CW-WR-76-020.73A
(DE82014579)

DESIGN AND DEVELOPMENT OF THE LIQUID FUELED HIGH TEMPERATURE COMBUSTOR FOR THE TURBINE SPOOL TECHNOLOGY RIG

High Temperature Turbine Technology Program. Phase II. Technology Test and Support Studies

Topical Report

June 1981

Work Performed Under Contract No. AC01-76ET10348

Curtiss-Wright Corporation
Power Systems Division
Wood-Ridge, New Jersey

U. S. DEPARTMENT OF ENERGY

DISCLAIMER

DISCLAIMER

CW-WR-76-020.73A
(DE82014579)
Distribution Category UC-90e

TOPICAL REPORT

DESIGN AND DEVELOPMENT OF THE LIQUID FUELED HIGH TEMPERATURE COMBUSTOR FOR THE TURBINE SPOOL TECHNOLOGY RIG

High Temperature Turbine Technology Program
Phase II
Technology Test and Support Studies

June 1981

Work Performed Under Contract No. DE-AC01-76ET10348
For U.S. Department of Energy

Curtiss Wright Corporation . Power Systems Division . One Passaic Street
Wood-Ridge, New Jersey 07075

THIS PAGE

WAS INTENTIONALLY

LEFT BLANK

ABSTRACT

Integrated gas turbine combined cycle electric power generating systems offer the promise for using coal in an economic and environmentally acceptable manner. Power plant efficiencies well above 40% may be achieved with gas turbine firing temperatures of 2600°F and higher, if the turbine cooling requirements are not excessive. The U.S. Department of Energy has sponsored, through the High Temperature Turbine Technology (HTTT) Program, the development of advanced gas turbine components for such a system.

The concept selected by Curtiss-Wright for this program utilizes transpiration air-cooling of the turbine subsystem airfoils. With moderate quantities of cooling air, this method of cooling has been demonstrated to be effective in a 2600°F to 3000°F gas stream. Test results show that transpiration air-cooling also protects turbine components from the aggressive environment produced by the combustion of coal-derived fuels.

A new single-stage, high work transpiration air-cooled turbine has been designed and fabricated for evaluation in a rotating test vehicle designated the Turbine Spool Technology Rig (TSTR). This report describes the design and development of the annular combustor for the TSTR. Some pertinent design characteristics of the combustor are:

Fuel	Jet A
Inlet Temperature	525°F
Inlet Pressure	7.5 Atm.
Temperature Rise	2475°F
Efficiency	98.5%
Exit Temperature Pattern	0.25
Exit Mass Flow	92.7 pps

The development program was conducted on a 60° sector of the full-round annular combustor. Most design goals were achieved, with the exception of the peak gas exit temperature and local metal temperatures at the rear of the inner liner, both of which were higher than the design values.

LIST OF ILLUSTRATIONS

Figure Number	Title	Page
1.1	Turbine Spool Test Rig Engine Section	1-2
2.1	Comparison of Operating Conditions and Performance Parameters	2-3
2.2	Annular Vaporizing Combustor Loading and Size Comparisons	2-4
2.3	Vaporizer Combustor Flow Patterns	2-5
2.4	Combustor System Temperature Rise Requirements	2-7
2.5	Combustor Injector Loading Vs Space Heat Release Rate	2-8
2.6	Combustor Frontal Fuel Loading Comparison	2-9
2.7	Liner Cooling Methods	2-11
2.8	Liner Cooling Flux as a Function of Thermal Severity	2-13
2.9	Measured Vs Predicted Combustor Liner Temperatures	2-15
3.1	TSTR Engine Compressor Discharge Diffuser Flow Path	3-2
3.2	TSTR Annular Combustor Design	3-4
3.3	TSTR Combustor Liner Wall Temperature Analysis	3-9
3.4	TSTR Annular Combustor General Layout	3-10
3.5	Combustor Headplate Finite Element Model	3-14
3.6	Combustor Inner Liner Hoop and Longitudinal Stresses	3-15
3.7	Combustor Headplate Deflection	3-17
3.8	Combustor Shroud - Liner Spacer	3-19
3.9	Combustor Vibrational Deflection	3-20

TABLE OF CONTENTS

Section	Title	Page
1.0	INTRODUCTION	1-1
2.0	GENERAL DESIGN CONSIDERATIONS	2-1
2.1	SELECTION OF FUEL INJECTION SPACING AND HEAT RELEASE	2-6
2.2	COOLING CONSIDERATIONS	2-10
3.0	DESIGN AND ANALYSIS	3-1
3.1	DIFFUSER PERFORMANCE ESTIMATES	3-1
3.2	AEROTHERMO-COMBUSTION	3-3
3.3	AEROTHERMAL-COOLING ANALYSIS	3-7
3.4	COMBUSTOR MECHANICAL DESIGN	3-7
3.5	COMBUSTOR STRESS AND VIBRATION ANALYSIS	3-12
3.6	FUEL SYSTEM DESIGN	3-26
3.7	RETRACTABLE PRIMER/IGNITER SYSTEM DESIGN	3-31
4.0	COMBUSTOR FABRICATION	4-1
5.0	COMBUSTOR TEST RIG AND TEST FACILITY	5-1
5.1	COMBUSTOR TEST RIG	5-1
5.2	COMBUSTOR TEST FACILITIES AND INSTRUMENTATION	5-13
6.0	COMBUSTOR TEST PROGRAM	6-1
6.1	METHODS AND PROCEDURES	6-1
6.2	COMBUSTOR DEVELOPMENT TEST RESULTS	6-10
6.3	COMBUSTOR TEST CHRONOLOGY	6-32
7.0	CONCLUSION	7-1

Subsequent turbine vane cascade testing established the need to reduce both the peak gas temperature (for optimum vane cooling) and the inner liner metal temperature (for combustor durability). Further development of the 60° combustor sector achieved the required temperature reductions and the final configuration was incorporated in the TSTR full-annular burner.

LIST OF ILLUSTRATIONS (Continued)

Figure Number	Title	Page
3.10	Combustor Outer Shroud Modification	3-22
3.11	Vaporizer Tube Calculated Temperature Distribution	3-23
3.12	Vaporizer Tube Finite Element Model Stress Distribution	3-24
3.13	Combustor Housing Cross-Section	3-25
3.14	Vaporizer Tube Family of Sizes	3-29
3.15	Vaporizer Tube Design	3-30
3.16	Fuel Injector Design	3-32
3.17	Various Stages of Atomization for Simple Jets	3-33
3.18	Retractable Primer/Igniter Cross-Section	3-34
3.19	Primer/Igniter Assembly	3-35
3.20	Combustor-Igniter Relationship	3-37
3.21	Primer/Igniter Wiring and Pneumatic Systems	3-38
4.1	Annular Liquid Fuel Combustor Basket Without Cooling Shrouds	4-2
4.2	Annular Liquid Fuel Combustor Basket With Cooling Shrouds Installed	4-3
4.3	Combustor Outer Liner Assembly	4-4
4.4	Combustor Headplate Assembly	4-5
4.5	Combustor Outer Liner - Upstream View	4-7
5.1	Liquid Fuel 60° Sector Combustor Test Rig Cross-Section	5-2
5.2	Photograph of 60° Sector Combustor Test Rig	5-3
5.3	Combustor Test Rig Assembly - Upstream View	5-4
5.4	Combustor Test Rig Assembly - 3/4 Rear View	5-5
5.5	Combustor Test Rig Water Cooled Side Plate	5-6

LIST OF ILLUSTRATIONS (Continued)

Figure Number	Title	Page
5.6	Combustor Test Rig in Test Stand Pressure Vessel	5-7
5.7	Combustor Test Rig in Pressure Vessel - Downstream View	5-8
5.8	Combustor Test Rig in Pressure Vessel - Upstream View	5-9
5.9	Combustor Test Rig Sweep Probe Assembly	5-10
5.10	T-4 Test Cell Control Room	5-14
5.11	Data Acquisition System Schematic	5-16
5.12	T-4 Test Cell Data Acquisition and Computer Control Station	5-17
5.13A	Combustor Sector/Turbine Cascade Logic Diagram	5-19
5.13B	Combustor Sector/Turbine Cascade Safety Interlock System Logic Diagram	5-20
5.14	Combustor Test Rig Sweep Probe Installation	5-24
6.1	Combustor Test Rig Installation for Light-Off Tests	6-2
6.2	Combustor Test Rig Installation in T-4 Test Cell	6-3
6.3	Combustor Outer Liner Pressure and Temperature Instrumentation	6-6
6.4	Combustor Inner Liner Pressure and Temperature Instrumentation	6-7
6.5	Combustor Headplate Total Pressure and Thermocouple Installation	6-8
6.6	Vaporizer Tube Thermocouple Installation	6-9
6.7	Combustor Performance Evaluation Definitions	6-11
6.8	Primer/Igniter Light-Off Test	6-15
6.9	Combustor Ignition Test Results	6-16
6.10	Combustor Primer/Igniter Orientation	6-17
6.11	Combustor/Igniter Light-Off Envelopes	6-18

LIST OF ILLUSTRATIONS (Continued)

Figure Number	Title	Page
6.12	Combustor Cold Flow Total Pressure Surveys	6-20
6.13	Sweep Probe Total Pressure Data	6-21
6.14	Combustor Total Pressure Loss	6-23
6.15	Combustor Total Pressure Loss Corrections	6-24
6.16	Combustor Total Pressure Loss Comparisons	6-26
6.17	Combustor Cold Flow Pressure Loss and Air Flow Distribution Test Results	6-31
6.18	Combustion Efficiency Vs Fuel Air Ratio, Configuration I	6-33
6.19	Combustor Pattern Factor Vs Temperature Rise, Configuration I	6-34
6.20	Combustor Average Radial Exit Temperature Profile	6-35
6.21	Combustor Liner #3 Temperatures	6-36
6.22	Combustor Liner #3 Nugget Temperatures	6-37
6.23	Combustor Liner Typical Temperatures	6-38
6.24	Combustor Liner Typical Temperatures Vs Fuel-Air Ratio	6-39
6.25	Combustor Liner Temperatures Vs Pressure Vessel	6-40
6.26	Combustor Liner Temperatures Vs Pressure Vessel	6-41
6.27	Combustor Liner Temperatures Vs Fuel-Air Ratio	6-42
6.28	Vaporizer Tube Thermocouple Locations	6-43
6.29	Vaporizer Tube Wall Temperatures Vs Fuel-Air Ratios	6-44
6.30	Vaporizer Tube Wall Temperatures Vs Pressure Level	6-45
6.31	Combustor Air Flow Distribution, Configurations I, II, IIa	6-47
6.32	Combustion Efficiency Vs Fuel-Air Ratio, Configuration II	6-48
6.33	Combustor Exit Temperature Pattern Factor Vs Temperature Rise, Configuration II	6-49

LIST OF ILLUSTRATIONS (Continued)

Figure Number	Title	Page
6.34	Combustor Average Radial Exit Temperature Profile, Configuration II	6-50
6.35	Combustor Headplate Wall Temperature Vs Fuel Air Ratio	6-51
6.36	Combustor Inner Wall Temperatures Vs Fuel Air Ratio	6-52
6.37	Combustor Outer Wall Temperatures Vs Fuel Air Ratio	6-53
6.38	Vaporizer Tube Wall Temperatures Vs Fuel Air Ratio	6-55
6.39	Fuel Jet Deflection Estimate	6-56
6.40	Fuel Tube Injector Modifications	6-57
6.41	Fuel Spray Pattern in Free Air Stream	6-58
6.42	Combustion Efficiency Vs Fuel Air Ratio, Configuration IIa	6-60
6.43	Combustor Exit Temperature Pattern Factor Vs Temperature Rise, Configuration IIa	6-61
6.44	Combustor Average Radial Exit Temperature, Configuration IIa	6-62
6.45	Combustor Outer Liner Temperature Vs Fuel Air Ratio, Configuration IIa	6-63
6.46	Combustor Inner Liner Temperature Vs Fuel Air Ratio, Configuration IIa	6-64
6.47	Combustor Outer Liner Temperature Vs Fuel Air Ratio, Configuration IIa	6-65
6.48	Combustor Inner Liner Temperature Vs Fuel Air Ratio, Configuration IIa	6-66
6.49	Combustor Headplate Wall Temperature Vs Fuel Air Ratio	6-67
6.50	Vaporizer Tube Wall Temperature Vs Fuel Air Ratio	6-68
6.51	Combustor Performance at Off-Design Conditions, Configuration IIa	6-69
6.52	Combustor Performance with Overboard Bleed, Configuration IIa	6-70

LIST OF ILLUSTRATIONS (Continued)

Figure Number	Title	Page
6.53	Combustor Inner Wall Cooling Fix, Configuration IIIa	6-72
6.54	Combustor Air Flow Distribution, Configurations IIIa, IVa, Va	6-73
6.55	Combustor Inner Liner Temperature Vs Fuel Air Ratio, Configuration IIIa	6-74
6.56	Combustor Inner Liner Temperature Vs Fuel Air Ratio, Configuration IIIa	6-75
6.57	Combustor Inner Liner Cooling Fix, Configuration Va	6-78
6.58	Combustor Inner Liner Temperature Vs Fuel Air Ratio, Configuration Va	6-79
6.59	Combustor Exit Temperature Profile, Configuration Va	6-80
6.60	Combustor Exit Temperature Profile, Configuration Va	6-82
6.61	Combustor Exit Temperature Pattern, Configuration Va	6-83
6.62	Combustor Modified Exit Temperature Profile Targets	6-84
6.63	Combustor Air Flow Distribution, Configurations Va, VIa, VIIa	6-85
6.64	Combustor Air Flow Distribution, Configurations VIIIa, IXa, Xa	6-86
6.65	Combustor Exit Temperature Profile, Configuration Xa	6-90
6.66	Combustor Exit Temperature Pattern, Configuration Xa	6-91
6.67	Combustor Test Rig Durability	6-92

LIST OF TABLES

Table Number	Title	Page
3-1	Combustor Design Parameters	3-6
3-2	Liquid Fuel Combustor TSTR Cooling Analysis Summary	3-8
3-3	Combustor Cooling Air Hole Definition	3-11
3-4	Combustor Air Flow Distribution	3-13
3-5	Combustor Stress Rupture Evaluation	3-17
3-6	Combustor Low Cycle Fatigue Evaluation	3-17
3-7	Vaporizer Tube Stress Analysis	3-27
3-8	Combustor Housing Stress Analysis	3-28
5-1	Combustor Rig Stress Analysis	5-12
6-1	Combustor Test Plan Summary	6-4
6-2	Combustor Test Program Results Summary	6-12
6-3	Combustor Sector Pressure Drop Calibration	6-27
6-4	Combustor Performance Summary	6-76
6-5	Combustor Performance Summary	6-88
6-6	Comparison of Exit Temperature Profiles	6-89

Section 1.0
INTRODUCTION

The Turbine Spool Technology Rig (TSTR), Figure 1.1, is a liquid-fueled test vehicle for the development of a high temperature transpiration air-cooled turbine. Turbine operation at inlet temperatures ranging from 2600°F to 3000°F requires a combustor subsystem capable of efficient performance over the operational range from ignition to a burner temperature rise in excess of 2500°F. In addition, the combustor subsystem must be sufficiently durable to assure reliable operation at high temperature levels. This requires that the design and manufacturing processes utilized to produce the combustor subsystem meet the quality standards consistent with dependable gas turbine engine operation.

The TSTR is a modification of the single-spool J65 gas turbine, incorporating a single stage transpiration air-cooled turbine. Similar rig engines have been utilized in the past by Curtiss-Wright to test developmental transpiration air-cooled turbines. Sustained endurance and cyclic tests were previously completed at turbine inlet temperatures up to 2750°F. The annular combustor configurations of the earlier rig engines and the TSTR were patterned after similar successful burners developed by Curtiss-Wright for high performance aircraft engines.

The unique feature of Curtiss-Wright combustors is the selection of a reverse flow aerating fuel injector system known as "candy-canes" and "mushroom" vaporizer tubes. These descriptive titles are derived from the geometric shapes of the fuel injectors. The reverse flow injector concept accomplishes lower luminosity (clean) combustion and lower exit temperature level variation by pre-injection aeration of the liquid fuel as well as very uniform distribution of the fuel across the combustor annulus by the reverse flow action of the injectors.

3000°F TSTR - 7.5:1 PRESSURE RATIO

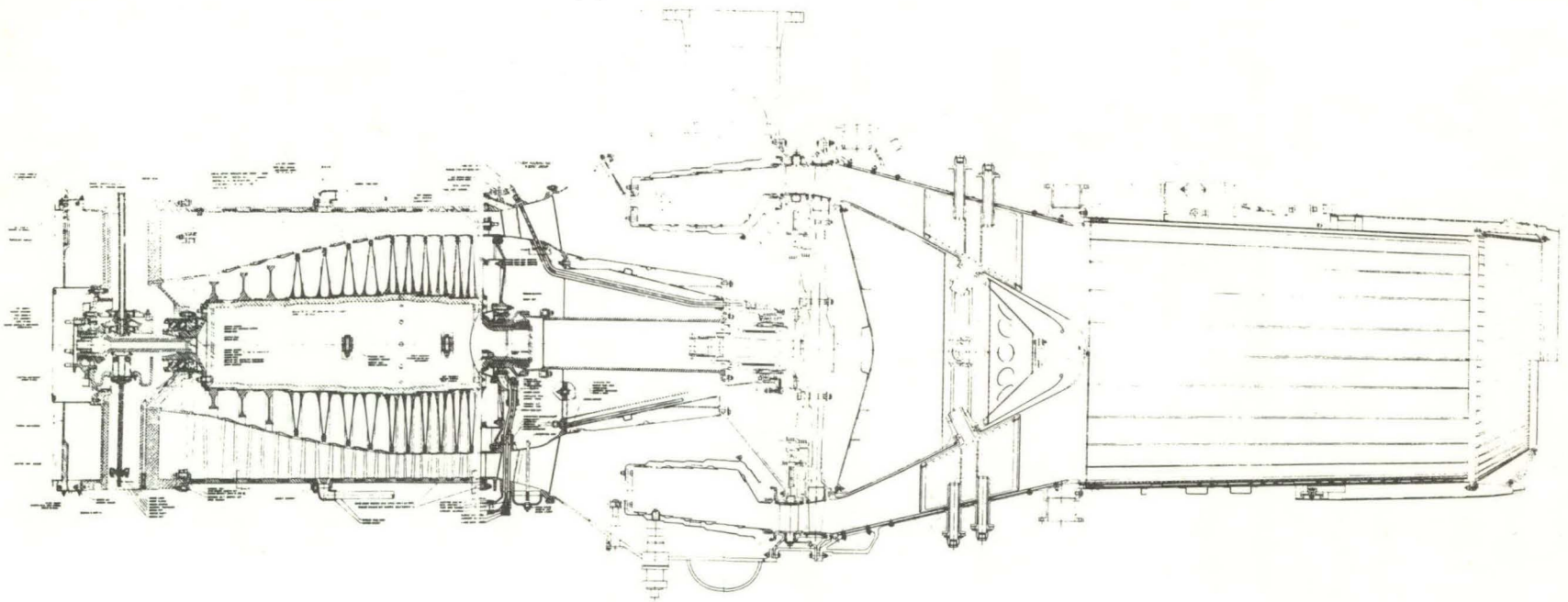

Figure 1.1
1-2

HTT-II-244

The TSTR is composed of a J65 compressor and main bearing support section and a new hot section. The new annular combustor of 41.0 inches outer diameter was designed to produce a 3000°F exit temperature at the following conditions:

Combustor Inlet Temperature	525°F
Combustor Inlet Pressure	7.5 ATM
Combustor Temperature Rise	2475°F

The combustor performance goals were established as follows for operation on Jet A fuel:

Combustor Efficiency	98.5%
Combustor Section Pressure Loss	6.0%
Combustor Exit Temperature Pattern	0.25
Combustor Liner Wall Temp (Max Avg)	1500°F (1000 LCF Cycles)

The TSTR combustor design incorporates 30 reverse flow (mushroom) fuel injectors, film cooled combustor walls with cooling air shrouds and six retractable torch igniters to initiate combustor light-off.

Section 2.0
GENERAL DESIGN CONSIDERATIONS

Differences in the approach taken in designing high temperature gas turbine combustors result in few outward changes in appearance, excepting size. The combustion chamber arrangement can be annular or can type, but in high temperature applications the reduced liner area of the annular combustor (30% less surface area) provides a significant reduction in cooling for this arrangement as combustor temperatures approach stoichiometric.

Liquid fuel injection systems may be the atomizing or vaporizing aerating type; the vaporizing aerating type is generally preferred for very high temperature rise and low emissions applications. The term vaporizer is really a misnomer since at nearly all conditions there is insufficient heat transfer surface to heat and fully vaporize the fuel, even with the assistance of inlet air which is admitted with the vaporizer tubes. Hence the device as a whole functions as a cross between a carburetor, an airblast atomizer and a true vaporizer.

Design of the primary combustion zone is very critical to the performance and durability of the combustor, and also to a major degree to the emission characteristics. The techniques involved are largely empirical. Parameters which must be considered for each design are overall residence time, primary air jet spread and intersection criteria, fuel-volume loading as dictated by emissions requirements and turn-down ratio, and internal velocity relationships as they affect combustion stability. The basic sizing of the primary zone is dictated by either aerodynamic loading or thermodynamic loading. Aerodynamic considerations are generally controlling on large engines but thermodynamics loading or reaction rate requirements tend to be dominant on small engines where it is difficult to provide sufficient residence time to complete combustion.

The mixing or dilution zone is designed to moderate the near-stoichiometric temperature gas stream exiting the primary combustion zone to produce the desired turbine inlet temperature profile by injection of air at combustor inlet temperature. Again, most of the design criteria are of an empirical nature relating to secondary air jet penetration and spreading characteristics.

The design methods practiced by Curtiss-Wright have produced successful combustor designs as proven by relatively trouble-free development and engine tests. Some examples of combustor designs similar in size to the TSTR combustor are shown in Figure 2.1.

The annular vaporizing combustor provides several advantages over other approaches verified by the broad range of burners developed at Curtiss-Wright, are enumerated as follows:

a. The primary zone consistently operates at near-stoichiometric fuel-air ratio at design temperature rise.

b. Stable combustion at high efficiency persists over a wide fuel-air ratio range because of excellent fuel preparation and mixing.

c. Carbon free operation, smokeless exhaust, and reduced radiant heat input to other components because vaporizing and/or aerating systems tend to burn with a relatively non-luminous flame.

d. A reliably consistent turbine inlet temperature distribution. A simple and relatively low pressure fuel supply system is required by the vaporizing combustor. Fuel metering orifices are relatively large and located outside the engine, thus minimizing sensitivity to fuel contamination and eliminating fouling due to the combustion process.

e. A maximum envelope of starting conditions is facilitated by a torch ignition system which is independent of the main fuel injectors.

The burner for the TSTR application is based upon scaling of the modified J65 high temperature combustor. The broad range of experience with variations in combustor geometry is illustrated in Figure 2.2.

A description of the air and fuel flow paths applicable to vaporizing-aerating burners is provided by Figure 2.3, which illustrates flow routing for typical 1800°F - 3000°F exit temperature burners.

CURTISS-WRIGHT ADVANCED COMBUSTION SYSTEMS

COMPARISON OF OPERATING CONDITIONS AND PERFORMANCE PARAMETERS

Combustor Design Details	J65 Production (1600°F T.I.T.)	J65 Modified for 2500°F T.I.T.	J65 Modified for 2750°F T.I.T.	J65 Modified for 2200°F T.I.T.	TJ60	NASA Segmentally-Constructed Liner Combustor	NASA Integrated Stator-Combustor System	WTF60	3000°F TSTR COMBUSTOR (ANNULAR)
Type of Combustor	Annular Vaporizing								
Number of Fuel Introduction Points	36				60	90	60	20	30
Dia: Outer Housing Max. - in.	36.0				30.0	40.2	30.0	20.0	48.0
Dia: Outer Liner Max. - in.	33.8				28.6	38.0	28.6	19.64	41.7
Length: Overall (Incl. Diffuser)-in	33.0				16.75	22.5	11.3	10.95	28.5
Length: Combustion Chamber - in.	22.0				10.75	15.9	5.3	7.3	17.0
Area: Compressor Discharge - $ft.^2$	1.535				0.67	1.11	0.67	0.238	1.535
Area: Combustor Reference* - $ft.^2$	5.74				2.90	7.46	2.90	1.39	2.61
Flight Condition	Mil. S.L.S.	Cruise	S.L.S.	S.L.S.	S.L.S.	Mil. S.L.S.	Cruise	S.L.S.	Cruise	Mil. S.L.S.	Cruise	S.L.S.	Cruise	Mil. S.L.S.	Emergency	
Inlet Conditions																
Airflow, lb/sec.	125	33	60	60	125	125	74.3	210	143	125	74.3	53.6	53.6	90.4
Total Pressure, in. HgA	203	54	90	90	203	270	161.3	270	183	270	161.3	451.2	451.2	188
Total Temperature, °R	960	810	760	760	960	1034	1276	1034	1610	1034	1276	1226	1226	983
Mach No.	.184	.178	.184	.184	.184	.379	.427	.379	.514	.379	.427	.287	.287	
Performance																
Fuel/Air Ratio	.016	.013	.035	.043	.027	.026	.023	.026	.0172	.026	.023	.023	.029	.043
Temperature Rise, Degrees	1100	840	2200	2450	1700	1626	1427	1626	1050	1626	1427	1434	1734	2477
Combustion Efficiency, %	98	98	99	99	99	99	99	99	98	99	99	99	98	98.5
Exit Temperature, °F	1600	1190	2500	2750	2200	2200	2243	2200	2200	2200	2243	2200	2500	3000
Primary Zone Air Flow (% of Compressor Discharge)	23.0	23.0	44.1	54.2	44.1	39.7		42.5		39.7				60
Total Pressure Loss: Overall (Incl. Diffuser) - % Inlet Total Pressure	5.0	4.6	9.26	9.26	9.26	11.0	13.5	4.8	8.1	10.0	12.3	5.0	5.1	6.0
Across Vaporizer Headplate - $\Delta P/q$ Reference*	28.52		31.4	31.4	31.4	17.8		17.9		17.8		25.4	25.4	-
Exit Temperature Distribution: Pattern Factor	.34 - .353		.175	.170	.200	.164	.189	.164	.20	.126	.152	.185	.170	.25
Max. Exit Ratio, $T_{max.}/T_{avg.}$ - °R/°R	1.18	1.18	1.135	1.135	1.13	1.10	1.10	1.10	1.08	1.08	1.08	1.14	1.14	1.18
Space Rate - BTU/hr/cu ft/atmos	2.72×10^6	2.2×10^6	7.2×10^6	9.2×10^6	4.6×10^6	11.5×10^6	10.1×10^6	6×10^6	3.97×10^6	24×10^6	21×10^6	9.0×10^6	11.4×10^6	7.0×10^6
Reference Velocity*, ft/sec	78	69	67	67	78	136	170	86	145	136	170	83	83	

*Reference Area from Outer Housing to Inner Housing

Figure 2.1
2-3

COMBUSTOR LOADING AND SIZE COMPARISONS

Annular Vaporizing Combustor Systems

	Space Rate BTU/hr/ft^3/atm		L/D Turbine Tip	
	Primary Zone	Overall	Flame Tube	System
J65 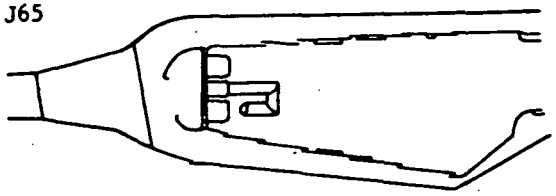	Production 9.7×10^6 Modified 12.1×10^6	2.7×10^6 9.3×10^6	0.72 0.72	1.08 1.08
TJ60 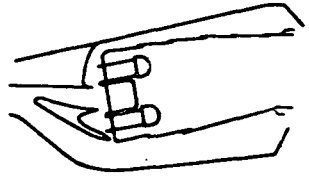	28.4×10^6	11.5×10^6	0.375	0.586
WTF60 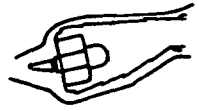	16.5×10^6	9.0×10^6	0.375	0.586

Figure 2.2

ANNULAR VAPORIZING COMBUSTOR FLOW PATTERNS - SCHEMATIC TYPE DESIGN

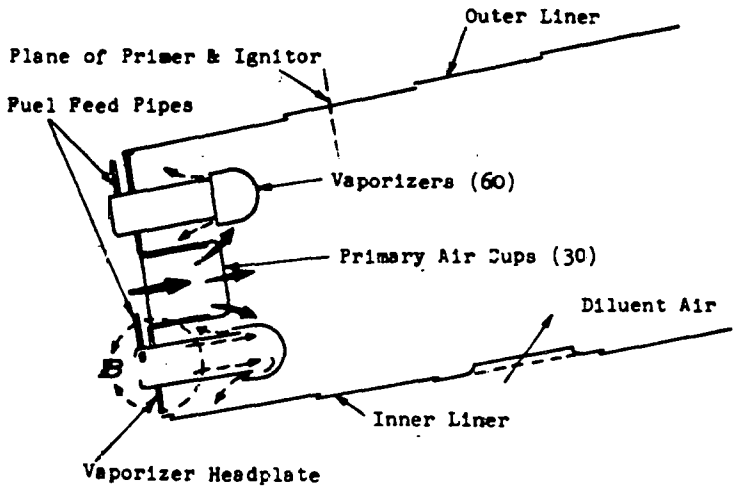

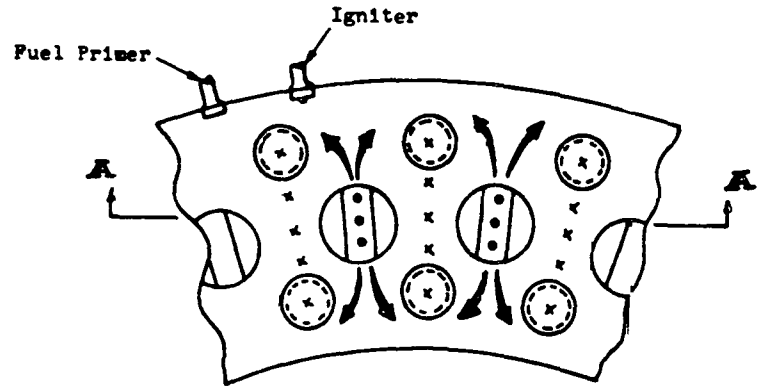

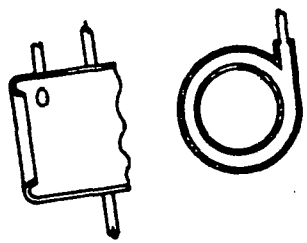

EXPLODED VIEW B

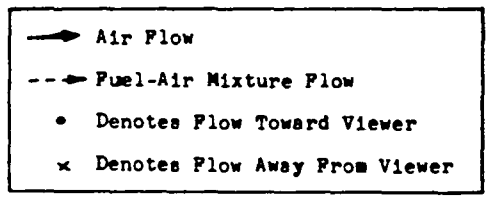

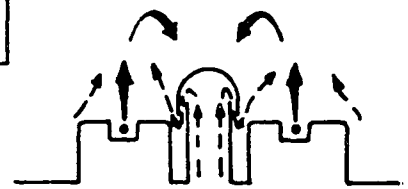

SECTION A-A

Figure 2.3

An appreciation of the salient features of the annular primary zone can be obtained by referring to the sketch of Figure 2.3 which describes the basic flow patterns and mechanism of operation. The fuel is burned at a fuel-air ratio close to stoichiometric in a relatively low velocity region downstream of the headplate. The primary air enters the combustion zone through the headplate, which contains reverse-flow "mushroom" fuel injectors and through the liner primary air holes. Externally metered fuel is delivered to each "mushroom" by large bore fuel feed tubes. The rich mixture of fuel and air passing through the "mushroom" tubes is heated by the combustion process surrounding the outside of the tubes and discharged in the forward direction in a state to burn immediately.

The essential function of the injector is to preheat the fuel and pre-mix it with air. The quantity of air in the tube must be sufficient to avoid fuel "cracking" and deposition while maintaining maximum carburetion. Combustor performance is not dependent on complete fuel pre-vaporization.

Ignition is accomplished by paired spark igniters and primer fuel injectors projecting through the outer combustor liner. Experience has shown this approach to be extremely flexible in providing the maximum starting envelope since the ignition system can be independently designed and developed for starting requirements.

The operating conditions of the TSTR combustor are compared to those of other Curtiss-Wright combustor systems in Figure 2.4; this figure also shows the wide range of fuel-air ratios over which this type of combustor has been utilized.

2.1 SELECTION OF FUEL INJECTION SPACING AND HEAT RELEASE

Selecting the number of fuel injection sources and the resultant fuel loading per source for a combustor system requires consideration of both physical limitations and performance experience. A survey of liquid fueled combustor/injector configurations has resulted in the experience guidelines of Figures 2.5 and 2.6, which show the range of fuel flow and frontal area loading in which satisfactory combustor exit temperature pattern control has been achieved as a function of burner temperature rise and space heat release rate.

COMBUSTOR SYSTEMS
VS.
PROGRAM REQUIREMENTS

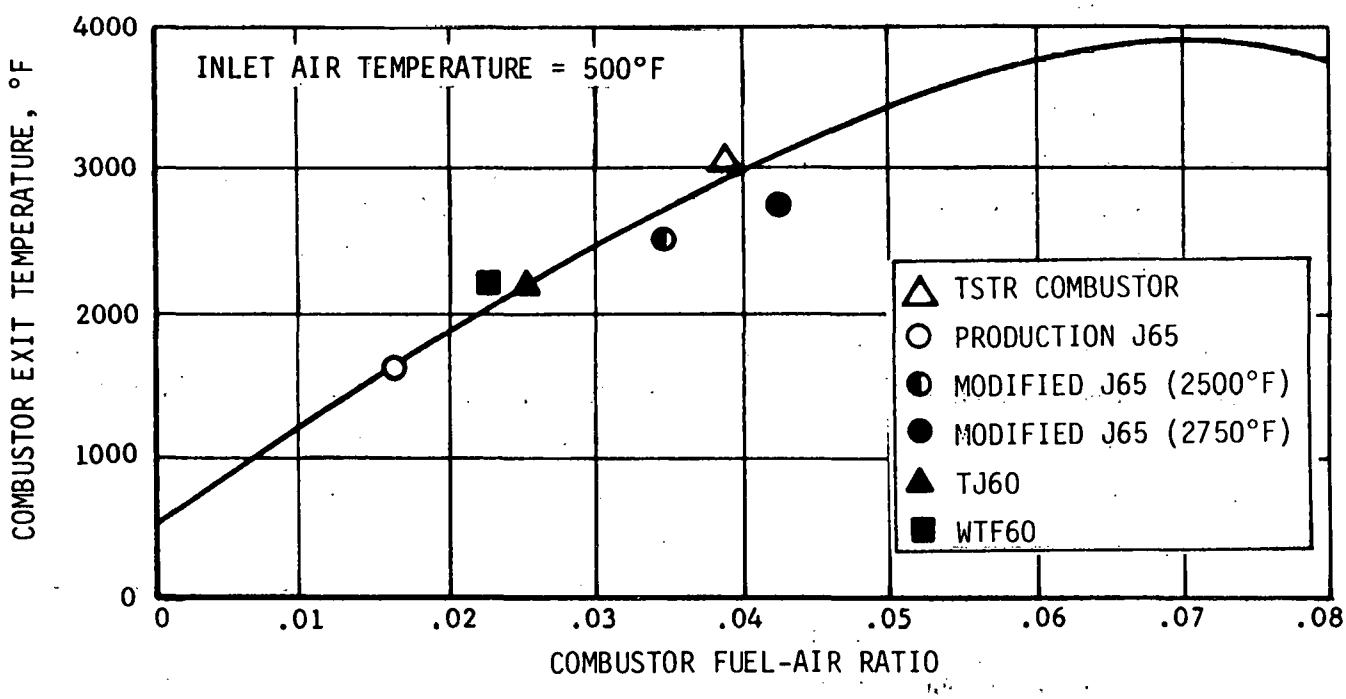

Figure 2.4

COMPARISON OF INJECTOR LOADING EXPERIENCE AS A FUNCTION OF
SPACE HEAT RELEASE RATE FOR VAPORIZER TUBE AND SPRAY COMBUSTION SYSTEMS

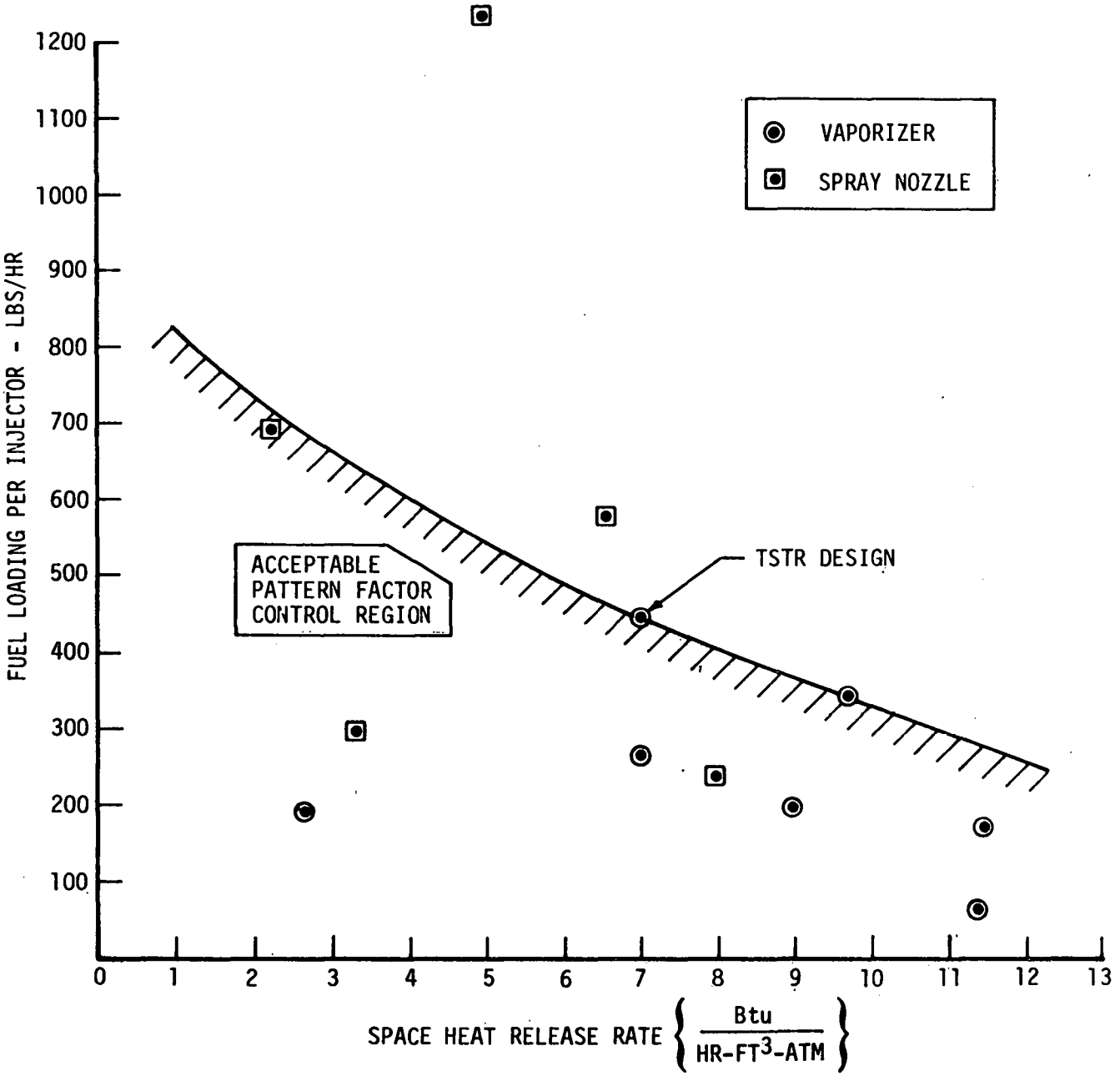

Figure 2.5

COMPARISON OF FRONTAL AREA FUEL LOADING LEVELS
FOR VAPORIZER TUBE AND SPRAY COMBUSTOR SYSTEMS

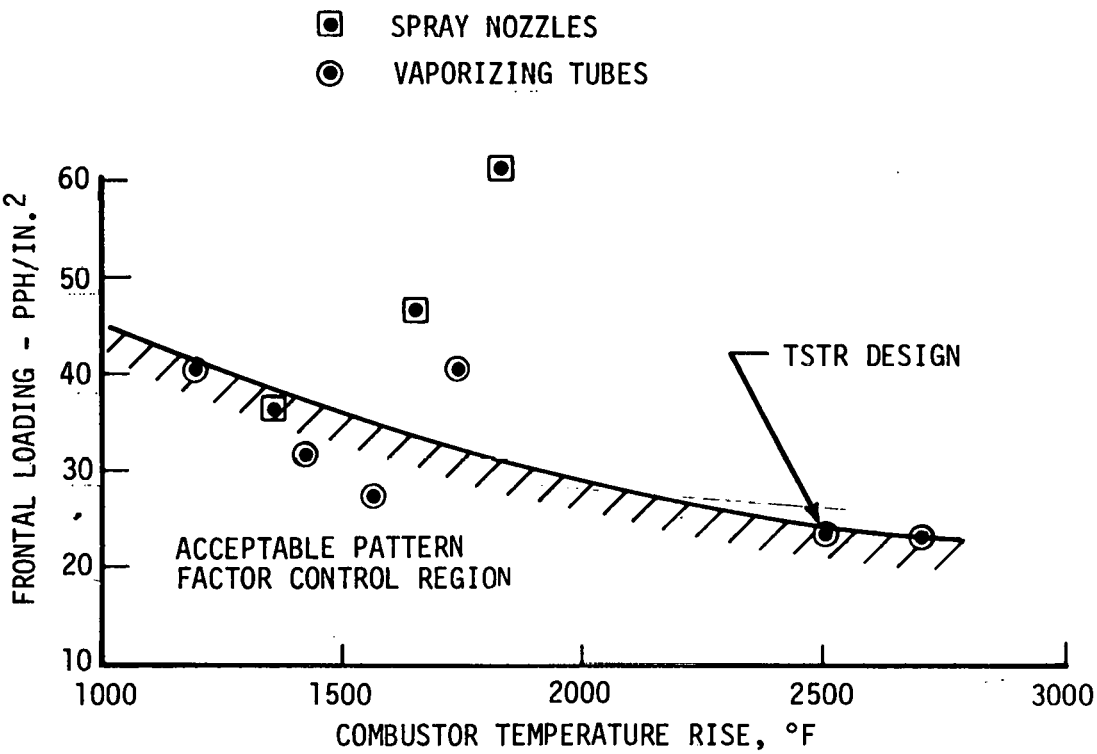

Figure 2.6

The figures are based on data obtained with both spray nozzle and vaporizer tube fuel injector devices incorporated in both moderate and high performance gas turbines. In the case of the TSTR it was found desirable to make the number of fuel injectors an integer multiple of the ten engine diffuser case struts. With a total of 30 injectors, the experience curves of Figures 2.5 and 2.6 show consistency at a frontal loading of approximately 24 pph/in.^{2} and a fuel loading of 450 pph per injector. This latter value yields a space heat release rate of approximately 7 x 10^6 Btu/Hr-Ft^3 ATM.

The aeration feature of the vaporizer tube injectors substantially reduces soot or exhaust smoke. However, there is no significant effect on the thermal NO_x generating processes which occur within the primary zone of high temperature combustors. Thermal NO_x reduction has been successfully demonstrated by techniques utilizing lean combustion (pre-aeration of air and fuel) coupled with short combustion residence times. Although the vaporizer tube design could be modified to incorporate the lean combustion concept, this was not investigated because of the work horse nature and relatively short operating time anticipated for this combustor.

2.2 COOLING CONSIDERATIONS

Operation of gas turbine combustors at high turbine inlet temperatures involves two broad technology areas: (1) materials and (2) combustor performance.

Air cooling is a practical method of limiting combustor liner temperatures since it imposes no penalties to the cycle and it is generally the least expensive cooling approach. Liner cooling methods that have been found satisfactory for application to combustors include (1) film cooled liners and (2) film cooled liners with regenerative convection cooling. Both of these schemes are illustrated in Figure 2.7.

Excessive temperatures or temperature gradients in the combustor liners may cause buckling, cracking, or oxidation, leading to major failures. It is therefore imperative that the liners be maintained at satisfactory temperatures (in the case of Hastelloy X material, no higher than 1500°F average or 1600°F maximum locally).

LINER COOLING METHODS

Tangential Film Cooling

Splash Plate Film Cooling

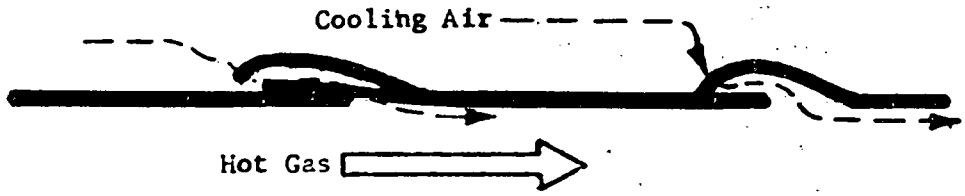

Transpiration Cooling

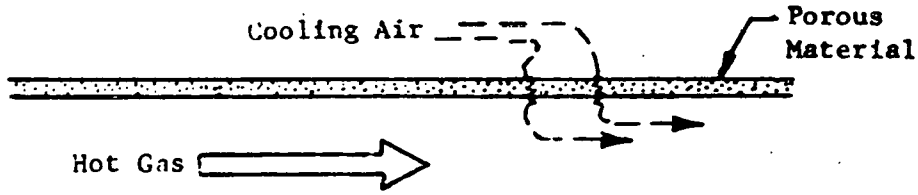

Regenerative Cooling

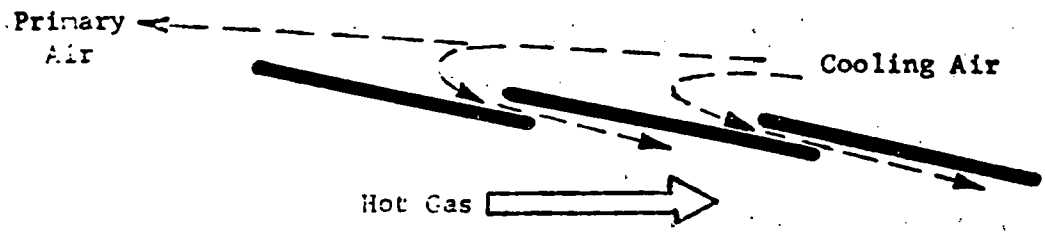

Figure 2.7

A correlation between satisfactory durability and heat sink availability, Figure 2.8, has been developed with various arrangements of fuel injectors and film cooled burner liners. This provides a reasonable starting point for cooling analysis and provides input data for performance prediction. The severity factor in the correlation represents the cooling required to maintain reasonable mechanical and thermal stresses in the liners.

A combustor design includes analytical predictions of coolant flow and temperature distribution for the particular combustor liner geometry, resulting in a complete thermal mapping of the liner surface temperatures under steady-state conditions. The computer program used by Curtiss-Wright for thermal mapping clearly delineates the advantages of specific materials and cooling schemes that exhibit lowered cooling requirements.

Steady-state analyses are done on a parametric basis, and involve the parameters listed below:

Fuel	Flame	Hot Gas	Coolant	Liner
L.H.V.	Temperature	Temperature	Temperature	Slot Height
Luminosity	Emissivity	Reynolds No.	Flow Rate	Permeability
Hydrogen/ carbon ratio	Radiation flux	Velocity	Velocity	Surface Area
		Density	Pressure Drop	View Factor
				Conductivity

The liner predicted temperature distribution is established from a heat balance of the following heat fluxes:

1. Luminous radiation from flame to liners
2. Convective heat transfer from hot gas to liners
3. Conduction within liners
4. External convection cooling of the liner by coolant

LINER COOLING FLUX COMPARISON WITH EXPERIENCE CURVE (ANNULAR COMBUSTOR)

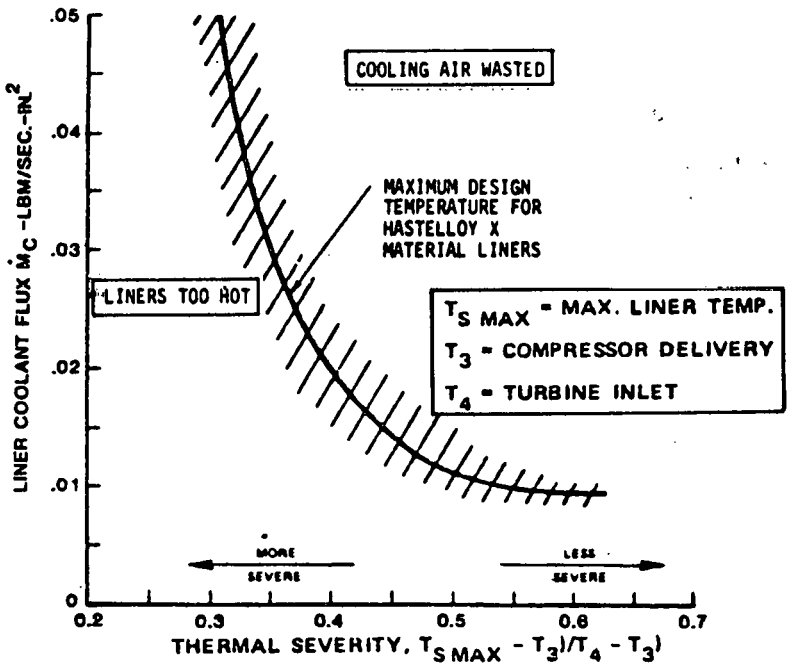

Figure 2.8

5. Radiation from liners to casing or cooling air duct

6. External convection cooling of casing or cooling air duct

7. Convection cooling and radiation heating within film cooling slots

Most combustor liner durability problems are temperature-related, and as noted earlier, the most suitable means of maintaining integrity is effective application of coolant to produce a controlled gas film temperature adjacent to the liner. Achieving the desired results involves combustor component rig development testing. Few test facilities are capable of producing the operating pressure levels (15 atmos or more) of modern high-performance gas turbines. Fortunately, earlier combustor development and rig research programs have established that testing at reduced pressure produces liner operating temperatures which are valid for the higher design pressure level. This applicability of data is indicated by Figure 2.9.

"Splash-plate" film cooling is used extensively in Curtiss-Wright combustors. Extensive experimental work was done in evaluating the relative merits of different types of film cooling configurations, including both cold flow aerodynamic tests and hot flow tests. Parametric studies have included slot height, lip thickness, plenum geometry, air introduction and metering methods, coolant Reynolds numbers, and velocity ratios. The results of these tests and studies provide a set of empirically defined relationships for calculation of film cooling effectiveness as a function of the above parameters.

Regenerative convective cooling is a technique primarily useful in augmenting the effectiveness of film cooling systems. Pure film cooling by slot injection involves a small additional heat removal from the metal on the coolant side by forced convection. This is obtained at some cost in effectiveness of the air as a film on the hot gas side due to the increase in air temperature before injection. In pure regenerative cooling, all of the cooling and primary combustion air is used in convection cooling of the liners before being introduced through the primary slots and headplate. In general, convective cooling effectiveness is not adequate unless liner velocities are high which results in high pressure losses.

COMPARISON OF MEASURED AND PREDICTED LINER TEMPERATURE

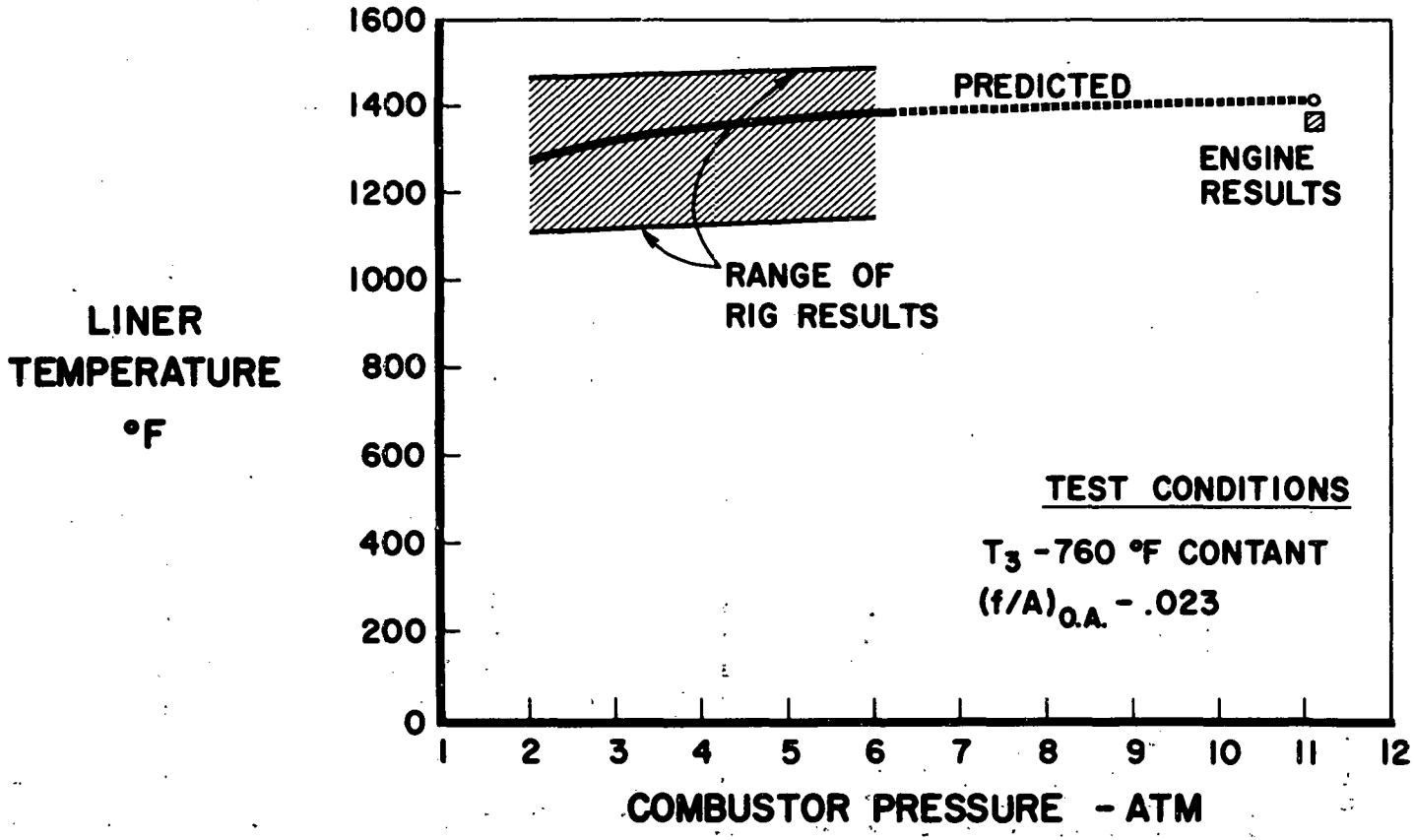

G.-203

Figure 2.9

Section 3.0

DESIGN AND ANALYSIS

3.1 DIFFUSER PERFORMANCE ESTIMATES

The Turbine Spool Technology Rig in which the new combustor must operate utilizes a J65 engine compressor assembly and diffuser case. The turbine component is at a considerably larger diameter. The resultant gas path elevation difference between compressor and turbine required analysis of the diffuser flow dynamics and pressure loss effects on the estimated performance of the overall combustor section installation. Based upon a design space heat rate criteria of greater than 7.0×10^6 Btu/Hr-Atm-ft^2, it would appear that the volume in the section between the compressor and turbine is so large (see Figure 1.1) that diffuser airflow dump conditions exist. The J65 diffuser flow path is shown in Figure 3.1. This flow path includes ten diffuser case support struts with symmetrical airfoil shape. Divergent wall angles at the diffuser inlet station are 8° at the inner wall and 14° on the outer wall. Inlet-to-exit area ratio is 2.48 without considering support strut blockage. With blockage, the area ratio to the station of maximum strut thickness is approximately 1.05 increasing to approximately 1.5 at a station 4.0 inches downstream of the diffuser entrance.

Past experimentation indicates that separation of the airflow occurs from both diffuser walls at this station and that a dump loss of approximately one velocity head would occur as the flow expands into the combustor case cavity. Using the empirical relationship for diffuser recovery efficiency (η_D), area ratio and total pressure loss ($\frac{\Delta P}{P_t} = \frac{\delta}{P_t} [1- \eta_D] [1-(\frac{A1}{A_2})^2]$, a diffusion pressure loss of approximately 0.70% was calculated for net area ratio of 1.62. The exit velocity head calculated at this station is approximately .9% for a potential total diffuser/dump loss of 1.60% $\Delta P/P_{t\ in.}$ when combined with the straight section loss.

TSTR ENGINE COMPRESSOR DISCHARGE DIFFUSER FLOW PATH

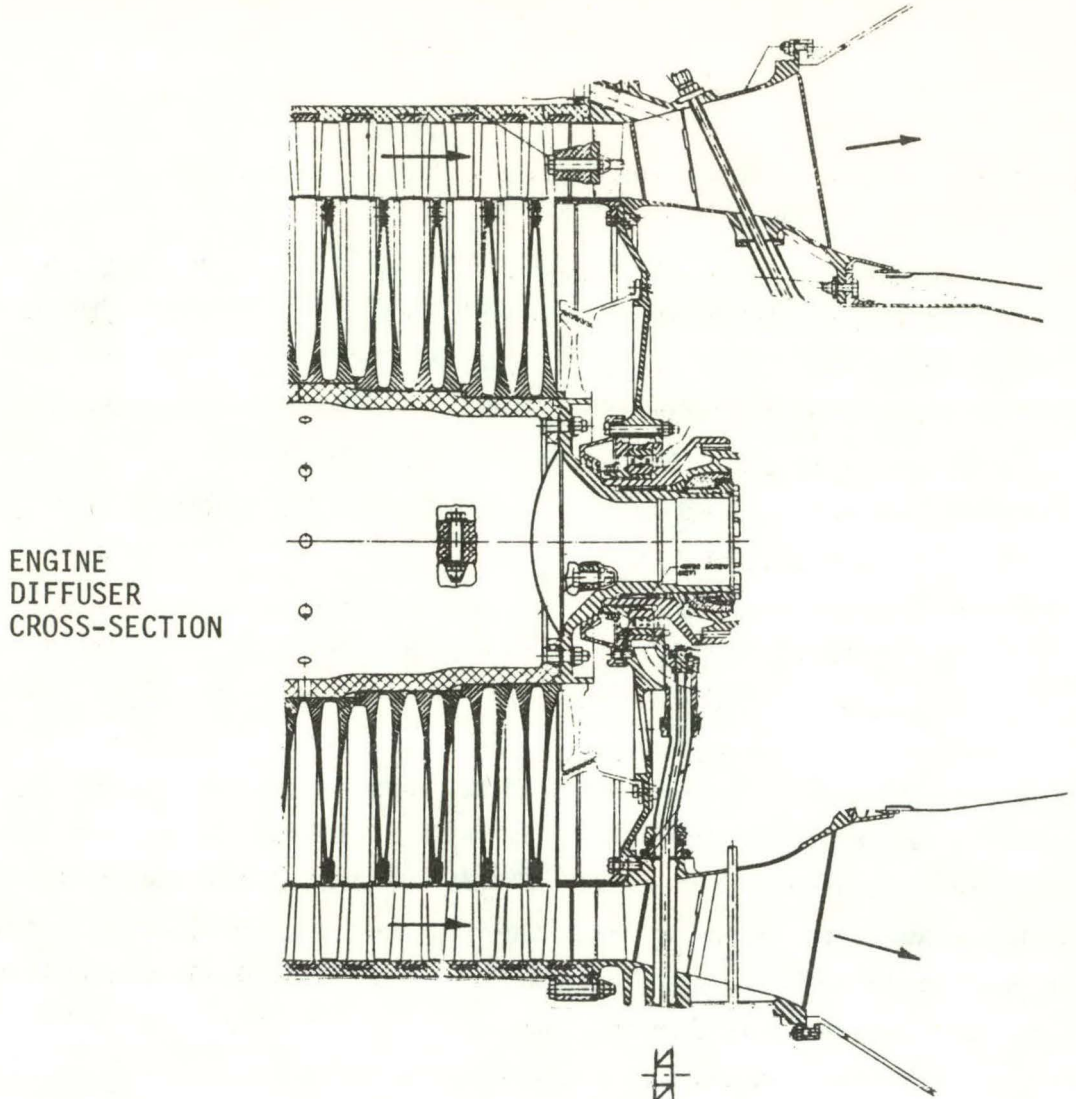

ENGINE
DIFFUSER
CROSS-SECTION

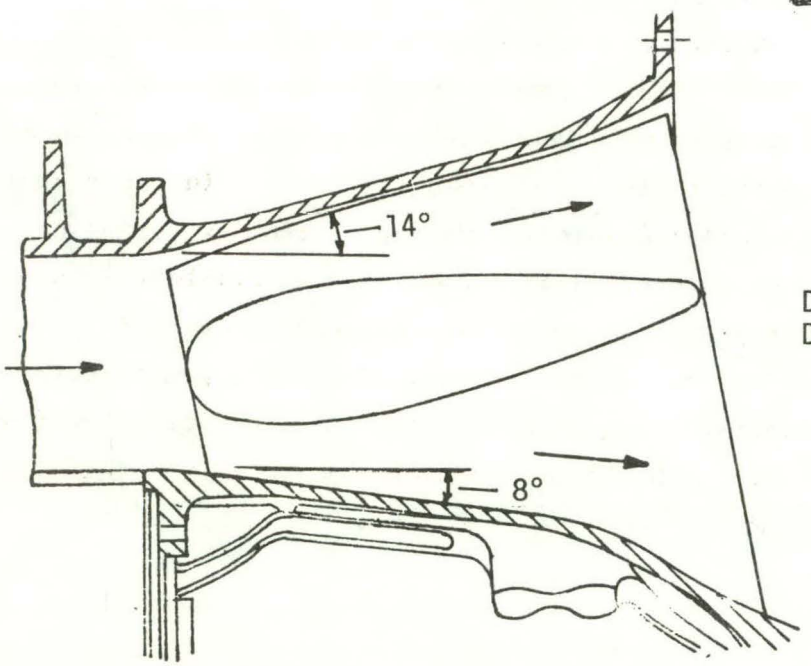

DIFFUSER
DETAIL VIEW

Figure 3.1

3.2 AEROTHERMO-COMBUSTION

The TSTR combustor design conditions are listed as follows:

Combustor inlet air flow rate	90.4	Lb/Sec
Combustor inlet air total pressure	106.5	Lb/Sq. In. Abs.
Combustor inlet air total temperature	523	°F
Fuel flow Jet A/JP-5	3.92	Lb/Sec
Combustor discharge gas flow rate	94.3	Lb/Sec
Combustor discharge gas total pressure	100.2	Lb/Sq. In. Abs.
Combustor discharge gas total temperature	3000	°F
Combustor exit temperature pattern factor	0.25	
Turbine rotor temperature profile variation	1.08	°R/°R
Combustion efficiency	.985	
$\frac{\Delta P}{P}$ Combustor pressure loss	6.0%	

To achieve a nominal turbine inlet temperature of 3,000°F with Jet A fuel the combustor must operate at an overall equivalence ratio (ratio of combustor fuel/air ratio to stoichiometric fuel/air ratio) of 0.65, which leaves 35% of the combustor inlet air flow for combustor wall cooling and turbine inlet temperature profile control.

The combustor design selected for the TSTR is an annular configuration with reverse-flow "mushroom" type vaporizer tubes as shown in Figure 3.2; design point nominal space rate is 7.0×10^6 Btu/Hr/Ft^3/Atmos. Using the given compressor exit annulus, turbine inlet annulus and available combustor envelope, a tradeoff study was performed which covering combustor design parameters of fuel/air mixing, emissions, residence time, dilution, pressure drop, temperature profile and liner cooling requirements. The results of this study were used to select a basic combustor geometry for further evaluation including design of liner cooling and mechanical design aspects.

TSTR ANNULAR COMBUSTOR DESIGN

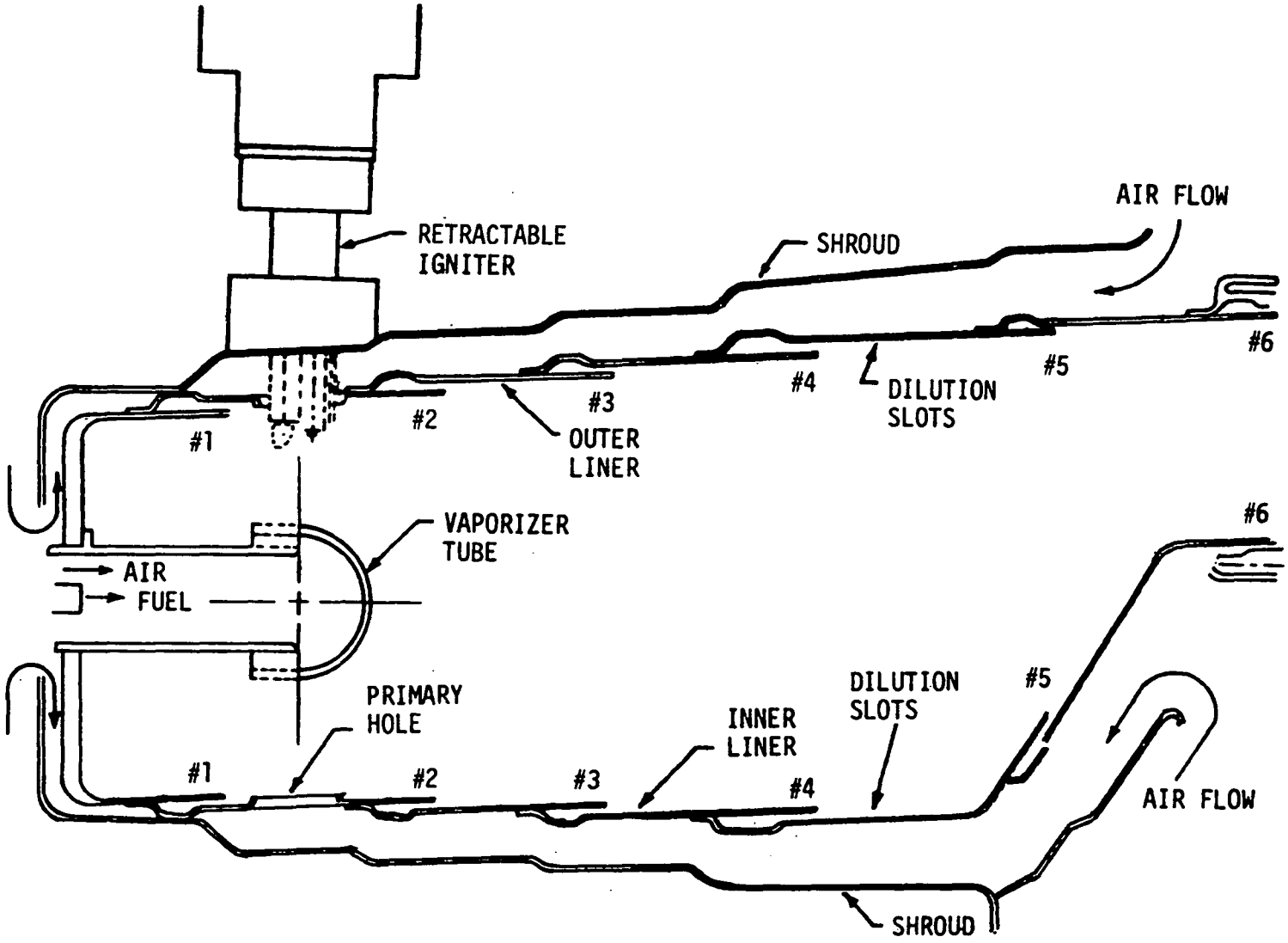

Figure 3.2

The nominal combustor length is 17 inches. The nominal headplate inner and outer radii are 14 inches and 19.1 inches, respectively. Three quarters of the air for the primary combustion zone enters the combustor through 30 plunged holes in each of the liners between the 30 vaporizer tubes. Liquid fuel and the remainder of the primary zone combustion air are injected into the combustor through the "mushroom" tubes. During combustor operation, the liquid fuel becomes partially vaporized prior to being discharged from the fuel tube. This fuel/air mixture impinges against the headplate, spreads out laterally and then mixes thoroughly with the remainder of the primary air entering the combustor.

Since the amount of air available for film cooling the combustor liners is limited, a combination of cold side convective cooling and hot side film-cooling was evolved for maximum cooling effectiveness. The amount of film-cooling air required is largely dependent on the magnitude of the convective velocity on the cold side of the combustor liners. The range of convective velocities considered was from 80 ft/sec to 200 ft/sec. Shrouds were designed external to the inner and outer liners to form flow passages to produce the desired cold side convective air velocities in a counterflow direction. The shrouds also contain in the flow passage the compressor discharge air to the various combustor entry holes.

Cooling analyses indicated that approximately 25% of the combustor air is required for the film-cooling slots. Film-cooling slot heights considered in the analysis varied from 0.10 to 0.20 inches. In this arrangement, the cooling air flowing between the shroud and liner enters a cooling plenum through a series of holes, impinges on the cooling lip and discharges into the combustor through the exit slot, forming the protective air film. The inlet holes are located either on the top or the end face of the plenum.

The list of selected combustor design parameters and liner dimensions is shown in Table 3-1.

Table 3-1

COMBUSTOR DESIGN PARAMETERS

Cooling Method:	Convective-Air/Cold Side Film-Air/Hot Side
Design Geometry	
Combustor Headplate Area	3.68 Ft^2
Number of Fuel Injectors	30
Number of Primary Holes	60
Number of Liner Cooling Bands	10 (Total)
Liner Surface Area	25.3 Ft^2
Combustor Volume	5.59 Ft^3
Surface Area/Volume	4.51/Ft
Liner Wall Thickness	.053 In. (Outer) .043 In. (Inner)
Liner Axial Length	17.0 In.
Liner Maximum Diameter	41.67 In.
Turbine Entry O.D.	41.67 In.
Turbine Entry I.D.	35.47 In.
Dilution Holes, Inner Liner	30
Dilution Holes, Outer Liner	60

3.3 AEROTHERMAL - COOLING ANALYSIS

A heat transfer analysis was performed to establish the minimal cooling airflow required to maintain a maximum average metal temperature of 1500°F when operating the combustor at 3000°F exit temperature. The following major heat fluxes were calculated for the combustor liner temperature balance: (a) hot side convection, (b) hot side radiation, (c) cold side convection, (d) cold side radiation and (e) film-cooling effectiveness. Using the Curtiss-Wright cooling analysis computer program, trade-off studies were conducted to optimize air distribution, considering cooling air mass flow, cooling louver geometry (gap height, cooling lip length) and outside convective effectiveness as a function of velocity and local heat flow. Table 3-2 summarizes the final cooling analysis results and compromises reached for the definition of the design combustor cooling configuration. Temperature levels and gradients were calculated for the combustor headplate, cooling louver nuggets and lips also, as shown in Figure 3.3.

3.4 COMBUSTOR MECHANICAL DESIGN

The general layout of the combustor is shown in Figure 3.4. The inner and outer liners forming the circular walls of the combustor are cooled by a combination of convective cooling the external surfaces and splashplate film-cooling the internal surfaces. The air cooling the external surfaces flows between the liners and concentric shrouds at velocities of 150 to 180 FPS entering the annulus at the aft end. The temperature of the liners varies from 1000°F upstream of the vaporizers tubes to approximately 1140°F at the air impingement locations with local maximum average temperatures of 1500°F expected at the double wall liner joints. The cooling holes are sized to obtain the optimum pitch (l/d) with which a uniform and effective impingement of cooling air is achieved as shown in Table 3-3. A pitch of approximately 2 is considered optimum. For manufacturing considerations it is important that the hole diameters be no less than the corresponding liner thicknesses. The air is discharged into the combustion zone at the splash-plate locations through circumferential openings and provides film-cooling.

Table 3-2

TSTR LIQUID FUEL COMBUSTOR COOLING ANALYSIS SUMMARY

Outer Liner

X	SH	M	W_c	V_c	V_s	X Loc. V_s
2.00	0.11	1.3	1.74	66.0	175	3.98
4.76	0.10	1.3	1.83	75.2	176	6.46
7.24	0.10	1.3	1.86	75.2	174	8.93
10.02	0.14	1.0	2.41	68.5	165	12.67
13.29	0.08	1.0	2.36	115.3	155	14.94
15.56	0.08	0.84	2.28			
			12.48 lb/sec			

Inner Liner

X	SH	M	W_c	V_c	V_s	X Loc. V_s
2.00	0.11	1.3	1.28	65.9	180	3.96
4.74	0.10	1.3	1.32	75.2	183	6.47
7.25	0.10	1.3	1.32	75.2	180	8.95
10.13	0.15	1.0	1.57	59.8	162	12.73
13.26	0.11	1.0	1.84	85.9	131	14.98
15.61	0.08	0.84	1.95			
			9.28 lb/sec			

X = Dimension (inches) From Rear Face of Headplate

SH = Slot Height (inches)

M = Mass Velocity Ratio - $\rho_c V_c / \rho_g V_g$ (dimensionless) $\frac{\text{Coolant}}{\text{Hot Gas}}$

W_c = Coolant Flow Rate (lb/sec)

V_c = Coolant Velocity at Slot Exit (ft/sec)

V_s = Velocity of Coolant Between Shroud and Liner (Shroud Velocity) (ft/sec)

X Loc. V_s = X Location of Shroud Velocity

TSTR COMBUSTOR LINER WALL TEMPERATURE ANALYSIS

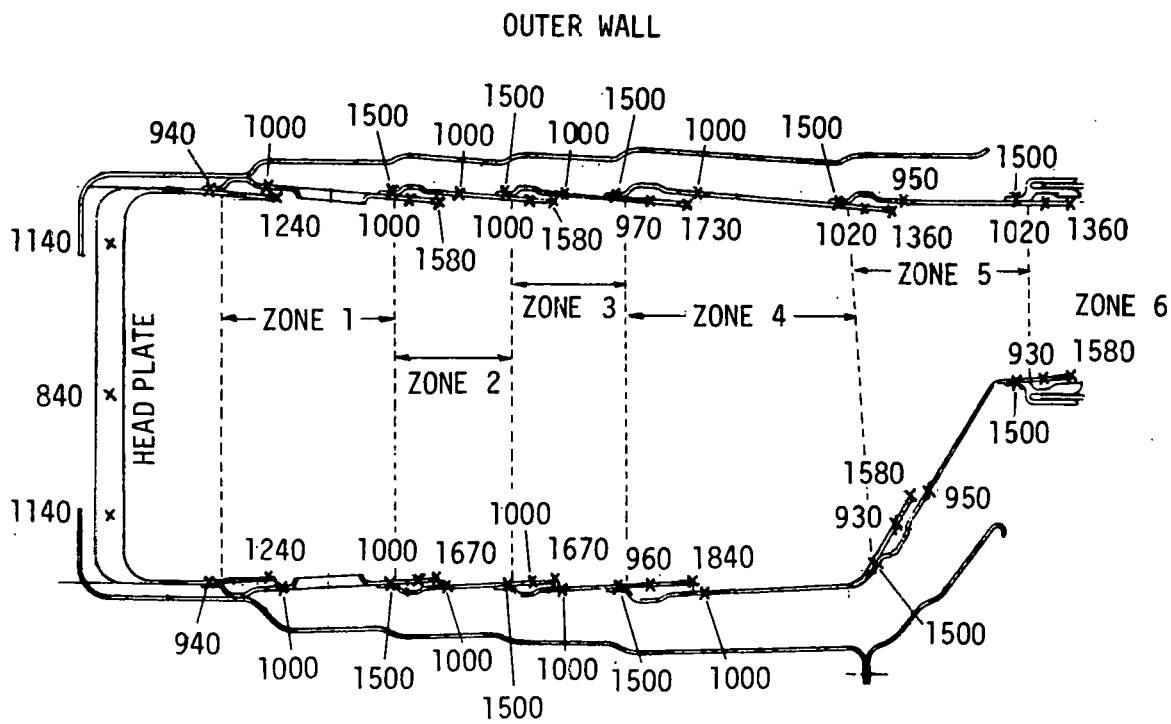

Figure 3.3

TSTR ANNULAR COMBUSTOR GENERAL LAYOUT

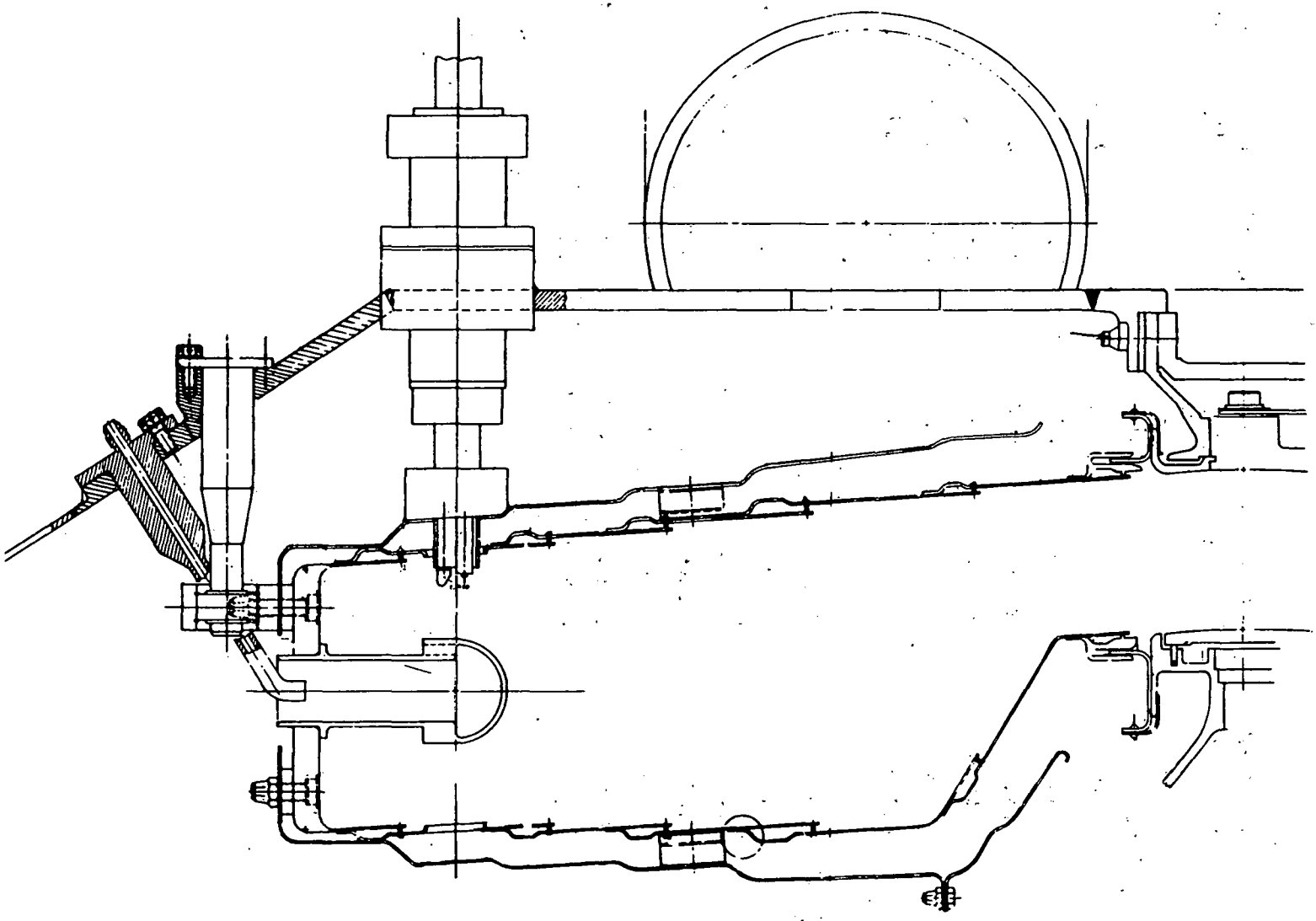

Figure 3.4

Table 3-3

TSTR COMBUSTOR COOLING AIR IMPINGEMENT

AIR-HOLE DEFINITION

Liner Number	Required Area (in^2)	Liner Radius (in)	Hole Dia. (in)	No. of Holes	Pitch =L/D	Actual Area (in^2)
Outer Liners						
1	2.368	18.953	.0550	1020	2.12	2.423
2	3.397	19.278	.0785	732	2.11	3.543
3	3.540	19.578	.0785	744	2.11	3.601
4	4.414	19.930	.0937	630	2.12	4.344
5	4.224	20.313	.0937	640	2.13	4.413
6	4.060	20.653	.0937	610	2.27	4.206
Inner Liners						
1	1.742	13.628	.0550	731	2.13	1.737
2	2.497	13.656	.0785	516	2.12	2.497
3	2.421	13.660	.0785	516	2.12	2.497
4	2.889	13.609	.0937	430	2.12	2.965
5	3.169	14.284	.0937	460	2.08	3.172
6	3.080	17.281	.0785	660	2.09	3.194

The inner and outer liners each have 30 primary air holes which are located circumferentially between the vaporizer tubes. In addition, located near the combustor exit, there are 30 diluent slots in the inner liner and 60 in the outer liner. The combustor overall airflow distribution through the various openings is shown in Table 3-4.

The liners are butt-welded to a single piece 1/2 inch thick circular headplate at their forward ends. The headplate is designed to limit rotation due to the eccentric pressure loading of the combustor. A gradual transition from the thick headplate to the thinner liners helps reduce the stresses at the joint resulting from the headplate rotation. The shrouds are fastened to the headplate and near the open end they are spaced from the liners with Z-shaped floating clips which permit differential axial and radial expansion of the components. The cooling louver design incorporates .070 diameter pins which serve as individual supports to limit local thermal growth of the cooling impingement lips.

3.5 COMBUSTOR STRESS AND VIBRATION ANALYSIS

The combustor was analyzed using an in-house finite-element computer program modeled for the ANSYS program using the quadrilateral elements shown in Figures 3.5 to 3.7. The design differential pressure loading on the liners is approximately 6 psi, however the analysis was performed with a differential pressure loading of 9 psi for a 50% overload condition.

In the stress-rupture evaluation the thermal stresses were not included since they can be considered as self-equilibrating and do not contribute to a "load-type" stress rupture failure. The significant mechanical stresses due to the pressure loading are shown in Table 3-5. These stresses when evaluated against the stress-rupture strength of the combustor material, Hastelloy X (inner and outer liner thicknesses of .045 and .056 inches respectively) were considered acceptable, except for the liner-segments at the headplate joints.

Table 3-4

TSTR COMBUSTOR AIRFLOW DISTRIBUTION

Location	Airflow, Percent
Vaporizer Tubes	16.19
Outer Liner	
Film Cooling Nugget 1	1.93
Primary Holes	22.03
Film Cooling Nugget 2	2.03
Film Cooling Nugget 3	2.06
Film Cooling Nugget 4	2.66
Dilution Holes	11.74
Film Cooling Nugget 5	2.61
Film Cooling Nugget 6	2.52
Inner Liner	
Film Cooling Nugget 1	1.41
Primary Holes	22.03
Film Cooling Nugget 2	1.46
Film Cooling Nugget 3	1.46
Film Cooling Nugget 4	1.74
Dilution Holes	3.92
Film Cooling Nugget 5	2.04
Film Cooling Nugget 6	2.16

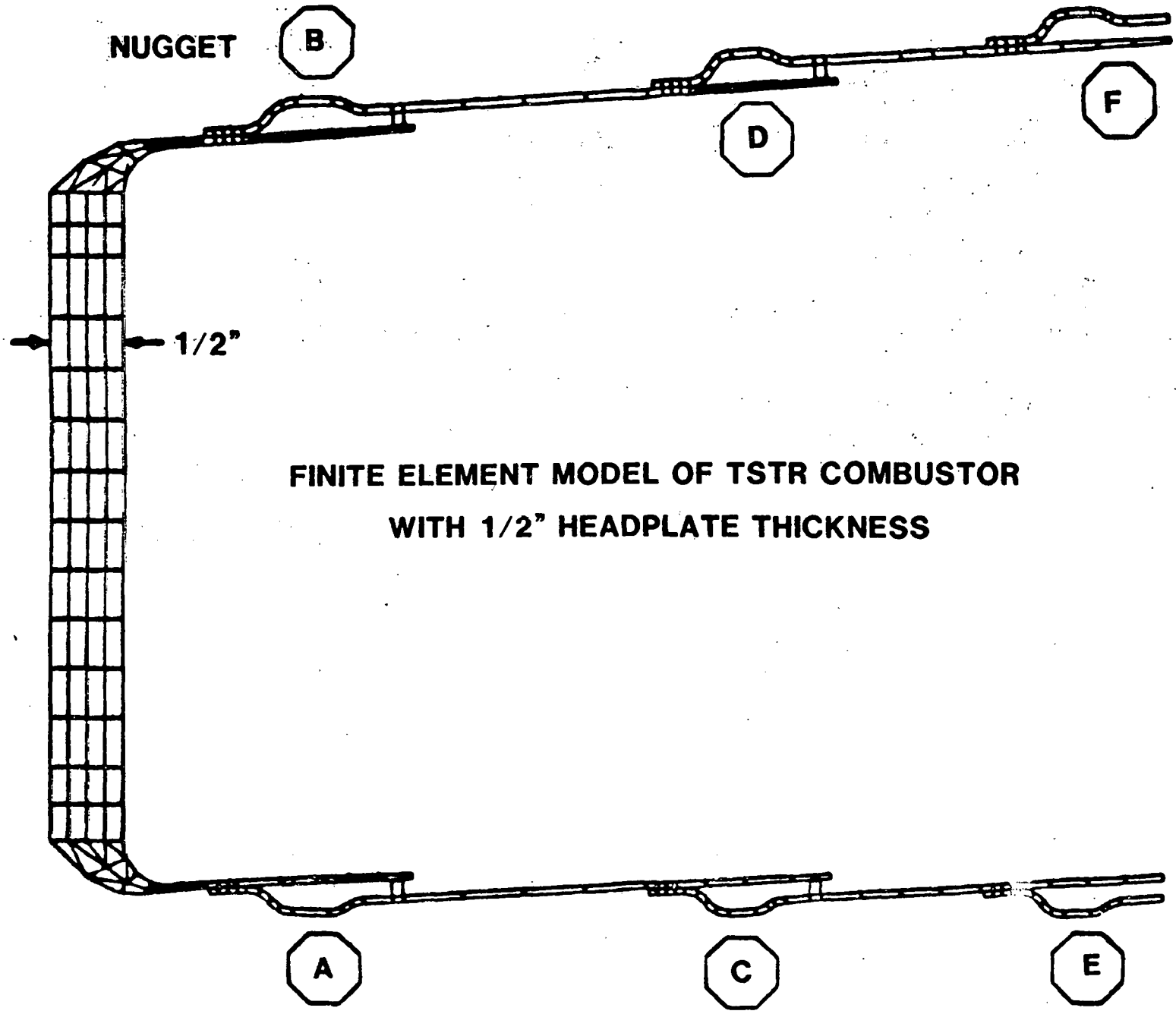

FINITE ELEMENT MODEL OF TSTR COMBUSTOR
WITH 1/2" HEADPLATE THICKNESS

Figure 3.5

TSTR COMBUSTOR INNER LINER

HOOP AND LONGITUDINAL STRESSES AT
CONE-CYLINDER TRANSITION

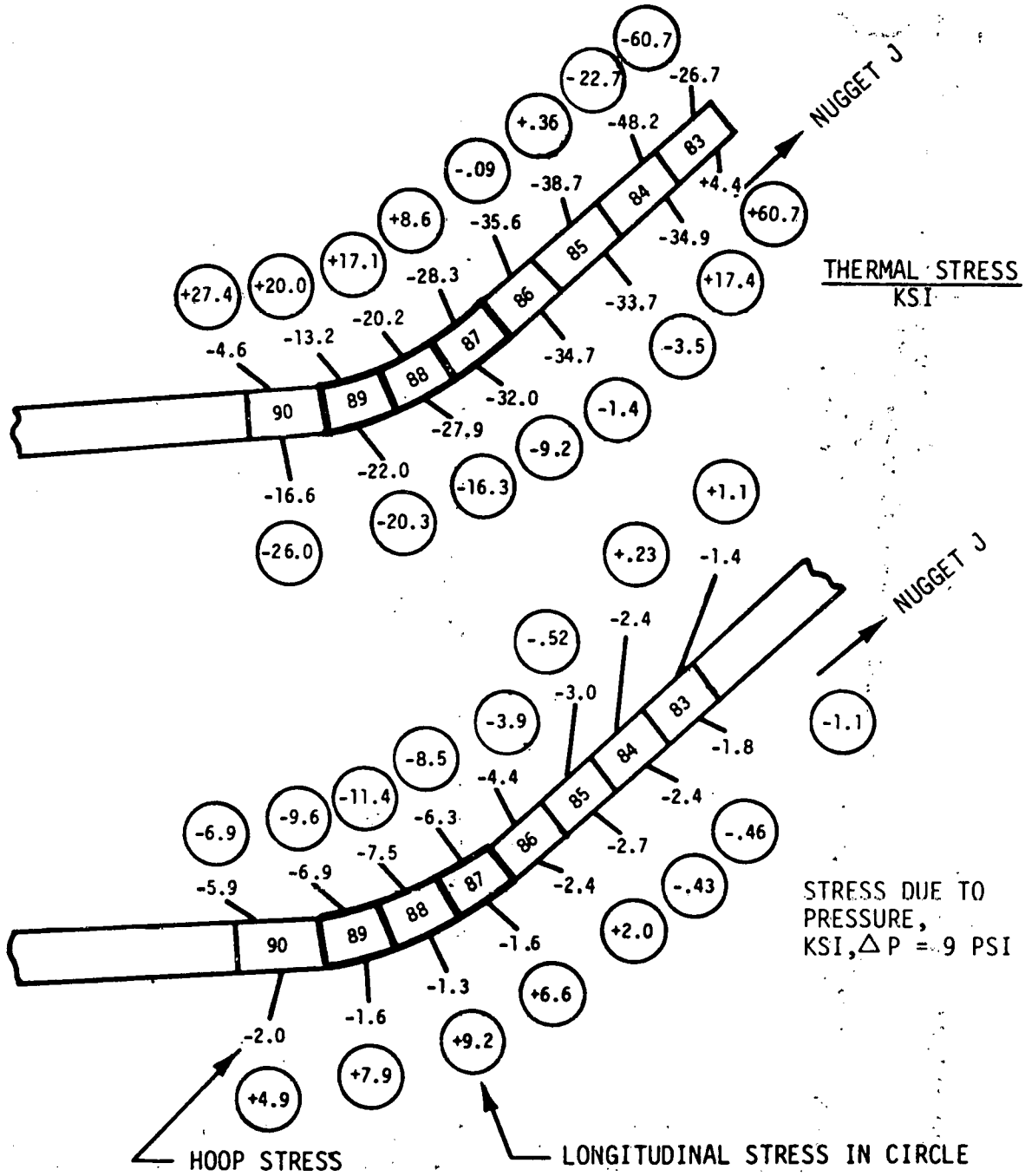

Figure 3.6

TSTR COMBUSTOR
HEAD-PLATE DEFLECTIONS

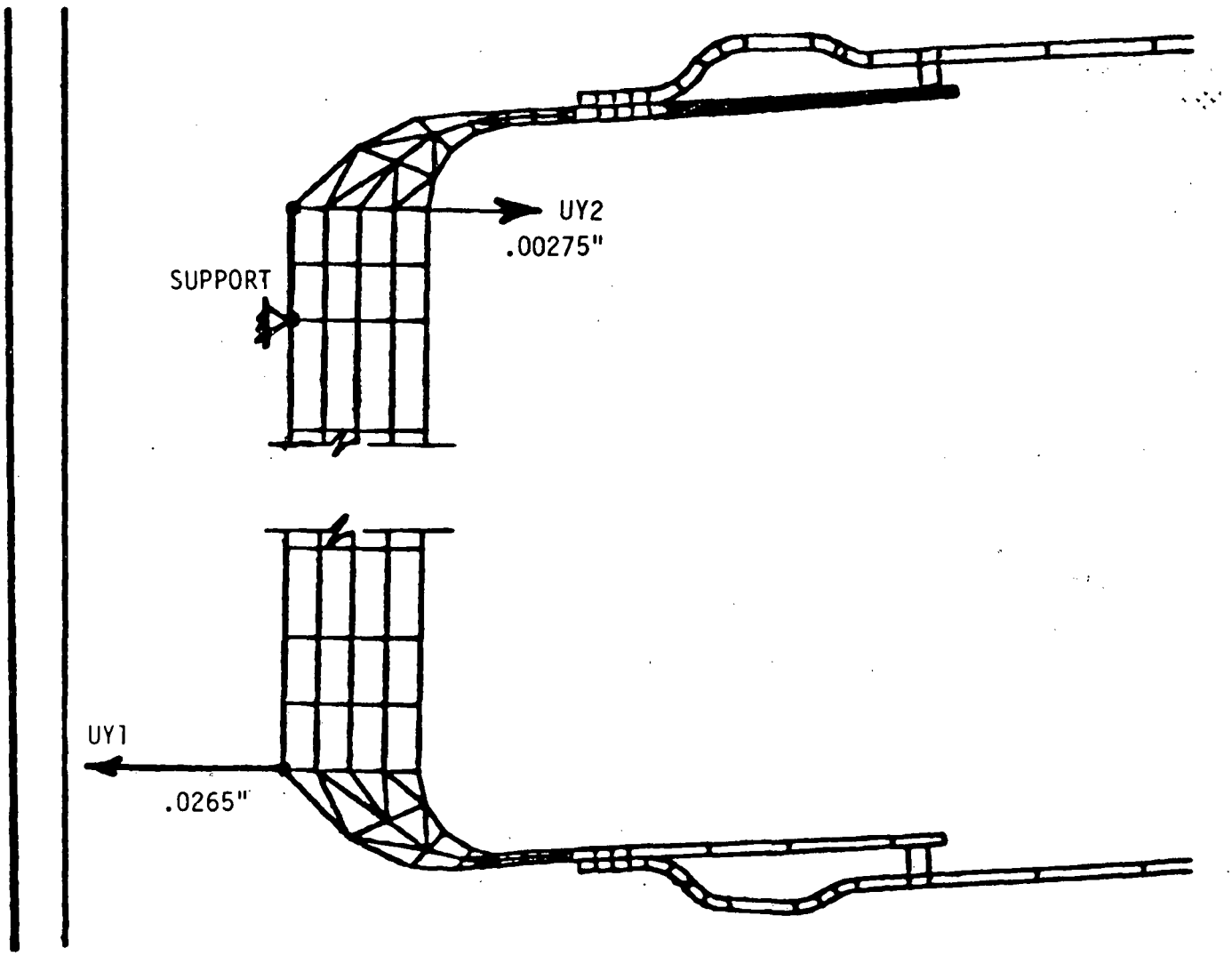

Figure 3.7

Table 3-5

TSTR COMBUSTOR STRESS-RUPTURE EVALUATION

Location	Longitudinal Stress (ksi)	Hoop Stress (ksi)	Equivalent Stress (ksi)	Metal Temperature (°F)	Minimum Stress Rupture Life (Hours)
Liner/Headplate Joint, Inner	-28.6	-14.6	24.8	1140	2000
Nugget C	-17.0	+ 0.5	17.3	1000	2000
Cone - Cylinder Transition	-11.4	- 7.5	10.9	1480	1500

Table 3-6

TSTR COMBUSTOR LOW-CYCLE FATIGUE EVALUATION

Location	Longitudinal Stress (ksi)	Hoop Stress (ksi)	Equivalent Stress (ksi)	Metal Temperature (°F)	Estimated Fatigue Life (cycles)
Liner/Headplate Joint, Outer	+45.5	- 5.7	48.6	1140	>100,000
Nugget D - Bead	-41.0	+105.1	130.5	1050	3,000
Nugget D - Lip	0	- 49.9	49.9	1610	>10,000
Cone - Cylinder Transition	59.6	12.6	54.4	1500	>10,000

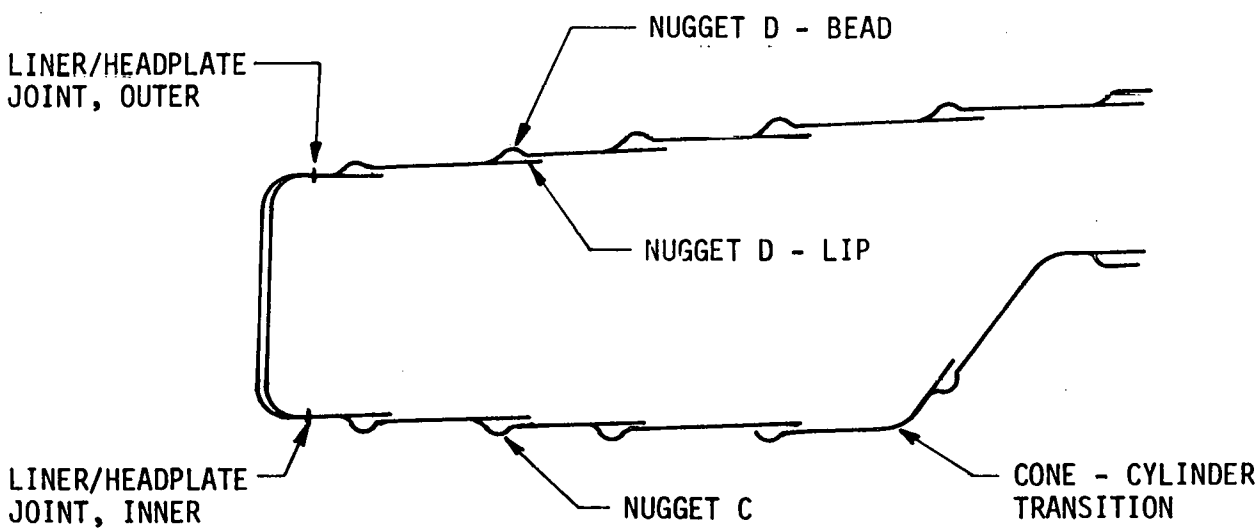

At these joints the stresses due the headplate rotation (Figure 3.7) were most significant, requiring that the inner and outer liner segment thicknesses be increased .056 and .062 inches respectively. An additional critical area was the cylinder-to-cone transition of the inner liner (Figure 3.6) where a minimum stress-rupture life of 1500 hours was calculated.

The low cycle fatigue evaluation of the combustor, which included the thermal loading, was based on the low-cycle fatigue data for Hastelloy X mate
The combined equivalent stresses at critical locations of the combustor are given in Table 3-5. The minimum low-cycle fatigue life was found to be 3000 cycles.

The radial buckling force on the outer liner and the axial buckling force on the inner liner due to the pressure differential were also computed. Based on published data (Bruhn) the analyses determined the margins of safety to be 5.6 for the outer liner and 19.7 for the inner liner.

There is no significant differential pressure loading on the cooling shrouds whose thickness is .056 inch and material is Inconel 600. The Z-shaped spacers between the shroud and liners are highly stressed due to the differential expansion of the hot liners and relatively cold shrouds (see Figure 3.8). At the calculated metal temperature of 1200°F and a stress of 68,000 psi, a low cycle fatigue life of 11,000 cycles is obtained from the published data for Hastelloy X material.

The combustor, including the shrouds, was also modeled for vibration analysis with the computer program. The spacers between the shrouds and liners were simulated as springs. A computer plot of the vibrational deflection in the first mode is shown in Figure 3.9. The frequency of 186 Hz is 30% above the operating speed of the TSTR. However, due to inherent constraints of the analytical modeling technique it is possible that not all modes of vibration were determined. Therefore, a vibration test of the physical combustor was performed on shaker equipment. A minor modification to the outer shroud was found necessary to eliminate the possibility of resonance at the TSTR operating speed.

TSTR COMBUSTOR
SHROUD-LINER SPACER

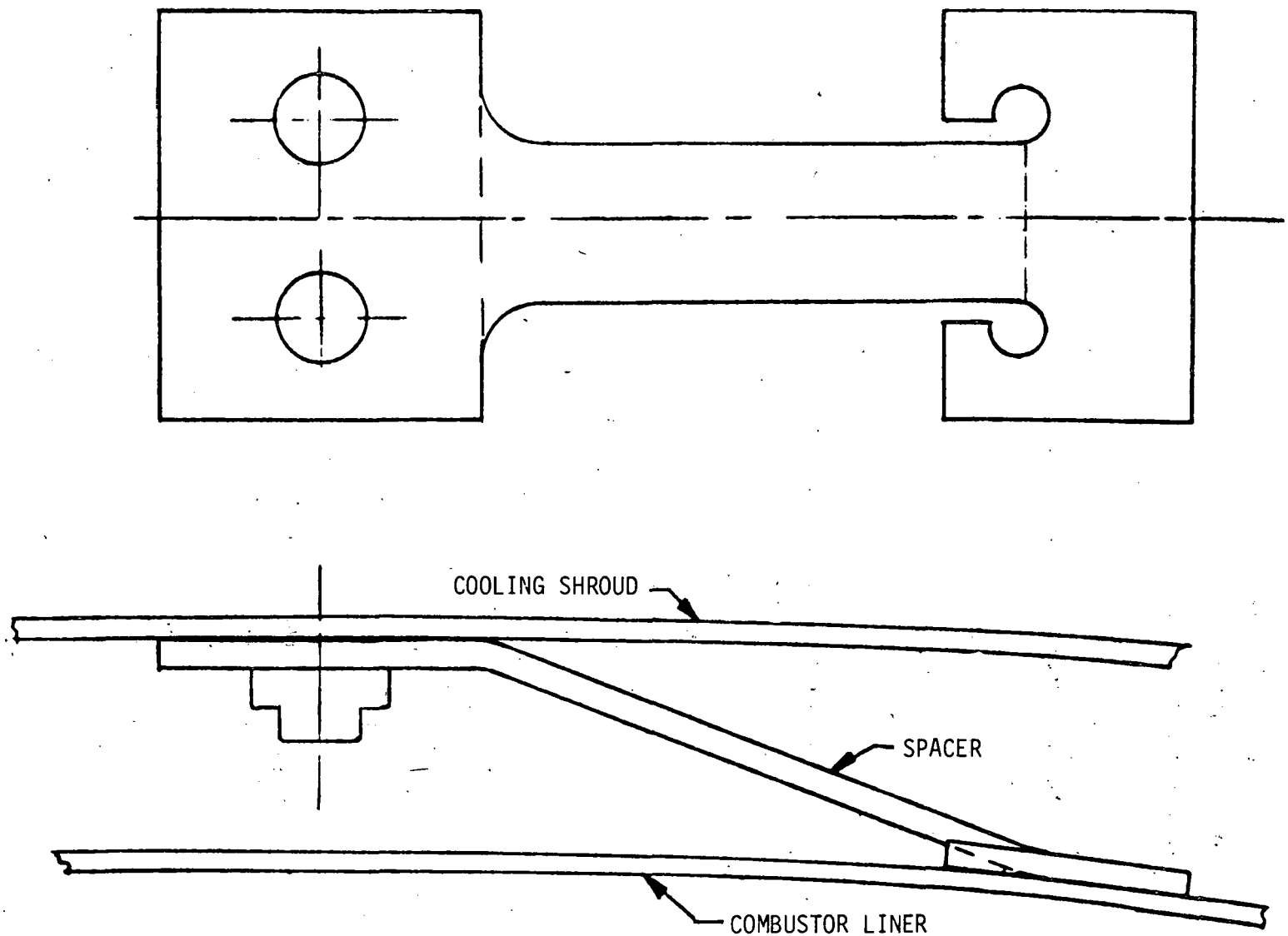

Figure 3.8

TSTR COMBUSTOR

PLOT OF MODE 1 VIBRATIONAL DEFLECTION

MODE 1 FREQUENCY 186 CPS = 11,160 RPM

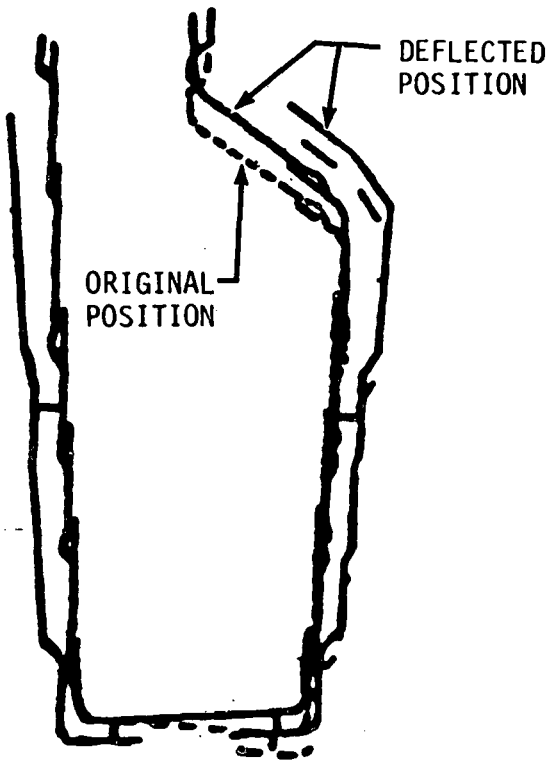

HTT - COMBUSTOR AND FREQUENCY ANALYSIS

Figure 3.9

Addition of a tube around the outer shroud as shown in Figure 3.10 yielded a first mode frequency of 184 cps, 28% above the TSTR speed. This mode is a "circumferential" vibration, rather than the "fore-aft" vibration depicted in Figure 3.9.

The fuel vaporizer tube, a drawing of which is shown in Figure 3.11, is integrally cast in one piece. The material is Hastelloy X. A finite-element computer program was used to analyze the vaporizer tube based on the temperature distribution shown in Figure 3.11. Pressure loading was calculated to be negligible. Significant calculated stresses are shown in Table 3-6 and the general stress distribution in Figure 3.12. The calculated stresses at some locations on the vaporizer tube are well above the yield stress of the material; however, since it is basically a thermal stress condition and self-limiting, failure is not expected. Evaluation of the vaporizer-tube for low-cycle fatigue indicates the tube to be structurally adequate for an excess of 50,000 cycles.

The combustor headplate has provisions for supporting the combustor in the diffuser case on radially directed pins. The pin and spherical bearing supports (Figure 3.13) permit thermal expansion of the combustor while keeping the entire unit centered in the housing and axially fixed. The calculated stress on the pins due to the aerodynamic thrust loads is 40,000 psi.

It was necessary to determine the vibration characteristics of the primer-igniter unit supported on the combustor housing. The first mode frequency is at 400 rpm and the second mode frequency is 17,200 rpm, both being adequately out of the TSTR idle and operating speed ranges. With a gravitational force of 10 G the cantilevered igniter assembly produces a moment of 660 in-lbs at the housing attachments. The stress in the bolts attaching the unit to the combustor housing does not exceed 6000 psi.

TSTR LIQUID FUEL COMBUSTOR

OUTER SHROUD MODIFICATION TO AVOID VIBRATORY EXCITATION

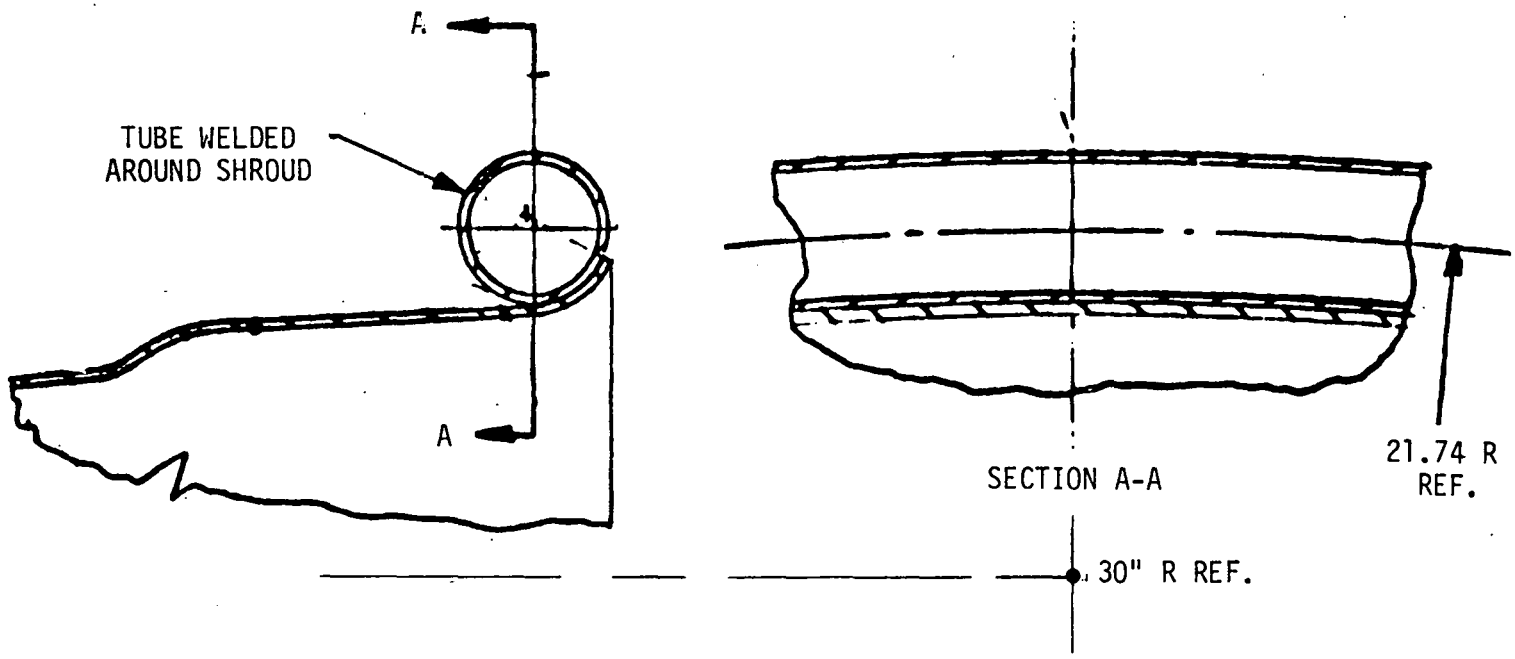

Figure 3.10

TSTR LIQUID FUEL COMBUSTOR VAPORIZER TUBE CALCULATED TEMPERATURE DISTRIBUTION

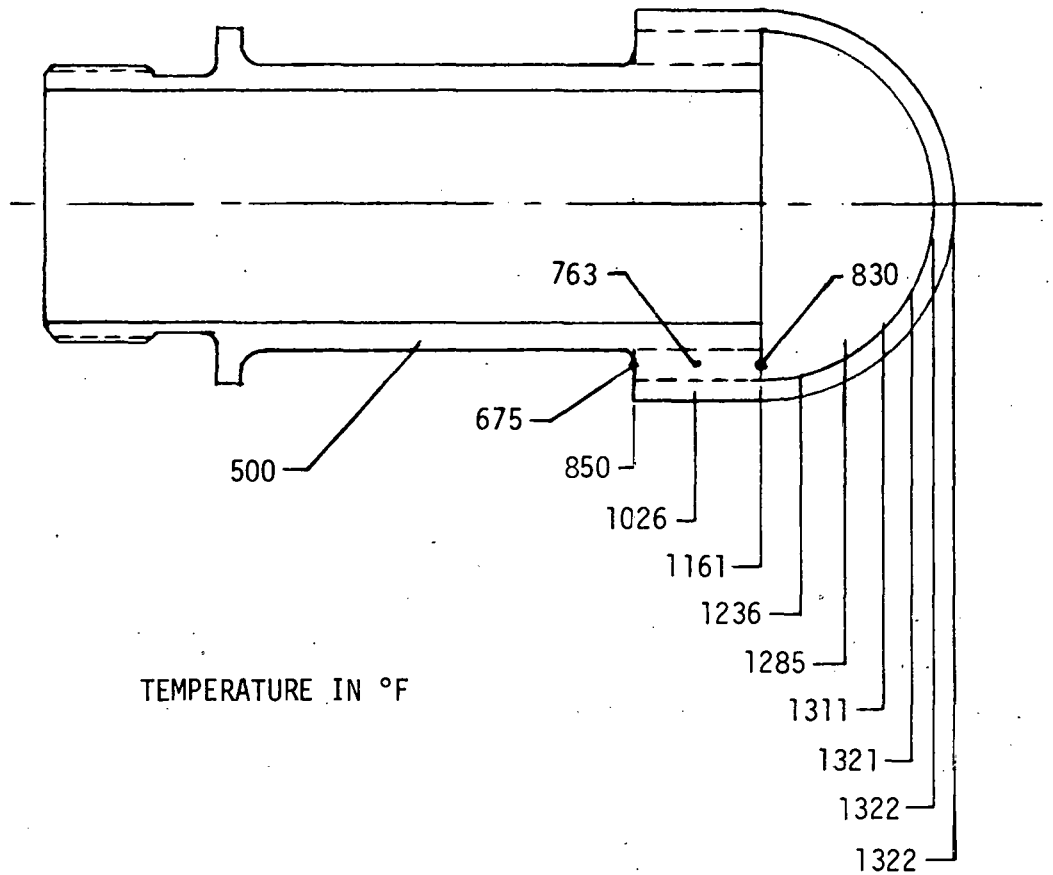

Figure 3.11

TSTR LIQUID FUEL COMBUSTOR VAPORIZER TUBE
FINITE-ELEMENT MODEL AND STRESS DISTRIBUTION

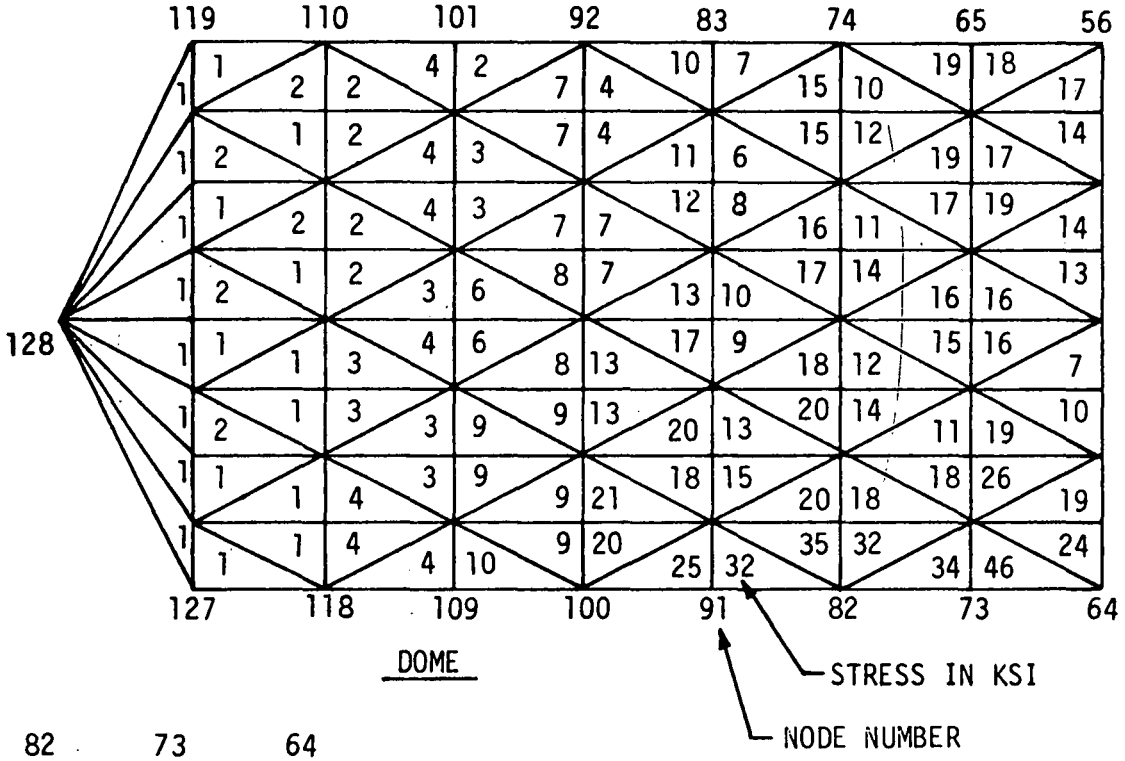

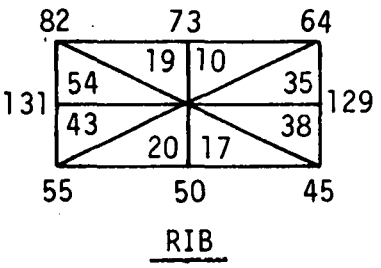

*STRESS NOT REALISTIC

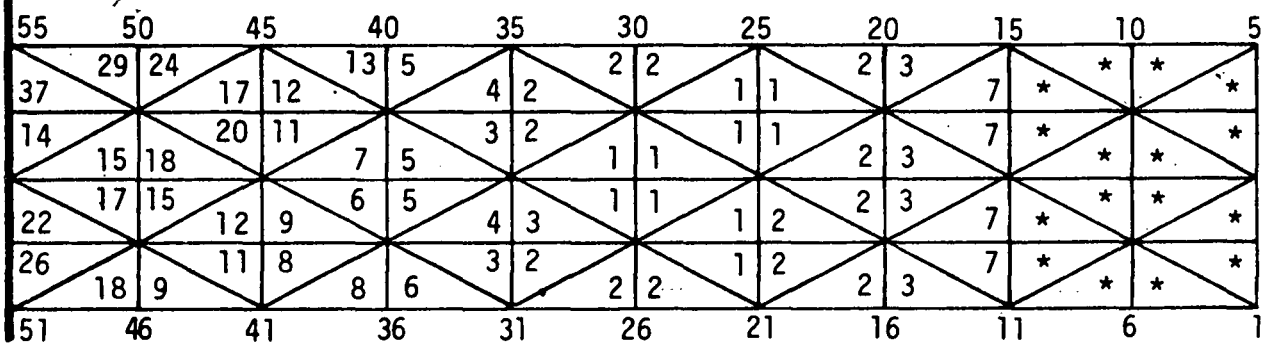

Figure 3.12

TSTR LIQUID FUEL COMBUSTOR HOUSING

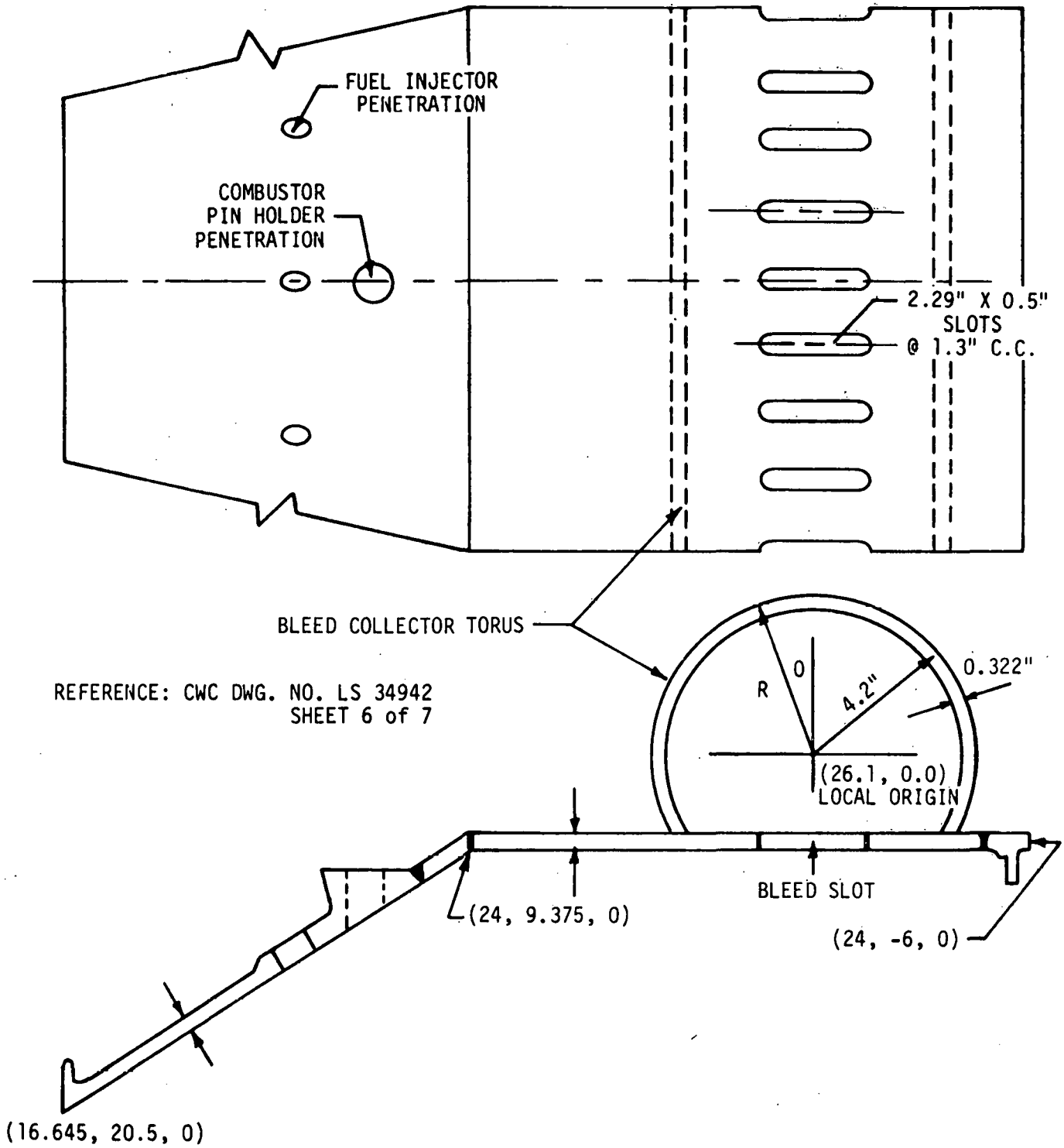

Figure 3.13

The axial thrust and weight of the combustor is transferred via radial pins to the combustor housing. In addition, the housing is subjected to the internal air pressure and a temperature differential. The structural analysis of the housing was performed with the finite-element program. Local stresses at the various bosses were determined using published analytical procedures (Bijlaard). Stress concentration factors were applied where appropriate. A summary of the significant stresses is given in Table 3-7. The effective stresses are below the yield strength of the material, stainless steel, AISI 410. Evaluation of the areas subjected to cyclic loads indicated that the combustor housing has a fatigue life in excess of 100,000 cycles as shown in Table 3-8.

3.6 FUEL SYSTEM DESIGN

The upstream fuel vaporizer tube injector system selected for the TSTR combustor is based upon long term development effort by the Curtiss-Wright Corporation. The range of mushroom vaporizer tube configurations and empirical design criteria developed over the years is shown in Figure 3.14. The development covered various dome shapes, length/diameter ratios as well as fuel/airflow ratios in the tube. The detail design of the TSTR vaporizer tube is shown in Figure 3.15. Variations of the liquid fuel injector configuration have also been evaluated for effectiveness of fuel distribution and atomization within the vaporizer fuel tube. Basically the vaporizer tube fuel injector concept utilizes a low-to-medium fuel pressure fuel system in that the fuel atomization and distribution within the vaporizer tube is accomplished by the airblast principle. Multi-port distribution valves are incorporated in the fuel system to ensure uniform distribution of fuel among the liquid fuel tube injectors. Various methods of injection of the liquid fuel into the vaporizer tube have been investigated to determine the optimum configuration and the effect on combustor performance. Tests indicated that direct injection at the centerline of the vaporizer is most effective. Fuel droplet atomization can be accomplished from simple jets by various degrees of hydraulic break-up and by airblast as generated by high velocity airflow perpendicular to the liquid fuel stream.

Table 3-7

VAPORIZER TUBE STRESS ANALYSIS

Location	Maximum Stress (ksi)	Temperature (°F)	Estimated Fatigue Life (cycles)
Inner Cylinder	37.30	500	>100,000
Rib	53.92	1161	>50,000
Outer Cylinder	45.57	1026	>100,000
Dome	35.37	1236	>50,000

Table 3-8

TSTR COMBUSTOR HOUSING STRESS ANALYSIS

Region/Material	Effective Stress (ksi)	Yield Strength At 500°F	Estimated Fatigue Life (Manson LCF)
1/8" Frustum Cone (AISI 410)	28	37	-
Fuel Injector Penetrations (AISI 410)	37	37	1.9×10^5
Combustor Pin Penetrations (AISI 410)	33	37	4.9×10^5
3/8" Frustum Cone/Cylindrical Shell Juncture (AISI 410)	17	37	-
Chamber Case/ Exhaust Manifold Juncture (AISI 410)	26	37	-
Chamber Case/ Exhaust Manifold Juncture Carbon Steel (C 1025)	9	27	-
Chamber Case Slots (AISI 410)	18	37	-
Flanges (AISI 410)	33	37	4.9×10^5

VAPORIZER TUBE SIZES

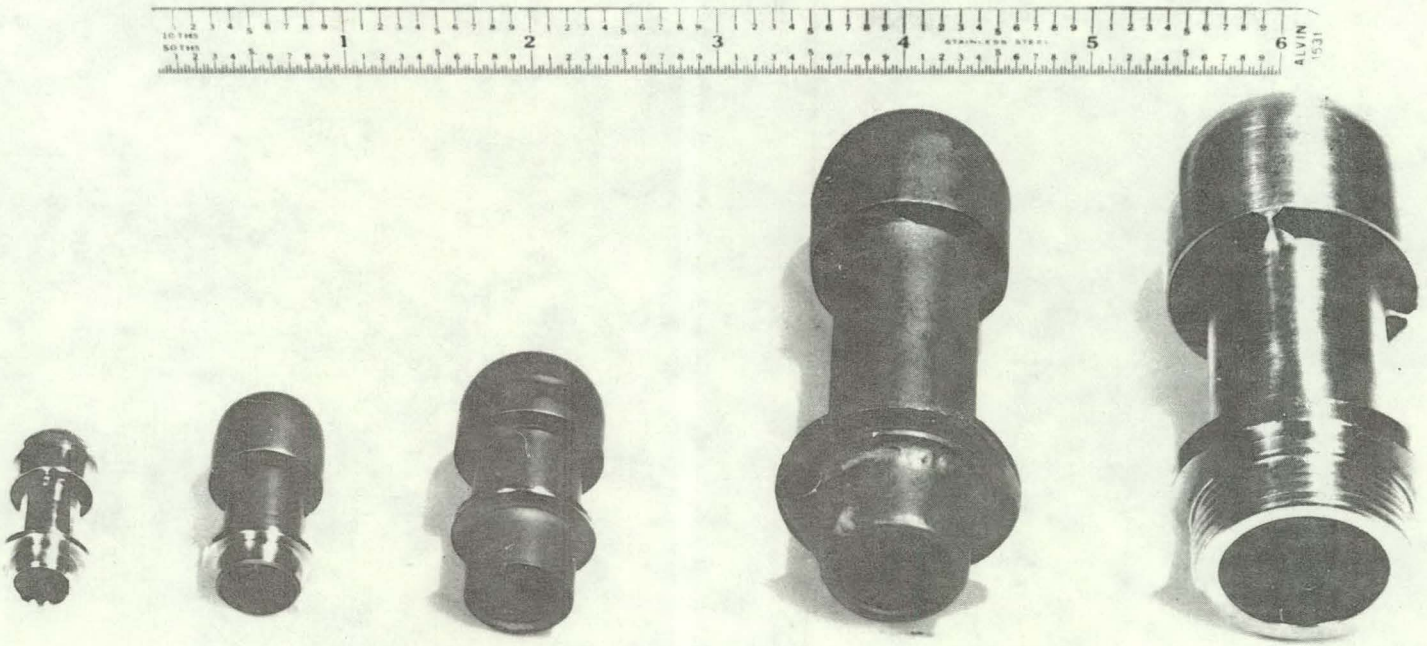

VAPORIZER TUBES

1. NUMBER BASED ON PRIMARY ZONE SIZING
2. SIZE FOR F/A = 0.25
3. L ~ 2.2H

   WHERE H = PRIMARY ZONE HEIGHT

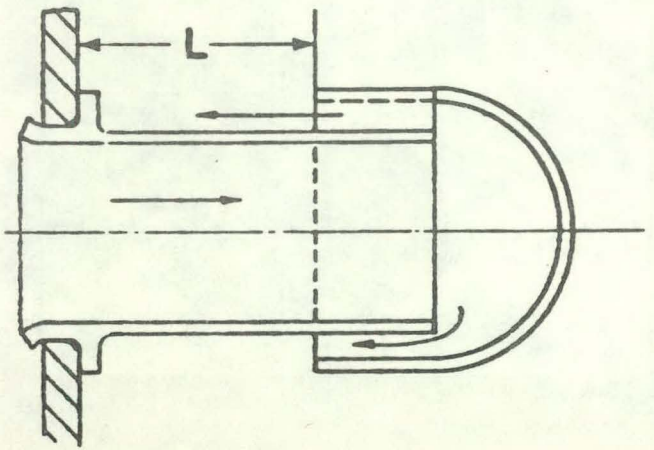

Figure 3.14

TSTR LIQUID FUEL COMBUSTOR VAPORIZER TUBE DESIGN

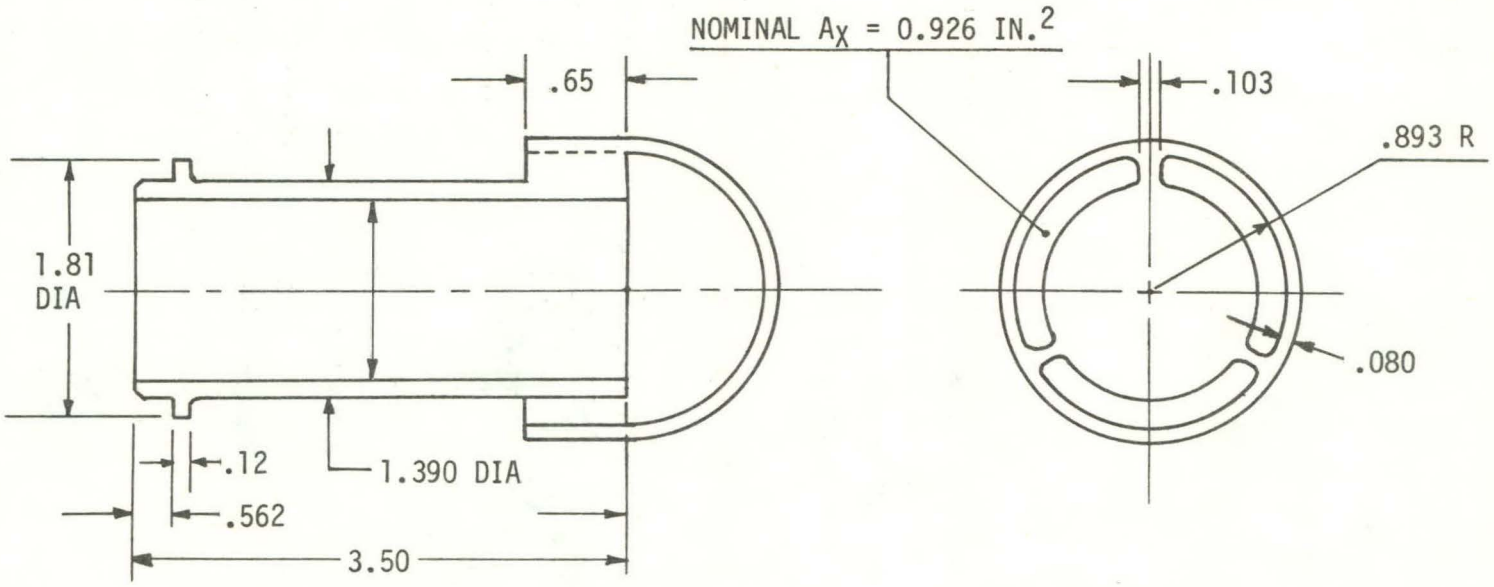

MATERIAL: HASTELLOY-X CAST.
AMS 5390

Figure 3.15

The TSTR fuel tube design shown in Figure 3.16 has a 0.1715 inch diameter bore resulting in a fluid jet velocity of approximately 16.4 FPS producing a jet break-up in the form of helicoidal waves characteristic of Region II of Figure 3.17.

3.7 RETRACTABLE PRIMER/IGNITER SYSTEM DESIGN

Combustor systems incorporating liquid fuel vaporizer tube injectors require a significant increase of heat energy to promote satisfactory fuel vaporization and subsequent ignition at conditions encountered during the critical engine start-up sequence. Torch primer/igniter system designs have been developed by Curtiss-Wright which have demonstrated reliable operation and durability for both aircraft and ground gas turbine installations. The general configuration consists of a small flow pressure atomizing fuel nozzle and a low energy spark ignition source in close proximity to the spray nozzle. Ignition of the fine fuel spray results in a substantial flame brush depending on the primer fuel flow. When directed at the combustor vaporizer tubes in the primary combustion zone the torch provides the necessary local heat for vaporization and ignition. Reliable ignition of the primer/igniter is assured by the fine spray nozzle and the resultant torch within the combustor minimizes late lights and residual fuel burn-outs during the critical engine start-up sequence. To ensure high reliability and durability the primer/igniter assembly has been designed with a retractable feature which removes the igniter tip from the burner once combustion has been verified.

A cross-section of the TSTR retractable primer/igniter design is shown in Figure 3.18 and a photograph in Figure 3.19. The primer/igniter is extended into the combustor by applying air pressure at 80-90 psig to the effective area of a piston rod enclosed in stationary cylinder depressing the piston and compressing the piston spring. Special elongated igniters and fuel spray nozzles are fitted in the movable piston through rifle bores drilled to precision tolerances. Retraction is effected by venting the pressurizing air and permitting the compressed spring and air pressure to return the piston to the storage position.

TSTR LIQUID FUEL COMBUSTOR FUEL INJECTOR DESIGN

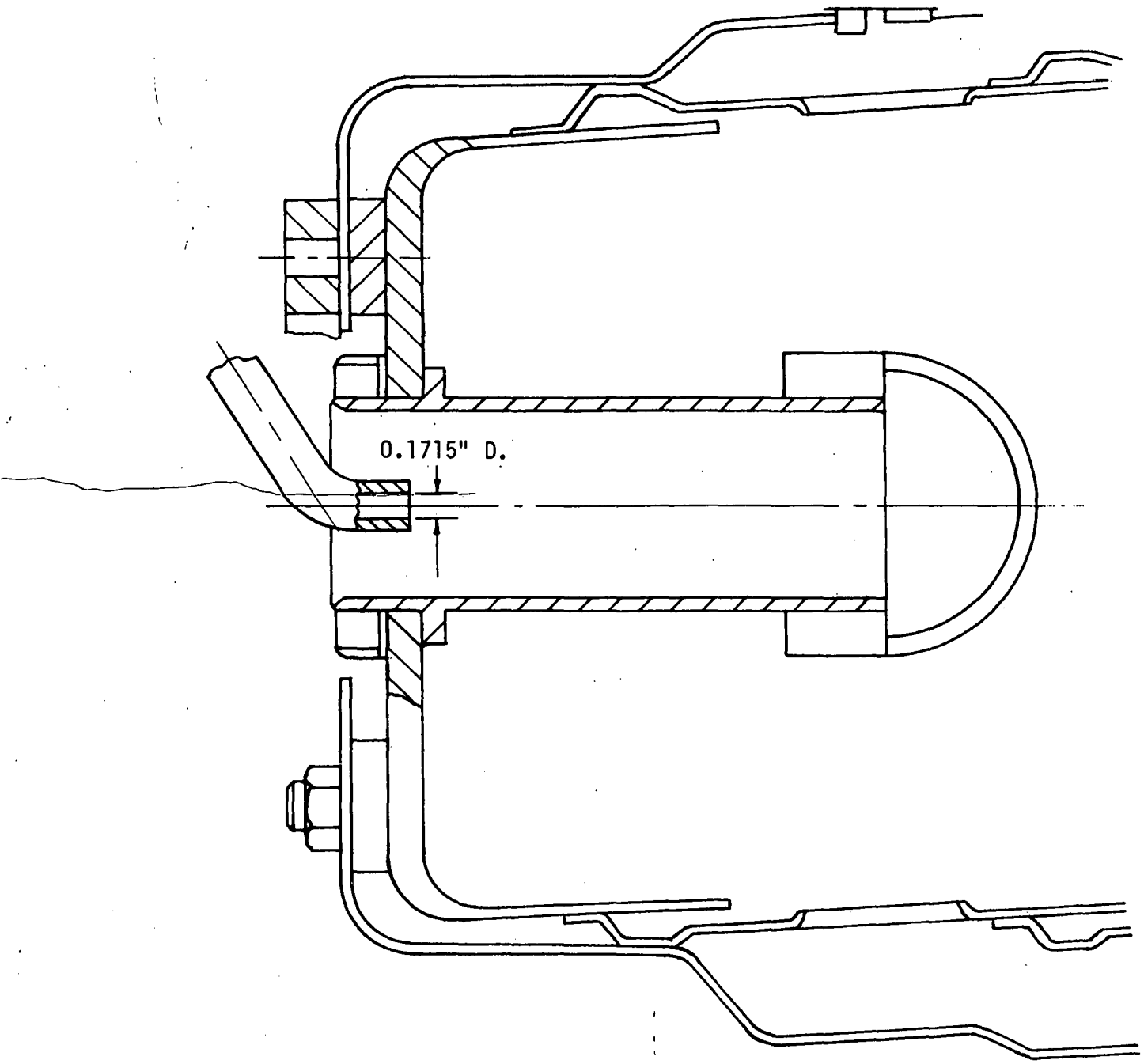

Figure 3.16

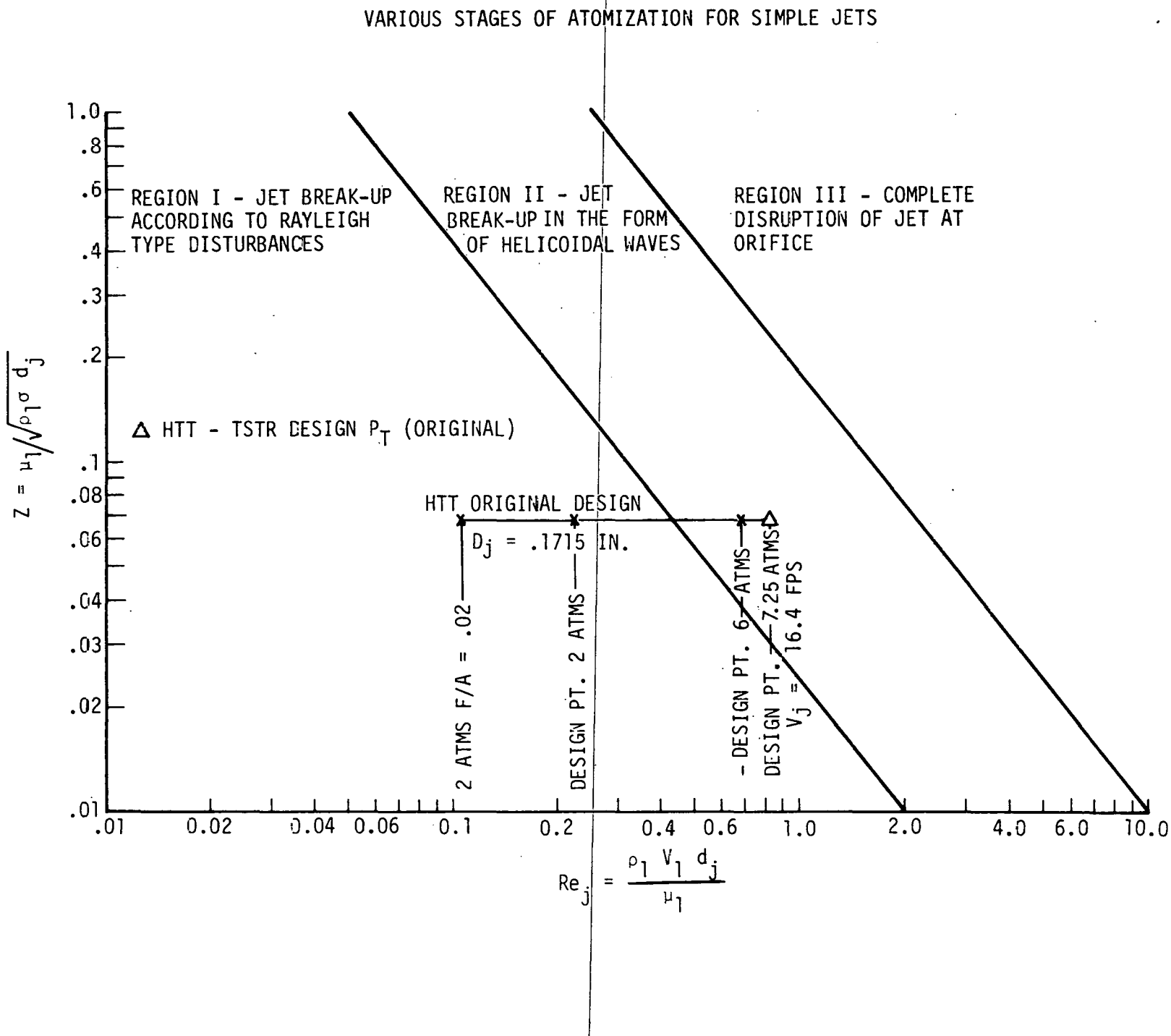
VARIOUS STAGES OF ATOMIZATION FOR SIMPLE JETS
REGION I - JET BREAK-UP ACCORDING TO RAYLEIGH TYPE DISTURBANCES
REGION II - JET BREAK-UP IN THE FORM OF HELICOIDAL WAVES
REGION III - COMPLETE DISRUPTION OF JET AT ORIFICE
Δ HTT - TSTR DESIGN P_T (ORIGINAL)
HTT ORIGINAL DESIGN
D_j = .1715 IN.
2 ATMS F/A = .02
DESIGN PT. 2 ATMS
DESIGN PT. 6 ATMS
DESIGN PT. 7.25 ATMS
V_j = 16.4 FPS
$\frac{f_p \rho_l d_j}{\sqrt{\mu_l}} = Z$
$Re_j = \frac{\rho_l V_l d_j}{\mu_l}$
1.0
.8
.6
.4
.3
.2
.1
.08
.06
.04
.03
.02
.01
.01
0.02
0.04
0.06
0.1
0.2
0.4
0.6
1.0
2.0
4.0
6.0
10.0

Figure 3.17

TSTR RETRACTABLE PRIMER/IGNITER
CROSS-SECTION VIEW

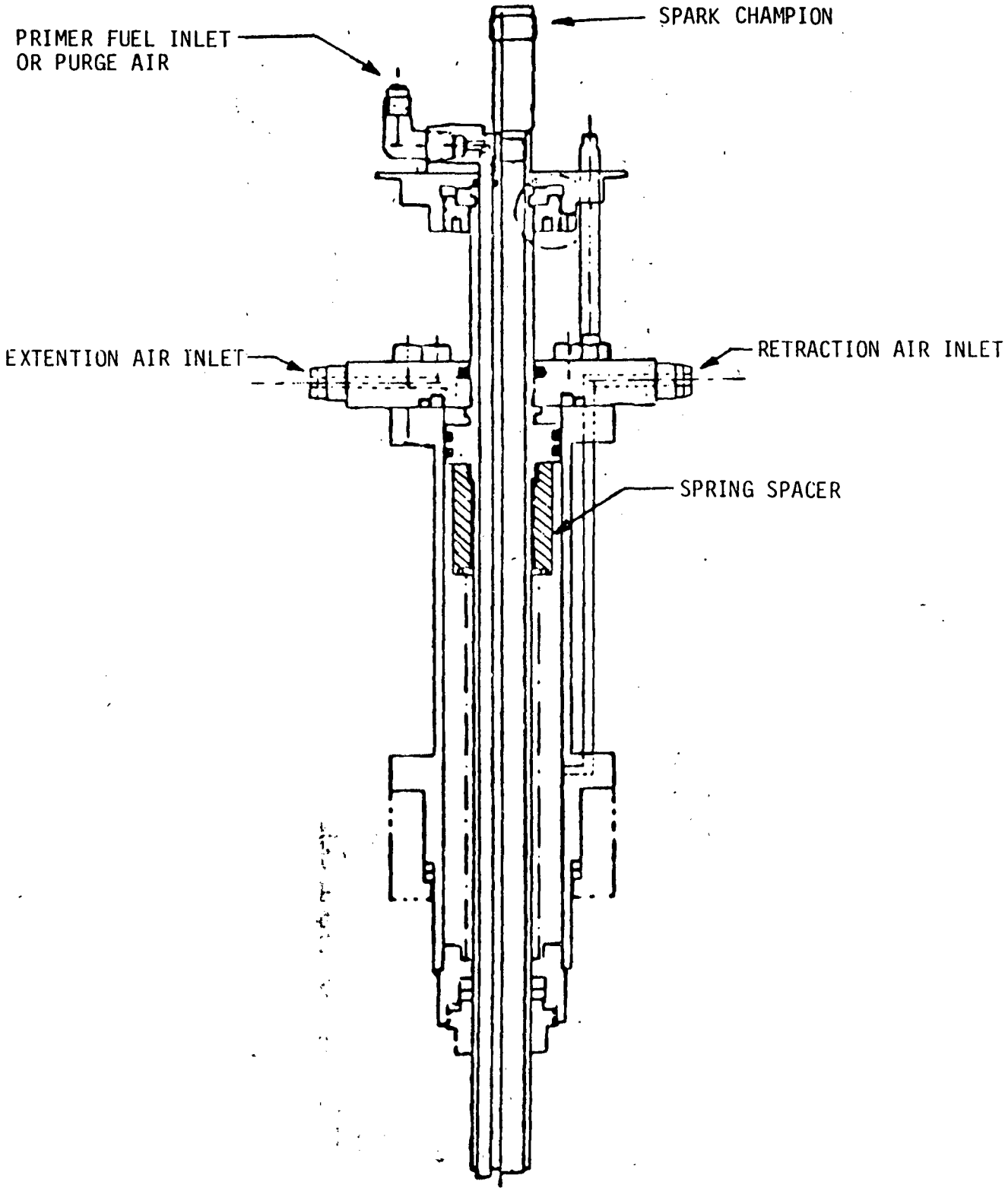

Figure 3.18

81-198

TSTR RETRACTABLE PRIMER/IGNITER ASSEMBLY

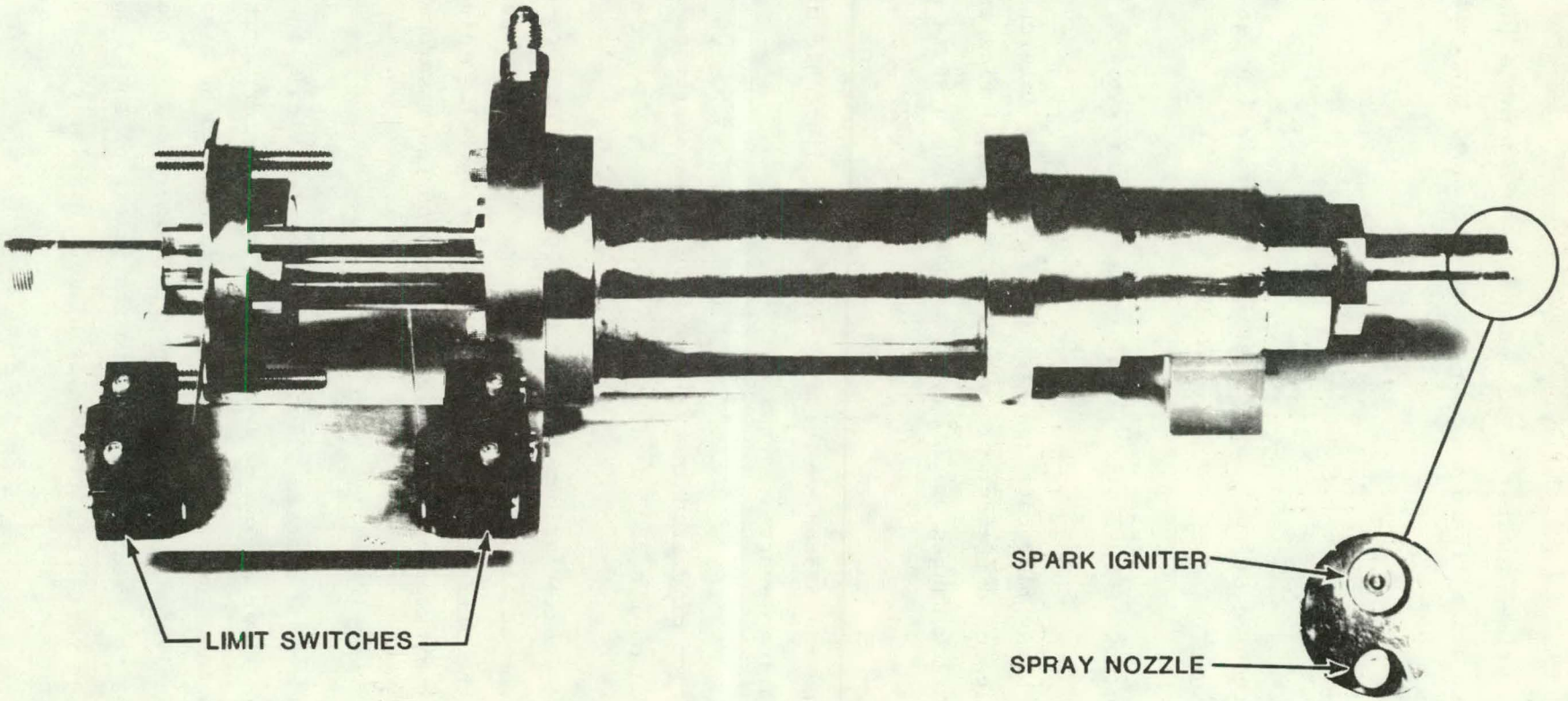

Figure 3.19

The retractable primer/igniter is designed for considerable installation flexibility. This is accomplished through incorporation of the following adjustments:

1. Extension Length - 2.2 inches maximum

2. Penetration of fuel spray nozzle relative to igniter - 0.25 inches maximum.

3. Direction of fuel spray relative to igniter - $\pm$ 45° arcs.

4. Fuel spray flow rate and atomization - Three interchangeable spray nozzles of different pressure flow characteristics were fabricated with flow ranges of 50 pph at 65 psid; 35 pph at 70 psid; and 20 pph at 30 psid.

5. Piston rod piston position indication - Adjustable microswitch actuating levers are provided.

6. Rotation of Piston in cylinder bore - Six positions at various areas cover a 360° periphery.

The retractable igniter/primer is mounted on the combustor case such that its extended position at light-off causes the spray nozzle and spark igniter to protrude into the primary combustion zone (Figure 3.20). This zone is downstream of the combustor headplate, which supports the mushroom type vaporizer tubes.

Figure 3.21 is a flow diagram illustrating the electrical, fuel, and air services, and associated equipment for three of the six retractable primer/igniters of the TSTR engine. As shown, each igniter is excited by a separate ignition box which is activated by the Data Center. Primer fuel is admitted through solenoid valves to a manifold common to the inlets of the 3 spray nozzles. Instrument air for radial positioning is divided similarly to the 3 piston rods.

TSTR COMBUSTOR - IGNITER RELATIONSHIP

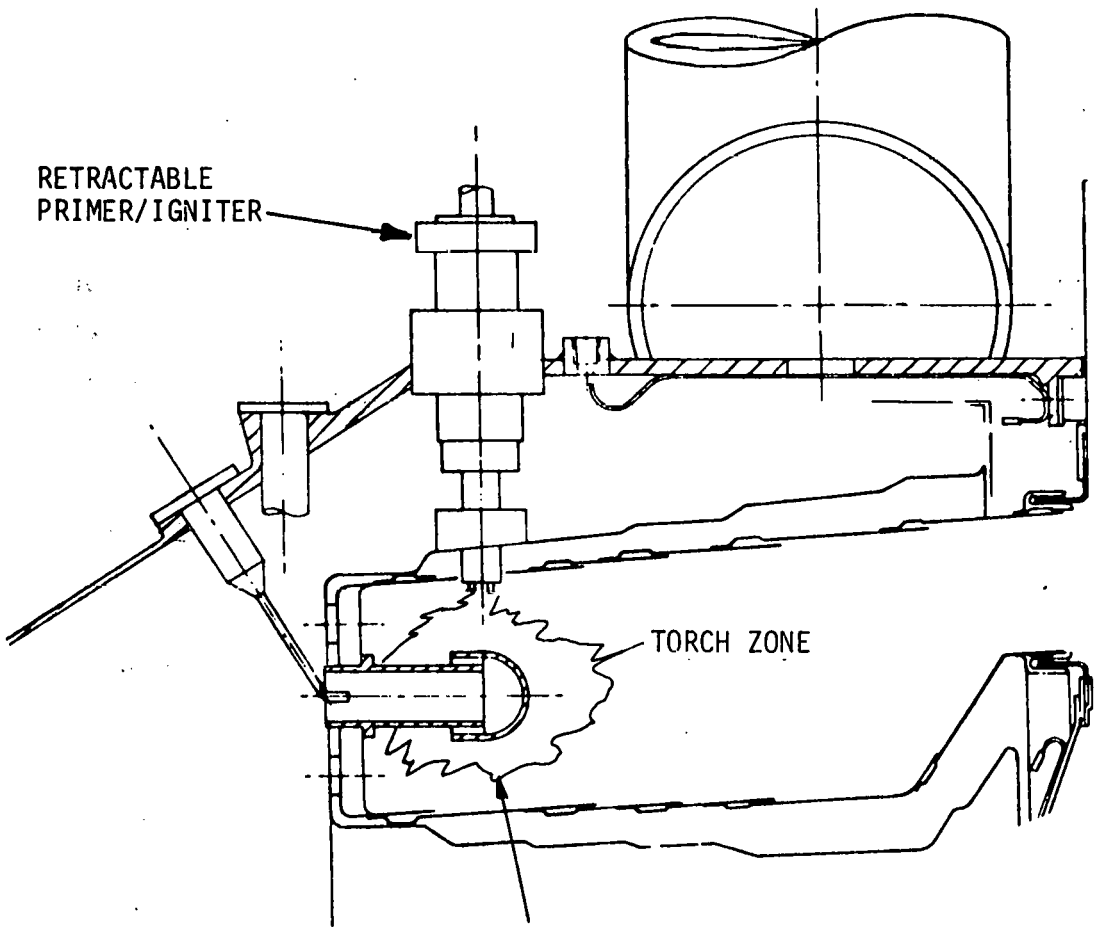

Figure 3.20

TSTR RETRACTABLE PRIMER/IGNITER WIRING
AND PNEUMATIC SYSTEMS

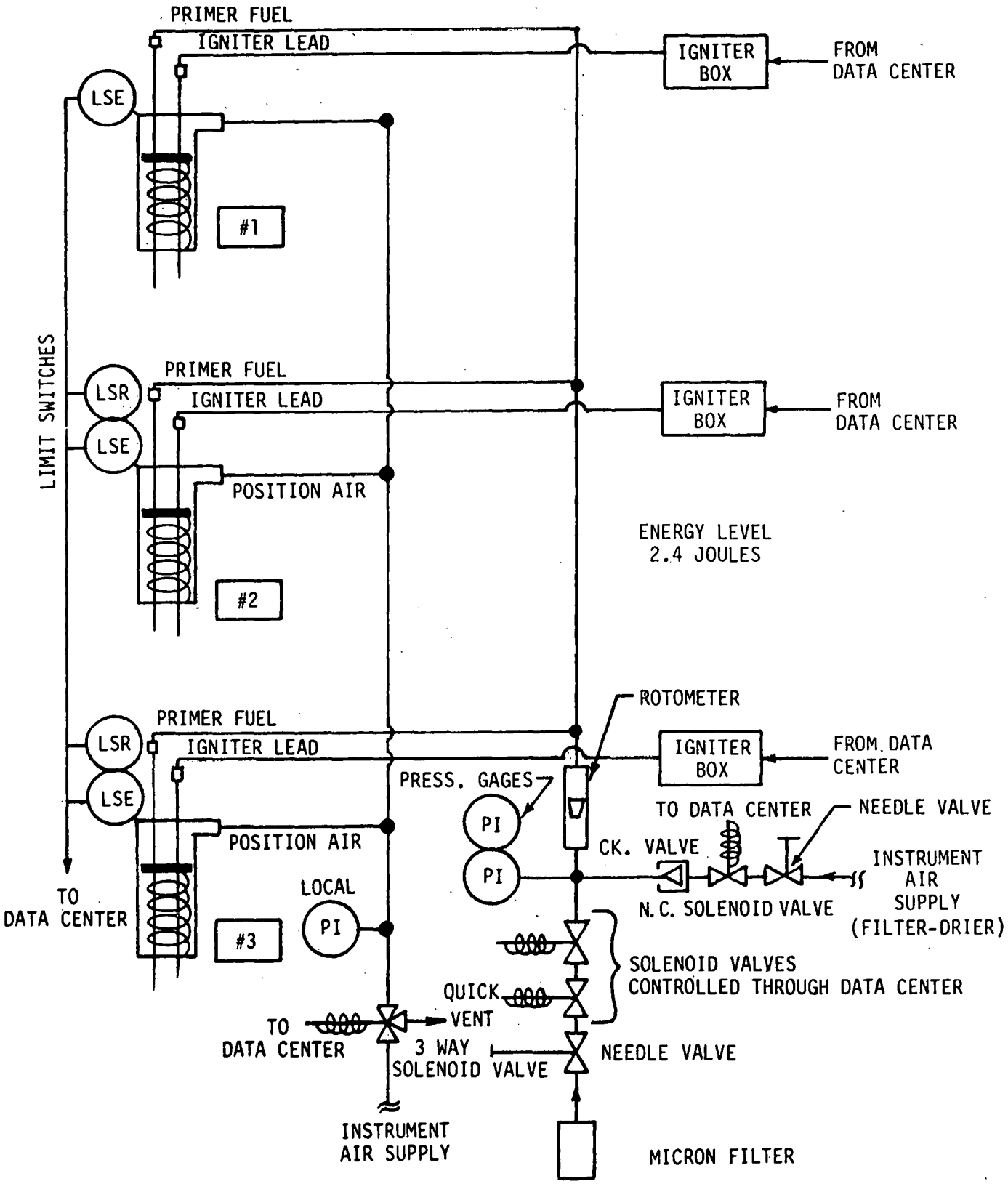

Figure 3.21

Instrument air is also used to purge fuel from the primer manifold following light-off and primer/igniter retraction. The Data Center sequences the various solenoid valves for functional control and displays fully extended fully retracted position feedback signals from the piston microswitches.

Section 4.0
COMBUSTOR FABRICATION

The combustor assembly for the TSTR consists of the headplate, inner liner, outer liner welded into one combustor assembly Figure 4.1. Complete assembly includes outer shroud, inner shroud and inner shroud extension (Figure 4.2).

Headplate assembly ES164641 includes 20 long and 40 short studs to support the inner and outer cooling shrouds. The headplate was machined fully from a flat plate of AMS 5536 Hastelloy X. Studs were machined fully from AMS 5754 bars, Hastelloy X and welded into the headplate (Figure 4.3, 4.4).

Combustor liner details were made from sheet stock. Cooling hole and combustion hole patterns were punched in the flat sheet form, then rolled and welded into a ring. Liner forms were produced on expansion dies for each detail. Cooling holes were punched in flat location since the size of cooling holes were not affected during forming. Weld expansion slots were performed after liner forming was completed. The primary airflow ports were pre-punched in a flat sheet and the plunged lips were die-extruded after forming the liners.

Inner liners 4 and 5, because of the complex rear design configuration were formed on dies. Liner 4 was fabricated in two (2) sections, 4A being conical cylinders and 4B a die formed part.

Rear supports were fabricated from rolled AMS 5754 (Hastelloy X) bar stock, welded and then fully machined.

The outer liner Figure 4.3 was made in one assembly. Liners and rear support were assembled and tach welded on a layout table to blueprint locations and then resistance welded.

TSTR ANNULAR LIQUID FUEL COMBUSTOR BASKET WITHOUT
COOLING SHROUDS (3/4 REAR VIEW)

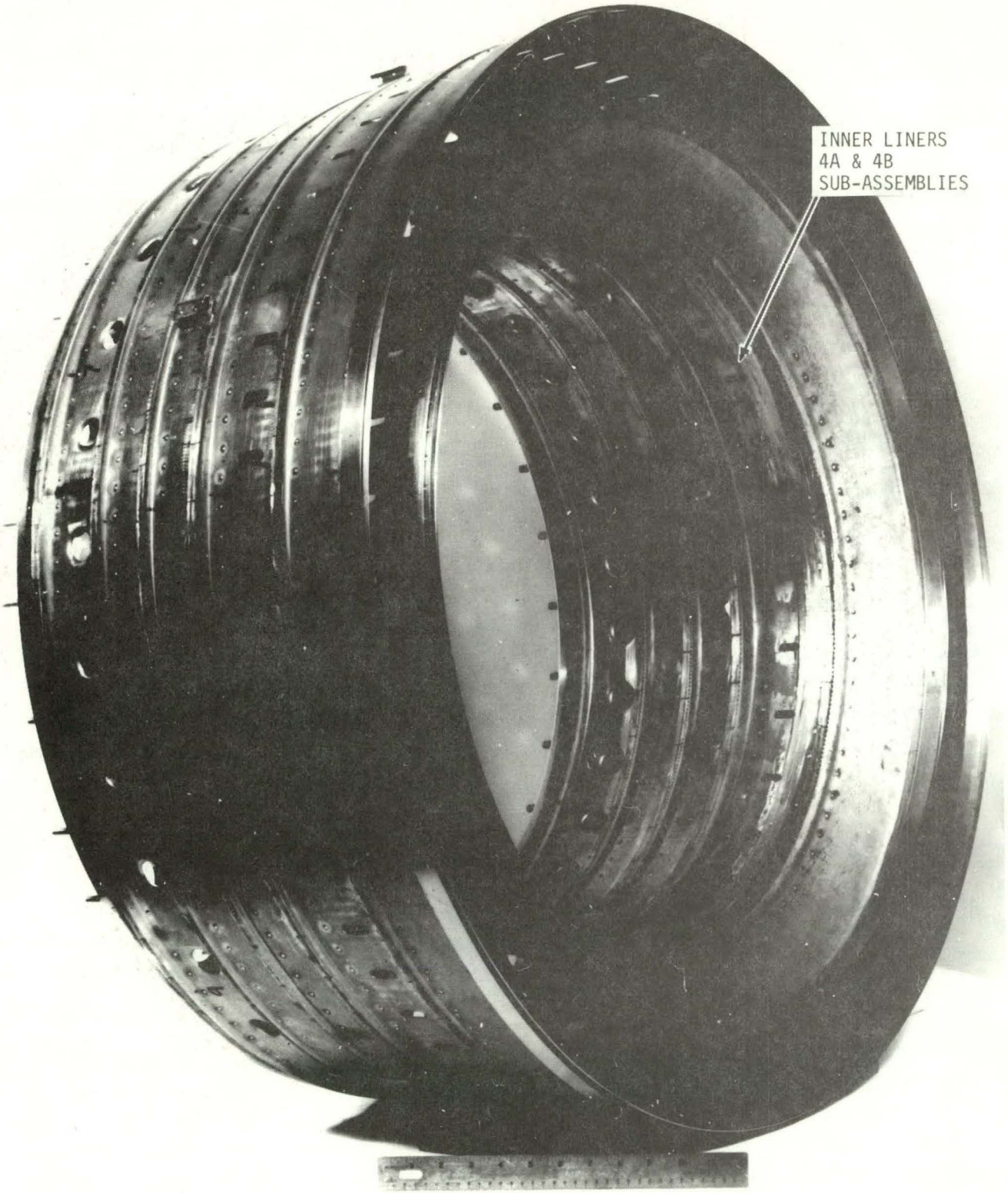

Figure 4.1

HTT-II-421A

TSTR ANNULAR LIQUID FUEL COMBUSTOR BASKET WITH COOLING SHROUDS INSTALLED (3/4 FRONT VIEW)

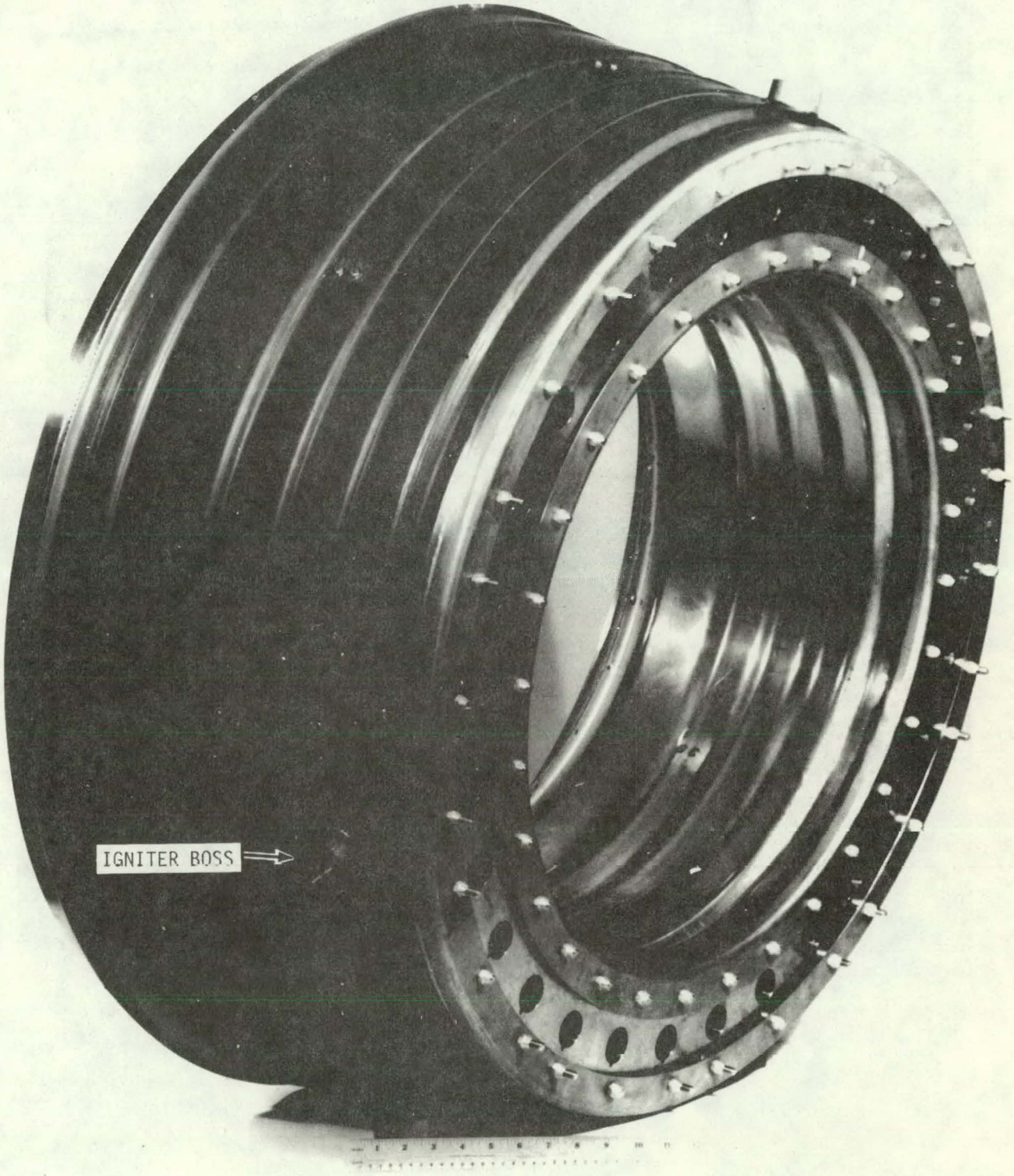

Figure 4.2

HTT-II-422A

TSTR COMBUSTOR OUTER LINER ASSEMBLY

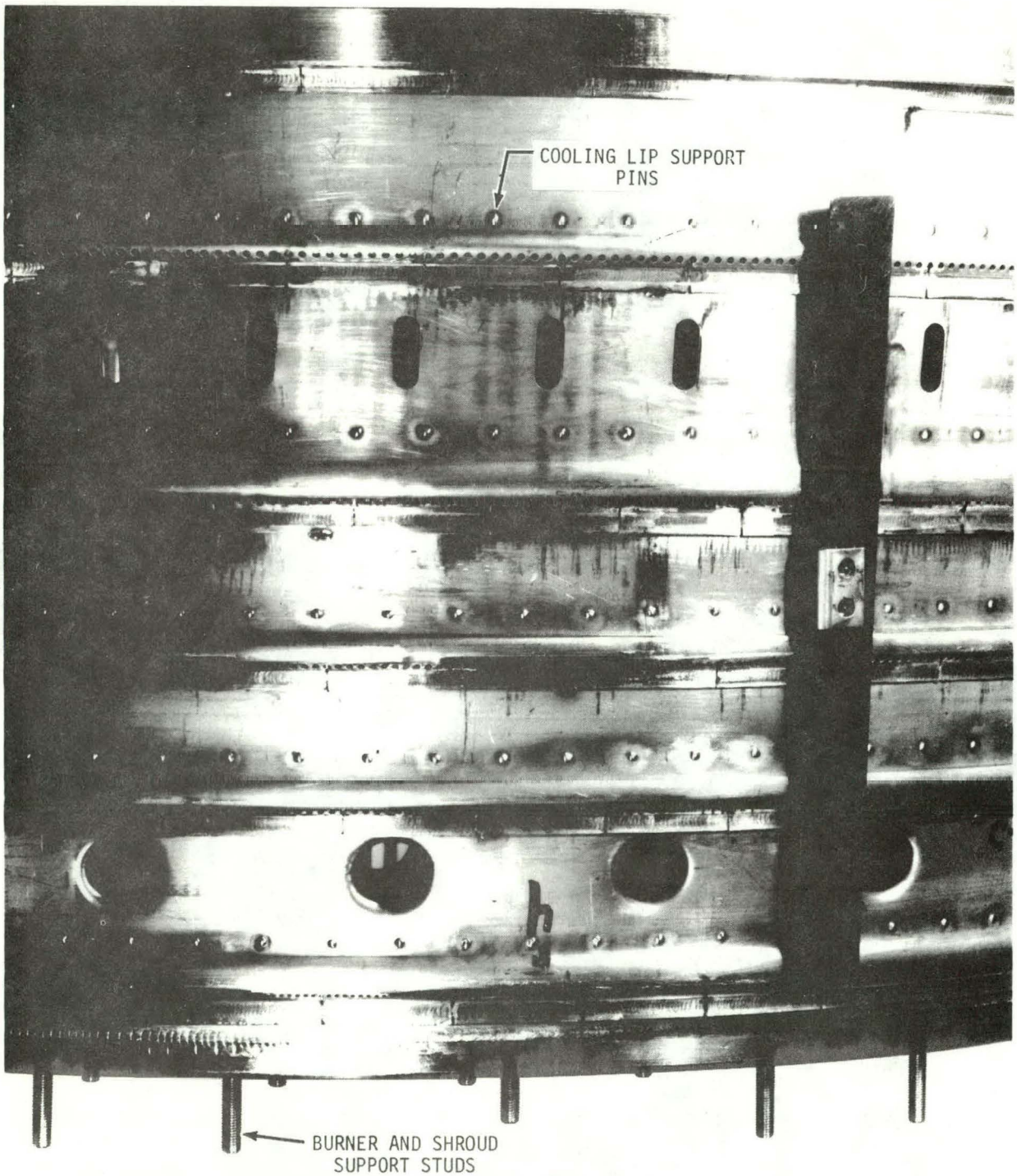

81-142

Figure 4.3

TSTR COMBUSTOR HEADPLATE ASSEMBLY

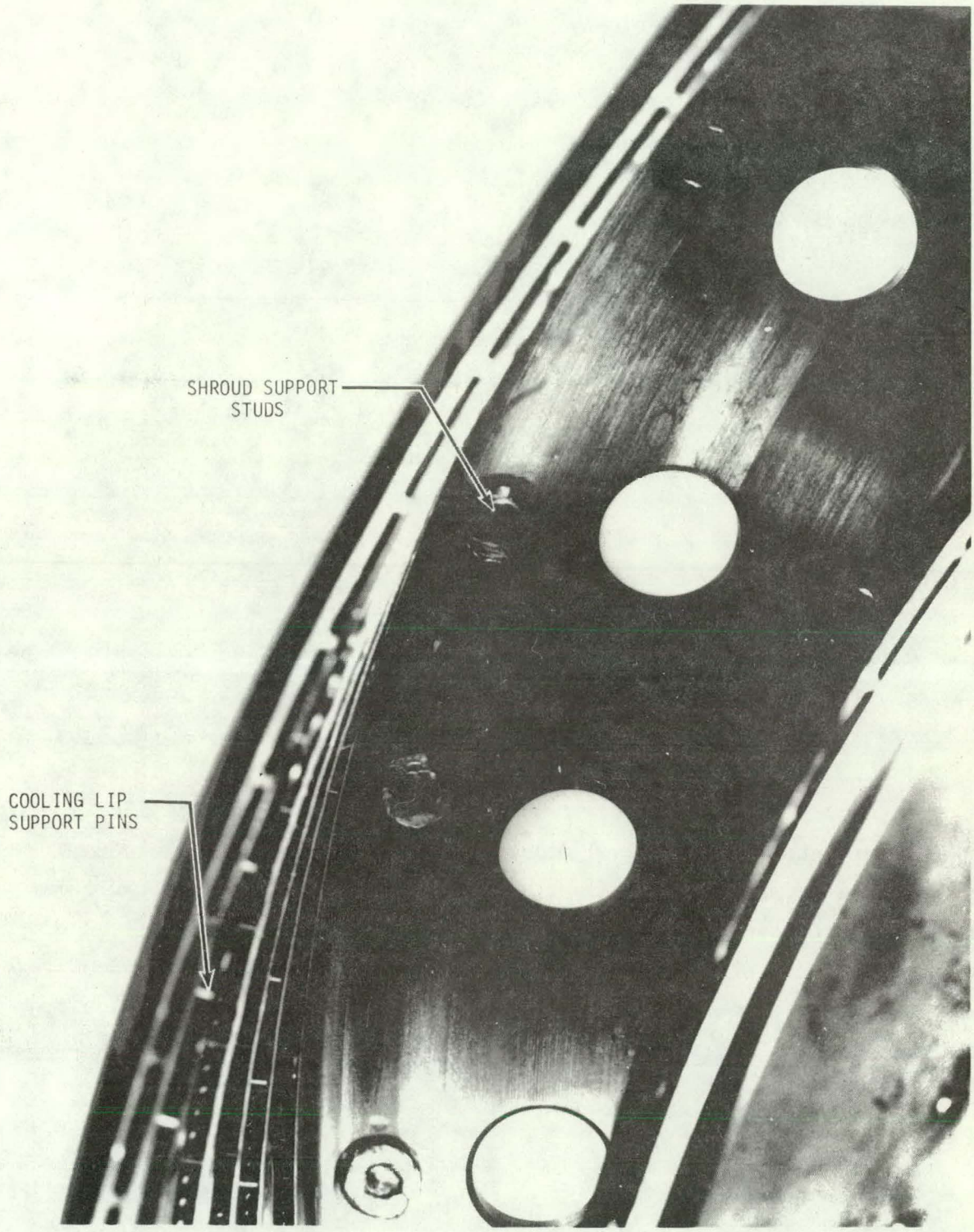

81-143

Figure 4.4

The inner liner was made in two subassemblies. The first assembly included liners 1 through 4A and headplate. The second assembly was accomplished on a universal fixture and included liners 4B, 5 and rear support. Fixturing was required in order to maintain concentricity of details 4B and 5.

All outer and inner liner weld assemblies were radiographically examined for acceptance upon completion of each weld.

Final assembly as shown in Figure 4.1 of inner liner subassemblies was performed on the same universal fixture used on details 4B and 5. Subassemblies were mounted on fixtures and located on the rear support groove while utilizing a centering plug on headplate liner. Weld joining details 4A and 4B was performed using manual TIG with gas back-up ring.

Basket assembly including headplate assembly, inner and outer liner assemblies was performed on the same universal fixture picking up the groove inside diameters on the rear supports and centering pins on I.D. of headplate. Back-up chills were used at the joint of headplate to headplate liner assembly. The weld was performed using manual TIG. Upon completion of all manual welds parts were zyglowed and then X-rayed.

The outer cooling shroud was manufactured from flat sheet welded into a cylinder and hydrospun on a cast iron mandrel. Attaching flange was also a spinning and weld to spun detail. Igniter bosses were machined from bar stock and welded into position. The inner shroud was fabricated from flat sheet rolled and welded into a cylinder and die-formed. The rear inner shroud extension is a die formed trimmed and outer bend formed on a bead roller. An upstream view of the completed combustor and shroud assembly is shown in Figure 4.5.

UPSTREAM VIEW OF TSTR COMBUSTOR
OUTER LINER

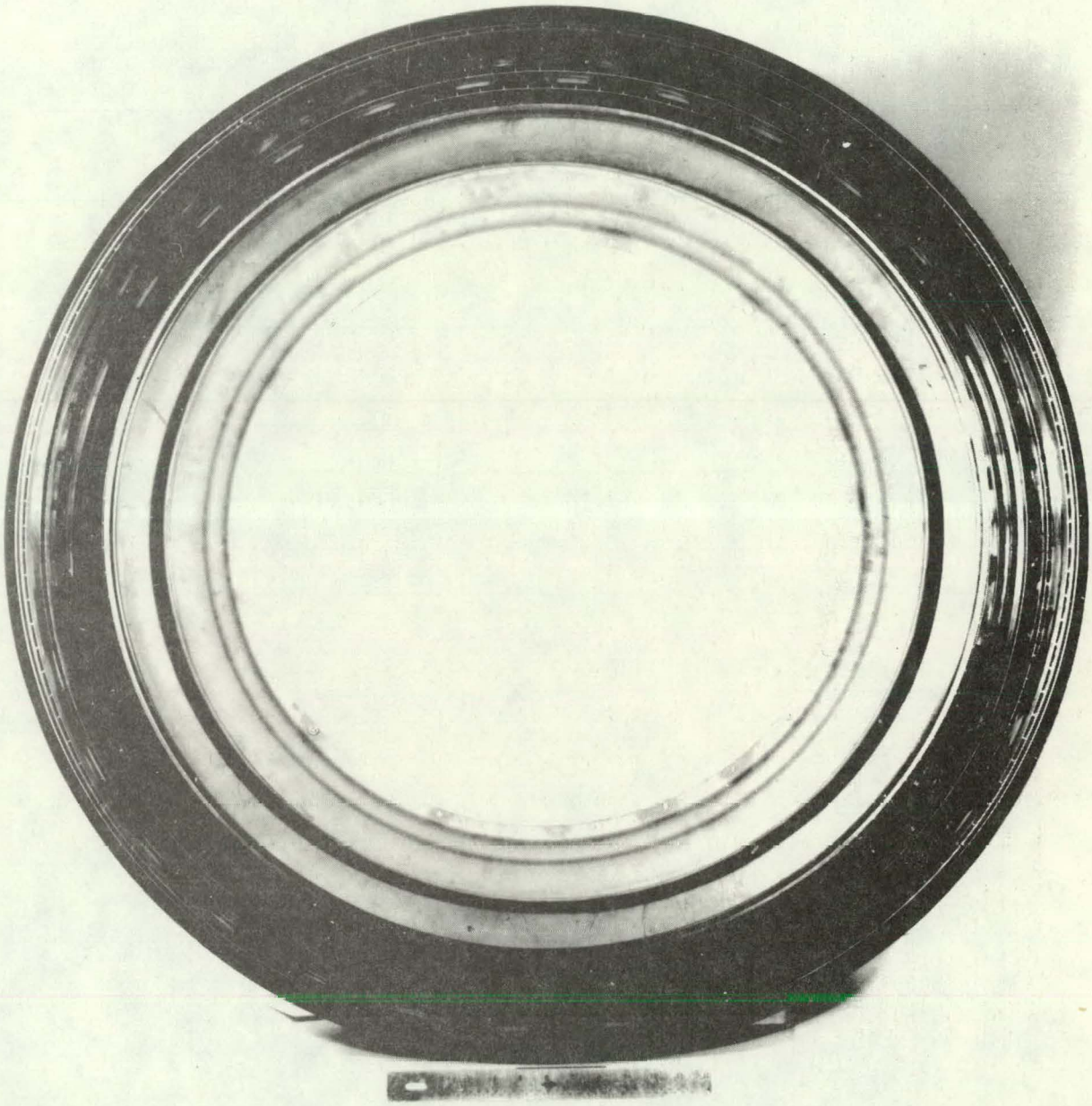

Figure 4.5

81-144

Section 5.0
COMBUSTOR TEST RIG AND TEST FACILITY

5.1 COMBUSTOR TEST RIG

A 60° test sector was selected as representative of the full annular TSTR combustor in terms of airflow and combustion processes thereby providing the vehicle with which to develop the burner configuration to meet the established goals of combustor exit temperature pattern and performance. The arrangement of the 60° sector test rig as shown in Figure 5.1 consists of a combustor section and an instrumentation probe section. The combustor sector is a true 60° arc of the full annular combustor as shown in Figure 5.2 and contains both inner and outer cooling shrouds. The sector (Figure 5.3) includes five vaporizer tubes, one primer/igniter assembly and provisions for a flame detector aperture. The 60° sector end walls are water cooled boxes coated with a thermal heat barrier on the hot side. Appropriate flanges and sheet metal seals are attached to the 60° combustor sector end wall edges for positioning and to prevent air leakage by the water end plates are shown in Figures 5.3 and 5.4. A cross-section of the water side plate design (Figure 5.5) shows a multitude of 1/2 inch wide by 1/8 inch high passages through which cooling water is passed at about 8 FPS, maintaining a maximum metal temperature of approximately 600°F at combustor design operating conditions. The test rig also includes a 60° section of the TSTR diffuser section with a bellmouth inlet as well as the inner and outer burner cover cases as shown in Figure 5.6. In addition, provisions to simulate both internal turbine cooling air bleed and overboard bleed from the burner section have been incorporated. As shown in Figures 5.7 and 5.8 the 60° sector assembly is mounted in a cylindrical pressure vessel 32 inches in diameter with a service capability of 6 atmospheres.

The exhaust duct and sweep probe section is fastened to the plate at the aft end of the combustor rig housing. This section (Figure 5.9) consists of a pressure vessel (48 inches in diameter, 3/8 inches wall-thickness) containing a short, film-cooled exhaust duct mounted directly downstream of the combustor exit station.

LIQUID FUEL TSTR 60° COMBUSTOR SECTOR RIG

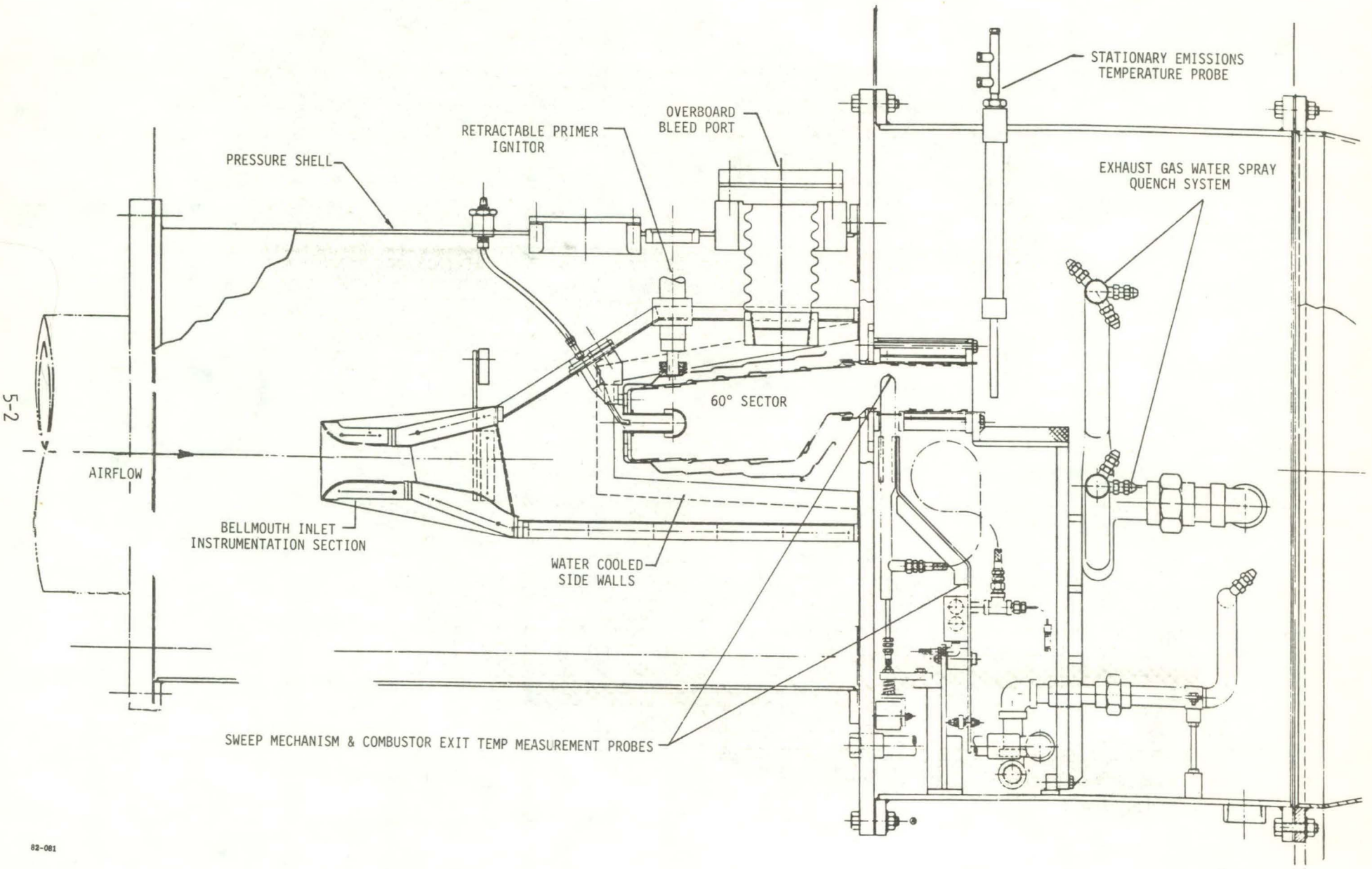

82-081

Figure 5.1

TSTR LIQUID FUELED 60° COMBUSTOR SECTOR

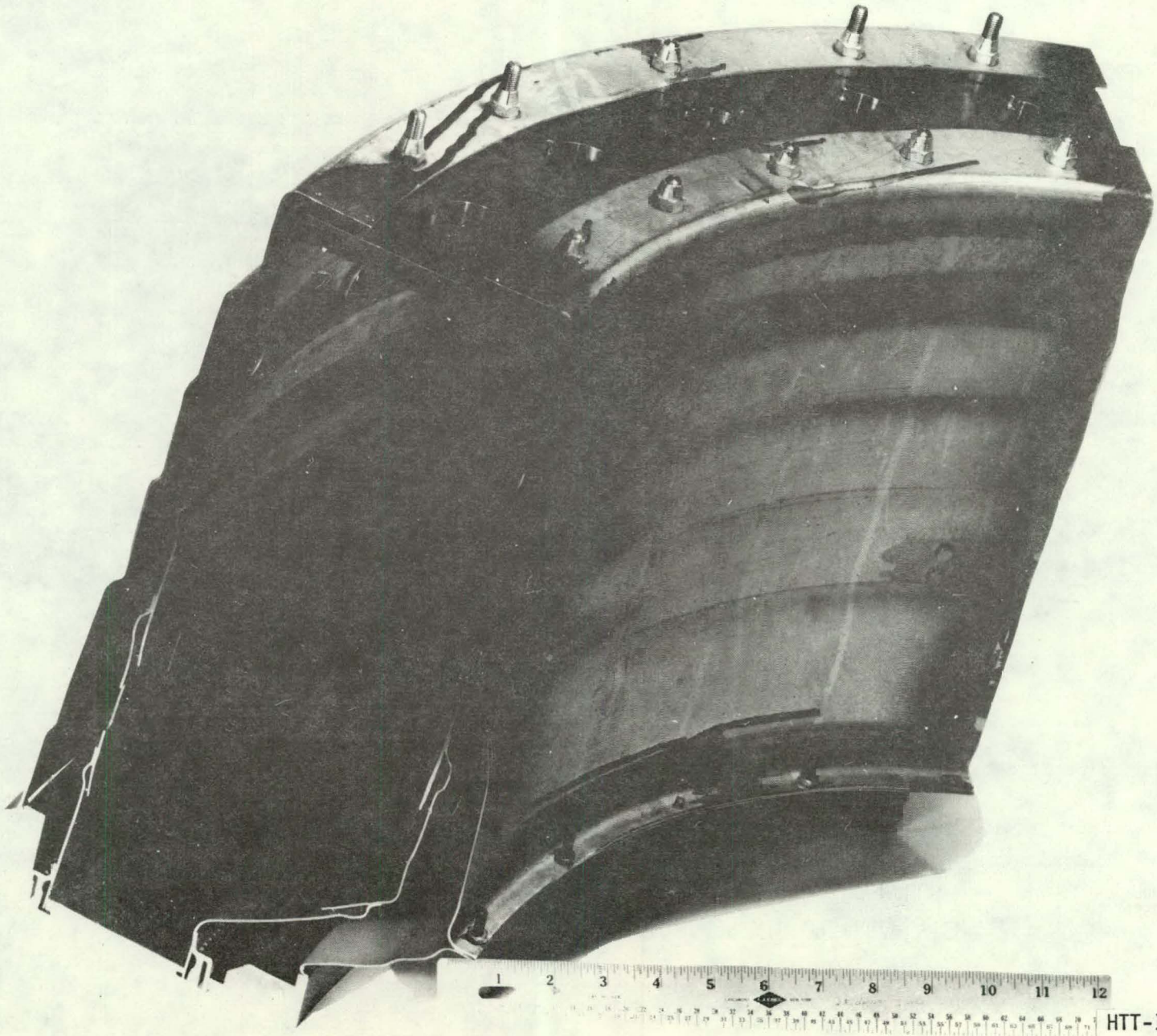

Figure 5.2
5-3

TSTR 60° SECTOR LIQUID FUEL COMBUSTOR RIG UPSTREAM VIEW
SHOWING VAPORIZER TUBES AND WATER COOLED SIDE WALLS

HTT-II-429A

Figure 5.3

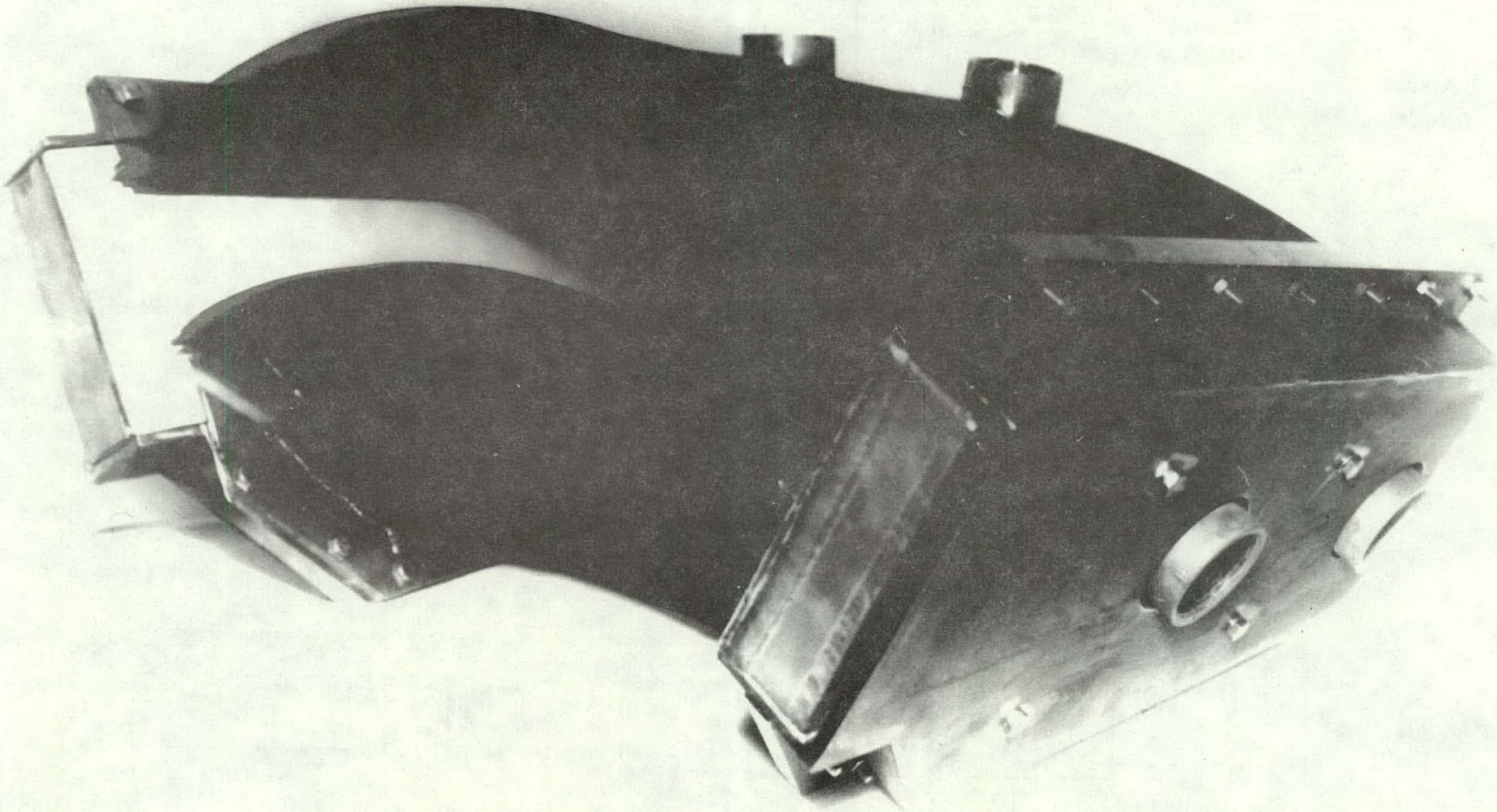

TSTR 60° SECTOR LIQUID FUEL COMBUSTOR RIG WITH WATER COOLED SIDE WALLS (3/4 REAR VIEW)

HTT-II-428

Figure 5.4

TSTR 60° SECTOR LIQUID FUEL COMBUSTOR TEST RIG

WATER COOLED SIDE PLATE

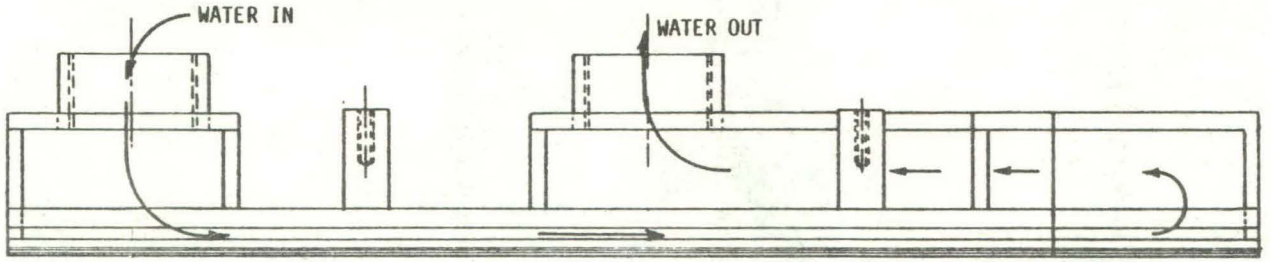

THERMAL BARRIER COATING (THERMAL CONDUCTIVITY 12 Btu-IN/HR-FT^2-°F)

LAYER	MATERIAL	THICKNESS
1	METCO P-443-10	(.003/.005)
2	75% METCO P-443/25% METCO 202NS MIX	(.005/.007)
3	50% METCO P-443/50% METCO 202NS MIX	(.005/.007)
4	75% METCO P-443/75% METCO 202NS MIX	(.005/.007)
5	METCO 202NS	(.030/.050)

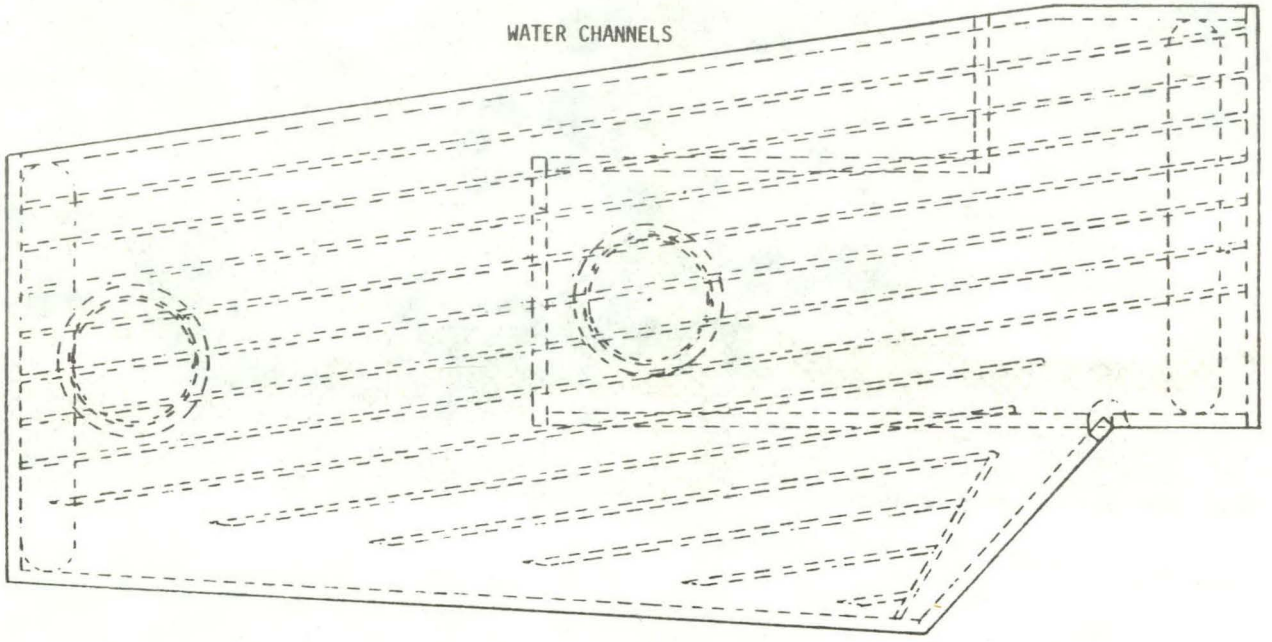

Figure 5.5

TSTR LIQUID FUELED 60° COMBUSTOR SECTOR RIG PRIOR TO INSERTION
WITHIN THE TEST STAND PRESSURE VESSEL

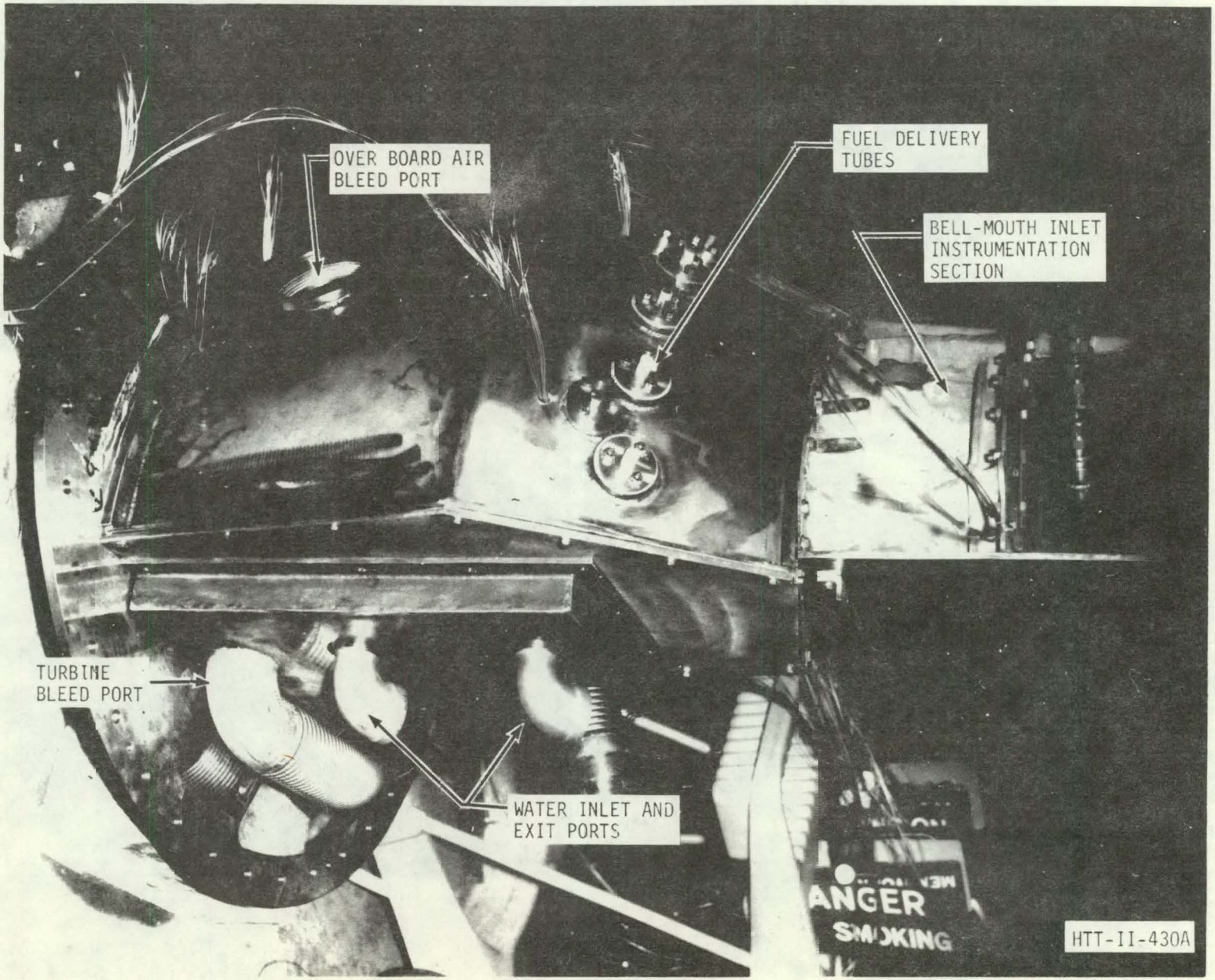

Figure 5.6

TSTR 60° SECTOR LIQUID FUEL COMBUSTOR RIG. DOWN STREAM VIEW
OF RIG INSTALLATION WITHIN THE TEST STAND PRESSURE VESSEL

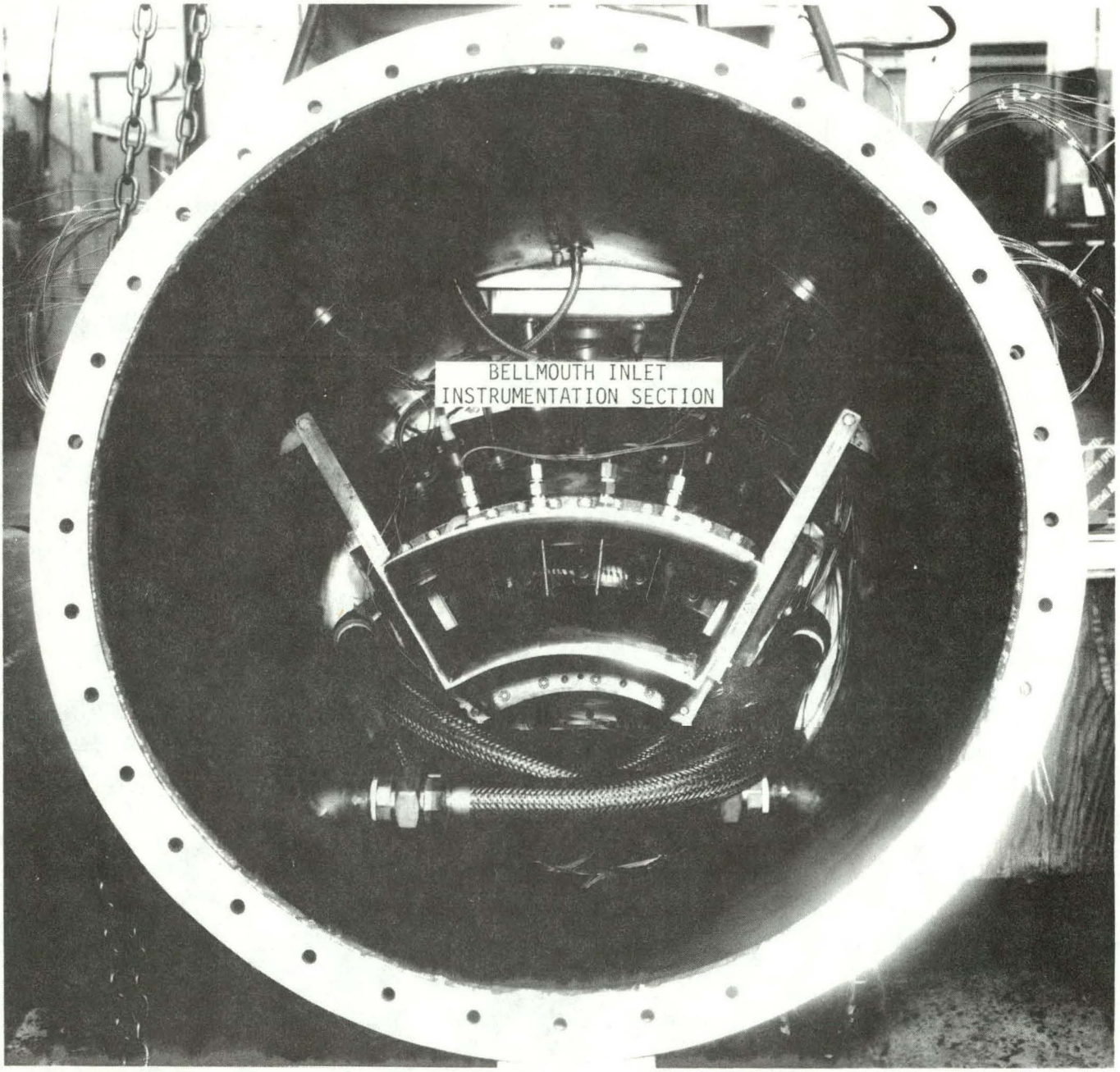

Figure 5.7

HTT-II-432A

80-174

TSTR LIQUID-FUELED 60° COMBUSTOR SECTOR RIG - REAR VIEW
OF RIG INSTALLATION WITHIN THE PRESSURE VESSEL

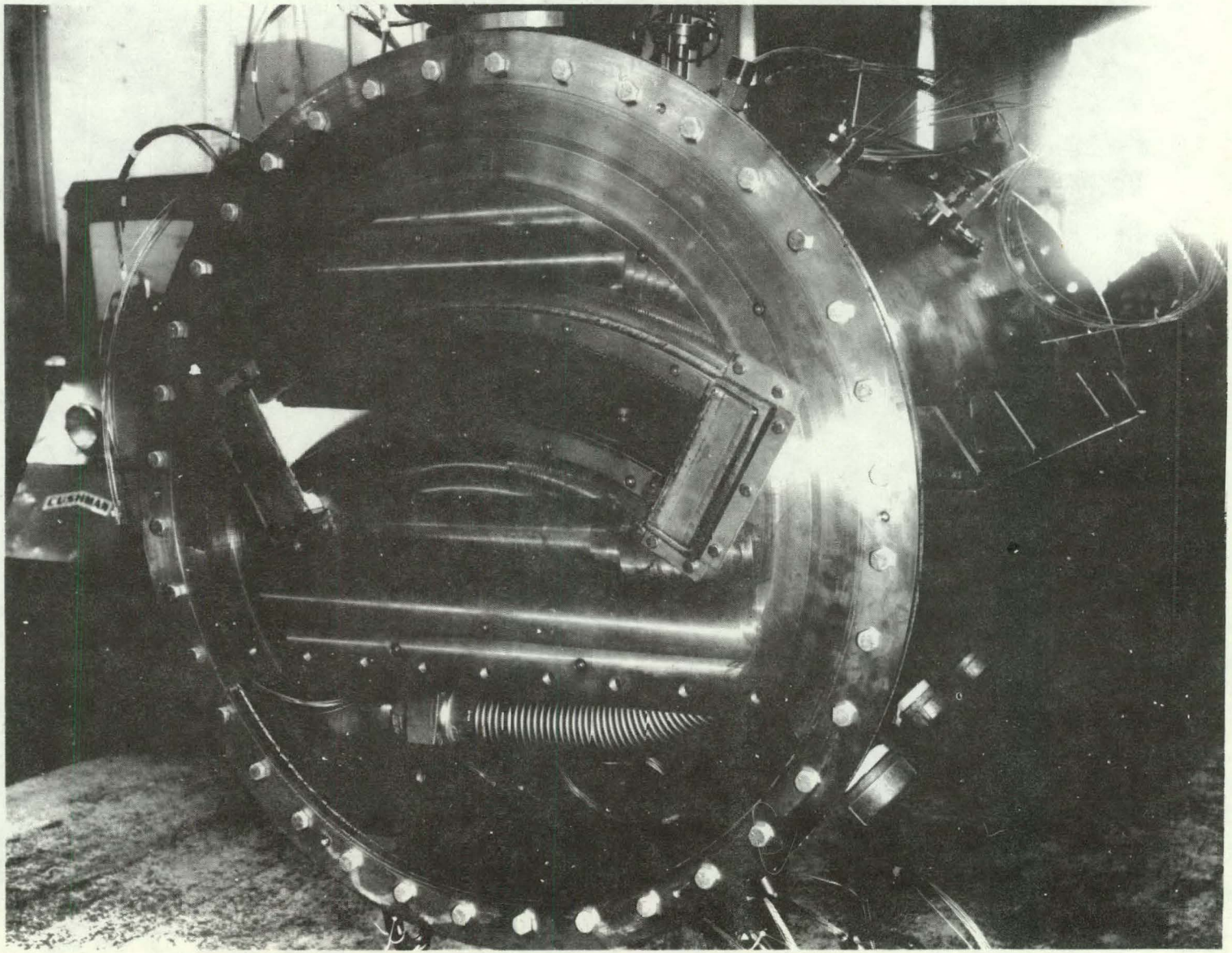

Figure 5.8

TSTR 60° COMBUSTOR SECTOR EXIT
SWEEP PROBE ASSEMBLY

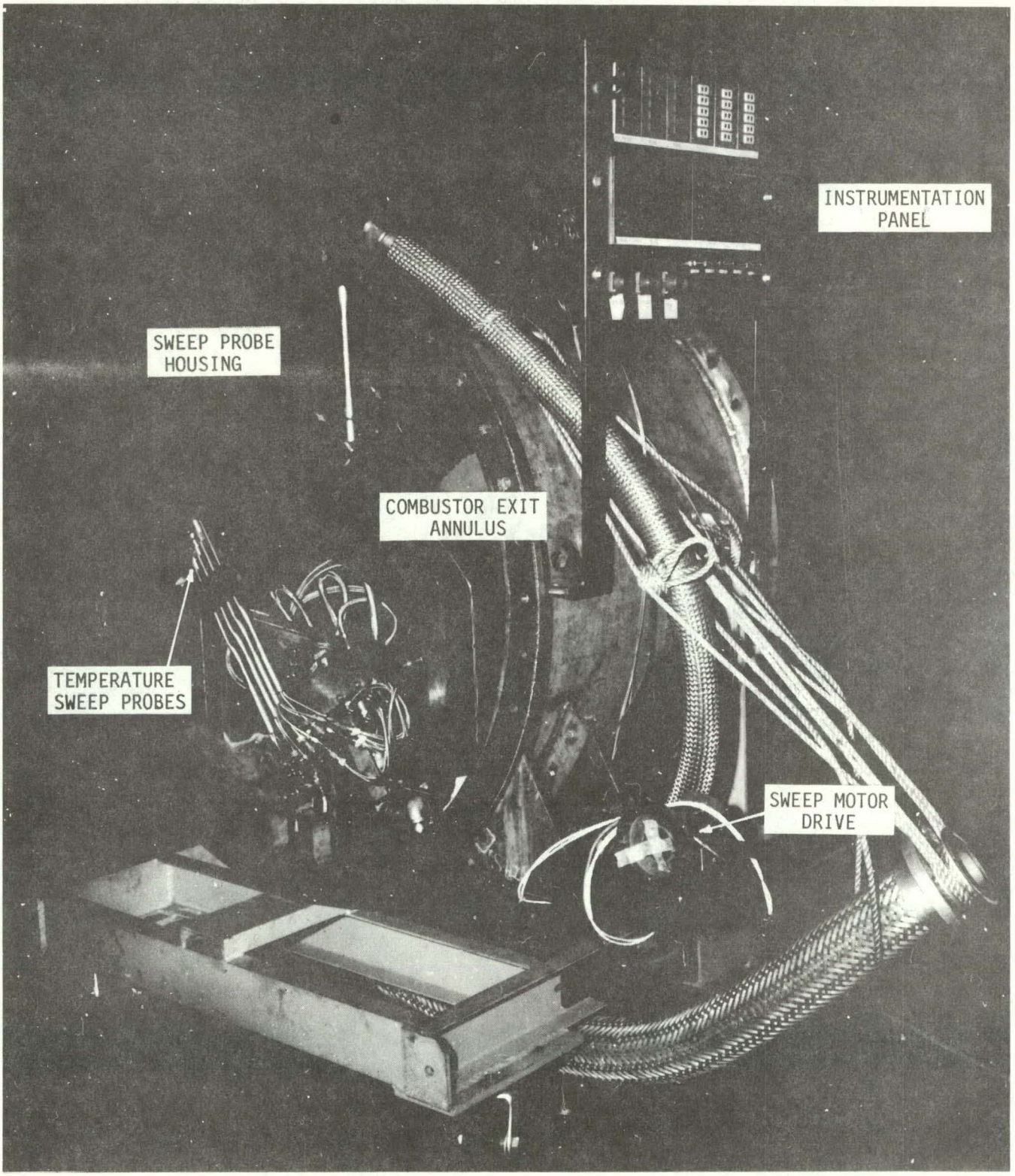

Figure 5.9

80-258

A water-spray manifold is positioned around and downstream of the exhaust duct to spray and cool the hot gas stream ahead of the test cell exhaust ducting, back-pressure valve and silencer. The previously-described combustor exit sweep probe assembly is pivoted in an enclosure within the instrumentation section housing. The enclosure provides protection for the electrical leads and pivot mechanism from the hot gas stream. The probe assembly traverses the combustor sector exit at approximately 0.5 ips and can be stopped at any position. The approximate time for a complete continuous sweep is 30 seconds. The drive is an externally mounted electric motor. The angular position of the probe assembly is indicated by a remote sensing instrument.

The probe sweep assembly consists of four water-cooled thermocouple units set at defined radial heights commensurate with equal annulus areas. An accurate profile of the entire combustor exit can be mapped in this manner. To lengthen the life of the thermocouples operating in the high temperature gas, the system is designed to move completely out of the gas stream when no data is being taken. A thin flexible metal band attached to the probe assembly and moving circumferentially with it seals the probe pivot mechanism and electrical leads from the hot gas stream. To assure protection of the mechanism, the enclosure is pressurized by facility air to a level higher than that of the hot gas stream, with a small controlled leakage of cool air across the seal from the enclosure into the hot gas stream. Water for cooling the probes is supplied via flexible hoses in the enclosure and is discharged into the exhaust housing. A gas sampling probe, also water-cooled, is inserted through the exhaust housing and is positioned at the mid-point of the combustor exit annulus.

The individual components of the test rig were analyzed for structural integrity, using a finite-element computer program and published analytical procedures (ASME Codes). Results of the stress analysis are presented in Table 5-1 based on a 90 psi design pressure differential. The material of all components is stainless steel AISI 321 while the bolting material is A-286.

Table 5-1

TSTR COMBUSTOR SECTOR RIG STRESS ANALYSIS SUMMARY

Component	Pressure (psi)	Maximum Stress (psi)	Allowable Stress (psi)
Combustor Vessel	90	17,560	22,000
Probe Vessel	90	17,390	22,000
Pivot Enclosure	90*		
Back Plate		25,700	30,000
Lower Flange		20,270	30,000
Plate Ring Weld		5,400	15,000
Bolts (Bottom)		86,730	90,000
Bolts (Top)		77,830	90,000
Plate, Vessel	50*	27,300	30,000
Exhaust Duct Flange Weld	90	11,466	13,450

*This pressure is effective only during initial pressurization of enclosure.

5.2 COMBUSTOR TEST FACILITIES AND INSTRUMENTATION

Test Facility General Description

All combustor rig air requirements are provided by the facility air supply. Primary combustor air is filtered to 10 microns and passes through an indirect fired heater before entering the rig. Airflow measurement is accomplished downstream of the heater. Inlet and differential pressures are sensed sequentially by a multi-input scanivalve pressure transducer and transmitted to the data center for data recording and calculation. Control of airflow to the combustor rig is accomplished by an eight-inch (coarse) and a three-inch (fine) adjustment valve, each being positioned from the control room, Figure 5.10, by separate remote pneumatic loading stations. Primary combustor air system capabilities are as follows:

Light-Off Air Flow	0.25 PPS
Controlled Air Flow/Temperature Range	1.5 to 13.5 PPS at 350°F to 600°F 13.5 to 17.0 PPS at 350°F to 550°F
Maximum Flow	18.6 PPS at Maximum Temperature
Pressure	1 to 6 Atmospheres

Exhaust housing cooling air service up to 7.5 pps at 90 psig is also available with manual and automatically controlled modes.

Annunciation and safety interlock protection functions are provided and are directed through the data acquisition system computer. An optical flame detector at the primary zone of the combustor and a rig exit temperature probe provide signals to detect flame out and over-temperature conditions.

Data Acquisition System

The basic functional capabilities of the data acquisition system are as follows:

1. Data Logging - The system is capable of performing the following measurement functions:

T-4 TEST CELL CONTROL PANEL

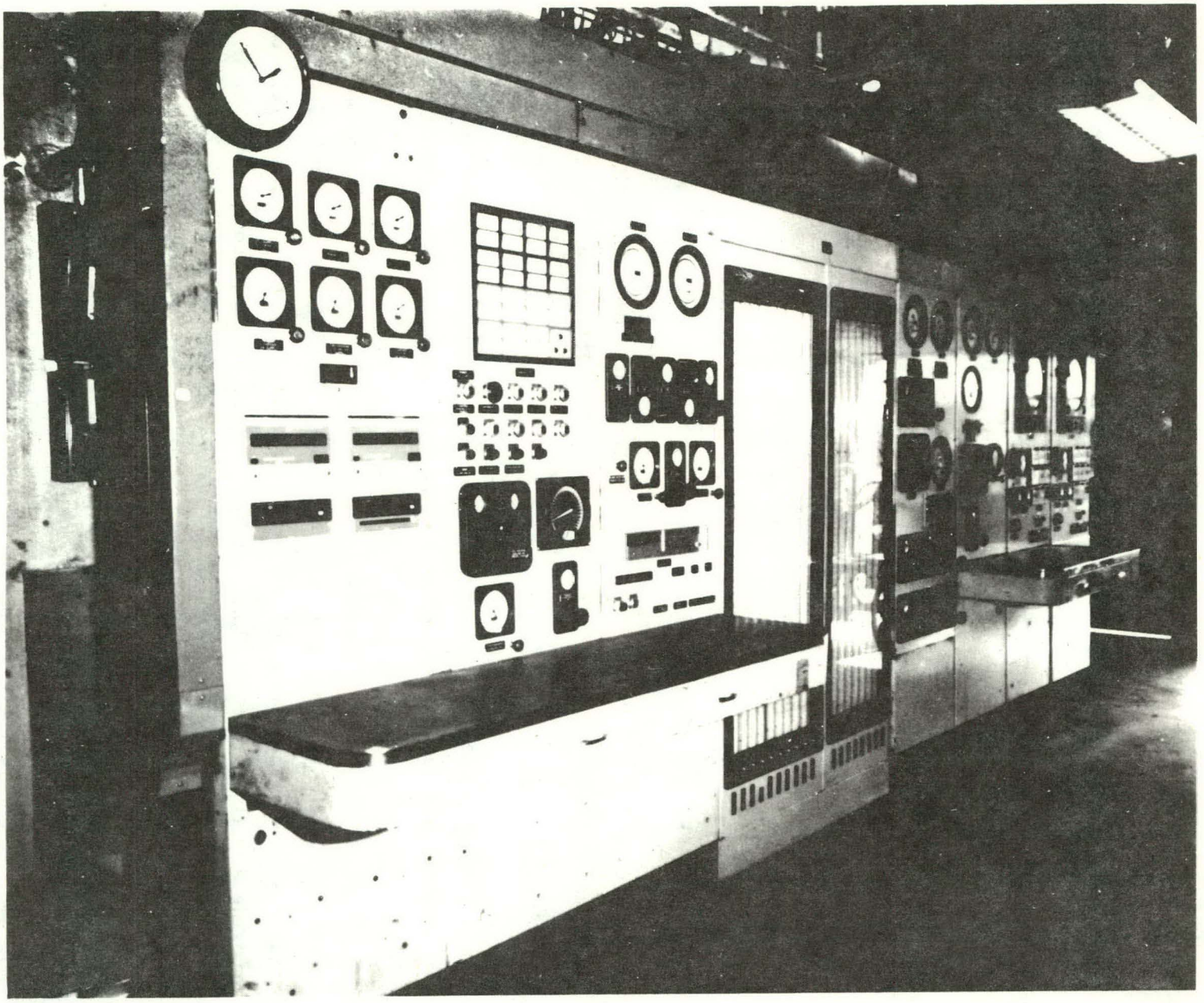

80-061

Figure 5.10

a. J, K, R, S, B, W, and V Thermocouples
b. Linear DC Voltages
c. Standard RTD's
d. Frequency Inputs

The system provides the required thermocouple linearizations and engineering scaling factors for all input channels.

2. Facility Control/Protection - The system is capable of assigning limits to each input channel and having these limits operate output relay contacts. These contacts interface with the control system to provide alarm/shutdown commands.

3. "On-Line" Data Reduction/Processing - Provides capability for reduction and processing of the raw input data for the following:

a. Conversion of input signals to proper engineering units
b. Correction of raw data to standard conditions
c. Data calculations
d. Periodic data reporting on hard copy with format
e. Alarm reporting
f. Various graphics (plotting, etc.)

The Hewlett-Packard Data Acquisition System consists of the major components discussed below and shown in Figures 5.11 and 5.12.

1. 9825A Desk Top Computer

This is the central control for the system. Through the HP-IB interface card, it controls the system scanners, digital voltmeter line printer, and optional graphics translator/CRT display. Through a 16-bit I/O card, it controls the Scanivalve pressure scanner. A real time clock is provided to enable time data on all printouts. The 9825A contains a 23K byte read/write memory. The program is stored on a magnetic tape cartridge and can be loaded into the computer conveniently.

DATA ACQUISITION SYSTEM

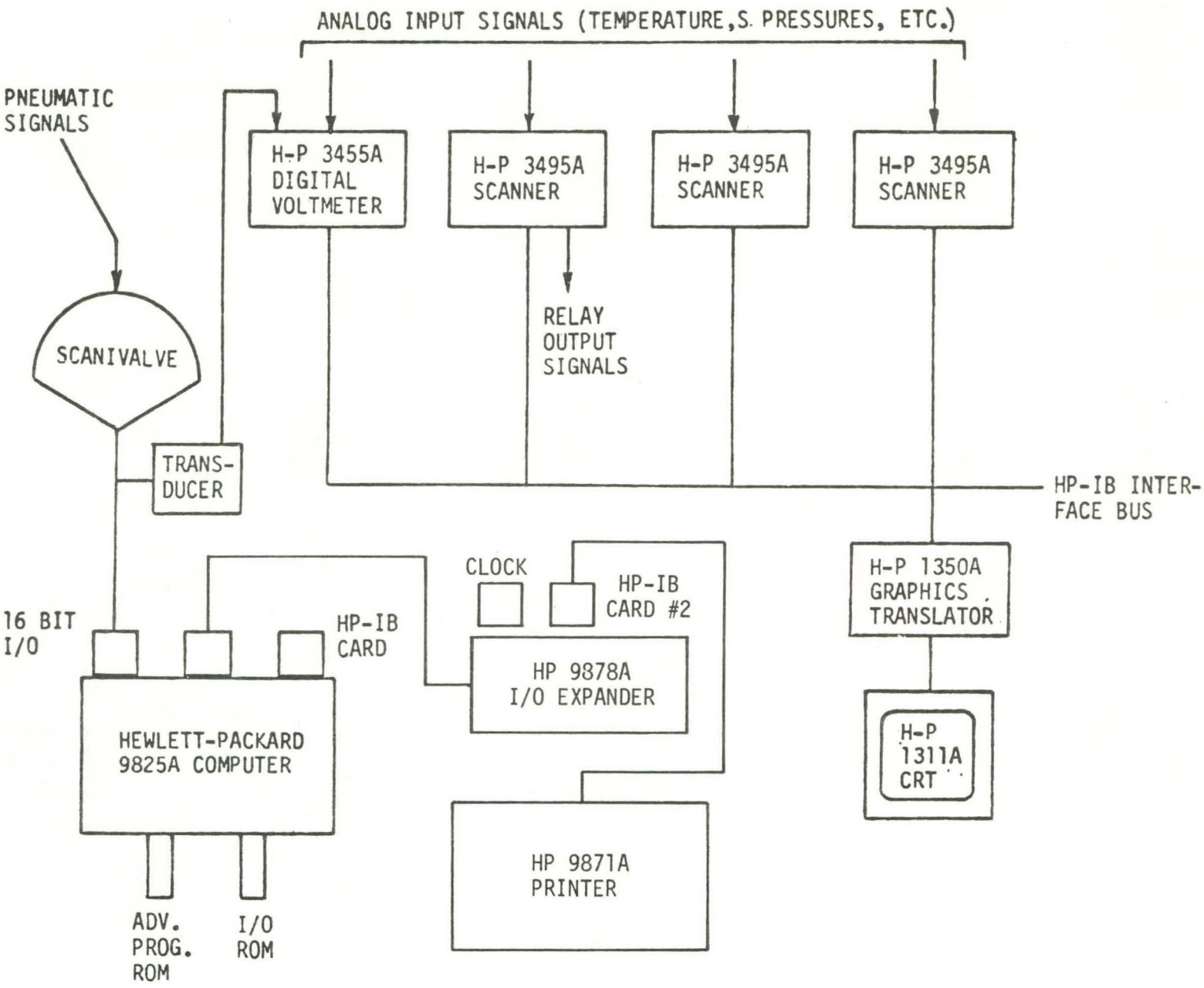

Figure 5.11

T-4 TEST FACILITY DATA ACQUISITION AND COMPUTER CONTROL STATION
FOR TSTR 60° COMBUSTOR COMPONENT TEST RIGS

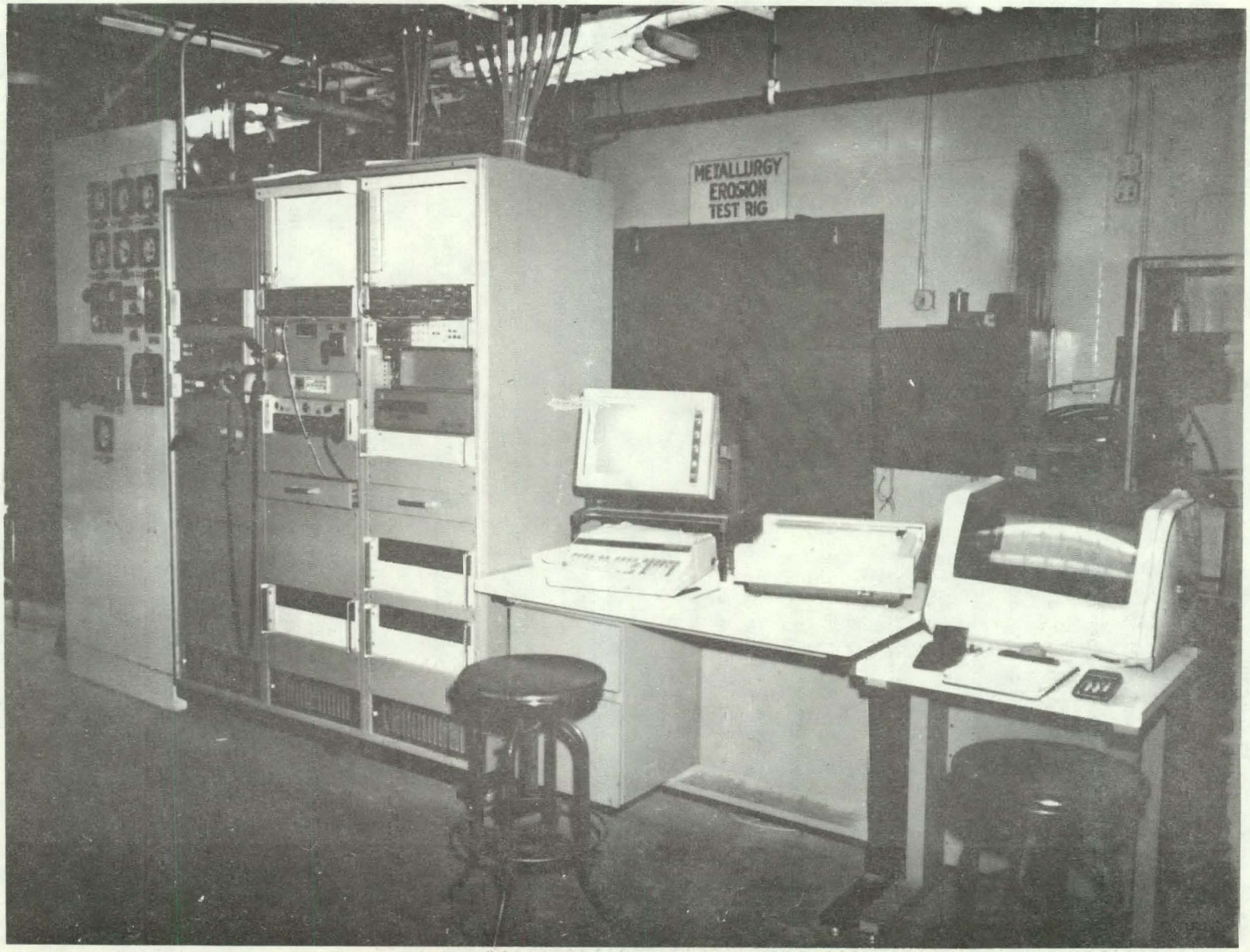

Figure 5.12

2. 3495 Scanner

The scanners provide the multiplexing of the raw input signals to the digital voltmeter for reading. A typical scanning speed of 20 channels/sec is attained. Each scanner may contain up to four (4) cards, which can be used for inputs or outputs. These cards are specifically designed for low level thermal or transducer inputs or dry contact outputs.

3. 3455A Digital Voltmeter

The digital voltmeter converts the multiplexed analog input signal to a digital signal for the computer. It is controlled through the HP-IB bus by the computer.

4. 9871A Printer/Plotter

The line printer/plotter provides the hard copy printout of both raw and reduced data. It is controlled by the computer and is also capable of graphic plotting of any variables.

5. 1311A CRT Display/1350A Graphics Translator

The CRT display provides a visual "logsheet" of critical test parameters (raw or reduced) updated for each system scan. The translator provides the interface between the display and the computer.

Safety Interlock System (SIS)

The SIS is a semi-manual system in which all start-up controls are operator set with the SIS simply providing the interlock logic necessary to allow start-up only in the proper order. Each step in the start-up sequence has certain prerequisites. Figures 5.13a and 5.13b show the logic developed for this SIS.

TSTR COMBUSTOR SECTOR LOGIC DIAGRAM

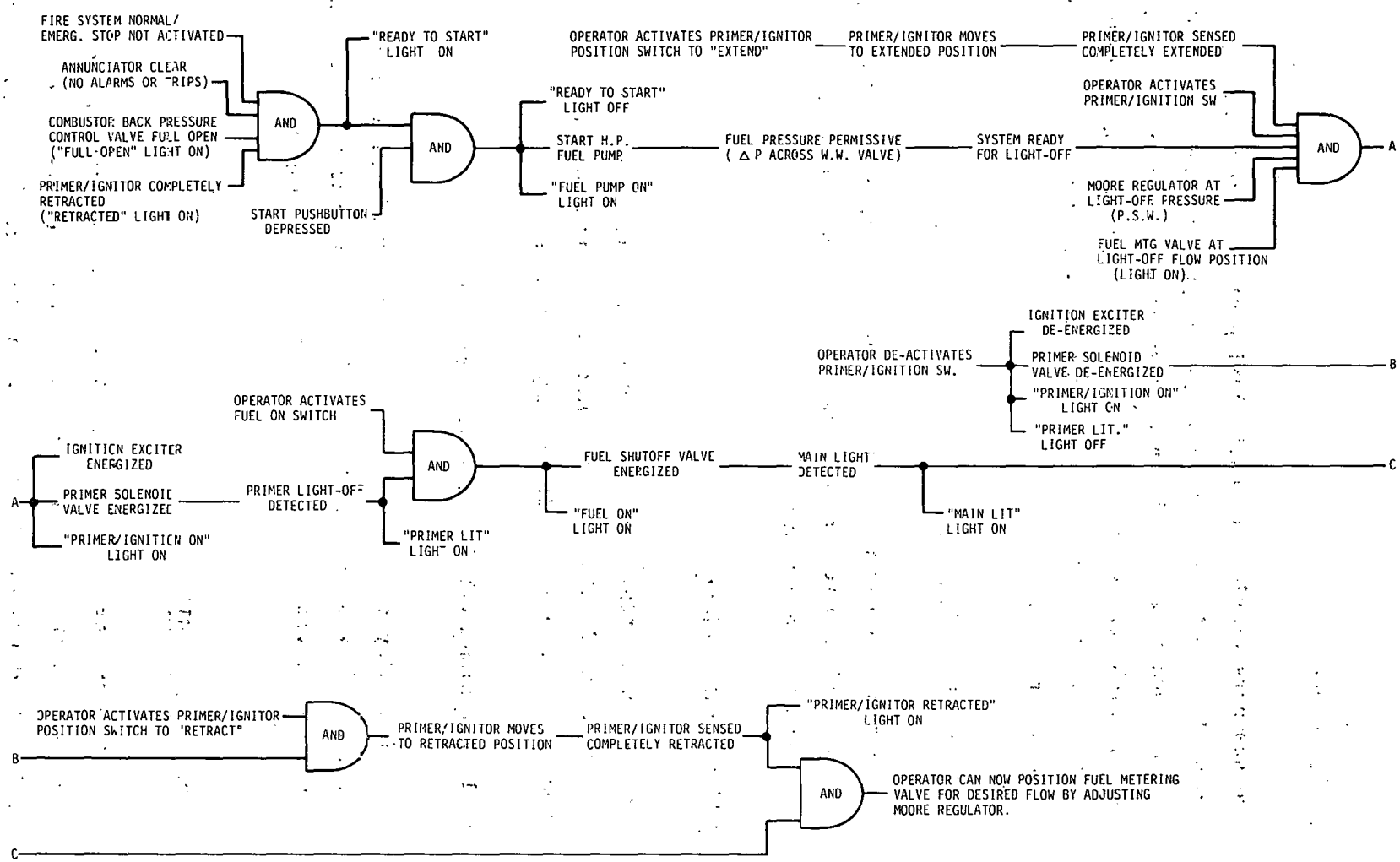

Figure 5.13A

TSTR COMBUSTOR SECTOR SAFETY INTERLOCK SYSTEM
LOGIC DIAGRAM

SHUTDOWN LOGIC

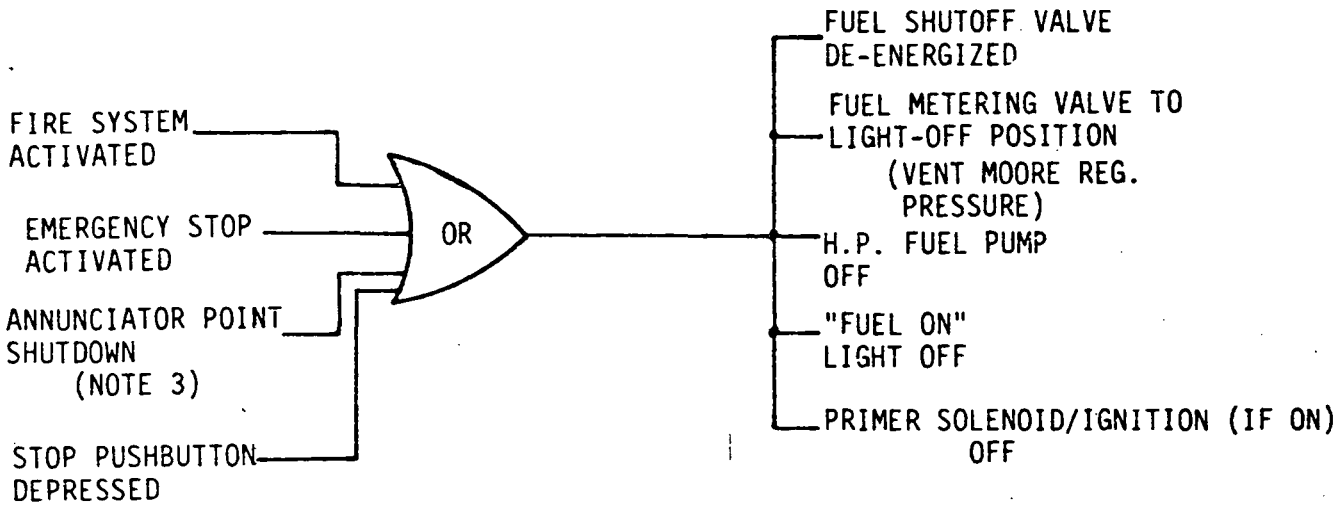

Figure 5.13B

1. Start-up Logic

Certain prerequisites are checked prior to allowing the start-up to be initiated. They are as follows:

a. Fire system active and in a safe condition. Facility emergency stop switches not activated.

b. No alarms or trips on annunciator. This requirement forces all facility systems to be operational and set in the proper condition for start-up.

c. Back pressure valve full open.

d. Retractable primer/igniter completely retracted.

When these prerequisites are satisfied, the "Ready to Start" light will be on, indicating that the rig start-up can be initiated.

When the operator depresses the Start pushbutton, the "Ready to Start" light goes off indicating a start in progress and the H.P. fuel pump (and light) is activated. Proper operation of the pump is verified by checking the development of the pressure drop across the Woodward fuel metering valve with a differential pressure switch. During this time period, the Operator extends the primer/igniter into the combustor by activating a switch and the position is then verified by the "Extended" light on.

With the fuel system operational and the primer/igniter extended, the logic checks that the fuel metering valve and its pressure regulator are in the light-off condition. When these checks are satisfied, the Operator can then activate the primer/ignition switch energizing the primer solenoid and the ignition exciter ("Primer/Ignition On" light on).

When the primer light-off is detected through either the stationary gas temperature probe or the optical flame detection system, the "Primer Lit" light comes on and the operator can then activate the fuel on switch. This then energizes the fuel shut-off valve and light-off flow is admitted to the combustor. When the indicator for the stationary gas temperature probe detects a main light-off, the "Main Lit" light comes on and the operator can now shut off the primer fuel and ignition. With primer fuel ignition off, the operator retracts the primer/igniter. When the primer/igniter is sensed as completely retracted ("Retracted" light on), the fuel metering valve can be positioned beyond light-off flow as desired.

2. Shutdown Logic

Shutdown of the system can be initiated by any of the following:

a. Fire condition or fire system malfunction. Facility emergency stop switch activated.

b. Annunciator trip

c. Stop pushbutton activated.

The shutdown then de-energizes the fuel shut-off valve, forces the fuel metering valve to its light-off position and stops the HP fuel pump. If the shutdown command was initiated while in the start-up sequence, the sequence immediately ceases and returns to time zero.

3. Optical Flame Detection System

The Honeywell gas turbine flame monitor system consists of an amplifier and two sensors. The sensors are designed to detect the ultraviolet radiation emitted by a hydrocarbon flame, and coupled with the amplifier, provide a logic signal to indicate the presence of a flame in the combustor. Correctly "aimed" to view both the primer/igniter

flame and the main flame, this system provides the necessary response as well as sensitivity needed for the logic signal to purge and retract the primer/igniter.

Instrumentation and Accuracies

The combustor exit temperatures were measured with dual junction water cooled thermocouple Type V probes. Four probes mounted in a sweep mechanism, as shown in Figure 5.14, traverse across the combustor exit annulus during a data acquisition point. As shown the probes are normally retracted from the combustor exit stream until a data point sweep is required. The actual temperature level is computed from the following relationships developed by the manufacturer of the temperature probes:

$$T_t = (T_w + T_c + T_r)/R$$

$$T_c = (T_w - T_b)\ \text{Sec}\ C$$

$$C = 3.62\ (MP)^{.25}$$

$$T_r = (1.82 \times 10^{-12})\left[\frac{Tw^4}{(MP)}\ .5\right]\left[1-\left(\frac{Td}{Tw}\right)4\right]$$

T_t = True Total Temp, °R

T_w = Primary Wire Temp, °R

T_c = Conduction Correction, °R

T_r = Radiation Correction, °R

R = Recovery Ratio

M = Mach Number

P = Static Press, Atm

T_b = Avg Base Junct Temp, °R

T_d = Outside Temp, °R

TSTR LIQUID FUEL 60° SECTOR COMBUSTOR TEST RIG SWEEP PROBE INSTALLATION

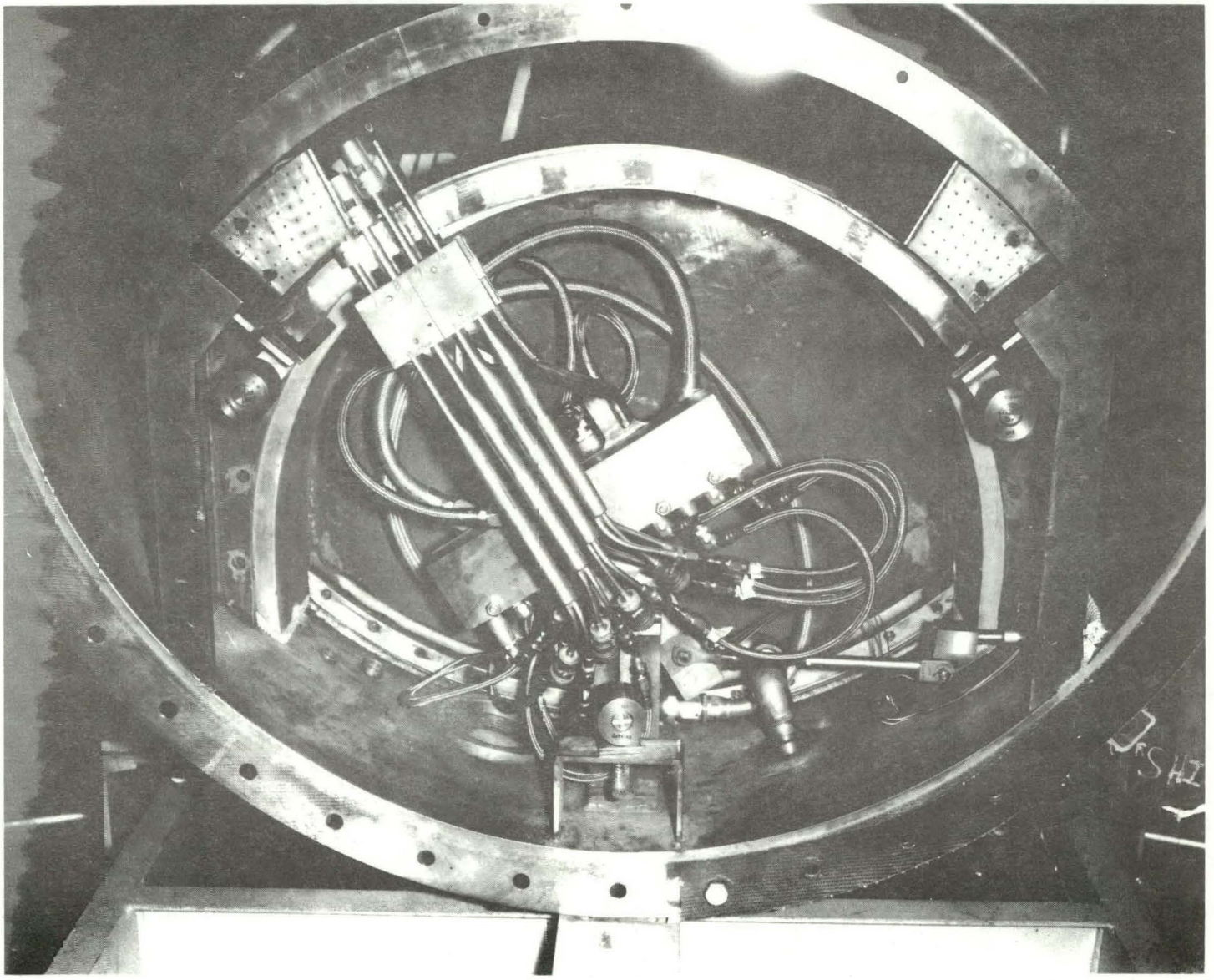

HTT-II-1005

Figure 5.14

Error Analysis

The pressure, temperature, fuel flow and airflow readings which are experimentally obtained through the various instruments are subject to errors caused by random electronic fluctuations in the data acquisition system, software errors, hardware errors, etc.

The theoretical uncertainties for the data were determined using the maximum limits of error listed in the specifications for the various instruments involved. The overall error of a given combination was determined by calculating the root mean square (RMS) of the individual errors.

Pressure

PSI	10	20	30	40	50	60	70
Max. possible error	±.100%	±.080%	±.073%	±.070%	±.070%	±.068%	±.067%

The above table illustrates the range of pressure reading uncertainties. The increase in uncertainty as the pressure decreases is attributed to the round-off error which results in the display.

Temperature

Max. Possible Temperature Uncertainties

T/C Type R-s	T/C Type J	T/C Type V Probe
2700°F ± .59%	1400°F ± .49%	3700°F ± .53%
2500°F ± .63%	1000°F ± .58%	3000°F ± .55%
1500°F ± .92%	750°F ± .70%	2500°F ± .57%
1000°F ± .32%		2000°F ± .61%

The main contribution to airflow and fuel flow error is the temperature measurements with its uncertainties of .58 to 4.8 percent.

Airflow

The uncertainty analysis for airflow is for the primary air orifice, only. The airflow rate is a function of several variables, each subject to an uncertainty. By dividing the partial derivatives of each variable, with the mass flow equation it can be applied to the RMS method to obtain the percent uncertainty in the mass flow rate.

Airflow Uncertainties

Assumed Conditions (Cold flow, high upstream pressure)

Pressure	(P)	-	105 psi $\pm$ .062%
Temp.	(T)	-	60°F $\pm$ 4.71%
	(P)	-	87.5" H_2O $\pm$ .062%
Dia.	(d)	-	7.744 $\pm$ .001 In.
Exp. Factor	(Y)	-	.996 $\pm$ .75%
Flow Coeff.	(K)	-	.6563 $\pm$ 1%

Flow Rate = 27 PPS $\pm$ .350 PPS (1.30%)

Assumed Conditions (Hot flow, high upstream pressure)

(P)	-	105 psi $\pm$ .062%
(T)	-	550-1/4F $\pm$ .82%
(P)	-	87.5" H_2O $\pm$ .062%

Flow Rate = 19.38 PPS $\pm$ .306 PPS (1.58%)

Assumed Conditions (Cold flow, low upstream pressure)

(P)	-	30 psi $\pm$ .062%
(T)	-	60-1/4F $\pm$ 4.71%
(P)	-	35" H_2O $\pm$ .062%

Flow Rate = 9.1 PPS $\pm$ .192 PPS (2.12%)

Fuel Flow

The fuel flow uncertainty is primarily comprised of random fluctuations in the turbine meter, flow rate indicator and the digital/analog converter. In addition, the uncertainties in the temperature and specific gravity measurements will account for errors in the corrected specific gravities computed by the data acquisition system.

Theoretically, the maximum possible uncertainty for fuel flow is $\pm$ 1.41%. The actual fuel flow calibration data resulted in errors approximately equal to the theoretical value.

Section 6.0
COMBUSTOR TEST PROGRAM

6.1 METHODS AND PROCEDURES

The TSTR combustor was tested in the 60° sector rig described in Section 5.1. This rig simulates the geometric and aerodynamic environment surrounding the TSTR combustor to permit investigation of the critical performance and durability characteristics of the combustor. The test program covers ignition, aerodynamic and combustion tests up to six atmospheres and 3000°F average combustor exit temperature and 530°F inlet temperature to simulate the TSTR engine design operating point. The test program was conducted in two separate Curtiss-Wright test cell installations, WX-37 and T-4. Combustor ignition/stability tests were conducted in the atmospheric test cell WX-37 as shown in Figure 6.1. On this test stand the burner rig exit gases are discharged directly from the rig to atmosphere, thereby enabling direct visual observations into the combustor for evaluation of the ignition/combustion stability characteristics during the test.

The aerodynamic and high pressure hot combustion tests were conducted in the T-4 test cell facility as shown in Figure 6.2. Three 60° combustor sectors and nine modifications were utilized during the test program, which covered over 130 hours of total rig test operation to evaluate the original design and develop satisfactory durability and performance. An outline of the tests conducted on the combustor is shown in Table 6-1. Initial testing defined the regions of successful primer torch and combustor ignition followed by combustor stability operation at various airflows and fuel flow ranges. Follow-on tests were conducted to validate the predicted airflow distribution through the burner and overall pressure loss across the diffuser/combustor section. The subsequent, and most significant portion of the development test effort, was directed toward achieving the combustor outlet temperature profile and durability design goals.

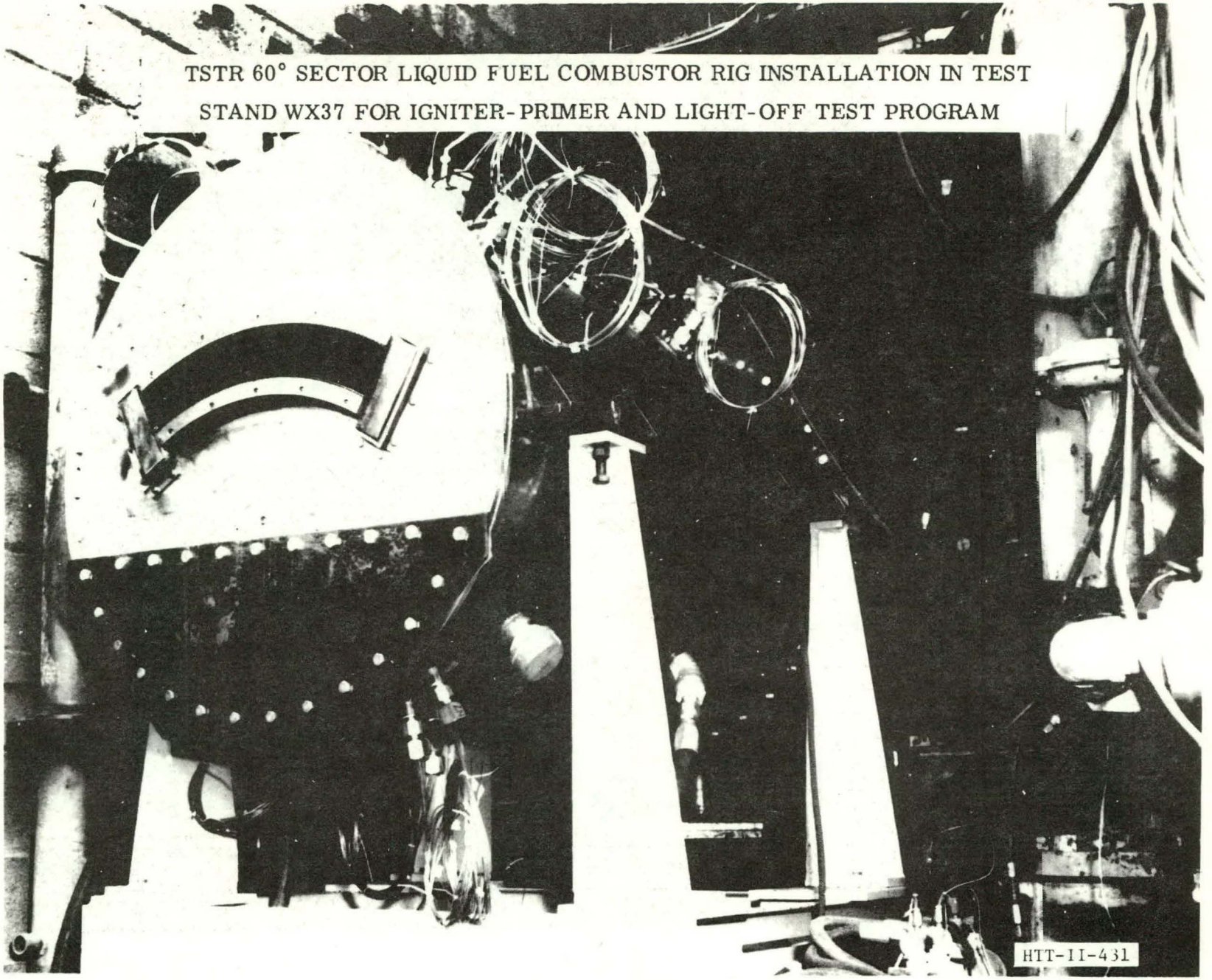

TSTR 60° SECTOR LIQUID FUEL COMBUSTOR RIG INSTALLATION IN TEST STAND WX37 FOR IGNITER-PRIMER AND LIGHT-OFF TEST PROGRAM

Figure 6.1
6-2

TSTR 60° SECTOR COMBUSTOR TEST RIG IN TEST CELL T-4

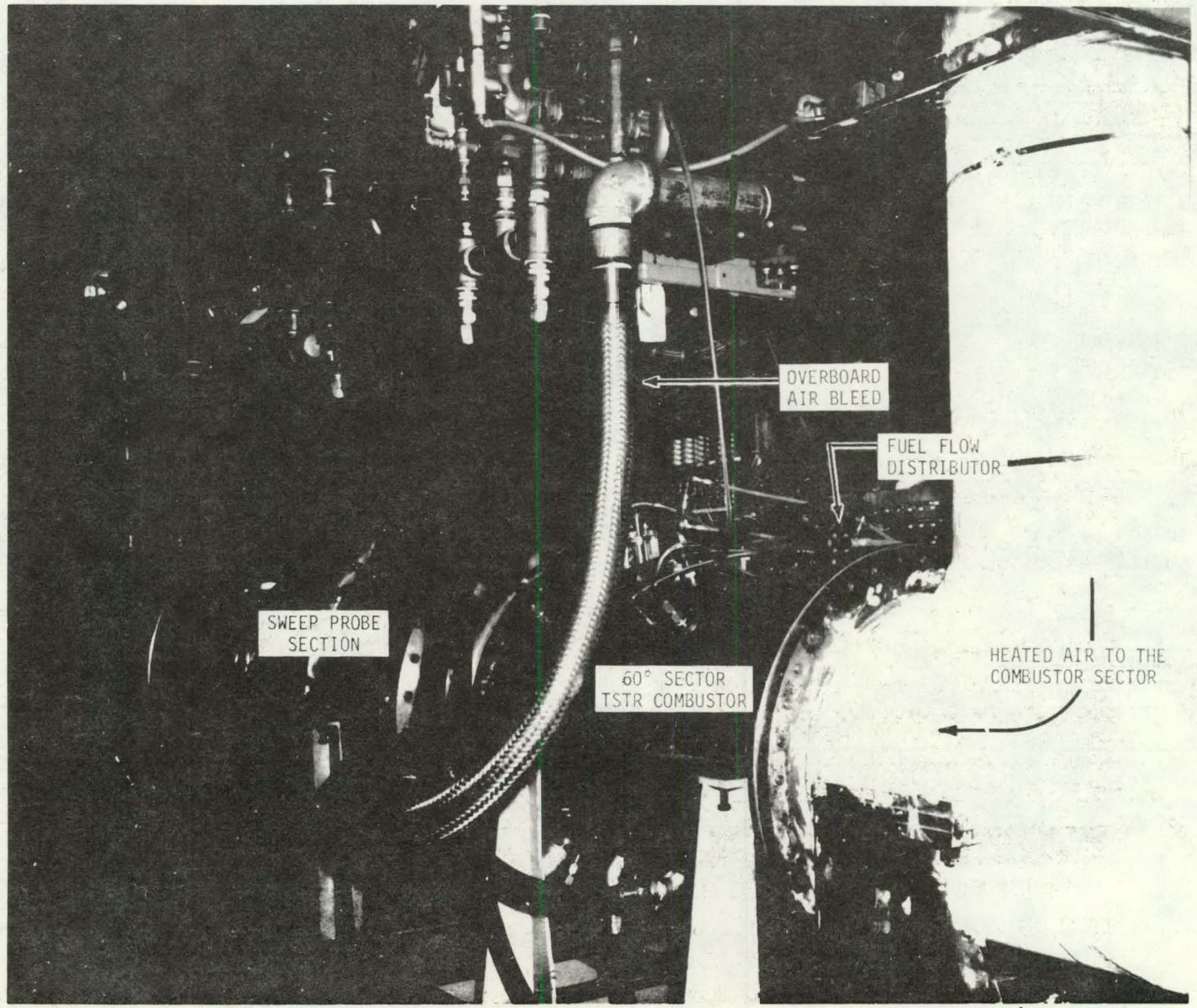

80-278

Figure 6.2

Table 6-1

SUMMARY OF TEST PLAN

Test Description	Air Temperature	Air Pressure	Objective of Tests	Output from Tests
I - Light-off Performance	Ambient	Atmos.Disch.	To determine light-off capabilities of combustor	To establish curve of (f/a) min. as a function of combustor $\frac{W\sqrt{T}}{P}$ for stable light-off.
II - Cold Flow Airflow Distribution	Ambient	Atmospheric and/or up to 6 Atmos.	To determine combustor airflow distribution for a range of pressure drops	To establish combustor corrected weight flow, $\frac{W\sqrt{T}}{P}$ as a function of pressure drop and to determine $[\frac{PS - PSREF}{PTREF}]$ at selected combustor locations
III - Combustor Evaluation at design f/a ratio	523°F	Atmos.Disch. 2 ATMS 4 ATMS 6 ATMS	To assess liner cooling, combustion efficiency and combustor stability at design f/a ratio	To achieve liner design temperature at design f/a ratio
IV - Combustor exit temperature profile development at design f/a ratio	523°F	6 ATMS	To achieve desired combustor exit profile and pattern factor	Combustor exit profiles, combustor efficiency
V Combustor performance along gas generator operating line		Actual PT3 up to limit of 6 ATMS	To determine combustor performance along operating line	Combustor exit profiles, wall temperatures

Build 1 of the 60° combustor sector was heavily instrumented with thermocouples and pressure probes in order to verify the design criteria utilized to define the burner airflow distribution and burner wall temperature level. Figures 6.3 through 6.6 show the extent of combustor liner, shroud and vaporizer tube installed instrumentation. A total of 120 thermocouples and 93 pressure probes/taps were installed in this build.

Combustor-Primer Ignition/Stability Test Sequence

The objective of this program was to determine the light-off primer igniter and main burner Jet A fuel flow schedules for the TSTR. During these tests the ignition and performance of the primer torch igniter were determined by varying the ambient temperature combustor airflow and primer fuel nozzle flow as well as orientation of the spark/spray relationship to the combustor vaporizer tubes. Once the primer torch igniter operating envelop was determined, main burner ignition tests were conducted at various main fuel flow rates and ambient temperature burner airflows.

Airflow Distribution - Cold Pressure Loss Test Sequence

The objective was to determine the overall cold pressure drop and airflow distribution of the initial TSTR combustor design.

The pressure drop measurements, which were performed first, utilized a combustor-exit plane four-element sweep probe. Tests were conducted at nominal upstream stagnation pressures of two, four and six atmospheres.

Following this, the airflow distribution measurements were performed at 1 atmosphere pressure, consisting of a sequence of 16 steps to determine incremental airflows for the various combustor openings proper, plus other combustor rig airflow paths which included water cooled side wall leakage, outer liner and inner liner downstream cooling slot flow and burner support leakage flow.

80-257

TSTR LIQUID-FUELED 60° COMBUSTOR SECTOR RIG
OUTER LINER PRESSURE AND TEMPERATURE INSTRUMENTATION

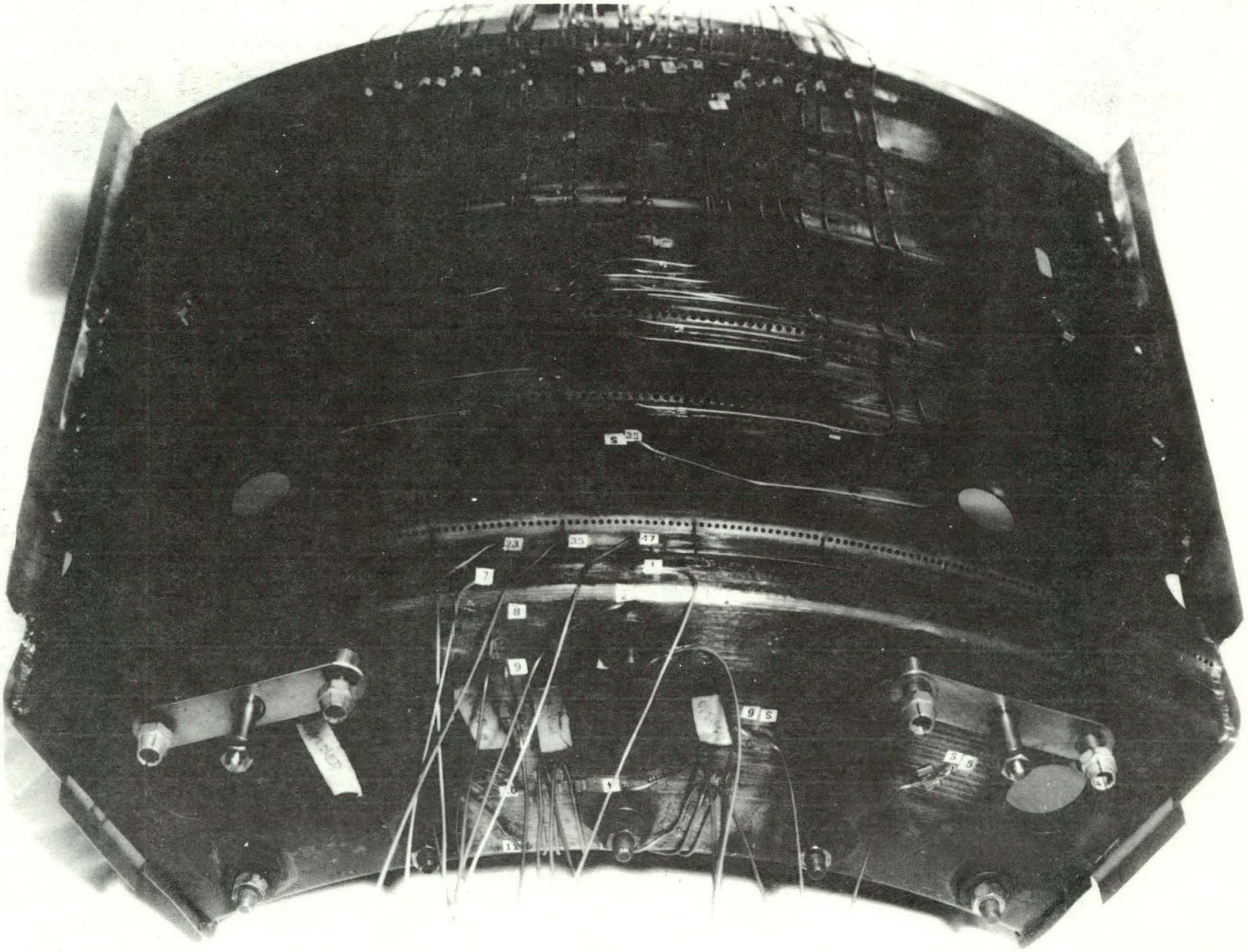

Figure 6.3

80-259

TSTR LIQUID-FUELED 60° COMBUSTOR SECTOR RIG
INNER LINER PRESSURE AND TEMPERATURE INSTRUMENTATION

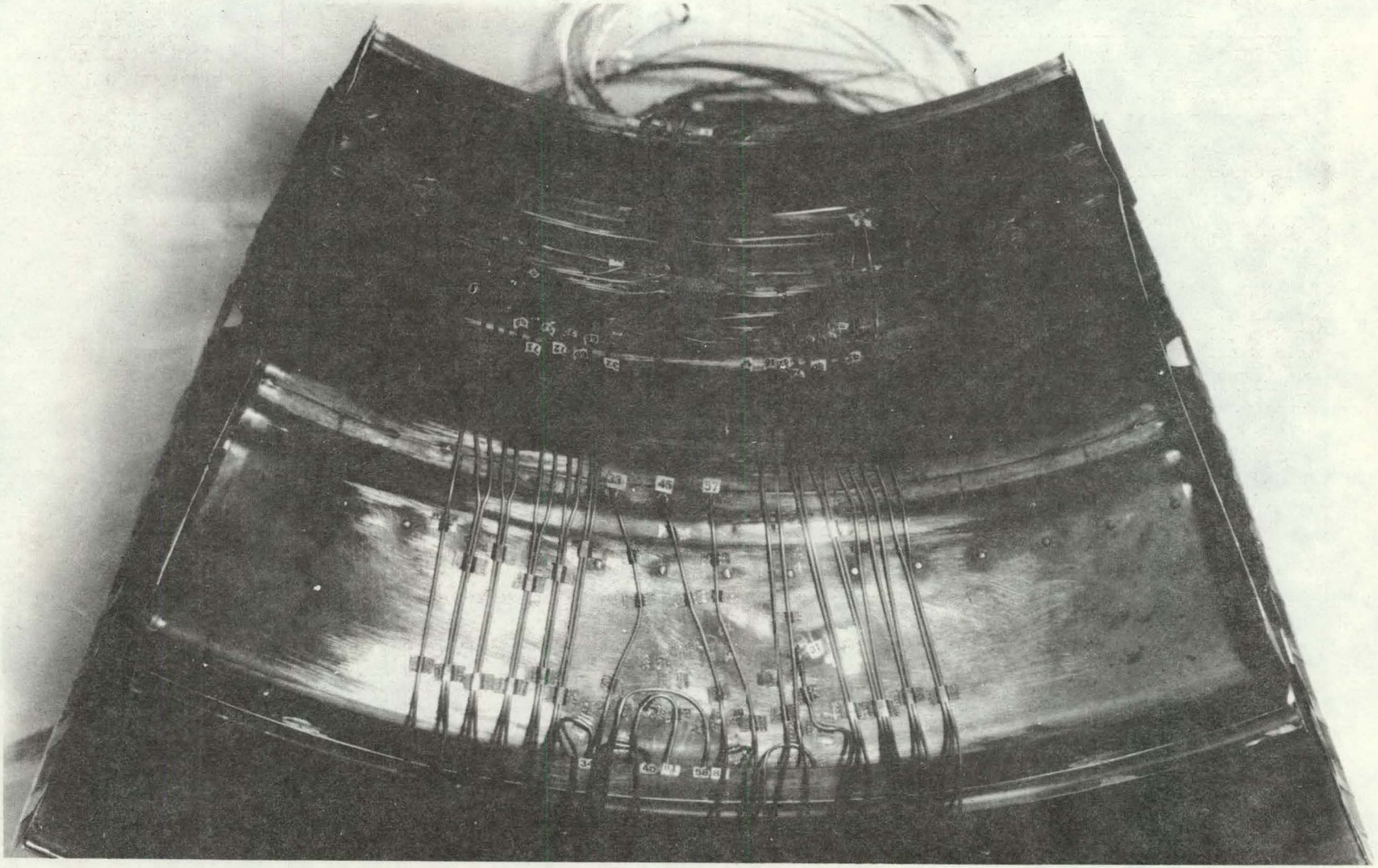

Figure 6.4

81-141

TSTR 60° SECTOR COMBUSTOR RIG HEADPLATE
TOTAL PRESSURE AND THERMOCOUPLE INSTALLATION

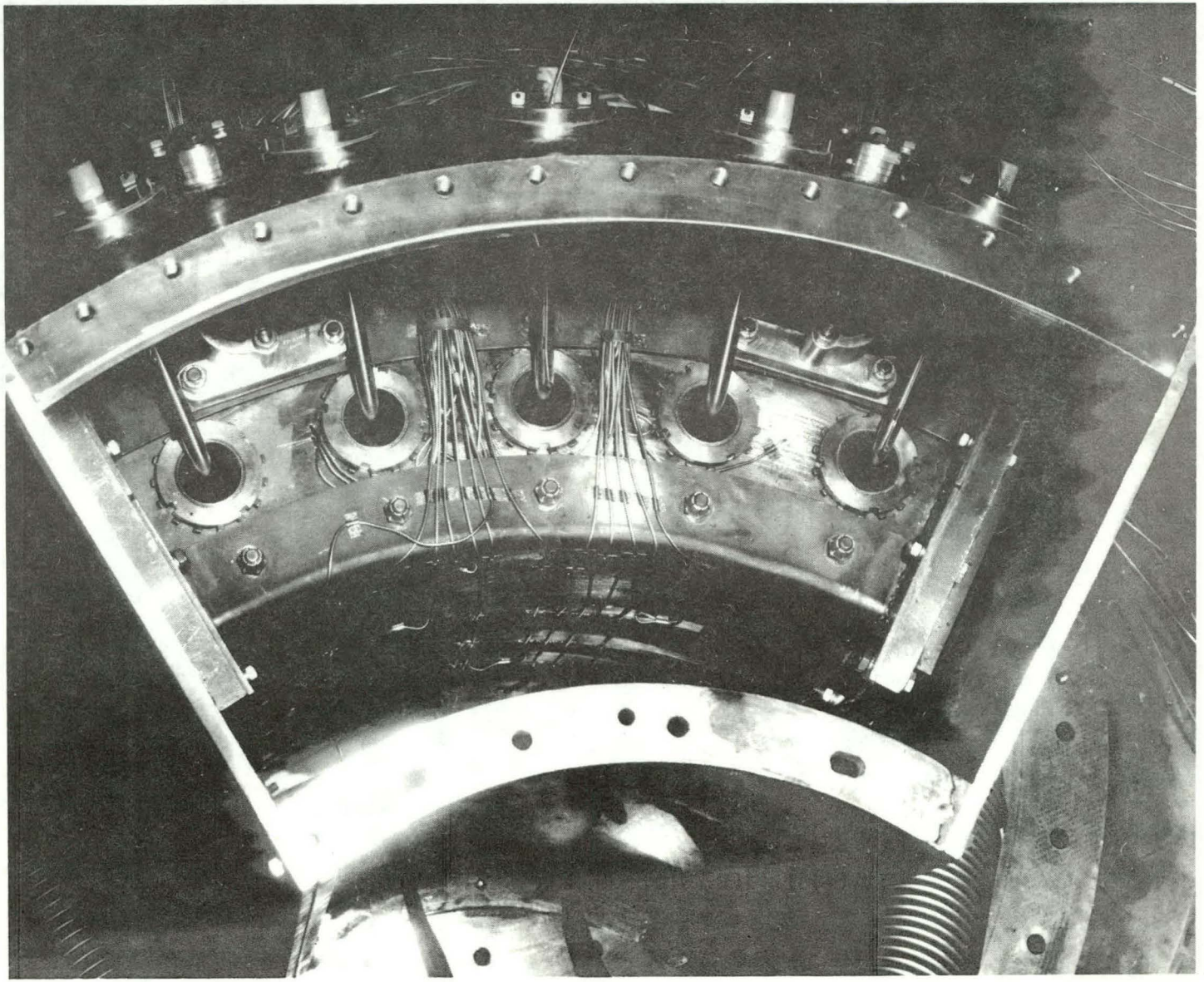

Figure 6.5

VAPORIZER TUBE THERMOCOUPLE INSTALLATION

TSTR COMBUSTOR 60° SECTOR TEST RIG

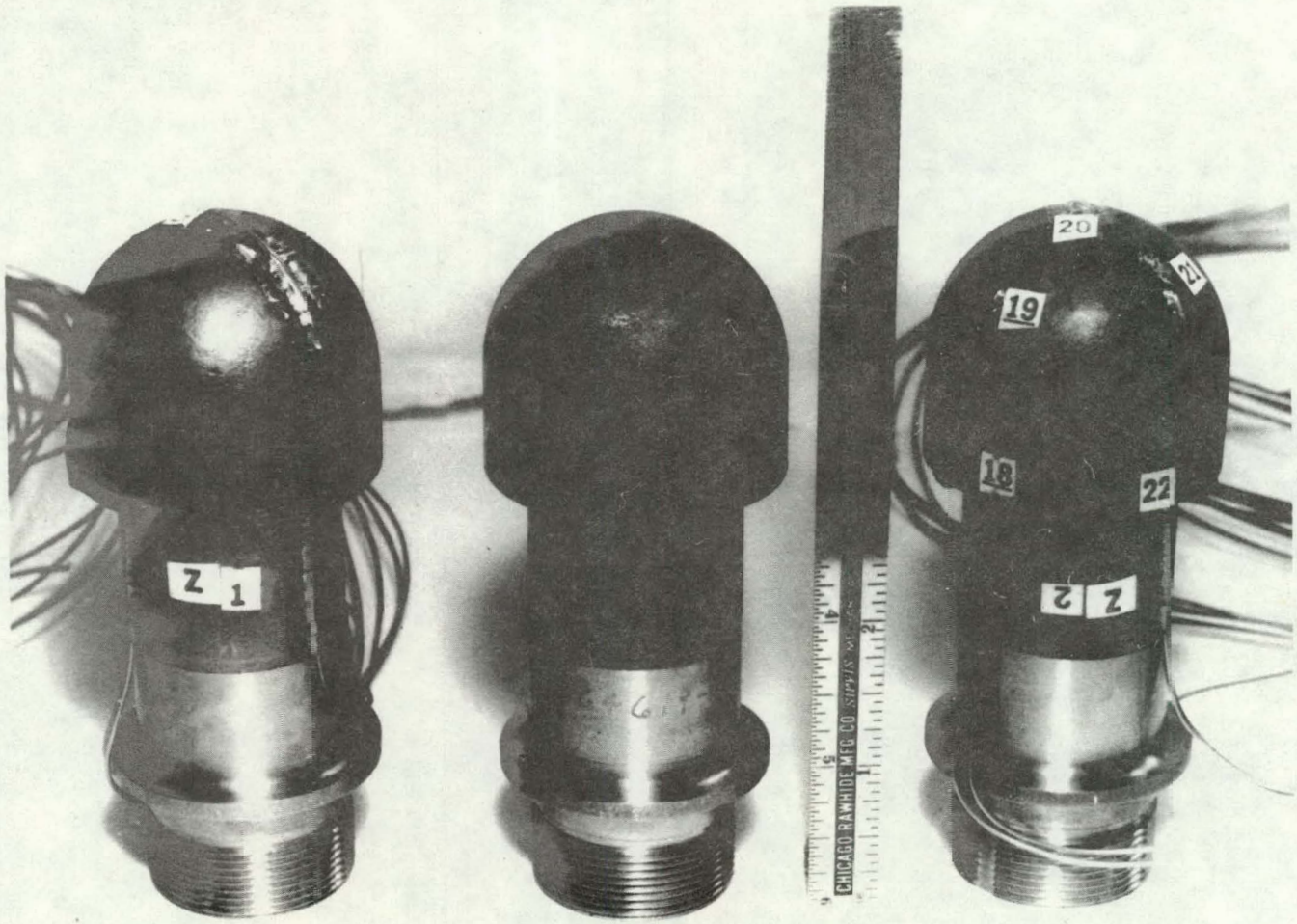

Figure 6.6

Durability and Combustor Exit Profile Development Test Sequence

Tests were conducted at various pressure levels, inlet temperatures and fuel-air ratios to define the areas in which durability or performance would require improvement.

Combustor nominal test conditions were set as follows:

Pressure Level	2 ATM	4 ATM	6 ATM
Inlet Temperature	525°F	525°F	525°F
Burner Airflow	4.6 PPS	10.0 PPS	14.2 PPS
Fuel/Air Range	.02 .05	.024	.024
$\frac{Wb\ \sqrt{T}}{P_T}$	4.25	4.25	4.25
Fuel	Jet A	Jet A	Jet A

At each test point the combustor inlet conditions were stabilized as close to the targets as practical, at which point the data acquisition process was energized. A complete scan of all measured temperatures and pressures as well as calculated parameters was recorded as a permanent log. Simultaneously a sweep traverse of the combustor exit plane recorded the thermocouple signal and angular position of each multi-junction temperature probe. Approximately 3 minutes of calculation time after data acquisition is required to display the reduced test results on the computer CRT screen. The definitions of combustor performance parameters utilized in this test sequence are shown in Figure 6.7. A combustor exit local temperature measurement was made approximately every 2.5 degrees through the 60° sweep of the temperature probes.

6.2 COMBUSTOR DEVELOPMENT TEST RESULTS

A summary outline of the entire 60° combustor sector test program listing rig builds, combustor configuration modifications and performance parameters is given in Table 6-2.

COMBUSTOR PERFORMANCE EVALUATION DEFINITIONS

PERFORMANCE PARAMETER	DEFINITION
EFFICIENCY	$\frac{\text{ACTUAL TEMPERATURE RISE}}{\text{IDEAL TEMPERATURE RISE}} = \frac{T_{AVG} - T_{IN}}{\Delta T_{IDEAL} \text{ FOR JET A AT 18,550 BTU/LB}}, \frac{°F}{°F}$
TEMPERATURE PATTERN FACTOR	$TPF = \frac{T_{MAX} - T_{AVG}}{T_{AVG} - T_{IN}} \quad \frac{°F}{°F}$
STATOR PROFILE DISTORTION FACTOR	$T_{MAX}/T_{AVG} \quad \frac{°R}{°R}$
ROTOR PROFILE DISTORTION FACTOR	$T_{IAVG}/T_{AVG} \quad \frac{°R}{°R}$
PERCENT COMBUSTOR AND DIFFUSER PRESSURE DROP	$\%\Delta P = \frac{P_{T\,(IN)} - P_{T\,(OUT)}}{P_{T\,(IN}} \times 100$

SWEEP EXIT TEMPERATURE RAKE

(FOUR IRIDIUM/RHODIUM/IRIDIUM DUAL JUNCTION THERMOCOUPLES, EACH LOCATED AT THE GEOMETRIC CENTER OF AN ANNULAR AREA WHICH IS 1/4 OF THE TOTAL EXIT ANNULAR AREA.)

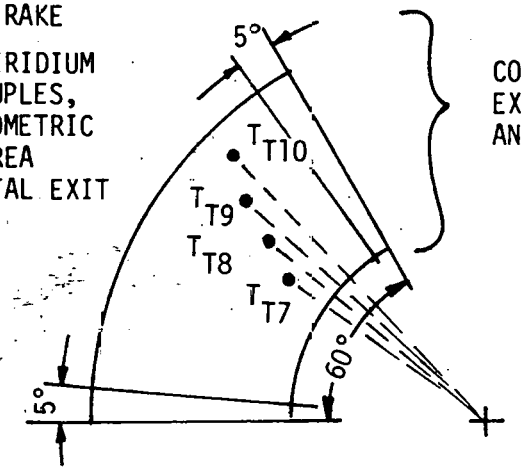

T_{IN} = COMBUSTOR INLET TEMPERATURE

$$T_{AVG} = \sum_{5°}^{55°} \frac{T_{1AVG} + T_{2AVG} + T_{3AVG} + T_{4AVG}}{4}$$

T_{IAVG} = HIGHEST OF T_{1AVG}, T_{2AVG}, T_{3AVG}, T_{4AVG}

T_{MAX} = MAXIMUM TEMPERATURE RECORDED BY ANY THERMOCOUPLES (T_1, T_2, T_3, T_4 AT ANY LOCATION)

Figure 6.7

Table 6-2

TSTR 60° COMBUSTOR TEST PROGRAM RESULTS SUMMARY

Rig Build	Combustor Configuration	Inlet Pressure Atmospheres	Inlet Temp °F	Exit Temp °F	Stator Profile Distortion Factor T_{max}/T_{avg} °R / °R	Rotor Profile Distortion Factor Ti_{avg}/T_{avg} °R / °R	Temp Pattern Factor TPF	Combustion Efficiency %	Objective
1.0	I	1	90°F	--	-- --	-- --	--	--	Ignition/Stability
1.1	I	2	90°F	--	-- --	-- --	--	--	Cold Flow Pressure Loss Survey
		4	90						
		6	90						
1.2	I	1	90°	--	-- --	-- --	--	--	Flow Distribution Survey
1.3	I	2	523	3009	1.21	-- --	.31	88.8	Hot Shakedown Liner Temperature and Performance Evaluation - Test Rig Failure Occurred
		4	530	2006	1.15	-- --	.28	95.5	
		6	532	2043	1.20	-- --	.35	99.9	
2.0	II	2	513	2802	1.23	-- --	.36	84.0	Hot Test Performance/ Profile/Durability Development
		4	519	2932	1.23	-- --	.34	89.4	
		6	481	3017	1.17	-- --	.253	95.9	
		1.3	199	1456	1.28	-- --	.44	96.4	
2.1	IIa	2	522	2688	1.21	-- --	.31	95.3	Hot Test Performance Development - With and Without Overboard Bleeds
		6	517	3077	1.17	1.12	.24	94.3	
		1.3	171	1315	1.27	-- --	.38	90.0	

Table 6-2

TSTR 60° COMBUSTOR TEST PROGRAM RESULTS SUMMARY (Continued)

Rig Build	Combustor Configuration	Inlet Pressure Atmospheres	Inlet Temp °F	Exit Temp °F	Stator Profile Distortion Factor T_{max}/T_{avg} °R / °R	Rotor Profile Distortion Factor Ti_{avg}/T_{avg} °R / °R	Temp Pattern Factor TPF	Combustion Efficiency %	Objective
3.0	IIIa	6	536	2783	1.22	1.13	.272	90.2	Durability Development
3.1	IVa	6	528	2938	1.17	1.08	.250	95.6	Durability Development
4.0	Va	6	514	2790	1.22	1.09	.31	98.5	Durability Development
5.0	VIa	6	522	1947	1.18	--	.297	99.5	Profile Development
6.0	VIIa	6	522	2780	1.20	1.12	.289	--	Profile Development
7.0	VIIIa	6	525	2913	1.16	1.13	.225	97.0	Profile Development
8.0	IXa	6	521	2917	1.18	1.15	.257	96.2	Profile Development
9.0	Xa	6	524	2851	1.21	1.18	.30	94.6	Profile Development

Exploratory test firings of the igniter-torch primer were conducted at ambient conditions with various fuel flow rates and fuel nozzle/spark orientations. These tests demonstrated excellent ignition and flame stability at static conditions over a wide range of fuel flow and nozzle/spark orientation.

The extent of flame brush resulting from a 20 PPH fuel flow into a static atmosphere is shown in Figure 6.8. Observation of the flame brush when the primer/igniter is immersed within the combustor indicates that the flame volume shrinks dramatically with increasing airflow through the combustor. Initial tests to determine the optimum relative orientation of the primer spray/igniter spark demonstrated good ignition and stability over the range of combustor airflow and primer fuel/air ratio shown in Figure 6.9 with the orientations marked by asterisks in Figure 6.10.

Based on the ignition and stability test data, the light-off primer nozzle and main fuel flow schedules shown in Figure 6.11 were established for the TSTR. The rig tests also indicated that combustion propagation in the TSTR engine would be significantly improved by increasing the number of primer/igniters from the original three to six.

A series of tests was performed to determine the overall cold pressure drop, airflow distribution and convection cooling air (shroud) Mach number using the pressure instrumented 60° sector combustor rig on T-4 test stand.

Verification of actual combustor airflow distribution is necessary because of the difficulty in accurately predicting hole airflow discharge coefficients in high velocity and rapidly turning passages. The airflow distribution is determined by a sequential process. Initially, all holes in the combustor are covered with metal tape except for the vaporizer tubes. The flow through the combustor is then measured over a range of combustor pressure drops.

81-145

RETRACTABLE PRIMER/IGNITER LIGHT-OFF TEST

EX-CELL-O CORPORATION
(TYPICAL FLAME PATTERN)

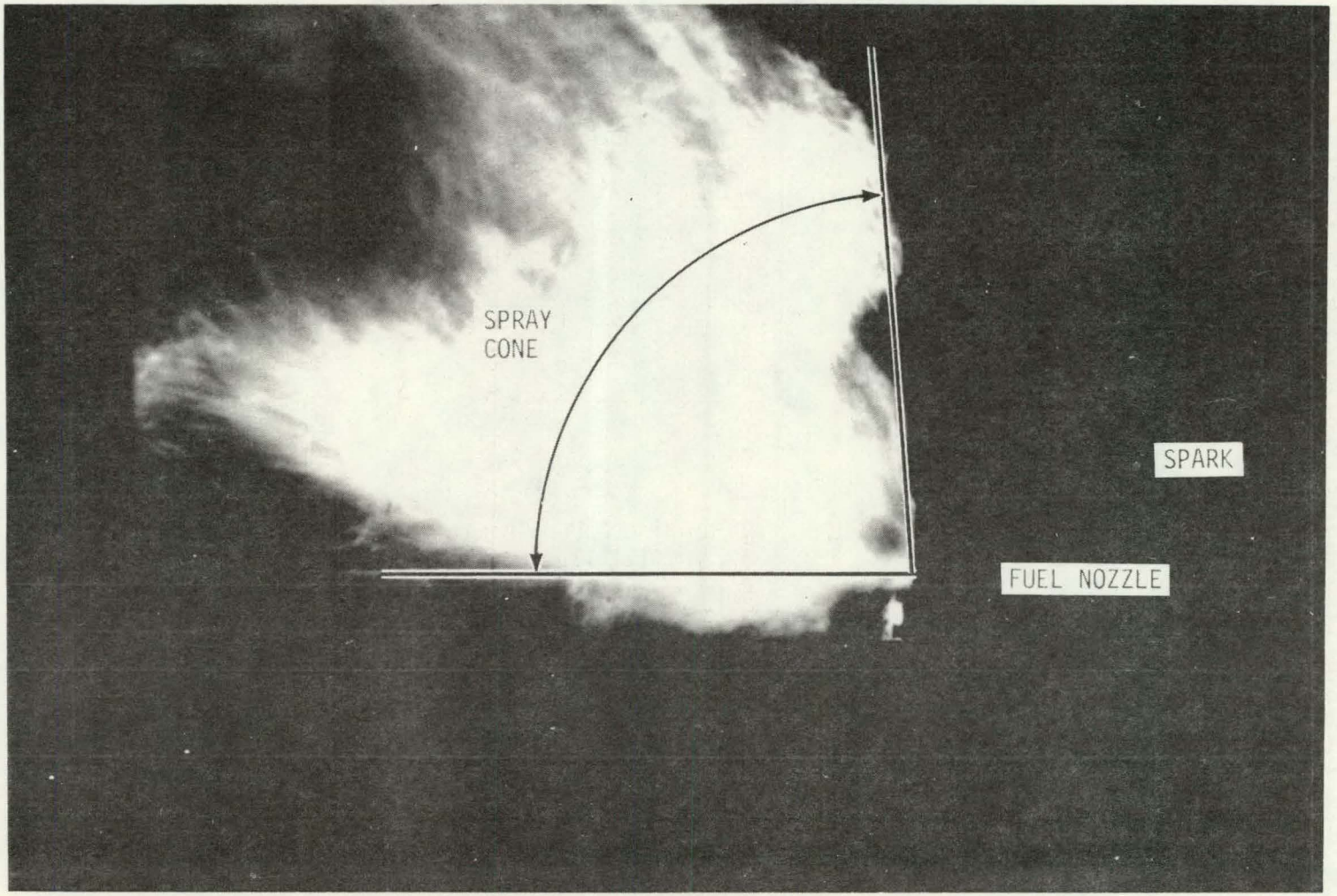

Figure 6.8

TSTR 60° SECTOR COMBUSTOR RIG IGNITION TEST RESULTS

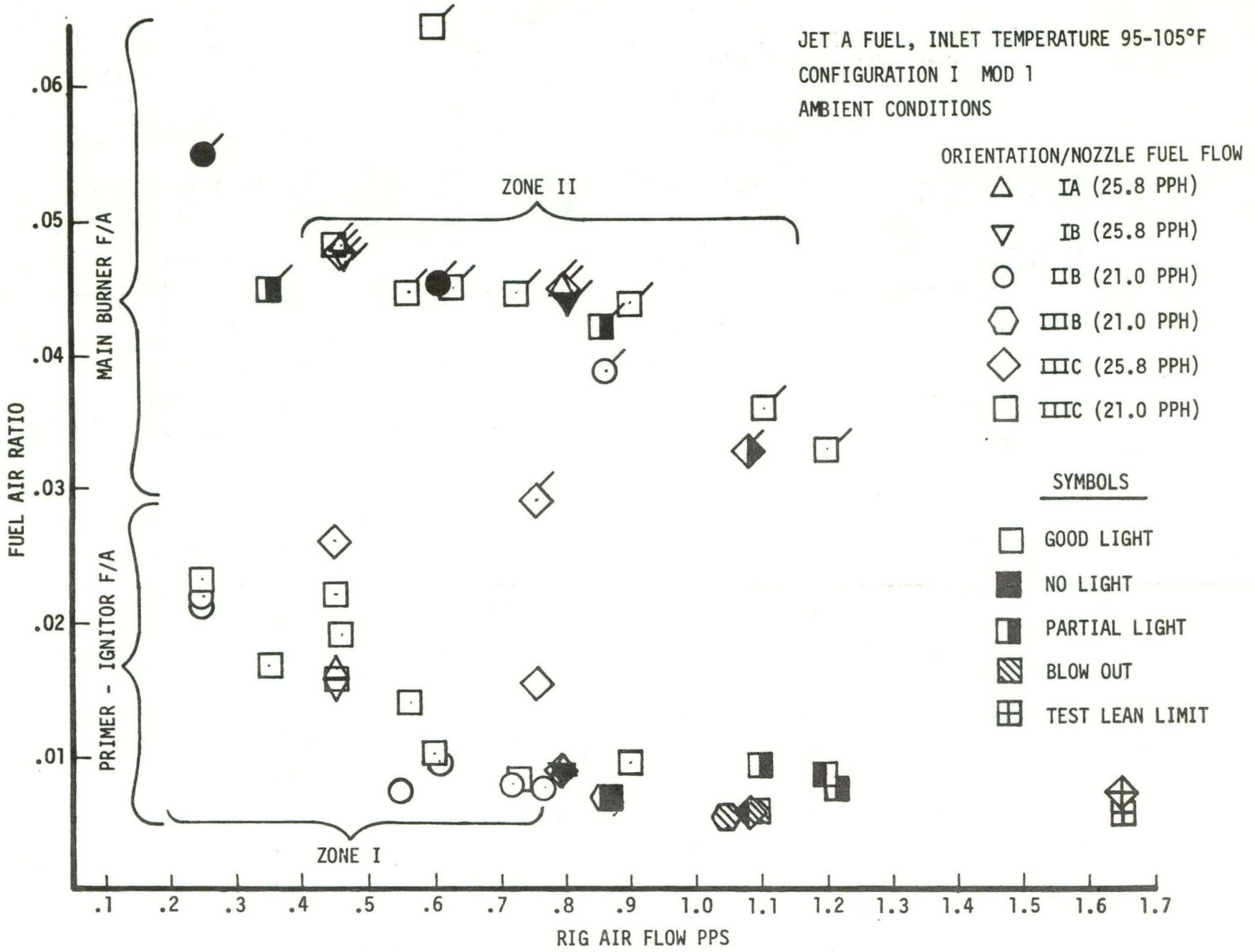

Figure 6.9
6-16

TSTR COMBUSTOR PRIMER-IGNITER ORIENTATION SURVEY

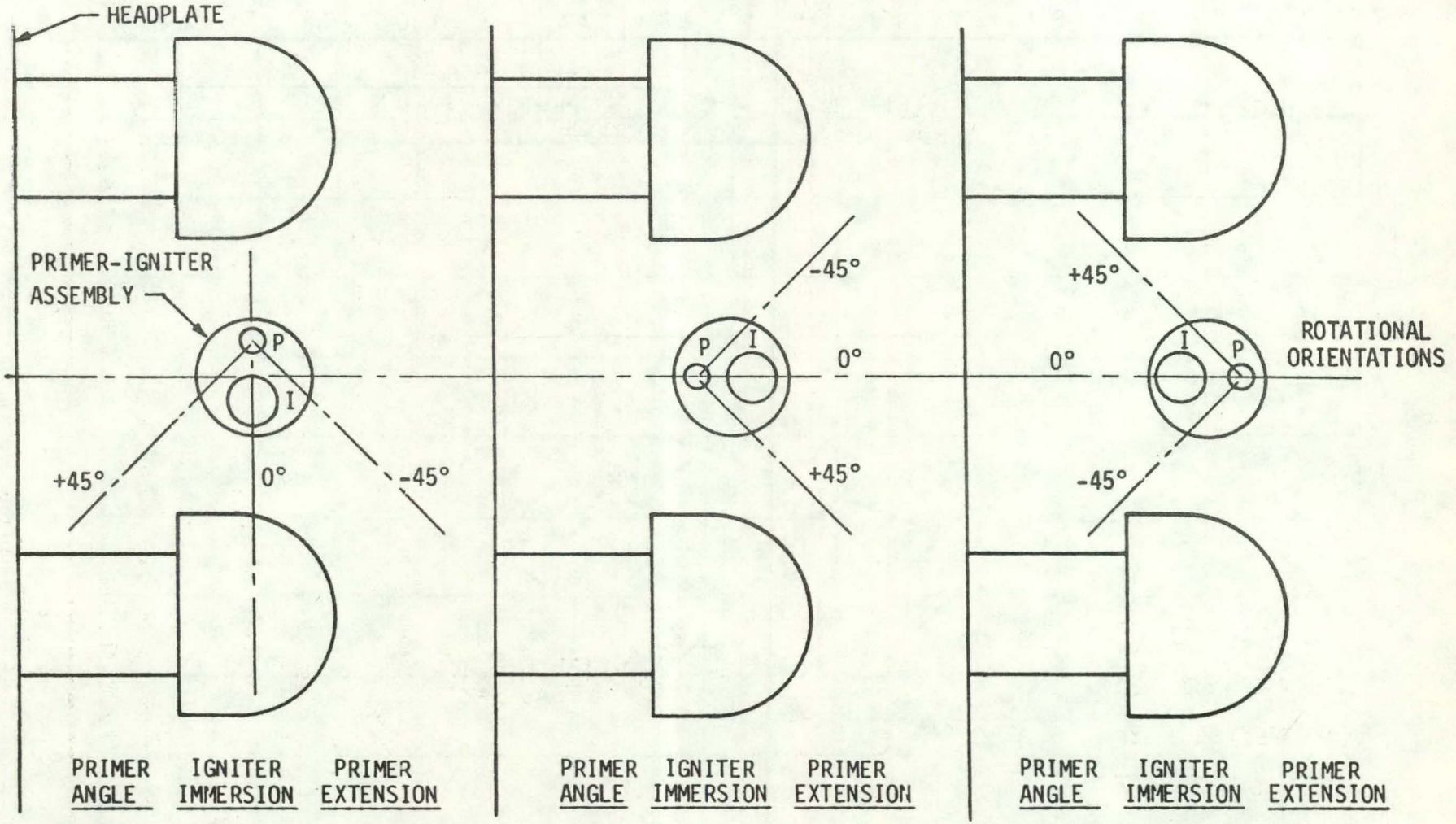

	PRIMER ANGLE	IGNITER IMMERSION	PRIMER EXTENSION
IA	+45°	0.500	NO SHIM
IB	0°		
IC	-45°		FULL SHIM
IAA	+45°		
IBB	0°		
ICC	-45°		

	PRIMER ANGLE	IGNITER IMMERSION	PRIMER EXTENSION
□A	+45°	0.500	NO SHIM
□B	0°		
□C	-45°		FULL SHIM
□AA	+45°		
□BB	0°		
□CC	-45°		

	PRIMER ANGLE	IGNITER IMMERSION	PRIMER EXTENSION
□□A	+45°	0.500	NO SHIM
□□B	* 0°		
□□C	*-45°		FULL SHIM
□□AA	+45°		
□□BB	0°		
□□CC	-45°		

*MOST EFFECTIVE

Figure 6.10

TSTR COMBUSTOR OBSERVED REGIONS OF STABLE OPERATION FOR LIGHT-OFF AND IDLE CONDITIONS

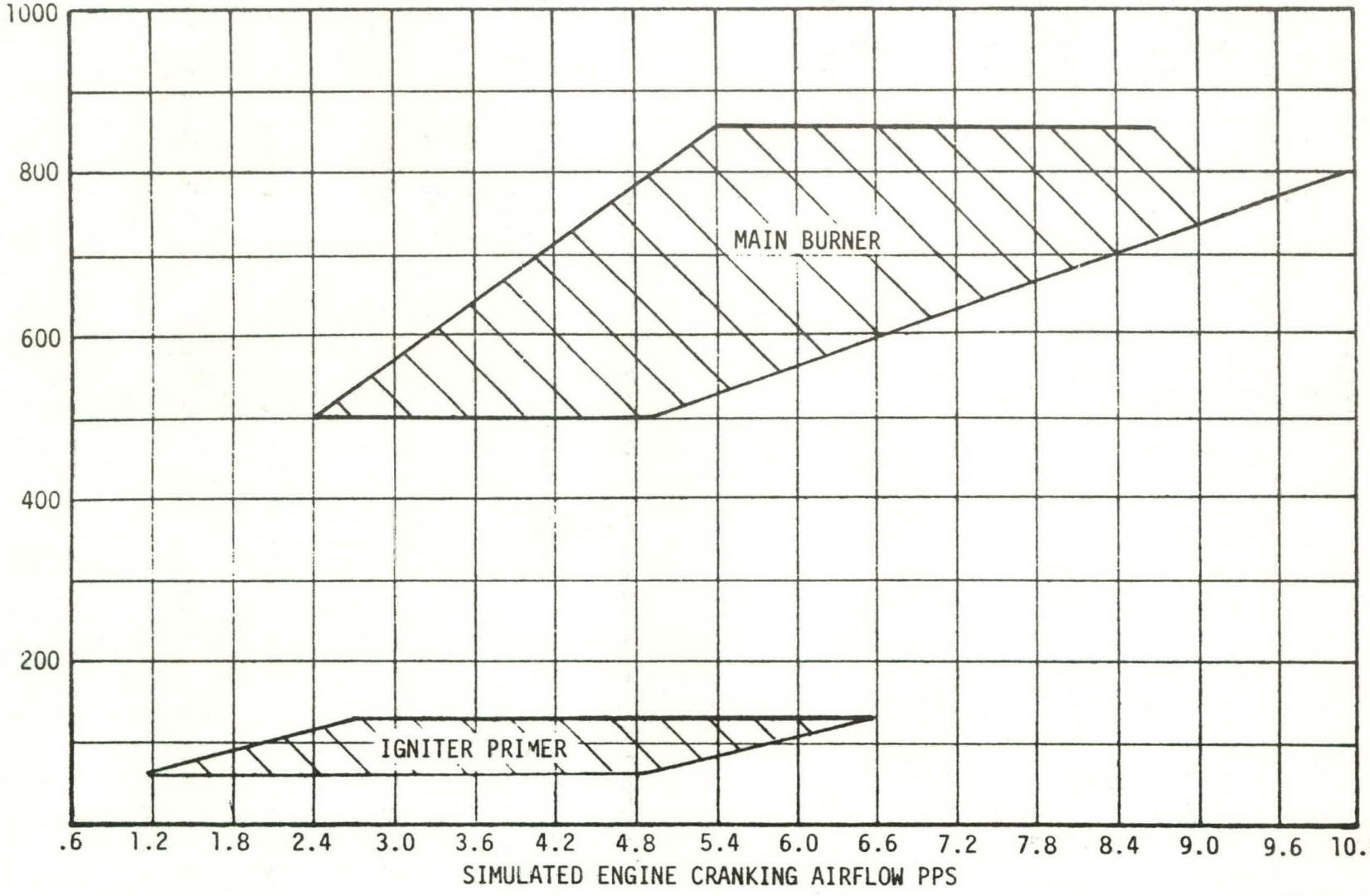

HTT-II-444

Figure 6.11

The blocked combustor holes are then systematically opened in an appropriate sequence until the entire combustor is uncovered. Determination of the flow distribution is based on a comparison of the flow measurements and static pressure differences across the liners between the taped and untaped hole tests. With all combustor holes unblocked and diffuser inlet flow at the design condition, the static and total pressures are measured. The static pressure differences are then calculated between upstream flowing locations at the inner, outer liner and headplate to downstream locations. To determine the flow for the vaporizer tubes, the data from the vaporizer tube flow test is reviewed to select the conditions which have the same vaporizer tube inlet-to-combustor exit static pressure differential as that of the test with all holes unblocked. The airflow rate measured for the vaporizer tube at the blocked condition is then assumed to be equal to the airflow at the unblocked condition. This is continued in an appropriate sequence until all holes are unblocked.

The pressure drop measurements, which were performed first, used a four probe rake to sweep the combustor exit plane. Tests were conducted at nominal upstream stagnation pressures of two, four and six atmospheres.

Following this, the airflow distribution measurements as previously described were performed at one atmosphere pressure and consisted of a sequence of 16 steps to determine incremental airflows for the various combustor openings proper, plus other combustor rig airflow paths which included water cooled side wall leakage, outer liner and inner liner downstream cooling slot flow and fishmouth leakage flow.

The Hewlett Packard Data Acquisition System was used to record the various pressure, temperature and flow measurements. A sample of the data system graphic and tabular printouts for the cold flow program is shown in Figures 6.12 and 6.13.

TSTR 60° COMBUSTOR SECTOR RIG - TYPICAL EXIT PRESSURE PROFILE PLOTS

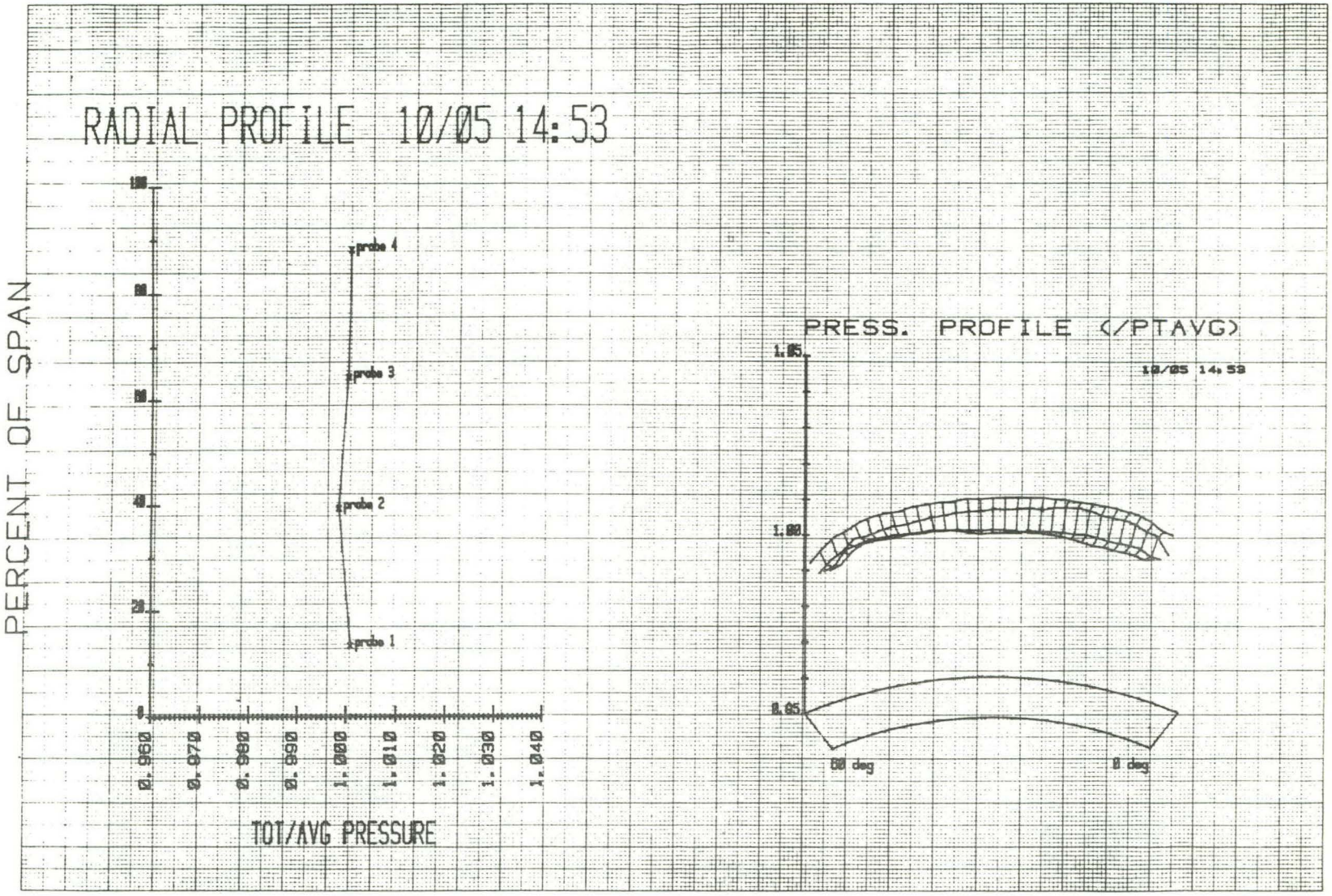

HTT-II-886

Figure 6.12

TSTR 60° COMBUSTOR SECTOR RIG - TYPICAL SWEEP-PROBE DATA PRINTOUT

HP COMBUSTOR - SWEEP PROBE CALCULATIONS 10/05 14:53

RIG9063 BUILD 0 BURNER CONFIG 1 BURNER MOD 1 IGNITER CONFIG 1 TEST RUN TEST STAND 4

WAP	:PRMARY AIR	4.31295	PPS	WP√T/P	:FLOW PARAM	3.40768		PTEXIT	:EXIT AVG	58.28988	IHGA
WATBL	:TURB BL L	0.05060	PPS	WB√T/P	:FLOW PARAM	2.97323		PTIN	:INLET AVG	59.82458	IHGA
WATBR	:TURB BL R	0.04135	PPS	TTIN	:INLET AVG	79.06840	DEGF	DEL P	:PRESS DROP	1.53471	IHGA
WAOB	:OB BLEED	0.45792	PPS					DP/PIN	:LOSS FACTR	0.02565	
WAB	:BURNER AIR	3.76309	PPS					PTMAX	:EXIT MAX	58.47970	IHGA
								PRATIO	:MAX/AVG R	1.00326	

HP COMBUSTOR - SWEEP PROBE DATA

PROBE 1		PROBE 2		PROBE 3		PROBE 4	
Pos (deg)	Press (inHga)	Pos (deg)	Press (inHga)	Pos (deg)	Press (inHga)	Pos (deg)	Press (inHga)
0.3	58.36	59.7	58.04	0.1	58.15	59.7	57.89
2.1	58.30	57.6	58.05	2.2	58.38	57.7	58.04
4.2	58.31	55.6	58.25	4.0	58.38	55.6	58.16
6.0	58.30	53.4	58.26	6.1	58.44	53.6	58.19
8.0	58.28	51.2	58.29	7.9	58.46	51.3	58.27
9.9	58.29	49.1	58.27	9.9	58.44	49.2	58.30
11.9	58.27	47.1	58.26	12.0	58.44	47.1	58.31
14.0	58.28	45.0	58.24	13.8	58.47	44.8	58.29
15.9	58.31	42.7	58.22	15.9	58.48	42.8	58.33
17.9	58.32	40.7	58.23	17.7	58.46	40.7	58.33
19.8	58.32	38.6	58.21	19.8	58.43	38.6	58.34
21.8	58.33	36.3	58.18	21.7	58.38	36.4	58.33
23.6	58.33	34.2	58.14	23.7	58.38	34.3	58.36
25.7	58.33	32.2	58.10	25.7	58.36	32.2	58.35
27.9	58.35	30.0	58.12	27.6	58.34	30.2	58.36
30.1	58.35	27.8	58.13	29.7	58.34	28.1	58.38
32.1	58.33	25.8	58.13	31.7	58.32	26.2	58.38
34.2	58.35	23.9	58.17	33.8	58.31	24.2	58.39
36.5	58.37	21.9	58.17	35.9	58.31	22.2	58.41
38.6	58.37	20.0	58.19	37.9	58.29	20.3	58.40
40.7	58.39	18.0	58.20	40.2	58.27	18.2	58.41
42.9	58.38	15.9	58.20	42.3	58.24	16.4	58.41
45.0	58.40	14.1	58.23	44.4	58.22	14.3	58.42
47.0	58.39	12.0	58.23	46.6	58.23	12.4	58.43
49.1	58.41	10.2	58.22	48.7	58.21	10.4	58.44
51.4	58.44	8.1	58.23	50.8	58.19	8.4	58.43
53.4	58.44	6.3	58.25	53.1	58.20	6.6	58.44
55.5	58.38	4.2	58.26	55.1	58.05	4.5	58.40
57.7	58.22	2.2	58.19	57.2	57.98	2.6	58.32
59.9	58.20	0.3	58.21	59.2	57.85	0.6	58.31

Figure 6.13

The combustor pressure-drop is defined as the overall total pressure drop from the compressor exit (rig bellmouth throat area) to combustor exit and as such includes compressor diffuser loss, total pressure loss due to cooling shroud and combustor liner and heat addition total pressure loss. The pressure drop measurements presented herein are for "cold" flow conditions only and therefore do not include losses associated with heat addition.

The overall cold total pressure drop measurements (in percent) as a function of $\frac{W\sqrt{T}}{P}$ as determined by the total pressure sweep rake (at a nominal inlet total pressure of two atmospheres) are shown in Figure 6.14 by the circle symbols. Here W excludes all bleed flows and T and P refer to total temperature and total pressure measured at the bellmouth throat at the inlet to the combustor sector.

The overall total pressure drop was also derived independently from airflow distribution measurements using the measured upstream total pressure, combustor exit static pressure and computed exit Mach number. The three points obtained by this method are shown as square symbols connected by a dotted line in Figure 6.14.

Examination of Figure 6.14 shows that the pressure drop computed from a single static pressure and exit Mach number is slightly higher than the more precise total pressure measurements.

Pressure drop as derived from measurements of combustor exit airflow plus $\Delta P \quad \frac{W\sqrt{T}}{P}$ fishmouth leakage is presented in Figure 6.15 as the solid line. From Figure 6.14, at $W\sqrt{T/P} = 4.254$ the difference between measured and derived pressure drop is 0.26 percentage points. This adjustment is then applied to Figure 6.15 data at $W\sqrt{T/P} = 4.254$ to give the corrected square relationship curve shown as a dotted line.

TSTR 60° COMBUSTOR SECTOR RIG
TOTAL PRESSURE LOSS AS A FUNCTION
OF $W\sqrt{T}/P$

2 ATMOSPHERES NOMINAL UPSTREAM TOTAL PRESSURE

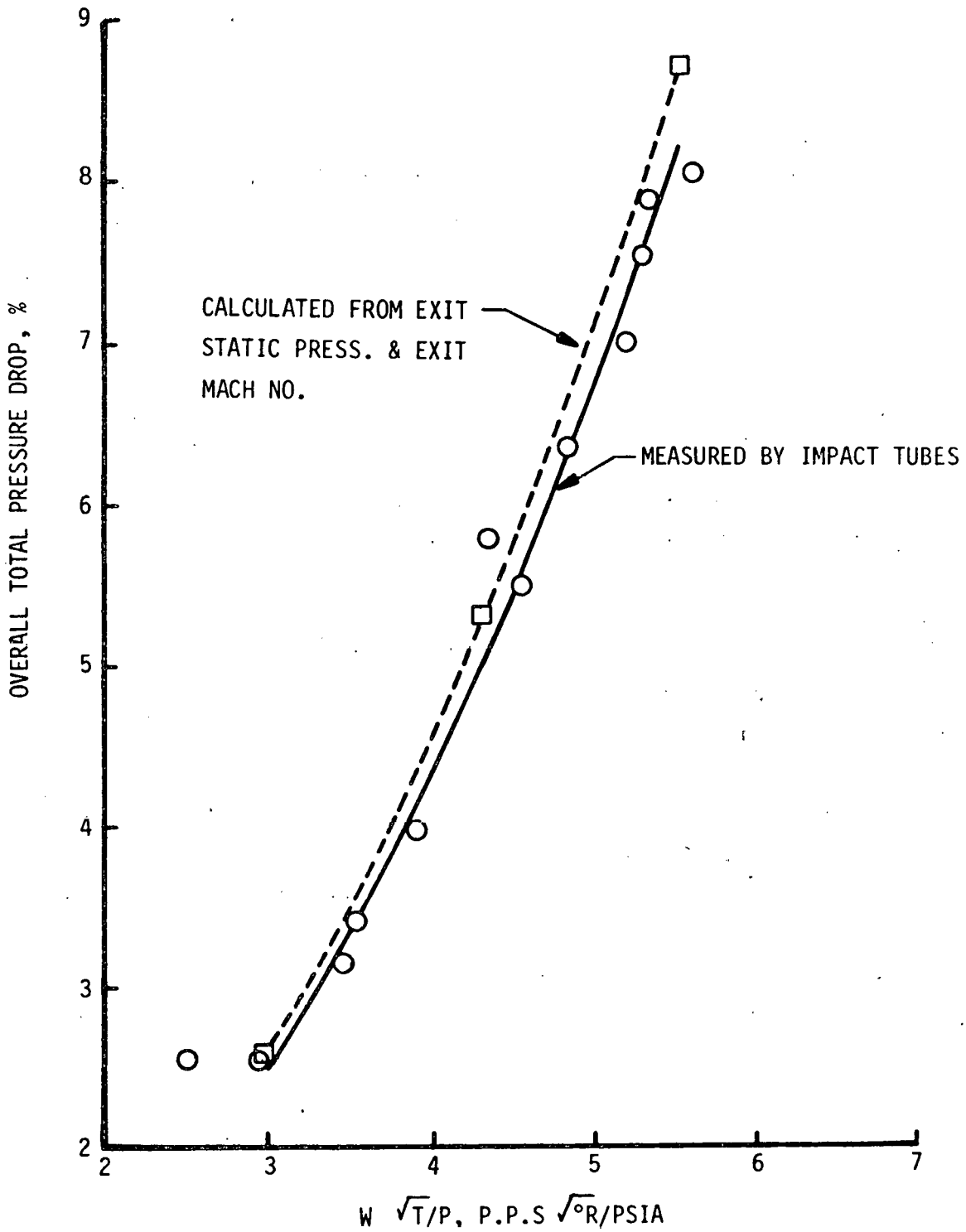

Figure 6.14

TSTR 60° COMBUSTOR SECTOR RIG
TOTAL PRESSURE LOSS AS A FUNCTION
OF $W\sqrt{T}/P$

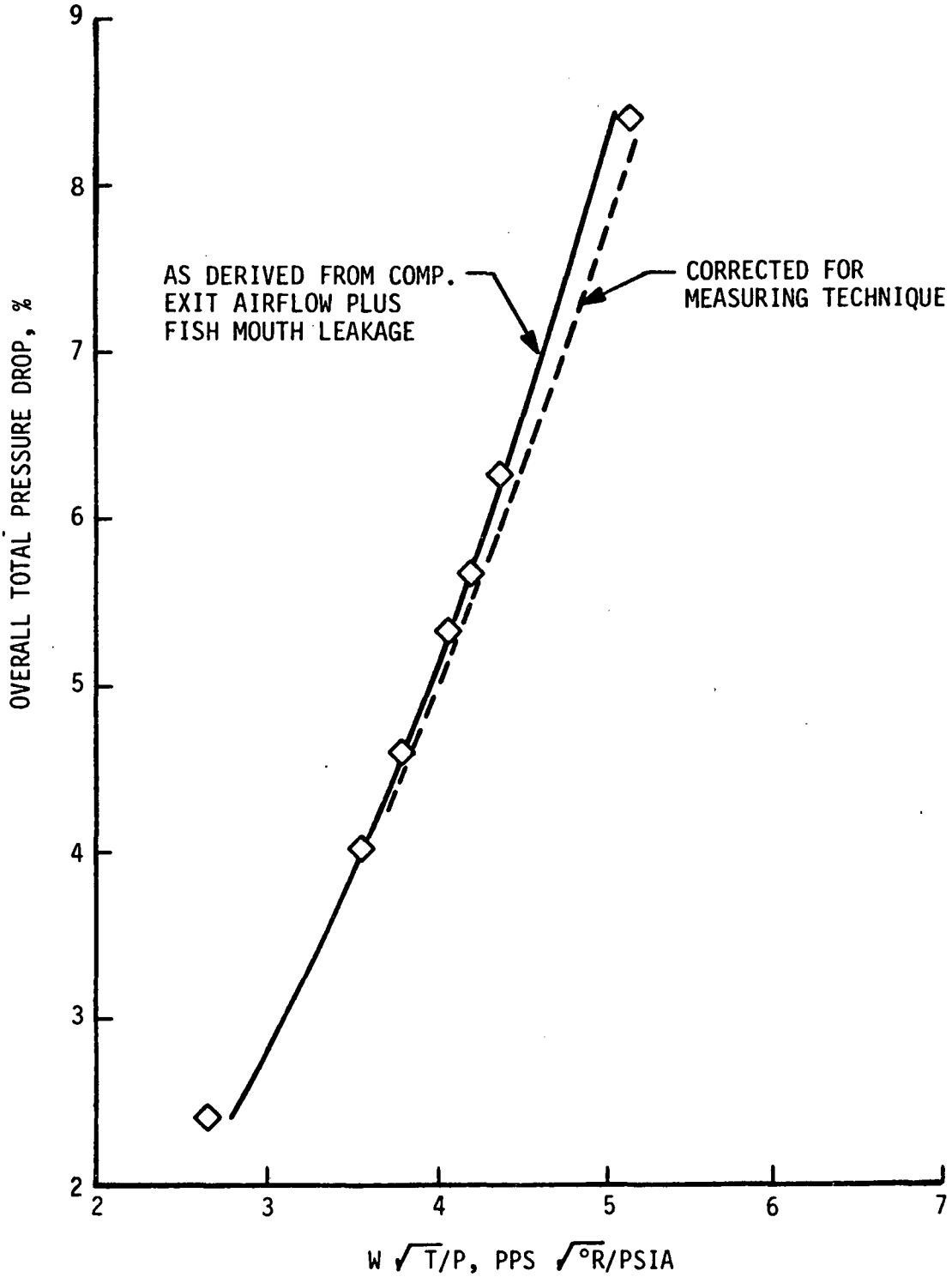

Figure 6.15

In order to be able to compare the test results with the predicted cold pressure drop, a further correction is required to exclude fishmouth leakage area and side wall leakage area. From the airflow distribution measurements (to be discussed later) the ratio of total effective area without fishmouth leakage and side wall leakage to total effective area with fishmouth leakage and side wall leakage is 0.9005. Therefore approximately 10% of the effective flow area is the sum of side wall leakage area and fishmouth leakage area. The revised pressure drop "as tested" using the corrected curve of Figure 6.15 and modified for leakage area by relationship $\frac{\Delta P}{P_T} \sim \frac{W\sqrt{T}}{P_T A_{eff}}$ is given as the top curve of Figure 6.16. Also shown in Figure 6.16 is the estimated cold pressure drop.

The initial estimate of overall cold pressure drop assumed that the compressor diffuser loss would be insignificant. However, measurement of the pressure drop from the bellmouth throat area (PT2) to total pressure ahead of the vertical centerline vaporizer tube (PT7) results in a diffuser pressure drop $\Delta p/q = .29$ which at the compressor design discharge Mach number results in a pressure drop $\frac{PT7-PT2}{PT7} \times 100$ equal to 0.7%. If this compressor diffuser loss is applied to the overall pressure drop at the combustor design flow parameter $W\sqrt{T}/P = 4.254$ the combustor shroud and liner cold pressure drop is (6.7 - .7) = 6.0% rather than the estimated value of 4.91%.

The airflow distribution measurements consisted of a sequence of 16 tests to determine incremental airflows through the various combustor openings, plus airflow through other airflow paths not present in the combustor but present in the combustor rig.

The results of this series of tests are given in Table 6-3. Listed for the 16 tests are the applicable results in Columns A through K. Column A and B are the sequence number and description of sequential flow increment. Column C is the pressure ratio used to establish the incremental flow. Column D is the numerical value of Column C taken from sequence 14 at $W\sqrt{T}/P = 4.254 + .168 = 4.422$, that is the design flow factor plus the fishmouth leakage. Column E is the measured cumulative $W\sqrt{T}/P$. Columns F and G are the incremental $W\sqrt{T}/P$ measured and estimated, respectively. Column H is the best assessment of the incremental airflow factor taking into account all variables.

TSTR 60° COMBUSTOR SECTOR RIG
TOTAL PRESSURE LOSS AS A FUNCTION
OF W $\sqrt{T/P}$

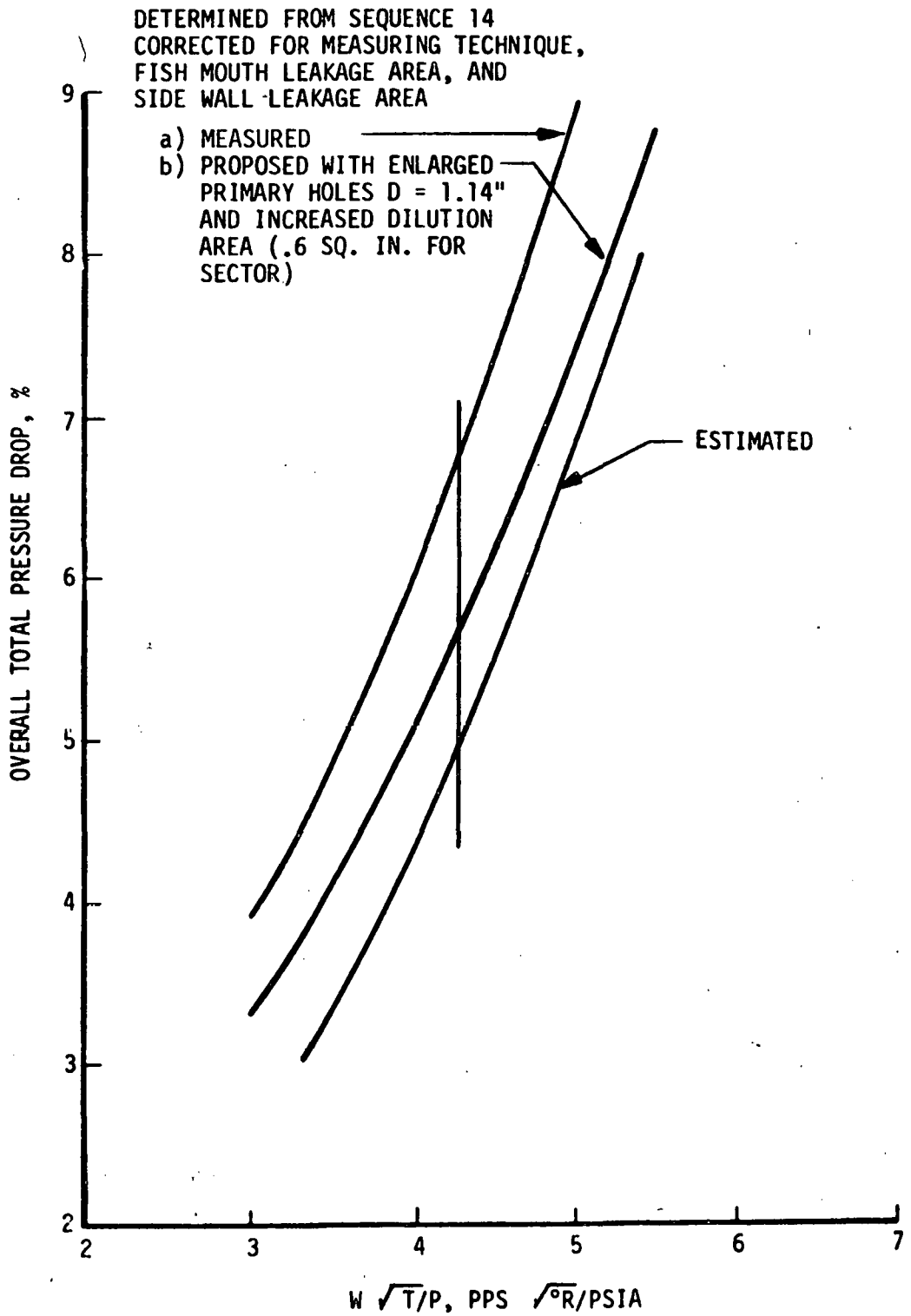

Figure 6.16

Table 6-3

TSTR 60° COMBUSTOR SECTOR PRESSURE DROP CALIBRATION

A	B	C	D	E	F	G	H	I	J	K
Sequence No.	Description of Sequence	Pressure Ratio Used For Sequence	Value of Pressure Ratio Used For Sequence	Measured Cumulative $W\sqrt{T}/P$	Measured Incremental $W\sqrt{T}/P$	Est $W\sqrt{T}/P$	Best Assessment of $W\sqrt{T}/P$	P.Z. $W\sqrt{T}/P$	Cooling Flow $W\sqrt{T}/P$	Dilution Flow $W\sqrt{T}/P$
1	Vaporizer Tubes Plus Sidewall Leakage	PT8-PS36 / PT8	.0521	.978	.978	.7057	.706**	.706	-	-
2	O.L. & I.L. Rear Seals	PS78-PS80 / PT2	.0563	1.146	.168	-	-	-	-	-
3	I.L. Cooling Nugget #1	PT7-PS36 / PT7	.0573	1.206	.060	.0556	.060*	-	.060	-
4	I.L. Primary Holes	PT11-PS36 / PT11	.0504	1.835	.629	.9603	.831**	.831	-	-
5	I.L. Cooling Nuggets #2,#3,#4	PT14-PS79 / PT14	.0572	2.220	.385	.1828	.183**	-	.183	-
6	I.L. Dilution Holes	PT17-PS79 / PT17	.0574	2.380	.160	.1708	.160*	-	-	.160
7	I.L. Cooling Nugget #5	PT17-PS79 / PT17	.0574	2.554	.174	.0799	.108	-	.108	-
8	I.L. Cooling Nugget #6	PS83-PS79 / PS83	.0608	2.628	.074	.0847	.074*	-	.074	-
9	O.L. Cooling Nugget #1	PT7-PS35 / PT7	.0575	2.660	.034	.0756	.100	-	.100	-
10	O.L. Primary Holes	PS9-PS35 / PS9	.0400	3.470	.810	.09603	.790**	.790	-	-

Table 6-3 (continued)

TSTR 60° COMBUSTOR SECTOR PRESSURE DROP CALIBRATION

A	B	C	D	E	F	G	H	I	J	K
Sequence No.	Description of Sequence	Pressure Ratio Used For Sequence	Value of Pressure Ratio Used For Sequence	Measured Cumulative $W\sqrt{T}/P$	Measured Incremental $W\sqrt{T}/P$	Est $W\sqrt{T}/P$	Best Assessment of $W\sqrt{T}/P$	P.Z. $W\sqrt{T}/P$	Cooling Flow $W\sqrt{T}/P$	Dilution Flow $W\sqrt{T}/P$
11	O.L. Cooling Holes #2,#3,#4	PT13-PS79 / PT13	.0566	3.715	.245	.2648	.265**	-	.265	-
12	O.L. Dilution Holes	PT13-PS79 / PT13	.0566	4.182	.467	.5123	.467**	-	-	.467
13	O.L. Cooling Nugget #5	PT13-PS79 / PT13	.0566	4.300	.118	.1025	.118*	-	.118	-
14	O.L. Cooling Nugget #6	PT13-PS79 / PT13	.0566	4.422	.120	.0990	.120	-	.120	-
15	O.L. & I.L. Downstream Cooling Slots	PT13-PS79 / PT13	.0566	4.720	.298	-	-	-	-	-
16	Water Cooled Side-Wall Leakage	PT13-PS79 / PT13	.0566	4.790	.070	-	-	-	-	-
		[.978 - .706 = .272]					.272			
			Totals		4.790	4.254	4.254	2.327	1.028	.627
	Proportional distribution of side wall leakage							.159	.070	.043
								3.486	1.098	.670
				Flow Breakdown Percentage from Measurements				58.4%	25.8%	15.8%
				Flow Breakdown Percentage Est.				61.7%	22.2%	16.1%

**Appropriate sum agrees with measured value.

*Agrees with measured value.

Sequence 1 includes side wall leakage, not independently measured, therefore the "best" assessment for sequence 1 flow factor was assumed to be the design value. Subsequently the difference between the measured flow factor and the design value was proportionally distributed among the primary zone air, cooling air and dilution air. Sequence 3 flow factor is the measured value. From pressure measurements it was observed that considerable flow interference existed in the shroud between sequences 4 and 5. Since the sum of sequence 4 and 5 equals the primary air plus the inner liner cooling nuggets #2, #3 and #4, it was decided to assign to the cooling nuggets the design value of the flow factor and the remainder of the flow factor $\frac{W\sqrt{T}}{P_T}$ was assumed to be the primary flow. Sequence 6 was consequently assigned the measured value. Based on analysis of the data scatter and trends, sequence 7 was assigned a value somewhat higher than design whereas sequence 8 used the measured value. Sequence 9 was assigned a value somewhat higher than the design value. Since considerable observed flow interference also existed between sequence 10 and sequence 11, it was decided to distribute the flow by assigning the design value for outer liner cooling nuggets #2, #3 and #4 and the remaining flow to the primary air. Sequence 12, 13 and 14 were assigned the measured values.

Columns I, J and K divide the flow given in Column H into primary zone, cooling flow and dilution flow. The side wall leakage flow was then divided proportionally to arrive at the measured percentage flow split. The design estimated flow split is also shown. Comparison of the test results with the design values indicates that the primary flow split was 3% below the predicted value while the cooling flow split was approximately 3% above the predicted value.

The measured convective outer liner shroud average Mach number was found to be equal to the design value of 0.108. Similarly, the actual convective inner liner shroud average Mach number was found equal to the design value of 0.101.

A review of the results shows that the primary zone airflow was less than predicted. The design of the primary holes was calculated using a discharge coefficient of .92. A review of the "best estimate" cold flow test results indicated the inner liner primary hole discharge coefficient to be .80 and the outer liner discharge coefficient to be .76.

Measured average radial pressure variation at the combustor exit was 0.2% while maximum variation was approximately 0.4%, thereby indicating no significant effects of dilution hole or other upstream disturbances.

Based on the test measurements, it appears that the primary holes should be increased from 1.024 inch diameter to 1.225 inch and the total dilution hole area increased by 8.550 square inches (1.425 square inch increase in the 60° sector) in order to achieve the design goal pressure drop of 4.91% (cold).

A summary of the predicted and measured flow splits and pressure drops is given below and in Figure 6.17. Also presented are the resulting flow splits and pressure drops for the indicated configuration change to achieve the design value overall pressure drop.

Summary of Results at $\frac{W\sqrt{T}}{P} = 4.254$

	% Airflow in P.Z.	% Cooling Air	% Dilution Air	% Compressor Diffuser Presssure Drop	Compressor Shroud and Liner % Pressure Drop (Cold)	% Overall Pressure Drop (Cold)
Measured	58.4	25.8	15.8	0.7	6.0	6.70
Configuration II	62.0	21.4	16.6	0.7	4.21	4.91

TSTR 60° COMBUSTOR SECTOR RIG TEST RESULTS
COLD FLOW PRESSURE LOSS & AIRFLOW
DISTRIBUTION TEST RESULTS (2, 4, 6 ATMS)

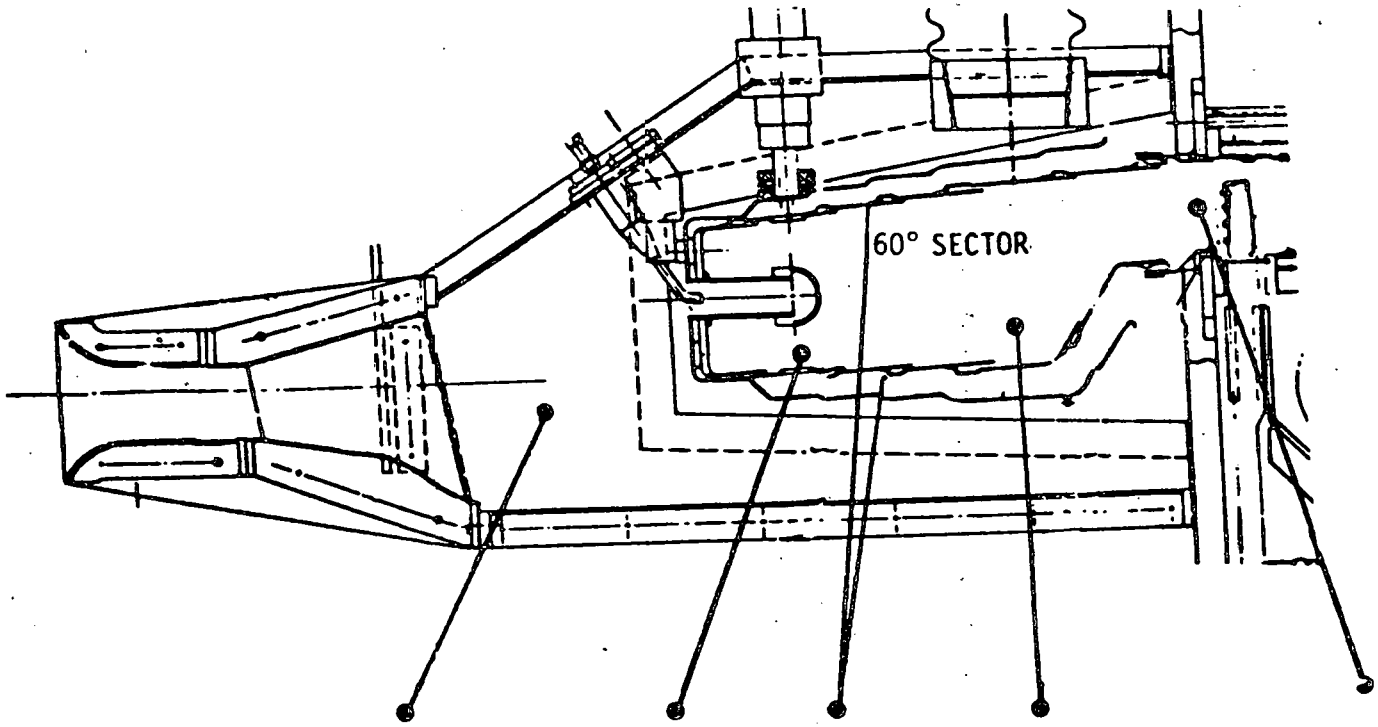

	DIFFUSER DUMP LOSS	PRIMARY ZONE AIRFLOW	BURNER COOLING AIRFLOW	DILUTION ZONE AIRFLOW	BURNER LINER LOSS	OVERALL PRESSURE LOSS
DESIGN	0%	51.7%	22.2%	16.1%	4.91%	4.91%
MEASURED	0.7%	58.4%	25.8%	15.8%	6.0%	6.70%

Figure 6.17

6.3 COMBUSTOR TEST CHRONOLOGY

Configuration I

Combustion tests with the instrumented Configuration I, the original design concept airflow distribution, were conducted at various pressure levels to evaluate the validity of the combustor design approach. The combustion tests were terminated prior to attaining the combustor design condition because of a test stand control failure which caused substantial damage to the 60° combustor and instrumentation, precluding further testing of this configuration. However, based on analysis of the performance and temperature data obtained, it was concluded that the selected combustor design concept demonstrated the potential to attain the TSTR performance goals at 3000°F exit temperature. The initial combustor performance results are shown in Figures 6.18 through 6.20. Combustion efficiency as shown in Figure 6.18 proved to be relatively insensitive to fuel-air ratio variation indicating that the primary combustion zone air-fuel loading was adequate for the required wide range of burner temperature rise. Although there was substantial scatter evident in the analysis of combustor exit temperature pattern factor, it appeared that combustor exit pattern would not be difficult to control. (See Figures 6.19 and 6.20.) Combustor wall and vaporizer wall temperature measurements results are shown in Figures 6.21 through 6.30. Measured temperatures as a function of fuel-air ratio and pressure level are shown in Figures 6.24, 6.25, 6.26 and 6.27. Measured temperature levels are significantly below the estimated levels described in Section 3 with the exception of nugget #6 which could exceed 1700°F when accounting for the effect of pressure level. The excessive temperature variation measured in the front section of the combustor (Liners #1 and #2) indicated non-axisymmetric fuel preparation in the primary zone with a resultant non-symmetric OD/ID temperature distribution (Figure 6.28). Louver lip temperatures of the #3 liner also exhibit an OD/ID temperature difference effect. However, the general temperature level of the lips and liner wall are significantly below the design objectives when accounting for effect of pressure level of 1320°F vs 1600°F estimated. Since the thermocouples were immersed into the sheet metal to provide an average bulk metal temperature measurement there was no reason to doubt the accuracy of these measurements.

TSTR 60° COMBUSTOR SECTOR RIG
VARIATION OF COMBUSTOR EFFICIENCY WITH
FUEL-AIR RATIO
CONFIGURATION I, JET A FUEL
2 ATMOSPHERES BURNER PRESSURE

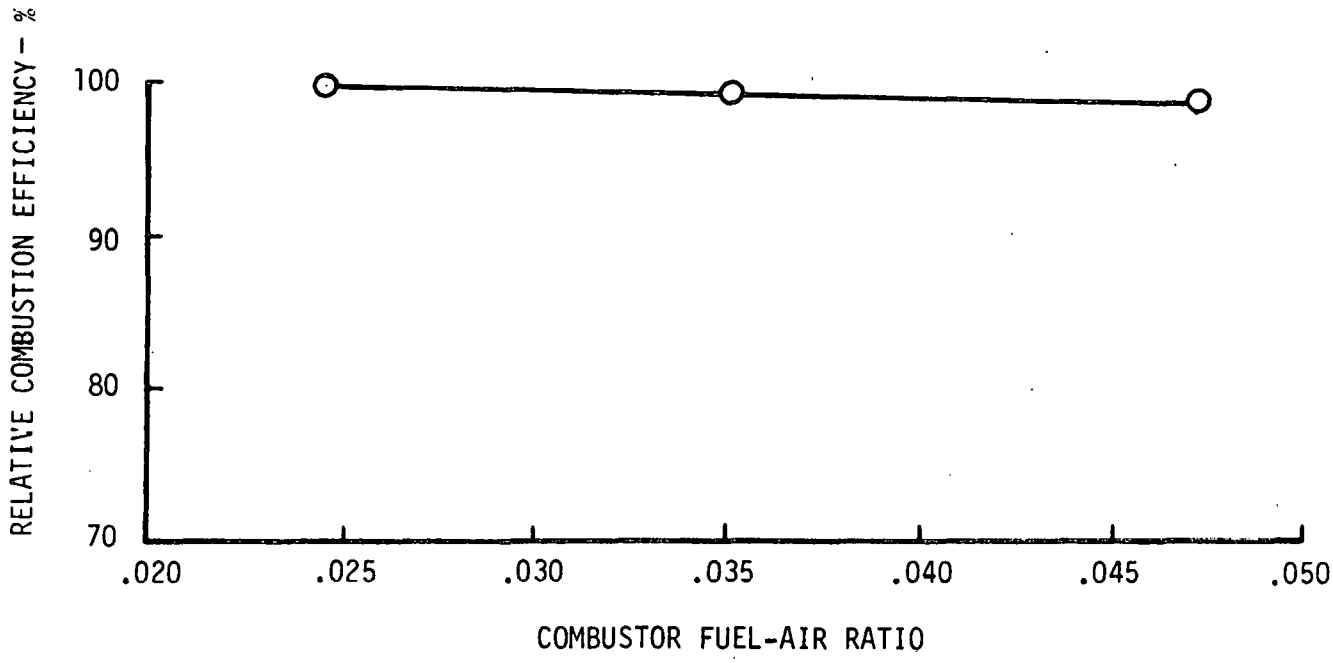

Figure 6.18

TSTR 60° COMBUSTOR SECTOR RIG
VARIATION OF COMBUSTOR EXIT PATTERN FACTOR
WITH TEMPERATURE RISE
CONFIGURATION I, JET A FUEL

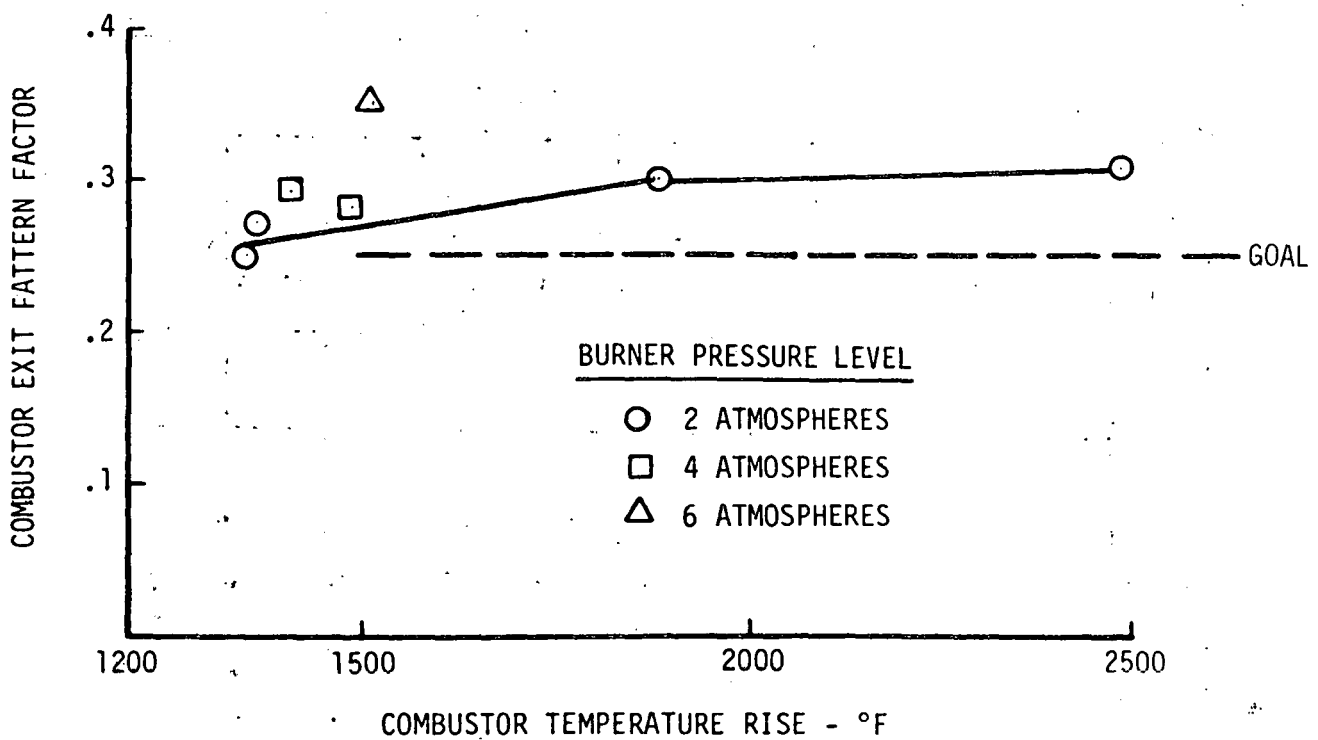

Figure 6.19

TSTR 60° COMBUSTOR SECTOR RIG
AVERAGE RADIAL PROFILE
CONFIGURATION I JET "A" FUEL
2 ATMOSPHERES PRESSURE LEVEL
FUEL-AIR RATIO .050

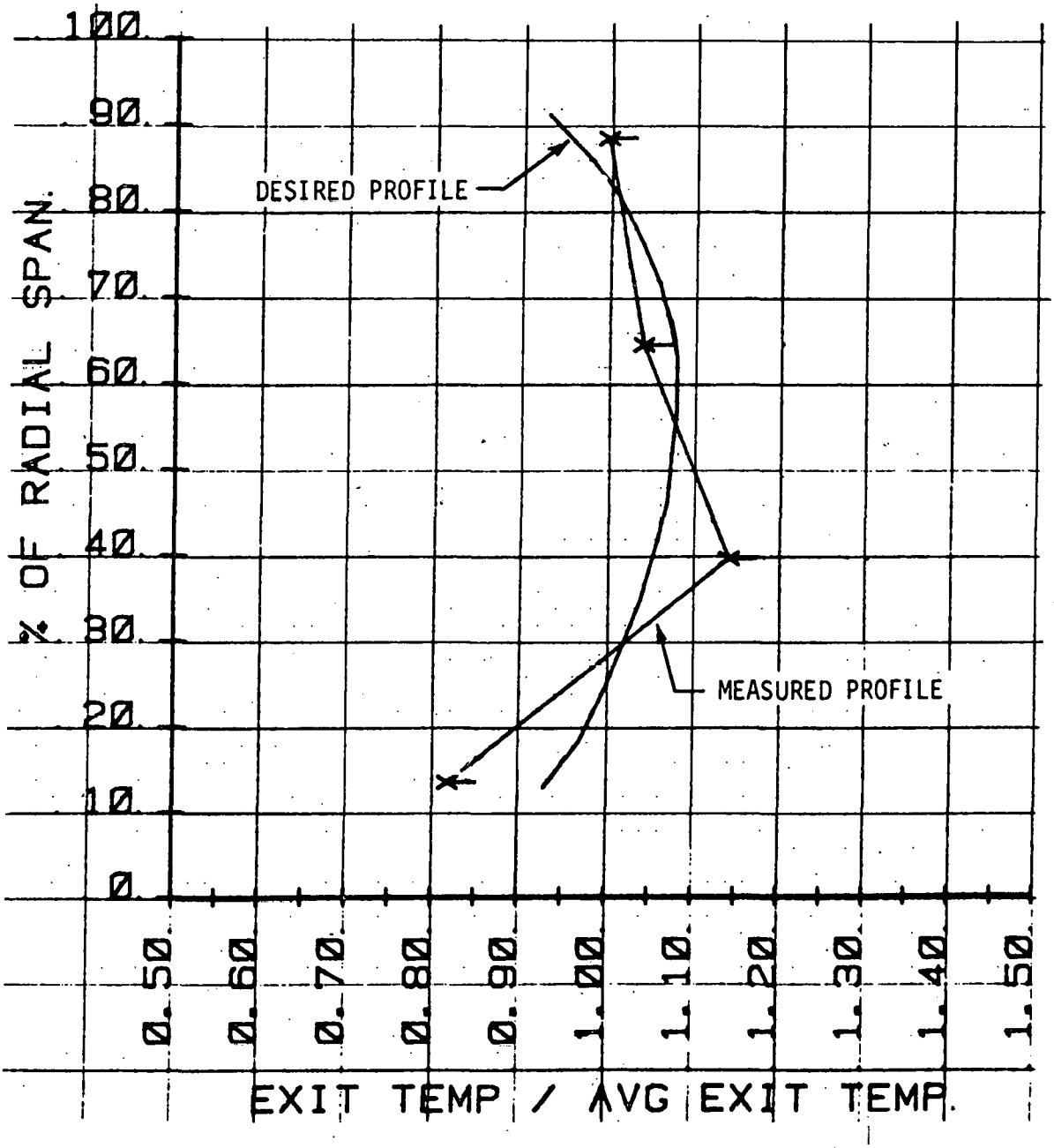

Figure 6.20

THERMOCOUPLE LOCATIONS ON COMBUSTOR LINER #3 CONFIGURATION I

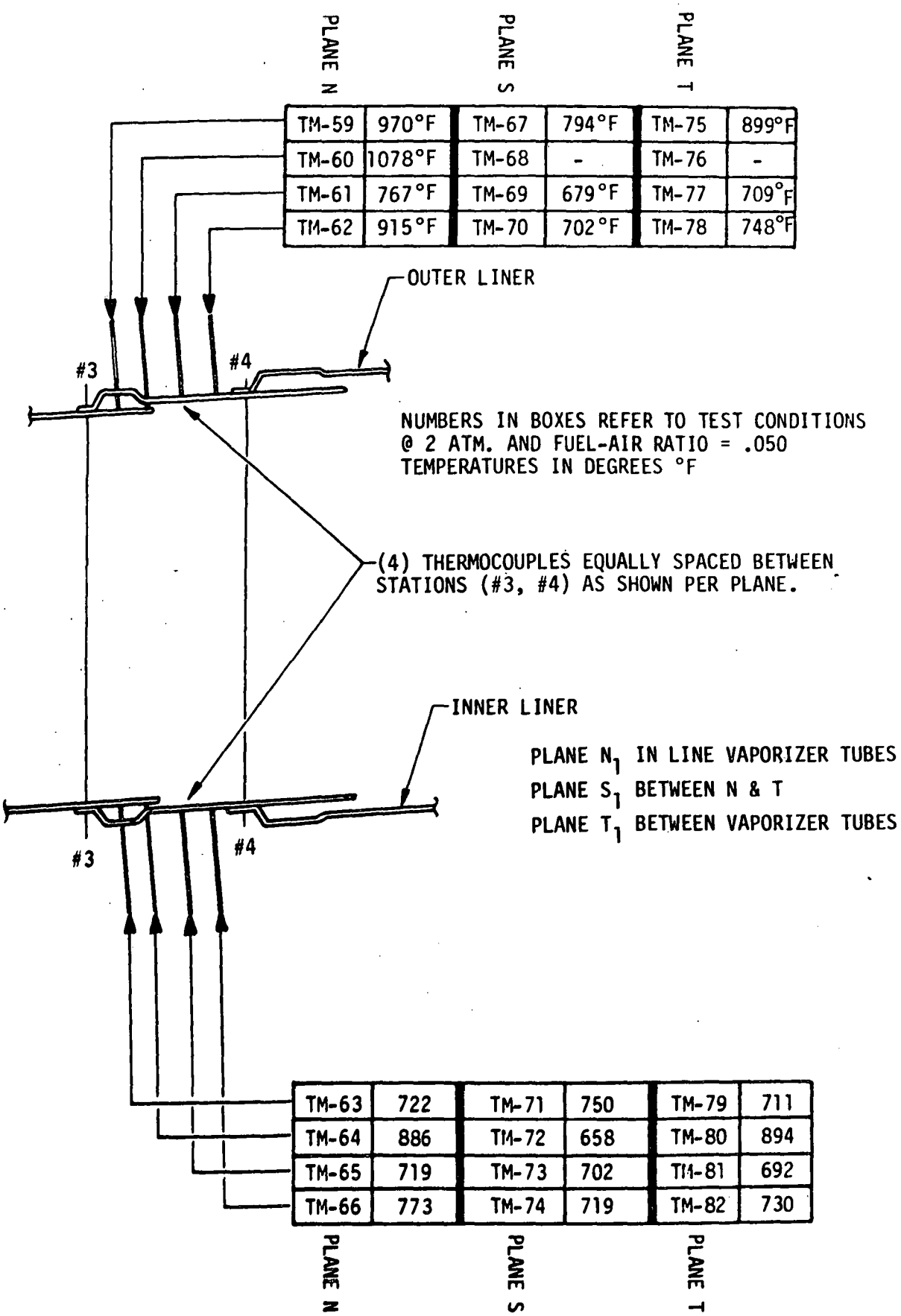

Figure 6.21

EFFECT OF FUEL-AIR RATIO ON METAL TEMPERATURES
DOWNSTREAM OF NUGGET #3 (O.L. AND I.L.)

AT 2 ATMS.
COMBUSTOR CONFIGURATION I
JET A FUEL

(See Figure 6.21)

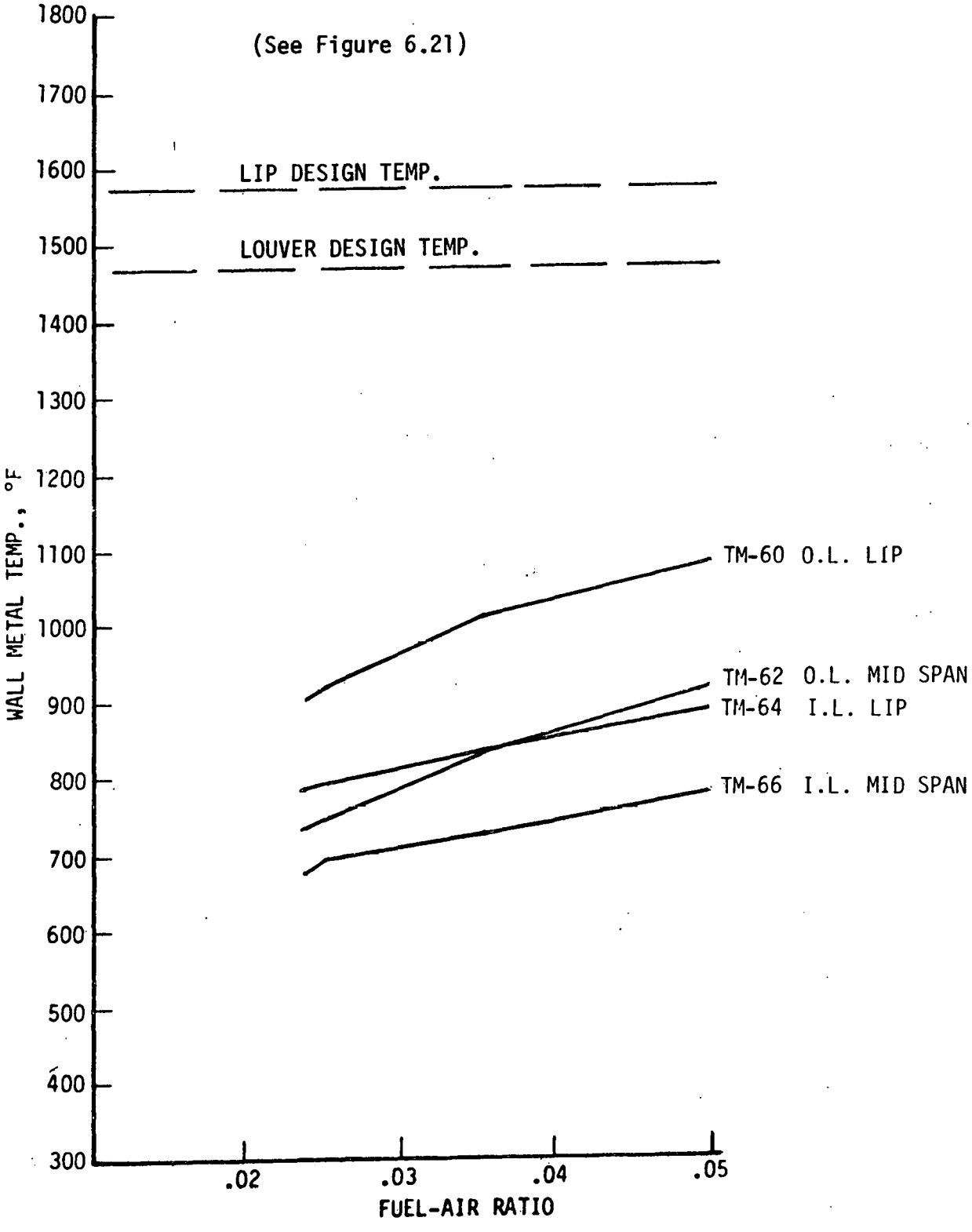

Figure 6.22

THERMOCOUPLE LOCATIONS ON COMBUSTOR WALL

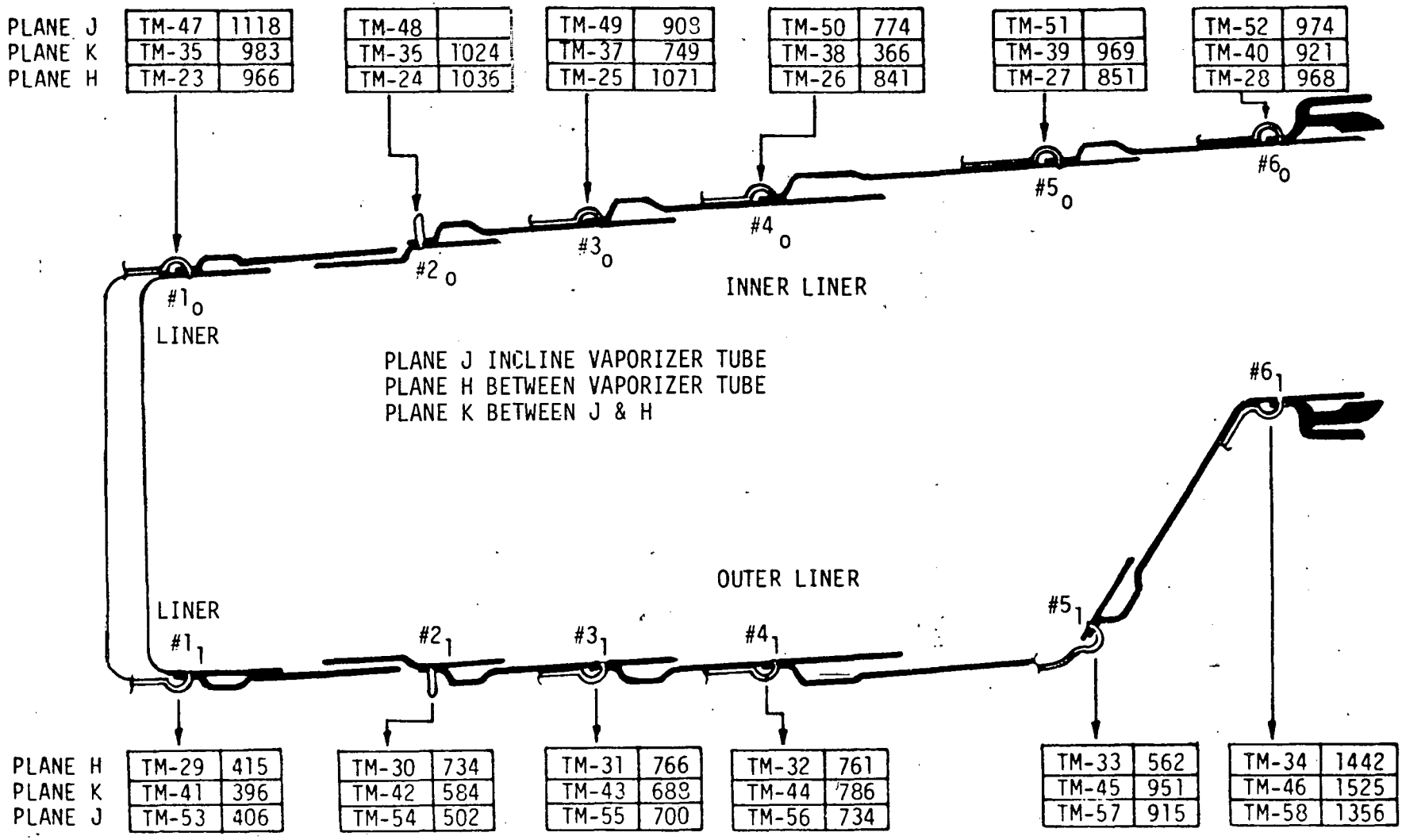

* NUMBER REFERENCE TO
TEST CONDITIONS @ 2 ATMS
& FUEL - AIR RATIO = .05
DEGREES °F

Figure 6.23

EFFECT OF FUEL-AIR RATIO ON COMBUSTOR LINER COOLING NUGGET "CRITICAL" POINTS

AT 2 ATMS.

COMBUSTOR CONFIGURATION I

JET A FUEL

(See Figure 6.23)

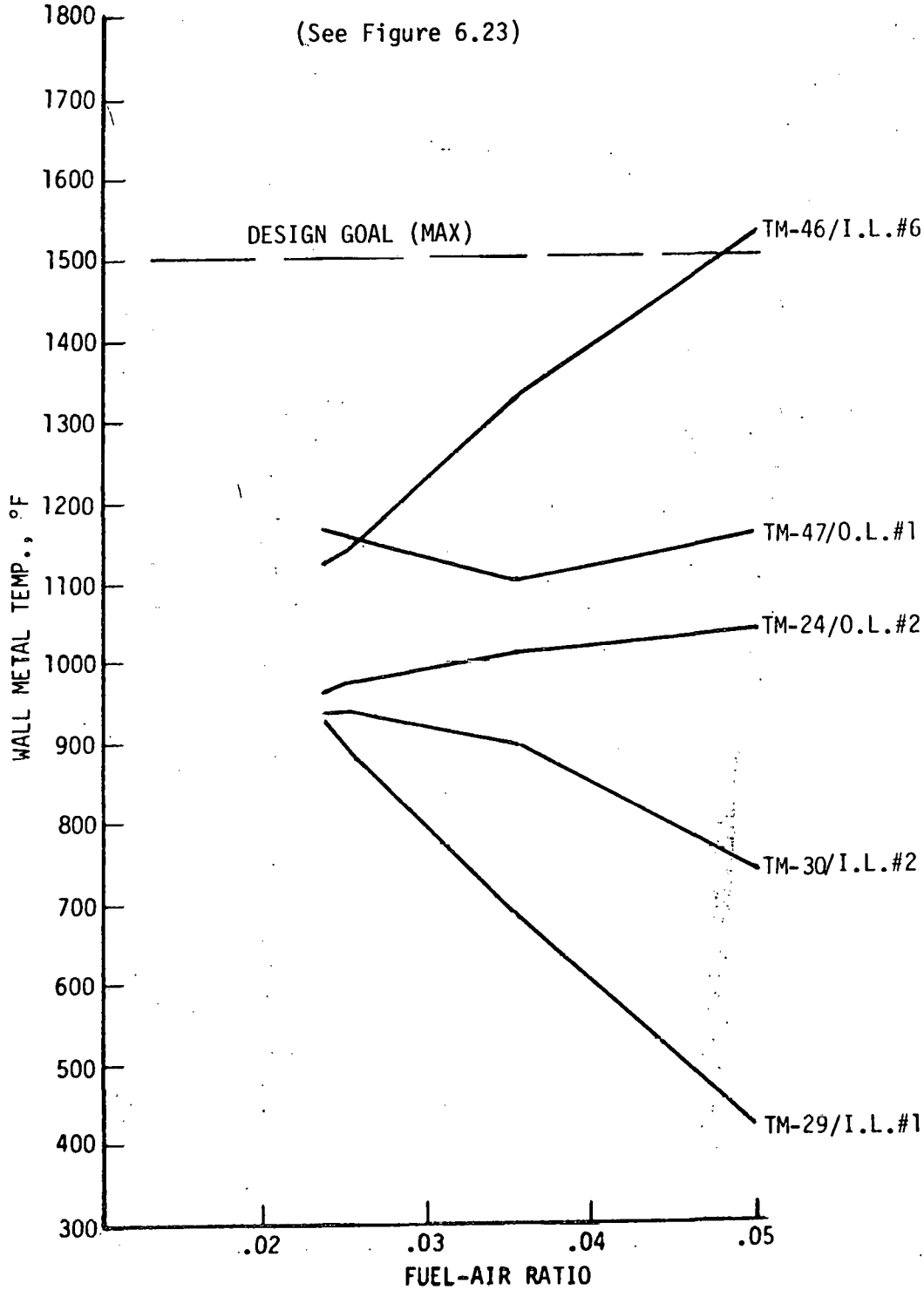

Figure 6.24

EFFECT OF PRESSURE LEVEL ON LINER COOLING NUGGET
"CRITICAL" POINTS

AT FUEL-AIR ≃ .023 TO .024
COMBUSTOR CONFIGURATION I
JET A FUEL
(See Figure 6.23)

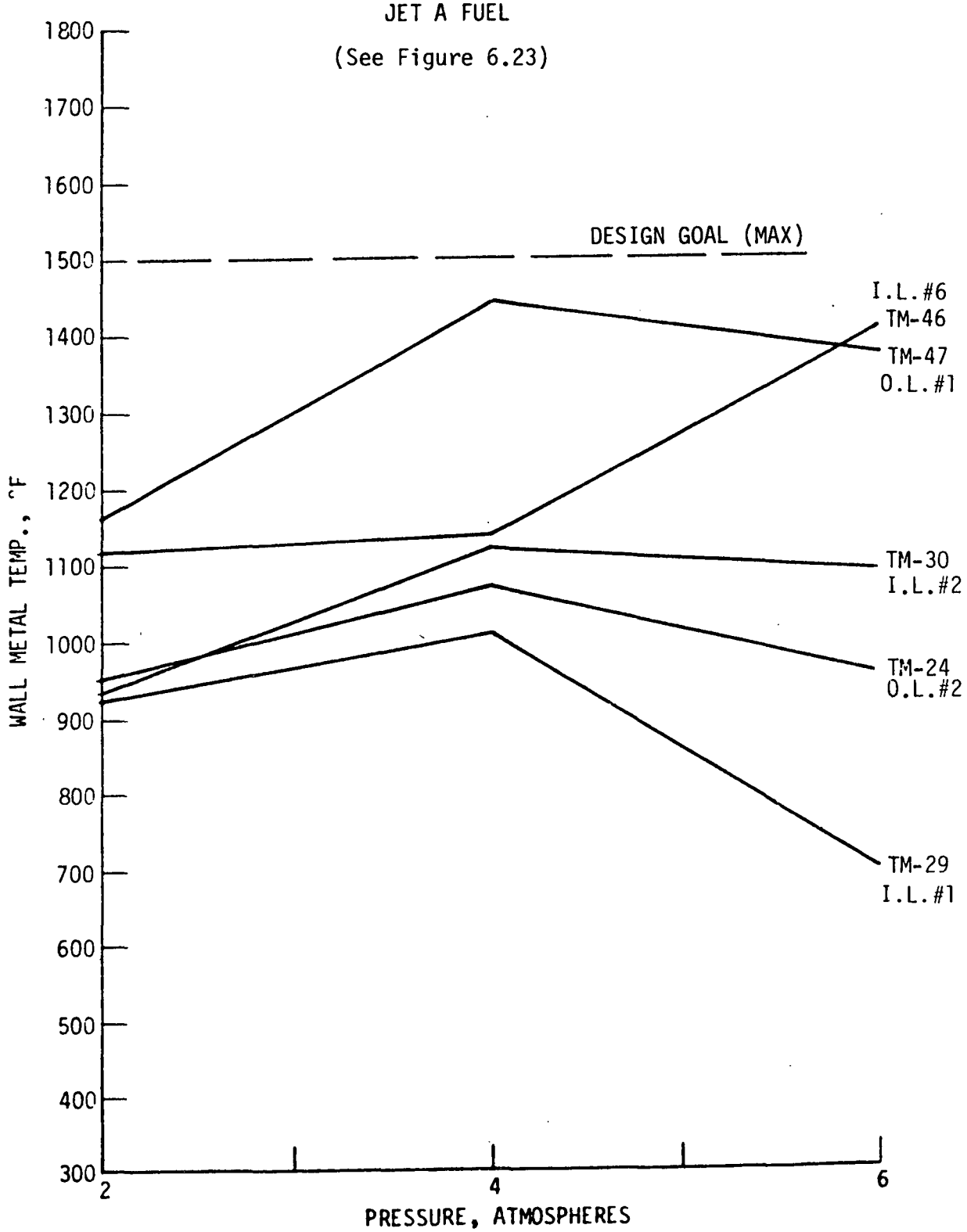

Figure 6.25

EFFECT OF PRESSURE LEVEL ON I.L. NUGGET #6 CRITICAL POINTS
FOR THREE PLANES

AT FUEL-AIR ≃ .023 TO .024
COMBUSTOR CONFIGURATION I
JET A FUEL

(See Figure 6.23)

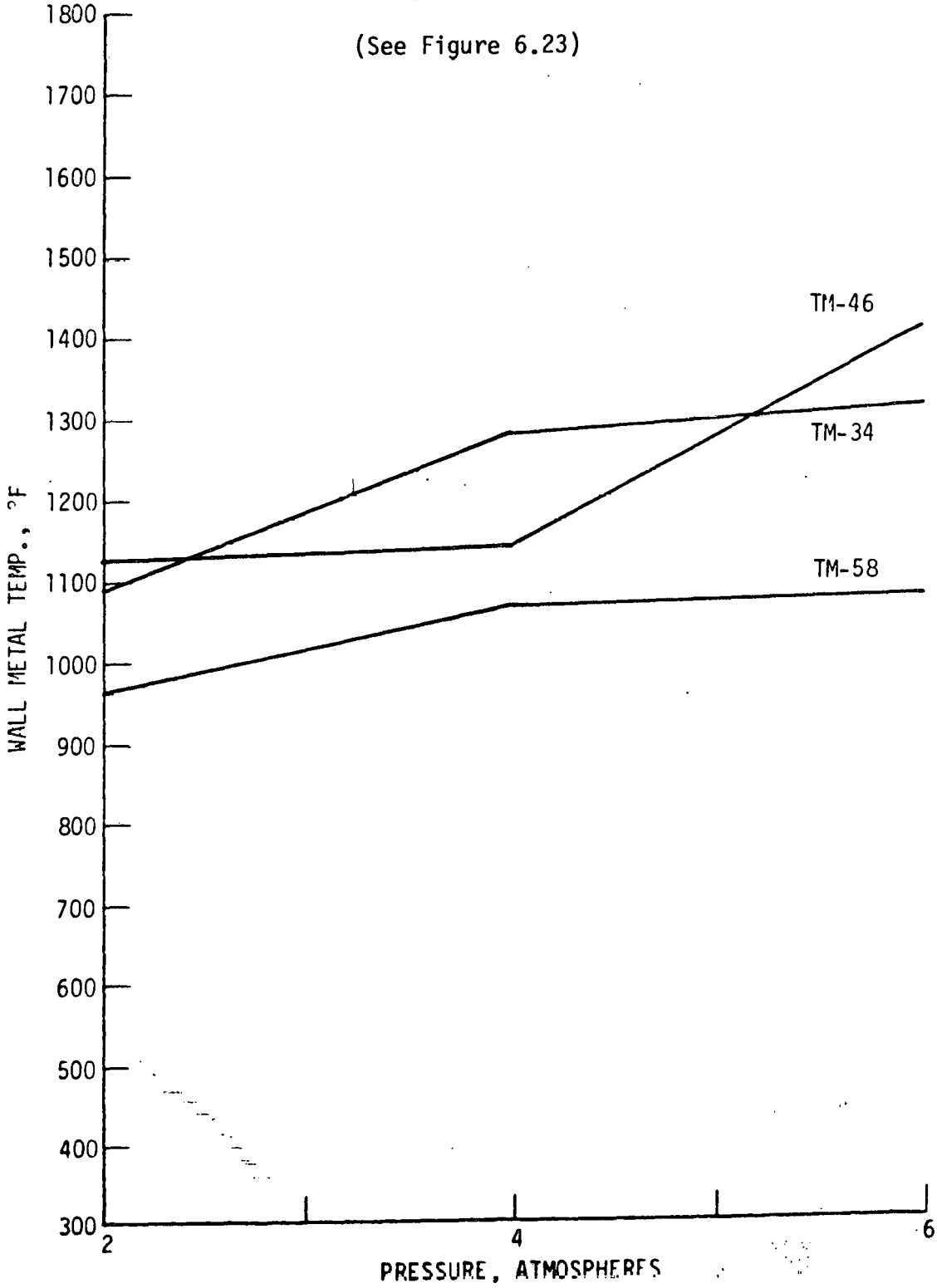

Figure 6.26

EFFECT OF FUEL-AIR RATIO ON INNER LINER NUGGET #6 CRITICAL POINTS FOR THREE PLANES

AT 2 ATMS.

COMBUSTOR CONFIGURATION I

JET A FUEL

(See Figure 6.23)

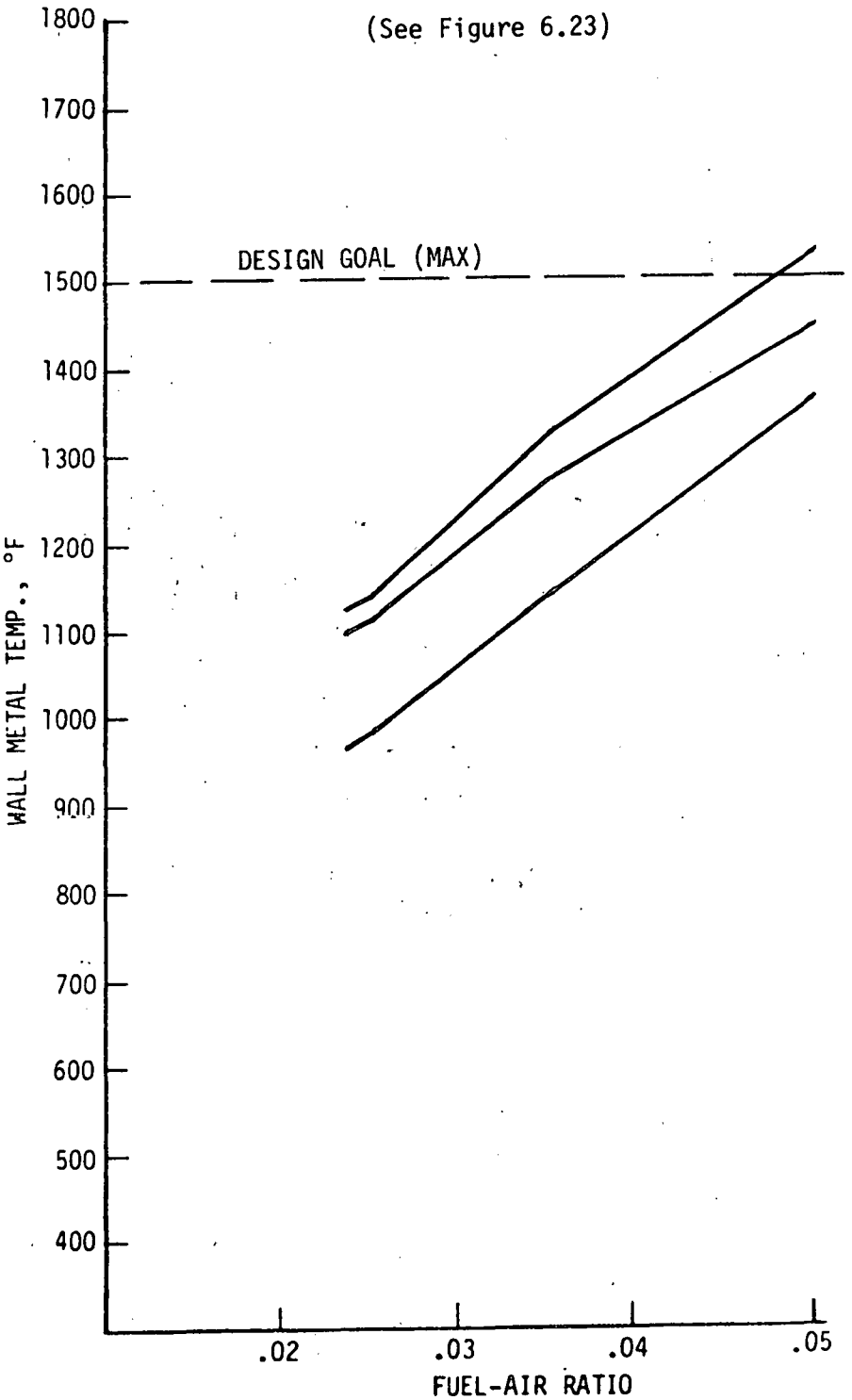

Figure 6.27

THERMOCOUPLE LOCATIONS ON THE VAPORIZER TUBE

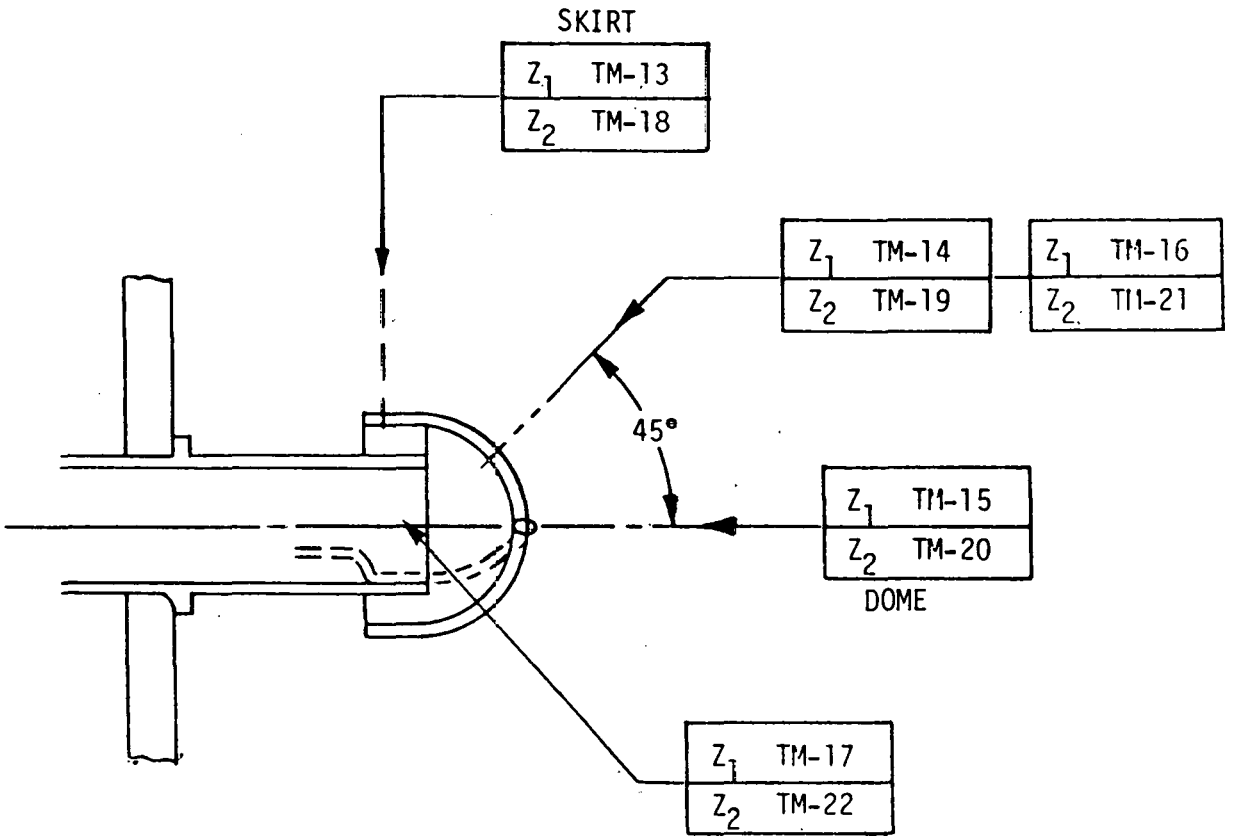

Figure 6.28

EFFECT OF FUEL-AIR RATIO ON VAPORIZING TUBE WALL TEMPERATURES
AT 2 ATMOSPHERES

COMBUSTOR CONFIGURATION I
JET A FUEL
(See Figure 6.28)

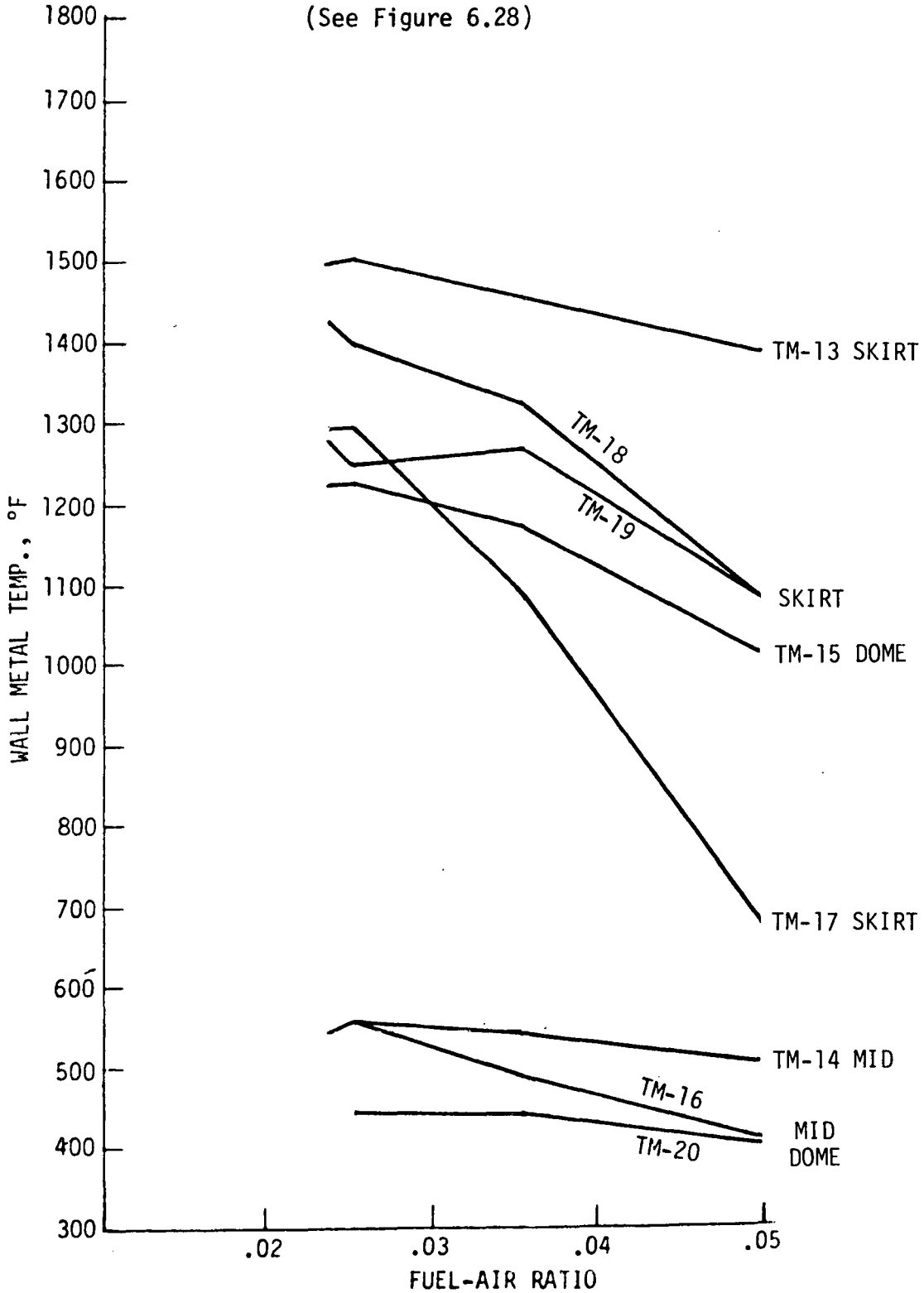

Figure 6.29

EFFECT OF PRESSURE LEVEL ON VAPORIZING TUBE WALL TEMPERATURES
AT FUEL-AIR .023 TO .024
COMBUSTOR CONFIGURATION I
JET A FUEL
(See Figure 6.28)

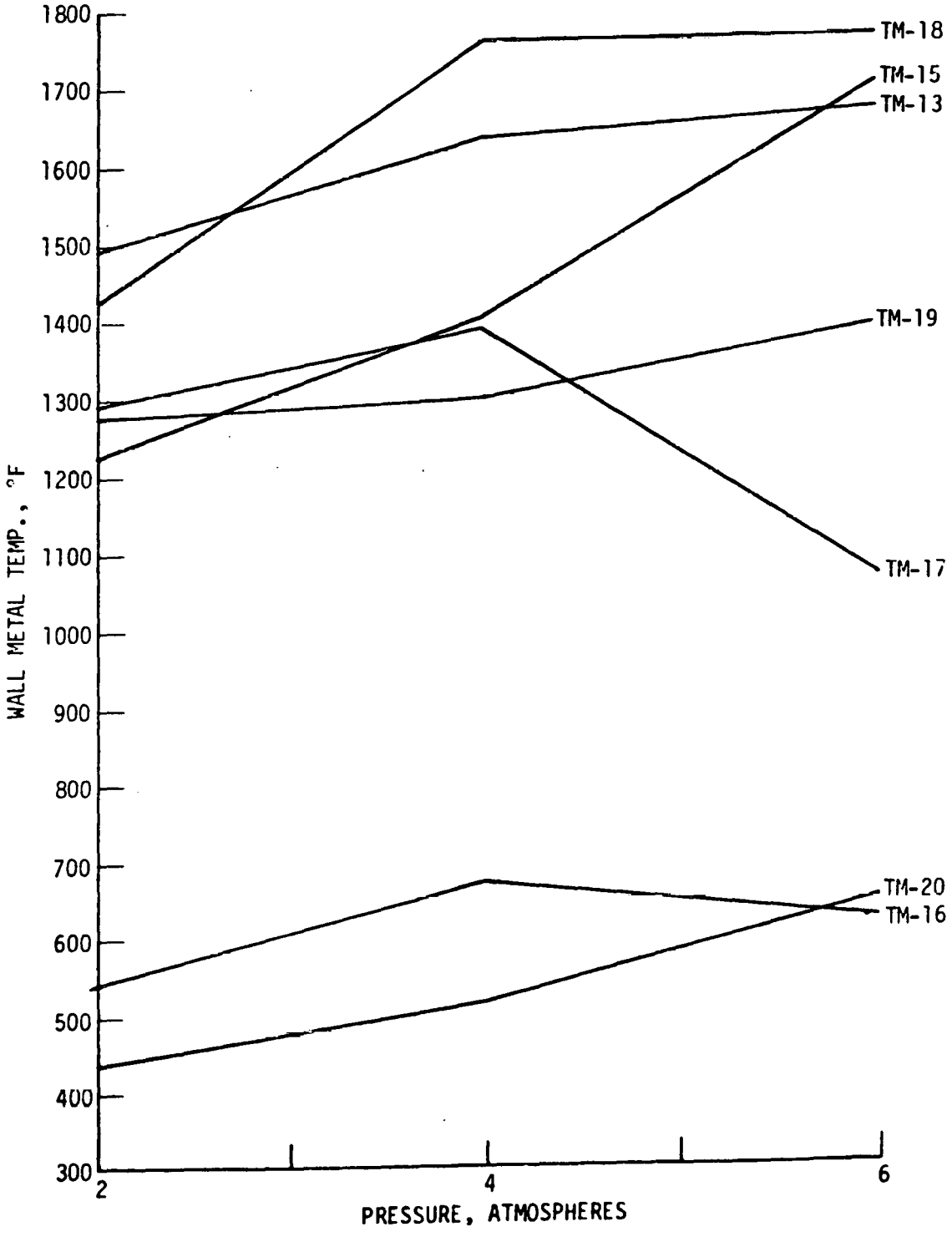

Figure 6.30

Visual inspection of the hardware after the pressure-induced failure confirmed the validity of the temperature measurements. Temperature measurements of the vaporizer tube (Figures 6.28 through 6.30) indicated the range of temperatures previously experienced and which are an operating characteristic of the mushroom vaporizer. In general, the overall temperature level decreases with fuel loading, with the skirts usually hotter than the dome of the tube. The effect of pressure level on vaporizer tube, determined to be 1.2 (approximately same as liners), will increase the maximum measured wall to approximately 1600°F at the TSTR engine design condition.

Configuration II

As previously described, the Configuration I measured overall burner section total pressure loss was slightly more than one percentage point above the design goal, the difference being attributed to a lower actual primary zone air injection flow coefficient. In addition, the combustor exit radial average temperature profile was found to peak below 50% span rather than at the target 62% span location. A second 60° combustor sector was prepared by increasing the primary combustion zone air holes and dilution slot areas to reduce the liner loss to meet the overall hot pressure drop goal of 6.0% and move the combustor exit radial average profile to peak at 62% span. This modified combustor was designated as Configuration II.

A comparison of the airflow distribution between Configurations I and II is shown in Figure 6.31. No changes in combustor wall cooling airflow were made since previously measured temperature levels and projections were consistently below the maximum design limit of 1600°F. The Configuration II 60° combustor sector was only minimally instrumented to measure those pressures and metal temperatures considered critical from the data obtained with Configuration I.

The Configuration II measured combustor performance and metal temperatures are shown in Figures 6.32 through 6.37. Analysis of the data found that this configuration did not meet the performance goals at 3000°F exit temperature.

TSTR 60° SECTOR COMBUSTOR RIG AIRFLOW DISTRIBUTION

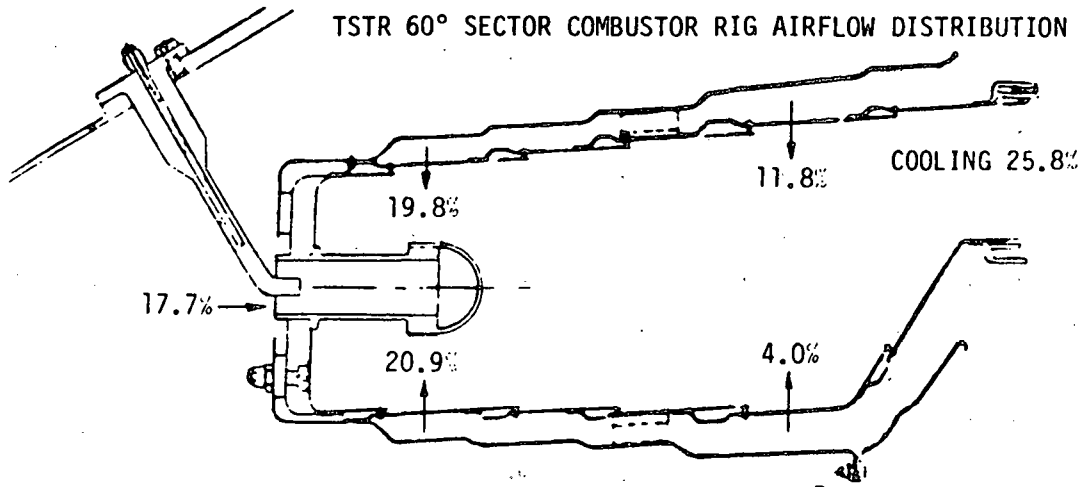

CONFIGURATION I (DESIGN) ~ 7.2% $\frac{\Delta P}{P}$

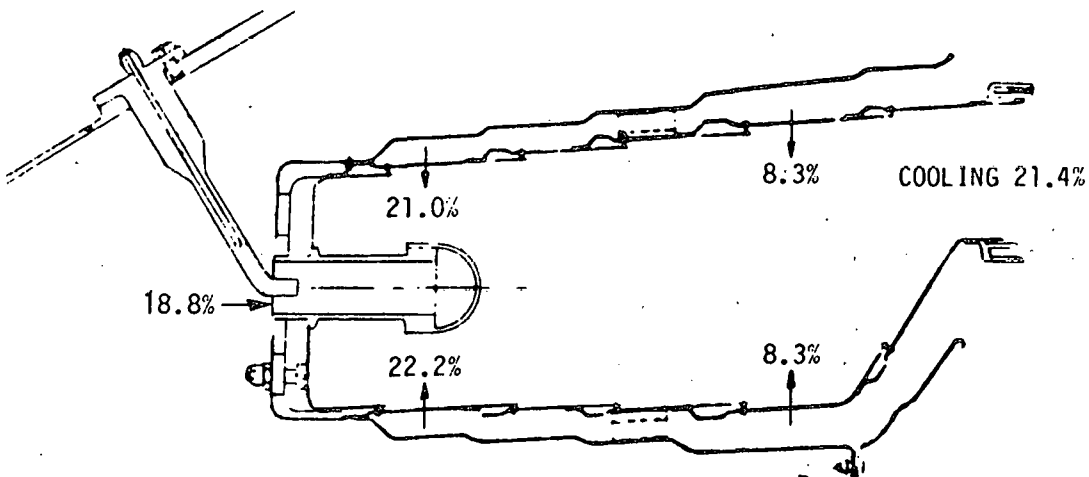

CONFIGURATION II - 6.0% $\frac{\Delta P}{P}$

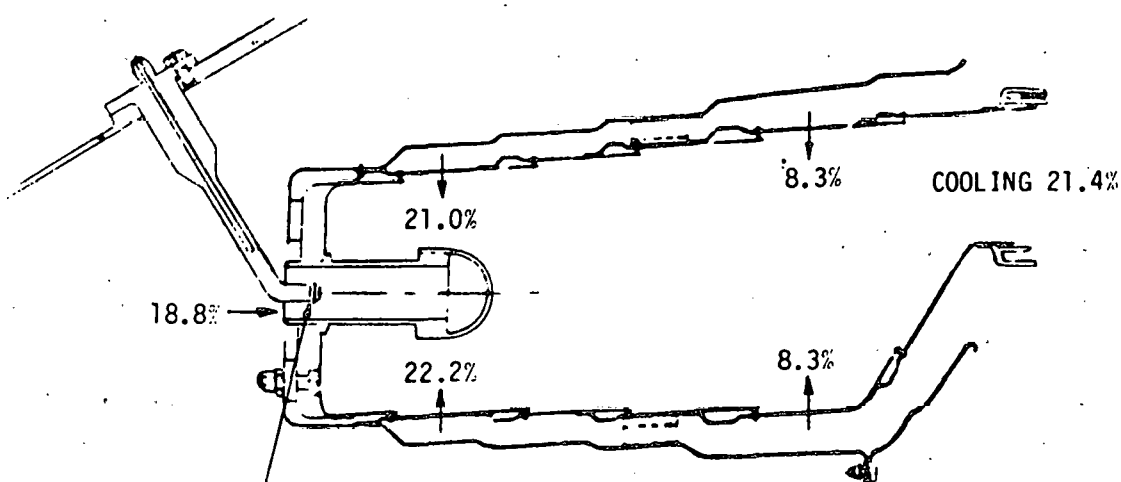

CONFIGURATION IIa* ~ 6.0% $\frac{\Delta P}{P}$

*ADDITION OF FUEL TUBE ATOMIZER DISC

Figure 6.31

TSTR 60° SECTOR COMBUSTION EFFICIENCY
AS A FUNCTION OF FUEL-AIR RATIO

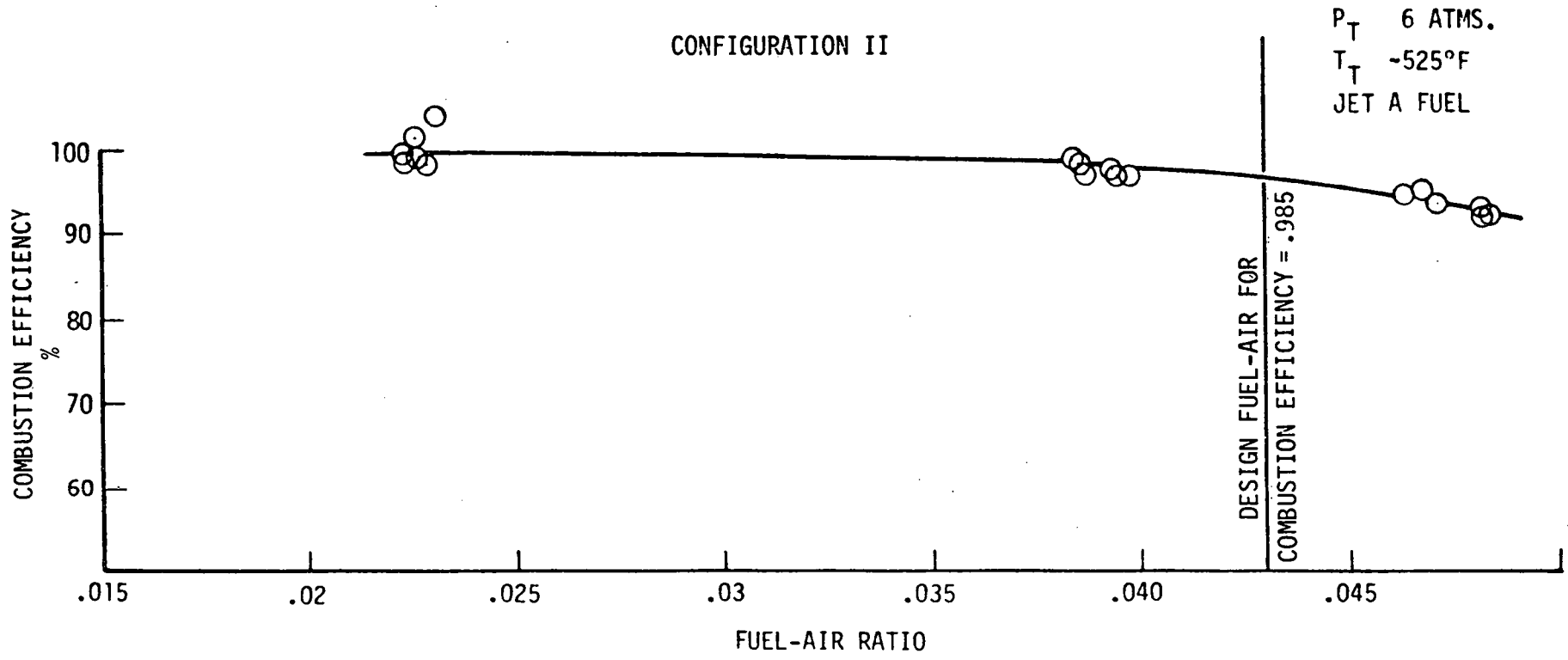

Figure 6.32

TSTR 60° SECTOR COMBUSTOR EXIT TEMPERATURE PATTERN FACTOR
AS A FUNCTION OF BURNER TEMPERATURE RISE

CONFIGURATION II

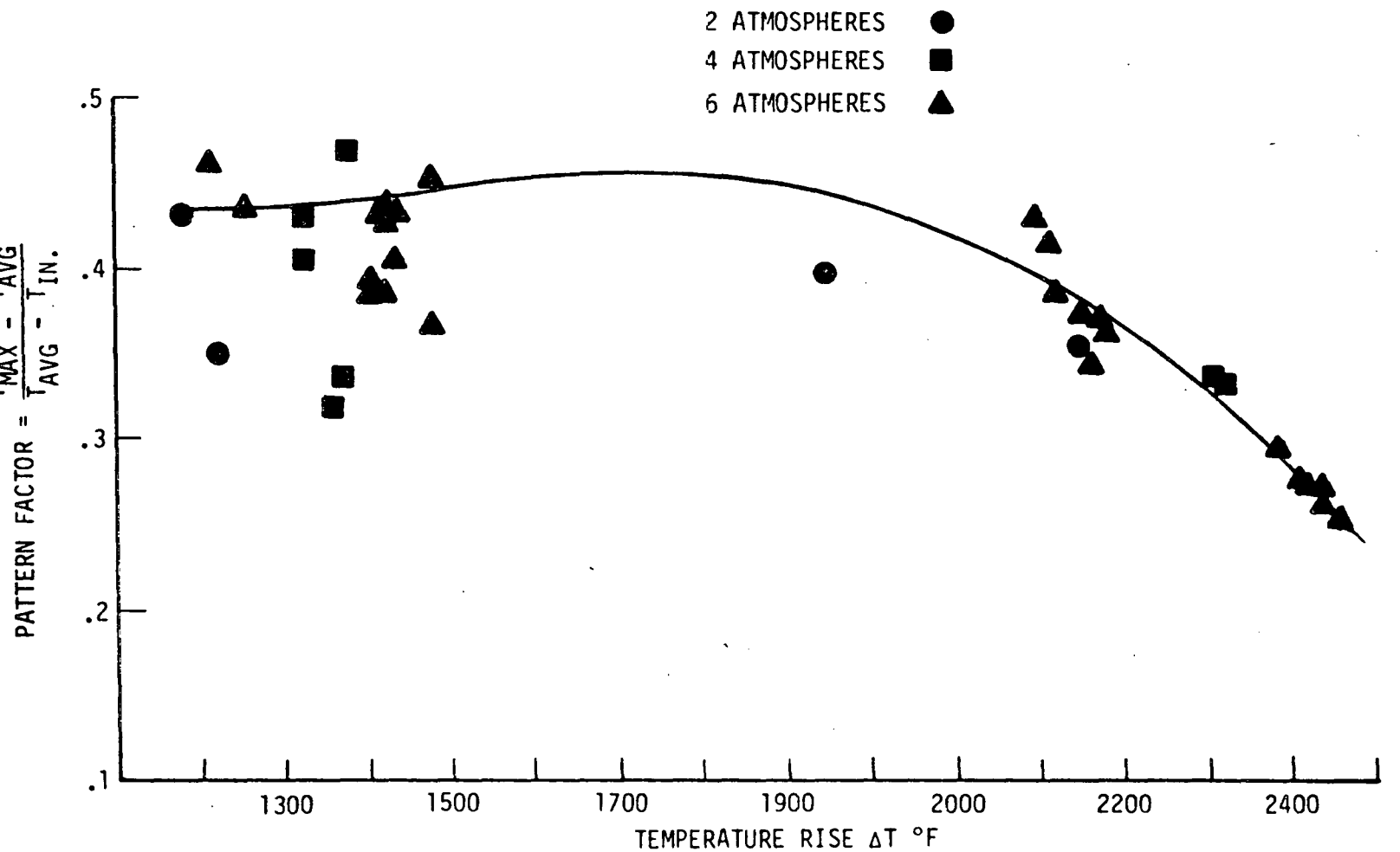

Figure 6.33

TSTR 60° SECTOR COMBUSTOR EXIT
AVERAGE RADIAL TEMPERATURE PROFILE
CONFIGURATION II

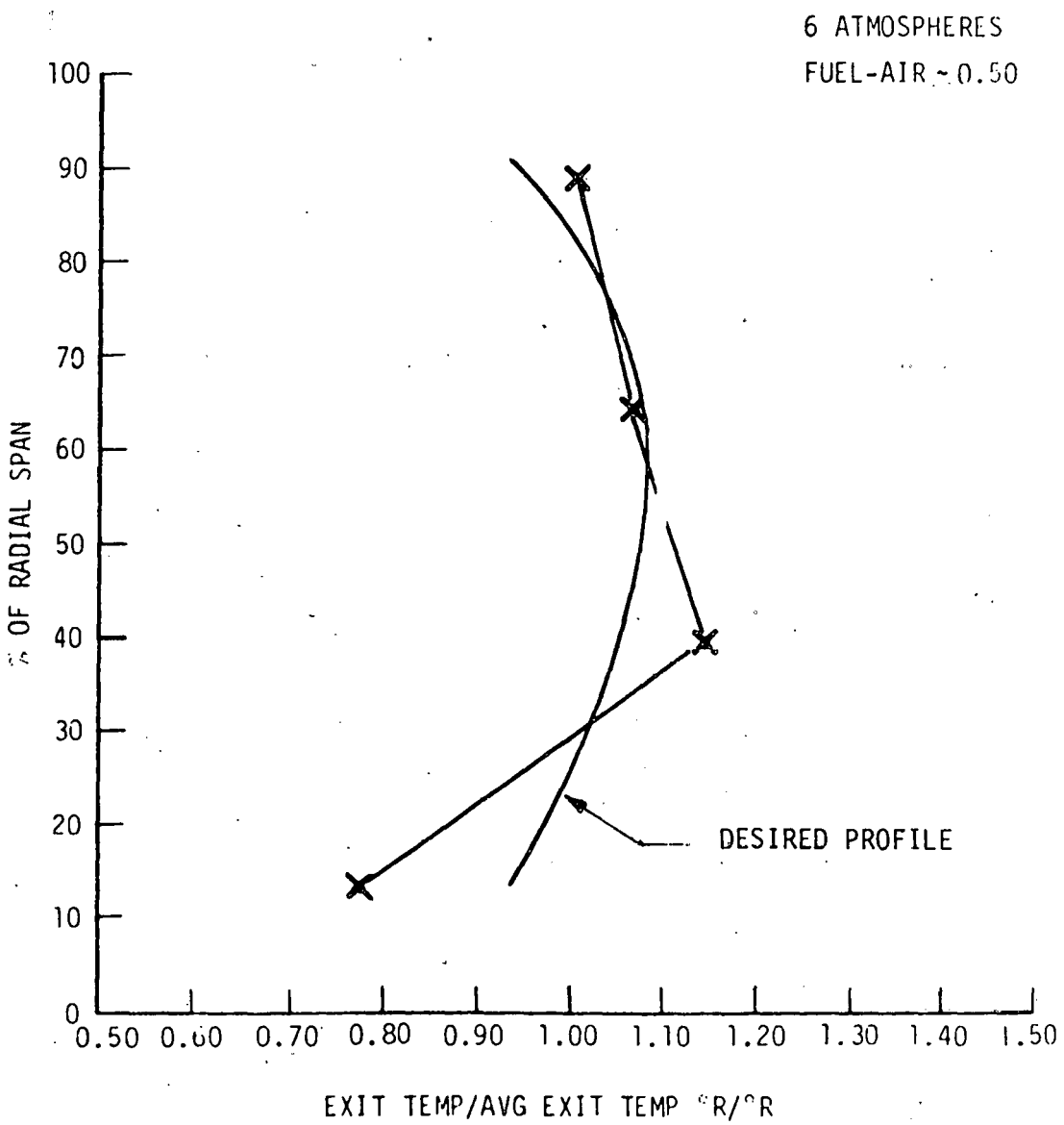

Figure 6.34

HEAD PLATE TEMPERATURE IN LINE WITH VAPORIZER TUBE
NOMINAL PRESSURE 6 ATMOSPHERES

COMBUSTOR CONFIGURATION II

JET A FUEL

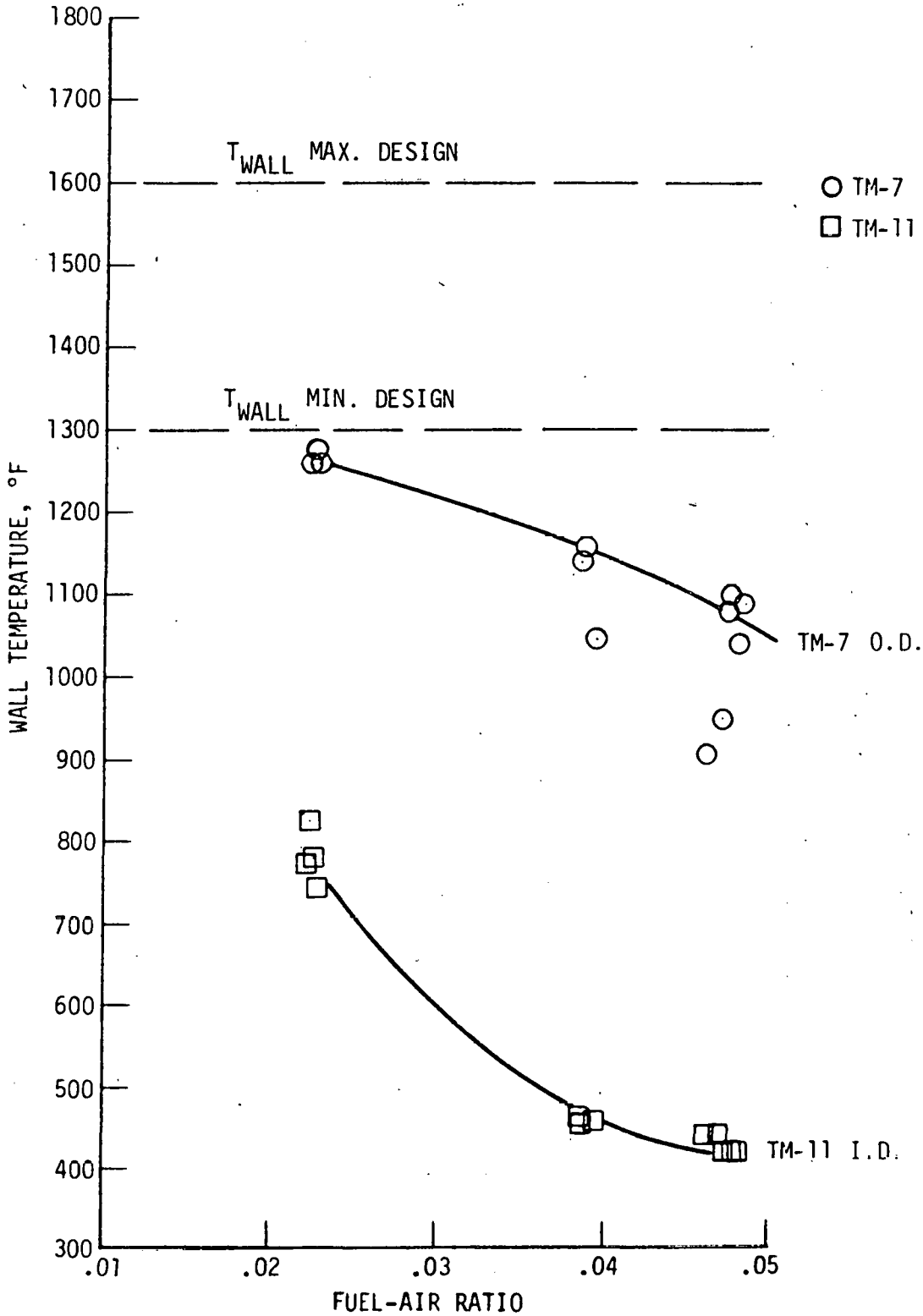

Figure 6.35

INNER LINER COOLING NUGGET CRITICAL POINTS
NOMINAL PRESSURE 6 ATMOSPHERES

COMBUSTOR CONFIGURATION II

JET A FUEL

(See Figure 6.23)

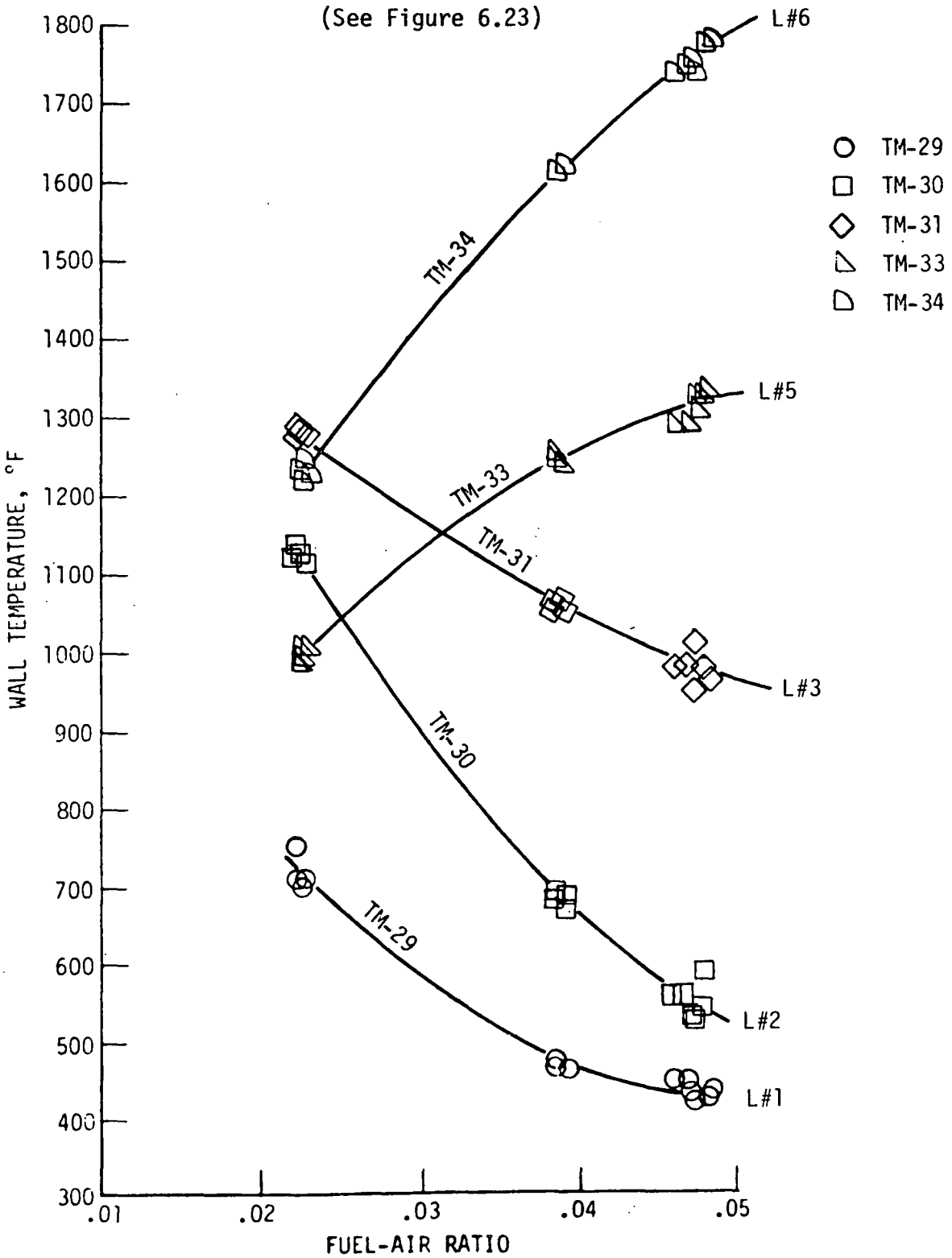

Figure 6.36

OUTER LINER COOLING NUGGET CRITICAL POINTS
NOMINAL PRESSURE 6 ATMOSPHERES

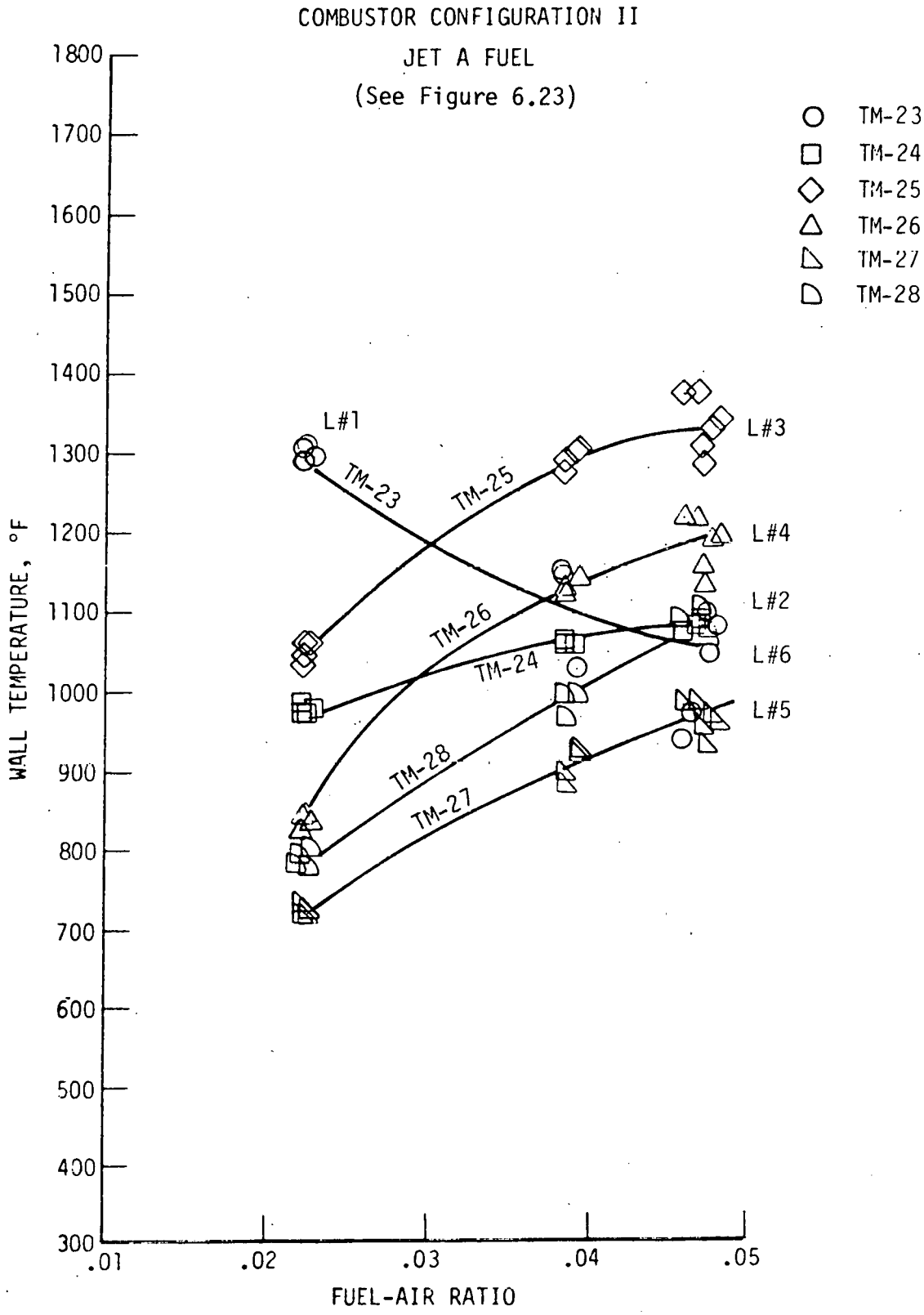

Figure 6.37

The performance deficiencies were concluded to be in part caused by inadequate fuel/air mixture preparation within the combustor mushroom vaporizer tube, producing less than optimum fuel distribution within the primary combustion zone of the burner. The actual pattern factor measured was .28 (Figure 6.33), which exceeds the goal of .25, while combustion efficiency was low by approximately 2.5 percentage points. Although, as shown by Figures 6.35 through 6.37, the majority of measured combustor wall temperatures were within the design goal of 1500°F, a small section at the rear of the inner liner exceeded 1700°F as shown in Figure 6.36.

Following the same trends as Configuration I, the combustor primary zone inner liner temperatures decreased as fuel-air ratio was increased, while the outer liner temperatures increased. These trends are shown by Figures 6.36 and 6.37. The headplate temperature measurements, Figure 6.35, verify this cooling effect of increasing fuel flow as well as the significant difference in temperature level between OD and ID regions of the primary zone. Temperature measurements of the mushroom vaporizer tube recorded at approximately design conditions indicate a maximum wall temperature of 1500°F to 1600°F (Figure 6.38) which compares favorably to the estimate of 1600°F based on the data from Configuration I testing.

Investigation into the causes of the difference in temperature from inner to outer liner in the primary zone found a gravitational deflection of the fuel jet trajectory within the mushroom vaporizer tube of approximately 0.1 inch below the vaporizer centerline as shown in Figure 6.39. Two alternate fuel tube arrangements were conceived to correct the vaporizer fuel jet deflection, and thus improve, at least partially, the fuel maldistribution indicated by the difference in primary zone liner temperatures. The two alternate fuel injection schemes are shown in Figure 6.40. Analysis of the original fuel injection tube design indicated that effectiveness of the vaporizer tube could be improved by utilizing air blast atomization energy scheme (a), or by high velocity liquids dynamics breakup scheme (b). Samples of both alternate arrangements were fabricated for bench test evaluation. Free stream testing of the air blast atomization scheme is shown in Figure 6.41, where an air blast is directed over the tip of the fuel injector as is the case in the vaporizer.

VAPORIZER TUBE TEMPERATURES
NOMINAL PRESSURE 6 ATMOSPHERES
COMBUSTOR CONFIGURATION II
JET A FUEL
(See Figure 6.28)

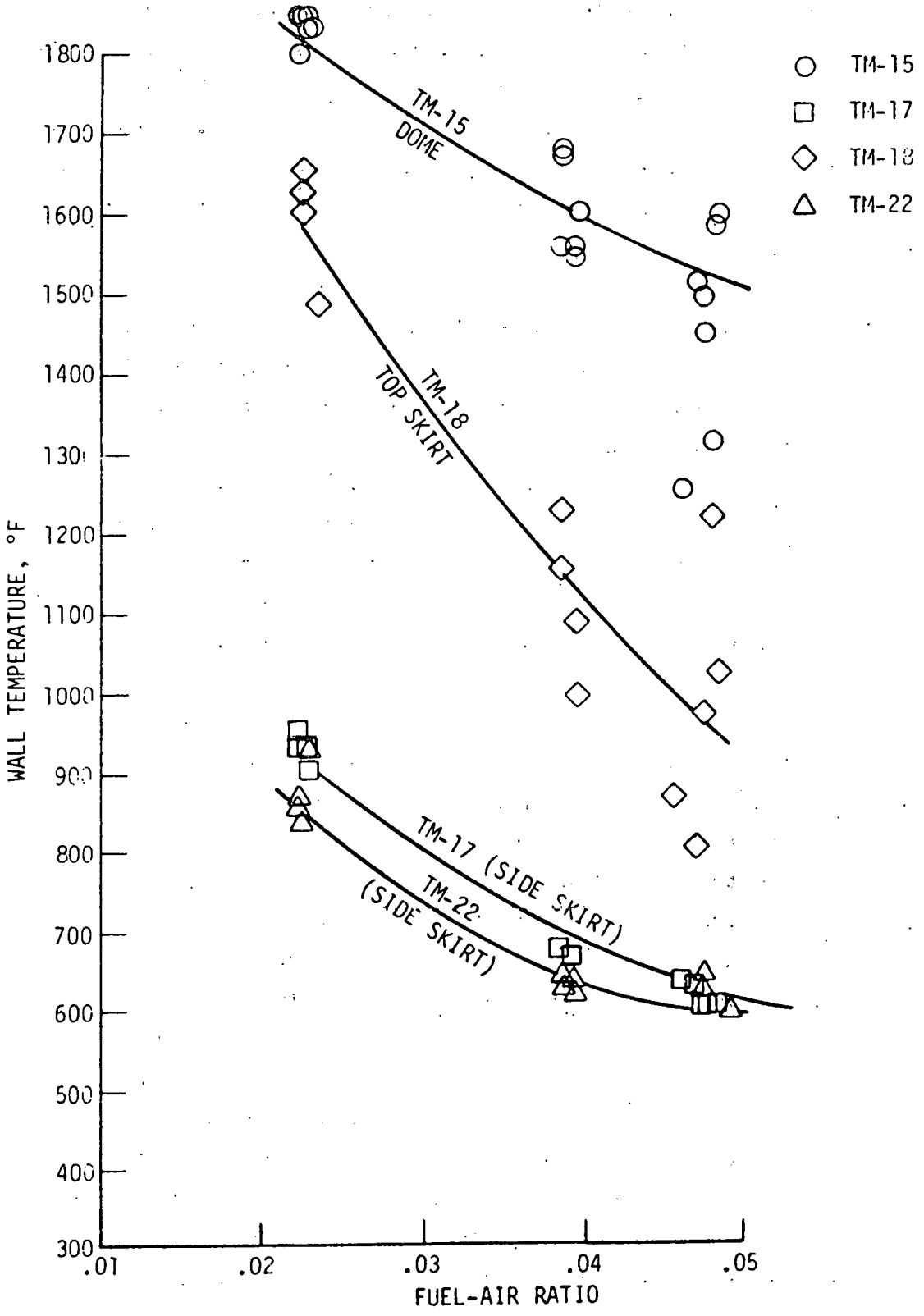

Figure 6.38

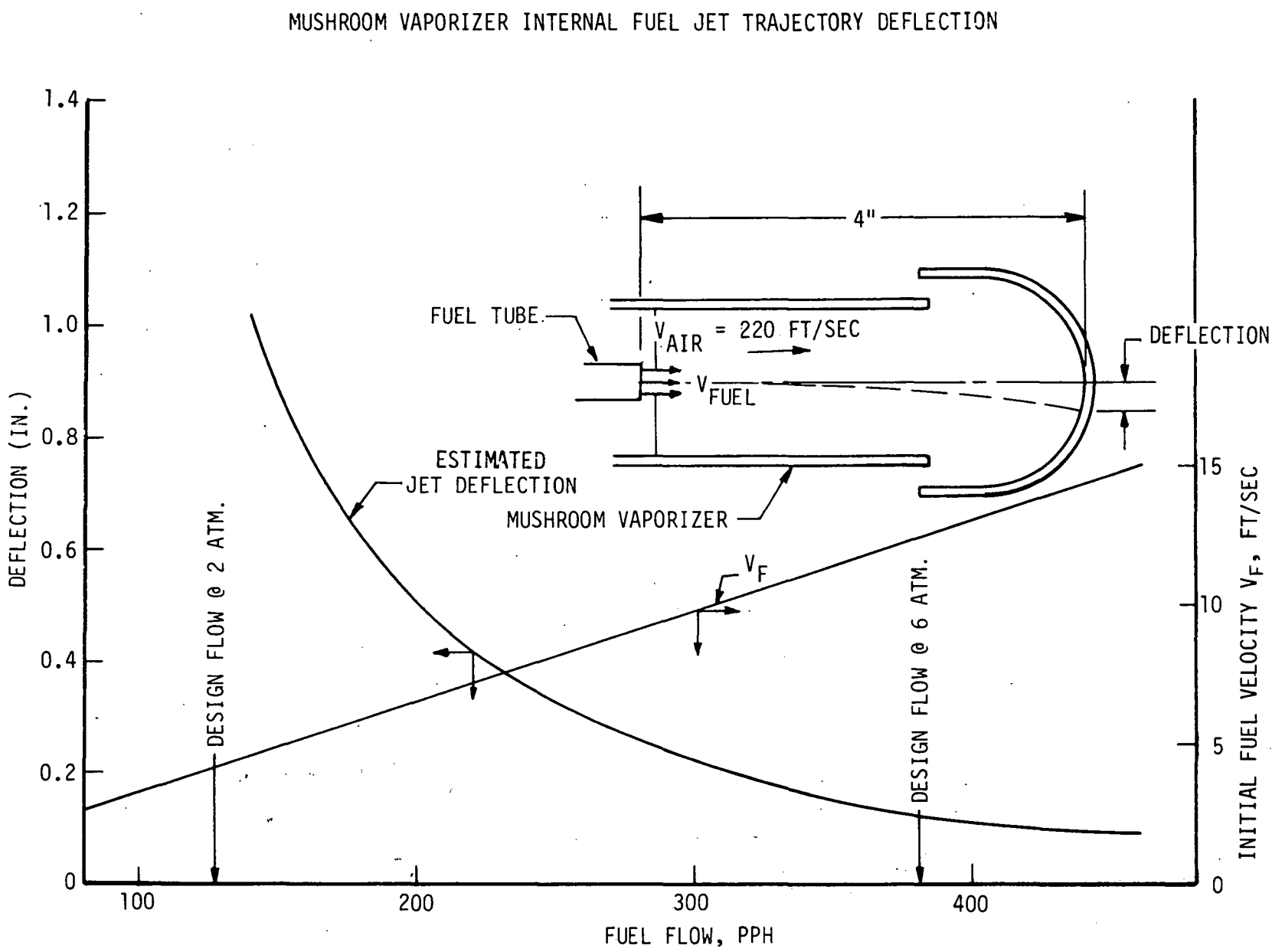
MUSHROOM VAPORIZER INTERNAL FUEL JET TRAJECTORY DEFLECTION
DEFLECTION (IN.)
1.4
1.2
1.0
0.8
0.6
0.4
0.2
0
100
200
300
400
FUEL FLOW, PPH
INITIAL FUEL VELOCITY V_F, FT/SEC
15
10
5
0
4"
FUEL TUBE
V_{AIR} = 220 FT/SEC
V_{FUEL}
DEFLECTION
ESTIMATED
JET DEFLECTION
MUSHROOM VAPORIZER
V_F
DESIGN FLOW @ 2 ATM.
DESIGN FLOW @ 6 ATM.

Figure 6.39

FUEL TUBE MODIFICATIONS

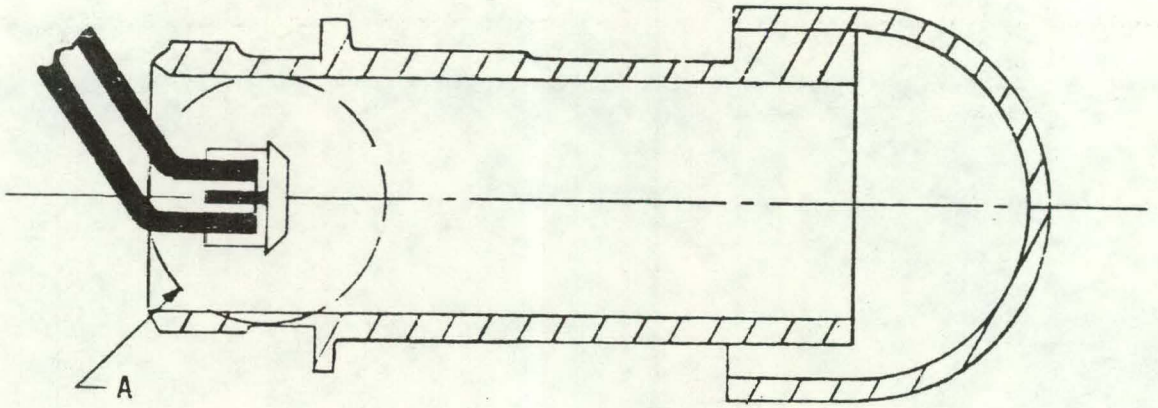

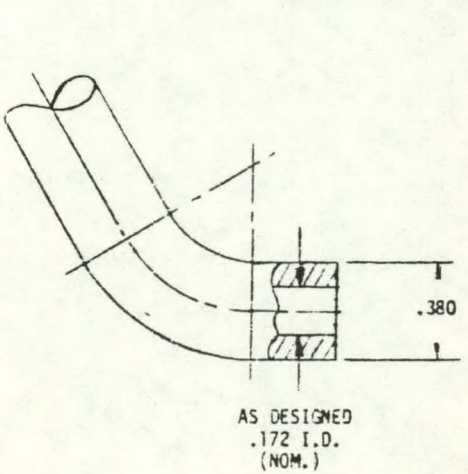

ORIG. CONFIG.

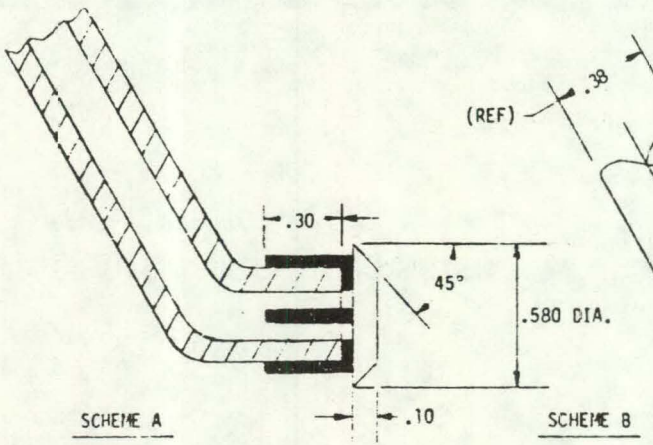

SCHEME A

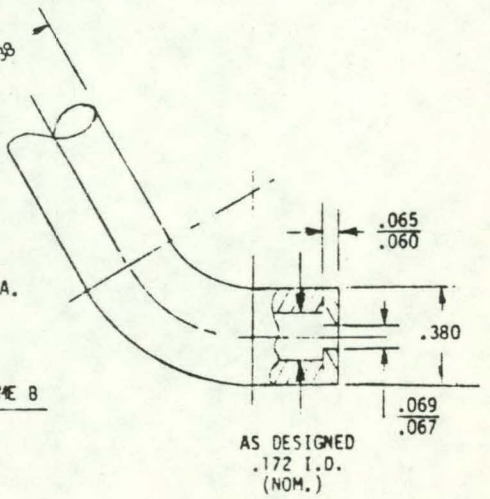

SCHEME B

Figure 6.40

80-288

FUEL SPRAY PATTERN IN FREE AIR STREAM FLOW
FUEL INJECTOR SCHEME A
FUEL FLOW ~1800 PPH

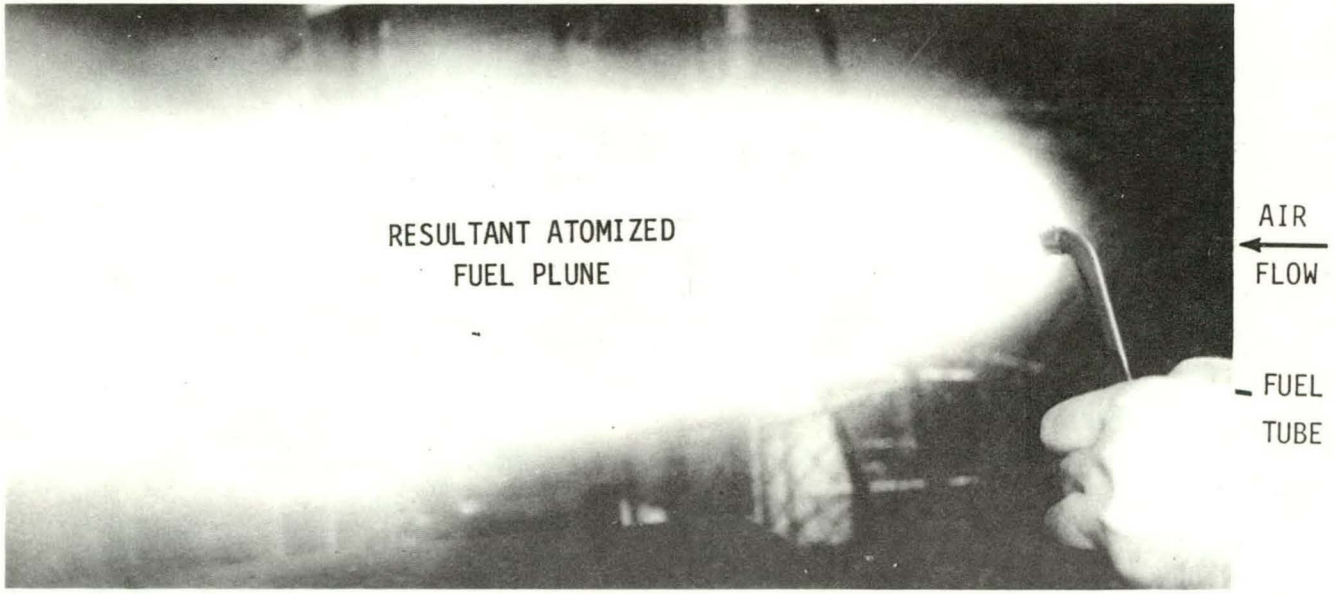

Figure 6.41
6-58

Configuration IIa

Another series of combustor tests was conducted with scheme (a) fuel injectors incorporated in combustor Configuration II. This arrangement was defined as Configuration IIa. Combustion performance tests at 6 atmospheres and at part power (including idle conditions), with and without overboard combustor air bleed were conducted. Test results are shown in Figures 6.42 through 6.44 as well as Figures 6.45 through 6.50. These results demonstrated that significant improvement in performance had been attained by incorporating the scheme (a) fuel injectors. Combustion efficiency (Figure 6.42) and pattern factor (Figure 6.43) goals were achieved with a reduction of the inner rear wall metal temperature (Figure 6.48) to the 1600°F range.

Comparison of the combustor primary zone liner headplate and vaporizer temperatures with comparable data from Configuration II indicates a significant improvement of symmetry between the inner and outer burner walls. The implication is that the fuel distribution is more uniform in the dome of the combustor with the scheme (a) fuel injector than with the originally-designed injector. This is graphically demonstrated by comparing Figures 6.47 and 6.48 and examining the comparison plot of Figure 6.49. These figures show that the ID dome temperature level and the OD dome temperature level have converged. Vaporizer metal temperatures were low, as shown in Figure 6.50. However, the combustor exit radial average profile of Configuration IIa shifted slighlty toward a higher temperature level at the outer portion of the annulus as shown in Figure 6.44. (Comparable data for Configuration II is shown in Figure 6.34.) The effect of part power operation and overboard air bleed from the combustor section on efficiency and pattern factor are shown by Figures 6.51 and 6.52 respectively. These indicate satisfactory performance with overboard bleed as well as off-design operation with Configuration IIa combustor. Post test inspection of the combustor hardware revealed that cooling at the rear wall of the inner liner was still marginal for longer term operation in the TSTR. It was determined that additional film cooling should be introduced into this section of the combustor and evaluated for effectiveness by follow-on 60° sector combustor testing.

TSTR 60° SECTOR COMBUSTION EFFICIENCY
AS A FUNCTION OF FUEL-AIR RATIO

CONFIGURATION IIa

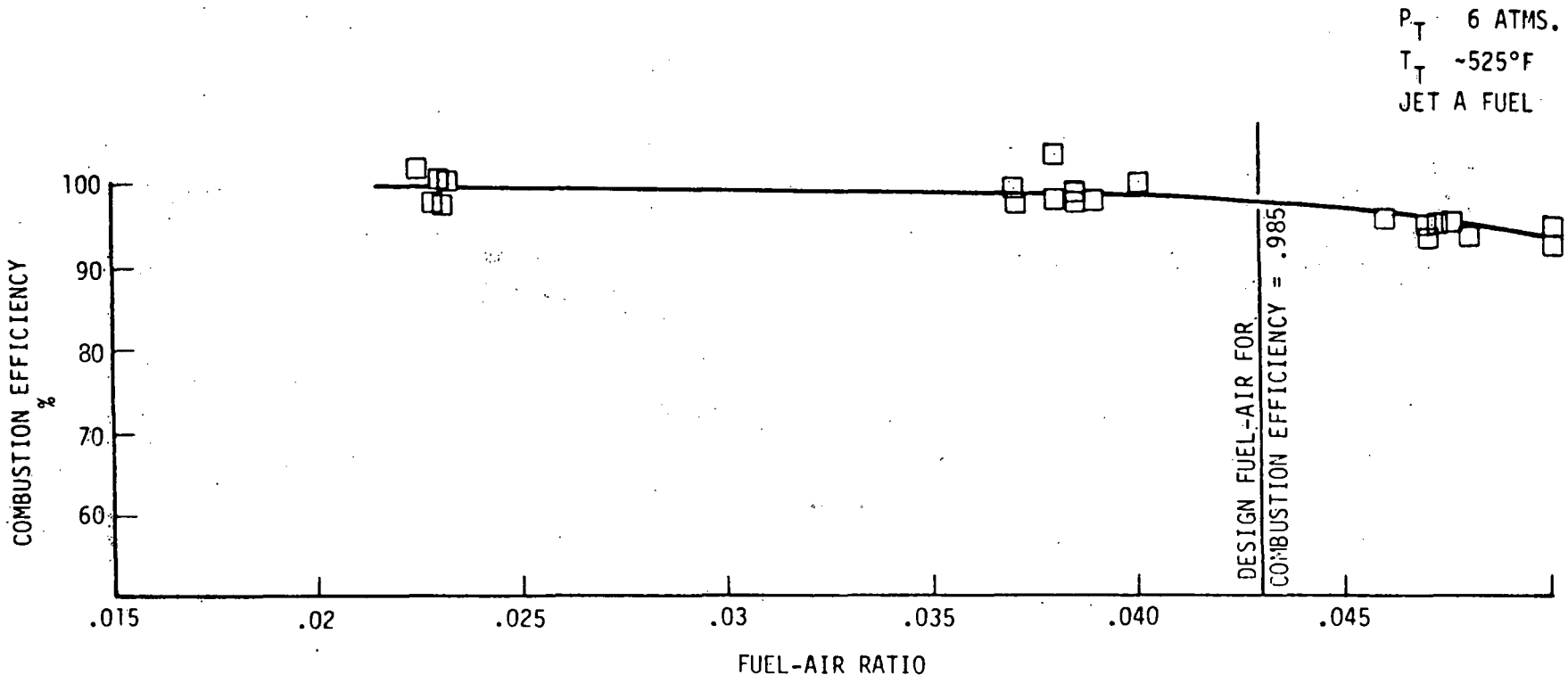

Figure 6.42

TSTR 60° SECTOR COMBUSTOR EXIT TEMPERATURE PATTERN FACTOR
AS A FUNCTION OF BURNER TEMPERATURE RISE

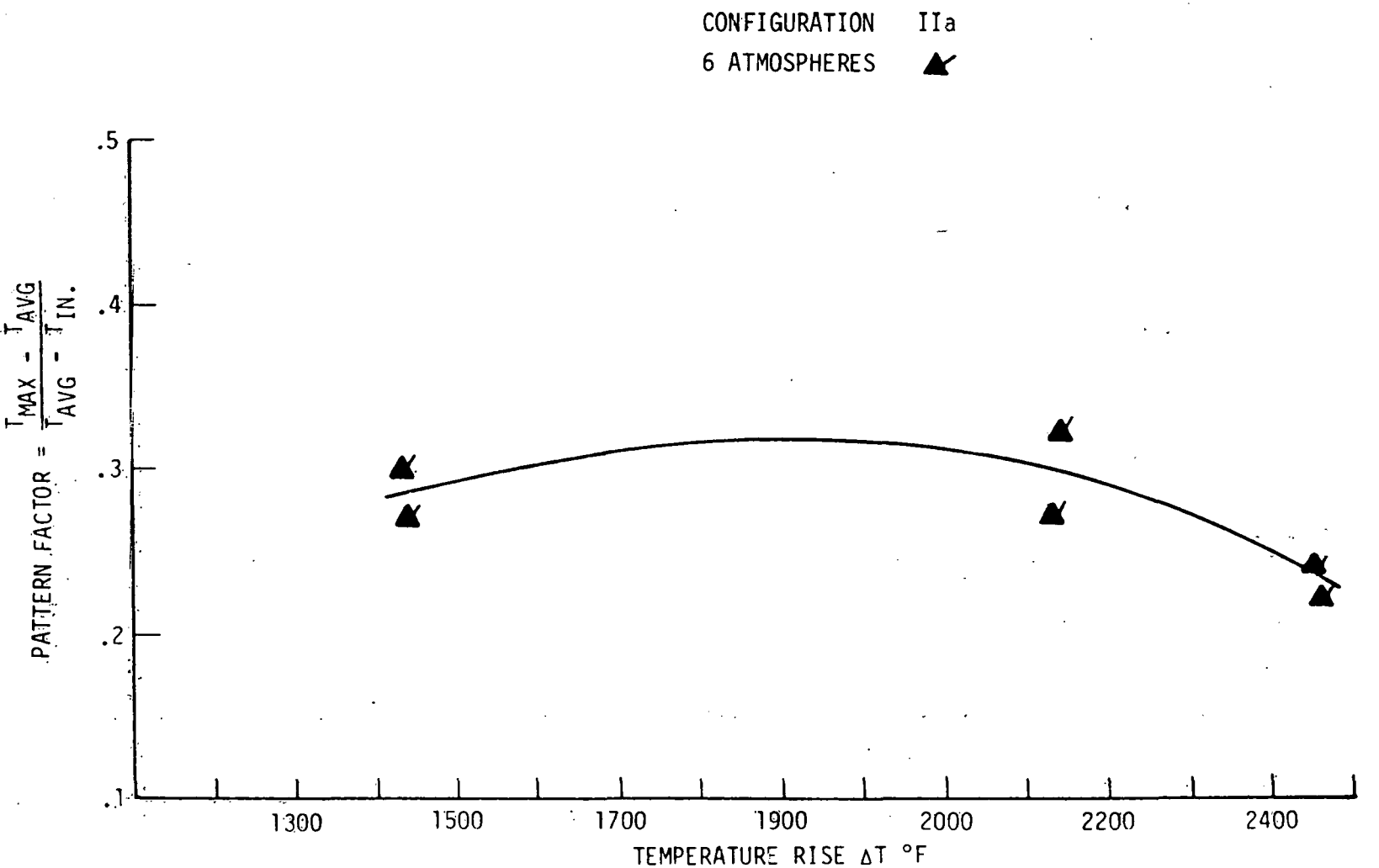

Figure 6.43

TSTR 60° SECTOR COMBUSTOR EXIT
AVERAGE RADIAL TEMPERATURE PROFILE
CONFIGURATION IIa

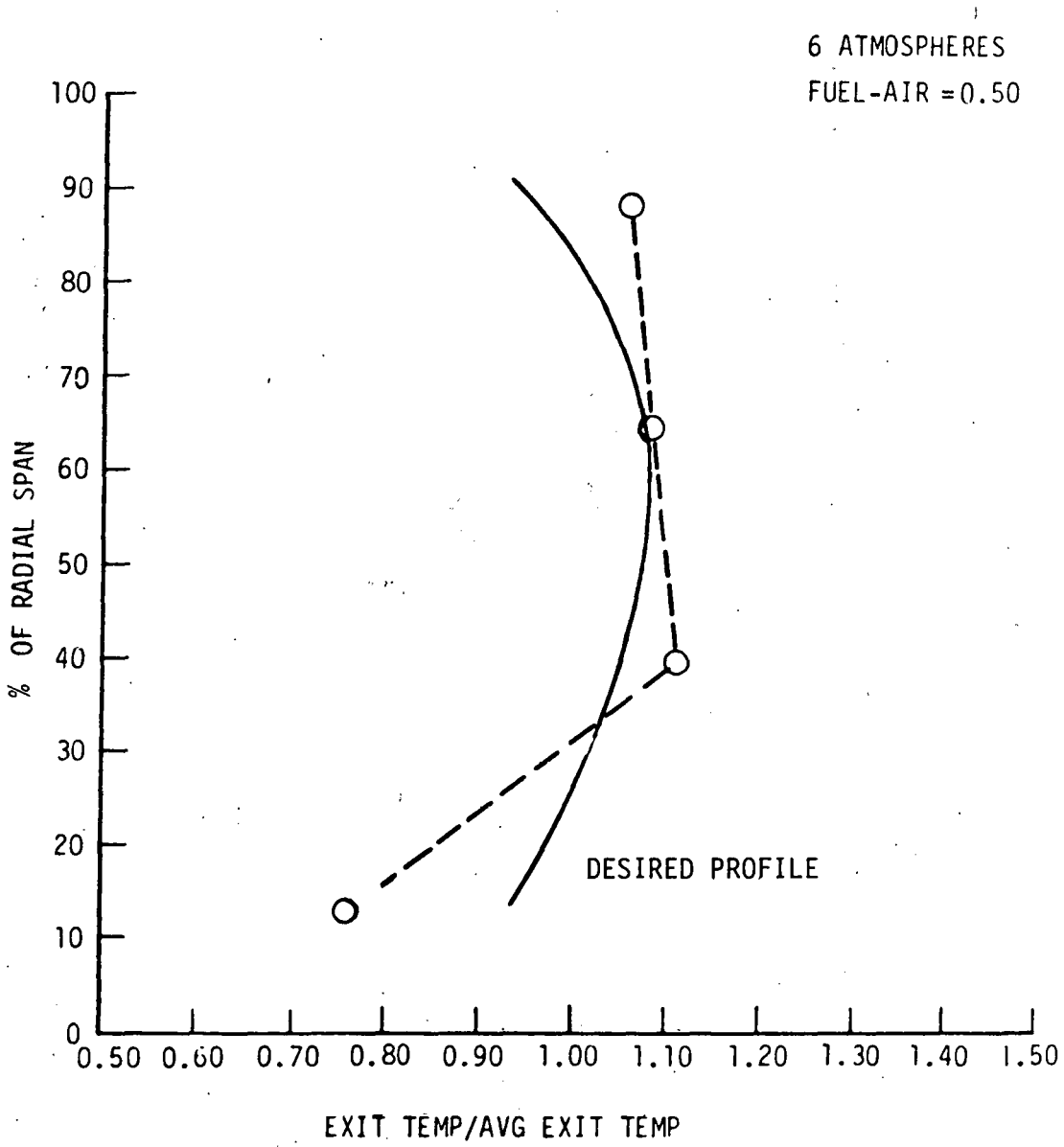

Figure 6.44

OUTER LINER COOLING NUGGET CRITICAL POINTS
NOMINAL PRESSURE 2 AND 4 ATMOSPHERES

FUEL TUBE WITH ATOMIZING DISK
COMBUSTOR CONFIGURATION IIa
JET A FUEL
(See Figure 6.23)

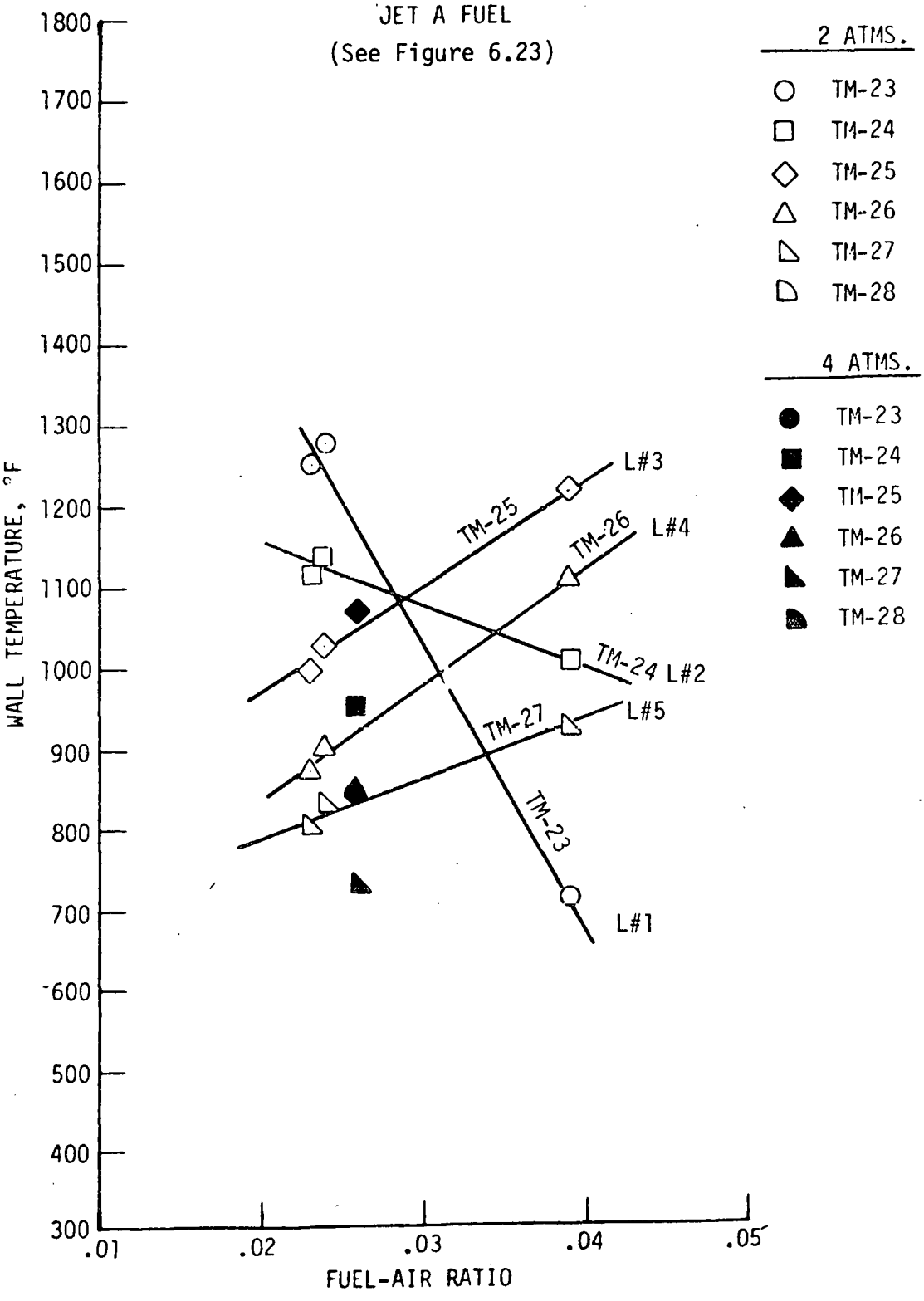

Figure 6.45

INNER LINER COOLING NUGGET CRITICAL POINTS
NOMINAL PRESSURE 2 AND 4 ATMOSPHERES

FUEL TUBE WITH ATOMIZING DISK
COMBUSTOR CONFIGURATION IIa
JET A FUEL
(See Figure 6.23)

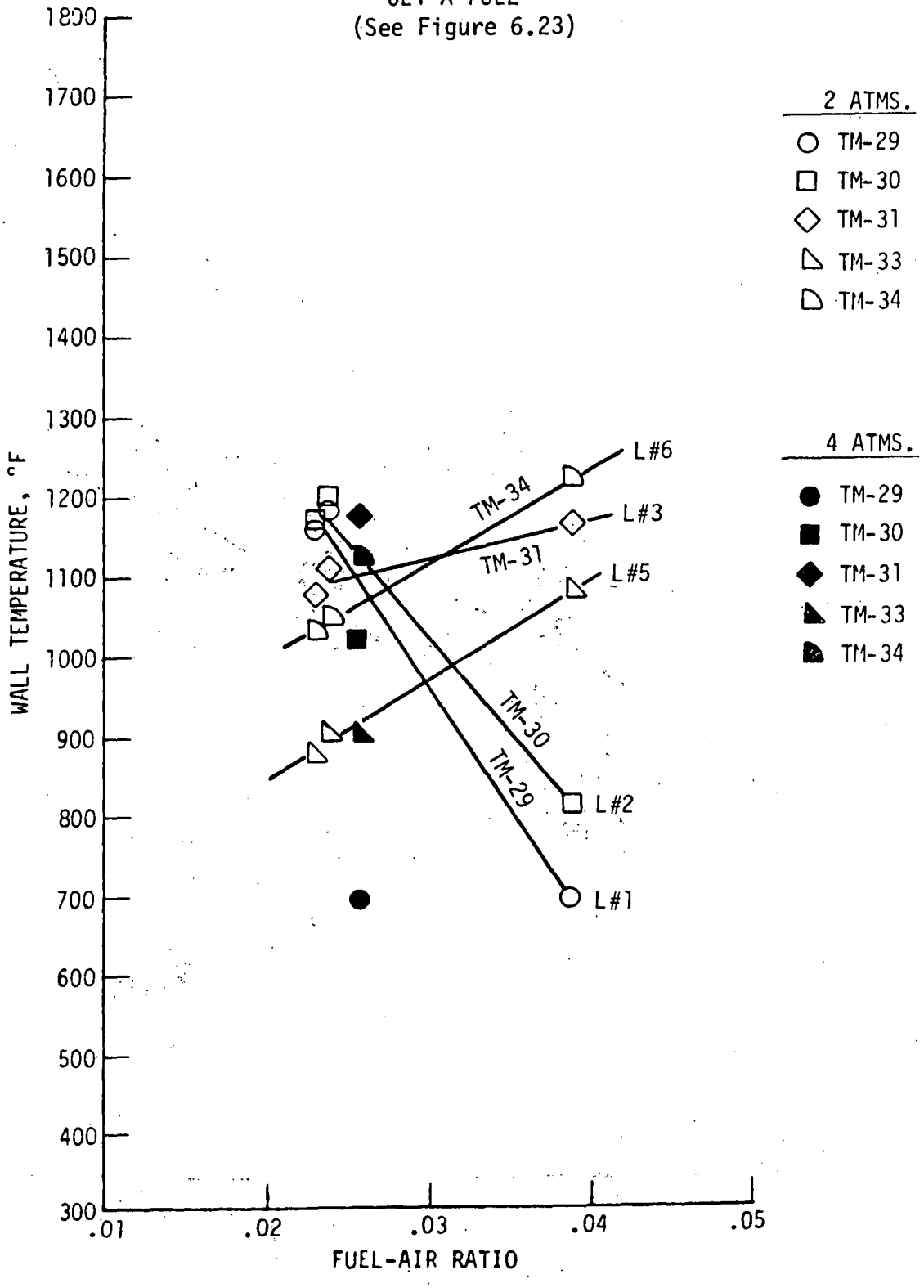

Figure 6.46

OUTER LINER COOLING NUGGET CRITICAL POINTS
NOMINAL PRESSURE 6 ATMOSPHERES

FUEL TUBE WITH ATOMIZING DISK
COMBUSTOR CONFIGURATION IIa
JET A FUEL
(See Figure 6.23)

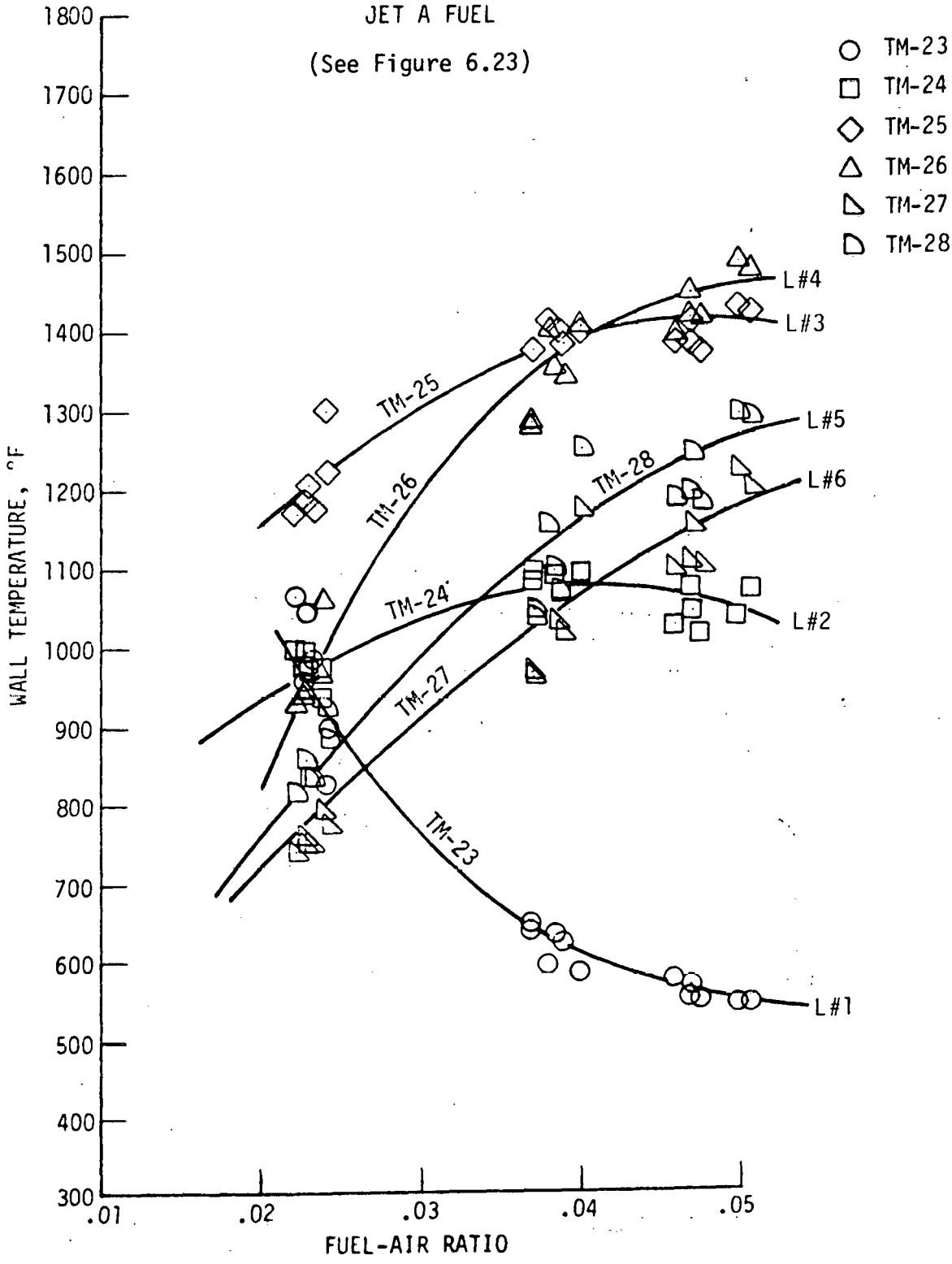

Figure 6.47

INNER LINER COOLING NUGGET CRITICAL POINTS
NOMINAL PRESSURE 6 ATMOSPHERES

FUEL TUBE WITH ATOMIZING DISK
COMBUSTOR CONFIGURATION IIa
JET A FUEL
(See Figure 6.23)

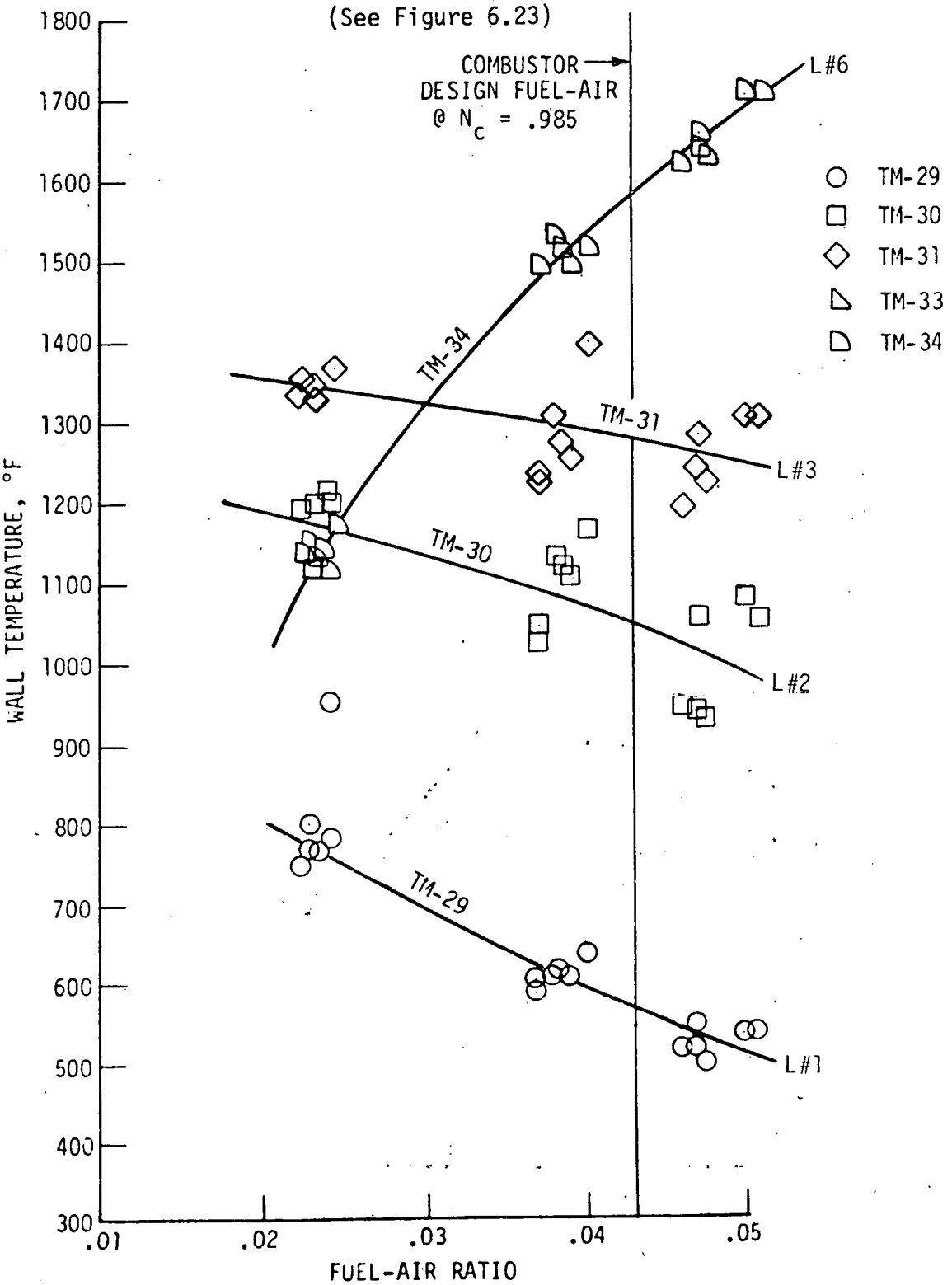

Figure 6.48

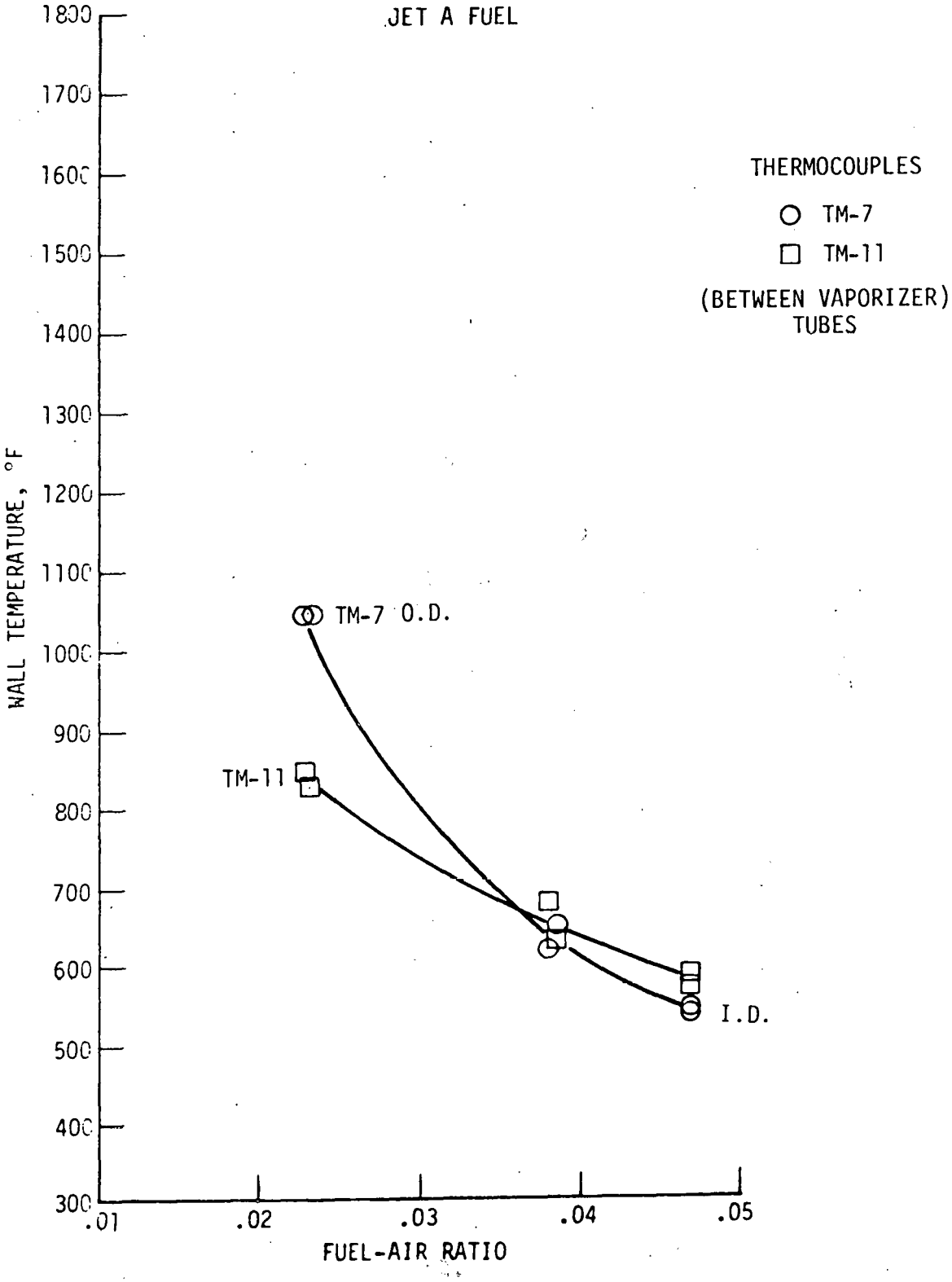
HEAD PLATE TEMPERATURE
NOMINAL PRESSURE 6 ATMOSPHERES
FUEL TUBE WITH ATOMIZING DISK
COMBUSTOR CONFIGURATION IIa
JET A FUEL
THERMOCOUPLES
TM-7
TM-11
(BETWEEN VAPORIZER) TUBES
WALL TEMPERATURE, °F
1800
1700
1600
1500
1400
1300
1200
1100
1000
900
800
700
600
500
400
300
TM-7 O.D.
TM-11
I.D.
.01
.02
.03
.04
.05
FUEL-AIR RATIO

Figure 6.49

VAPORIZER TUBE TEMPERATURES
NOMINAL PRESSURE 6 ATMOSPHERES

FUEL TUBE WITH ATOMIZING DISK
COMBUSTOR CONFIGURATION IIa
JET A FUEL
(See Figure 6.28)

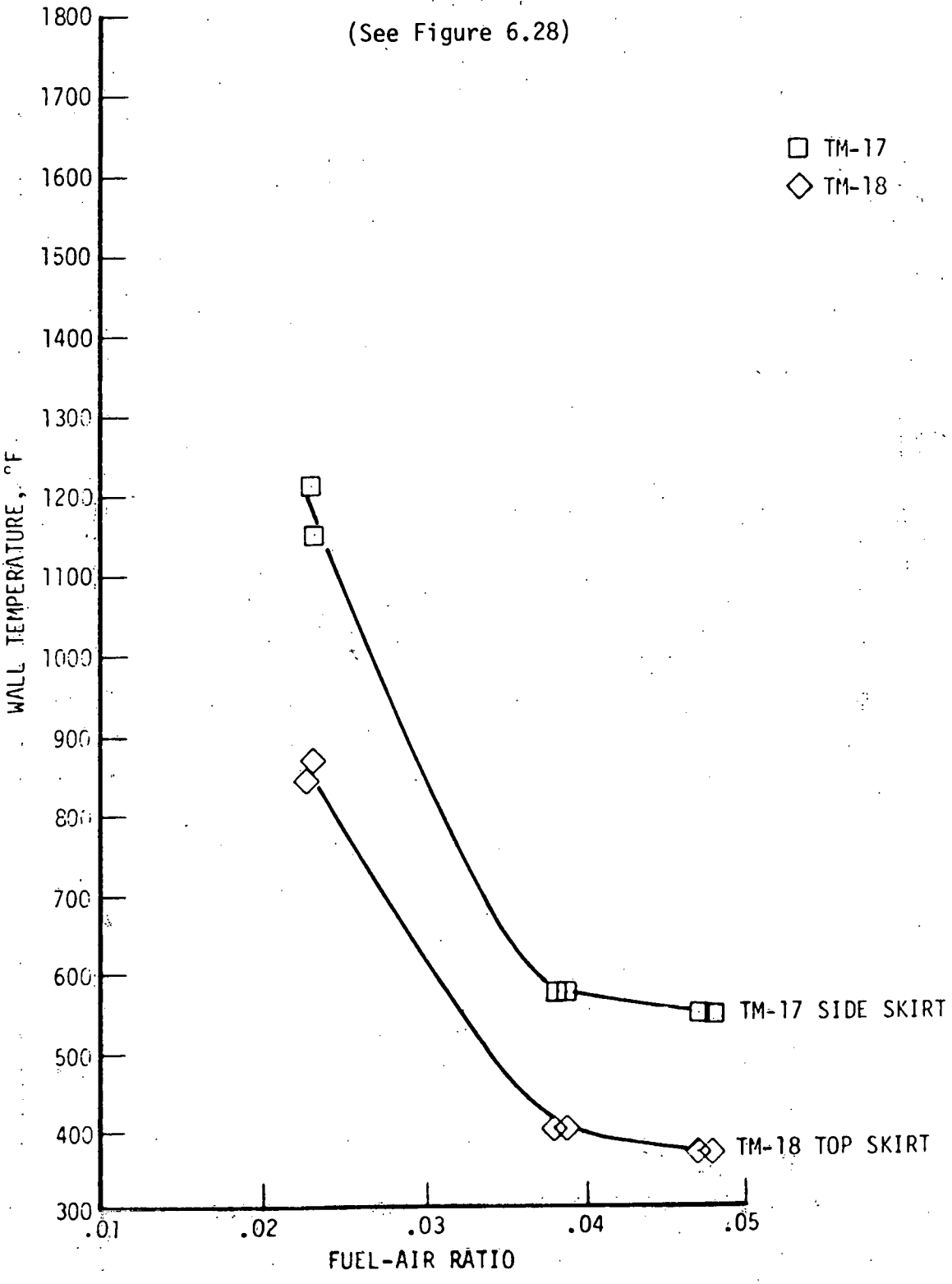

Figure 6.50

TSTR 60° SECTOR COMBUSTOR PERFORMANCE
AT OFF-DESIGN OPERATION CONDITIONS
JET A FUEL
COMBUSTOR CONFIG. IIa

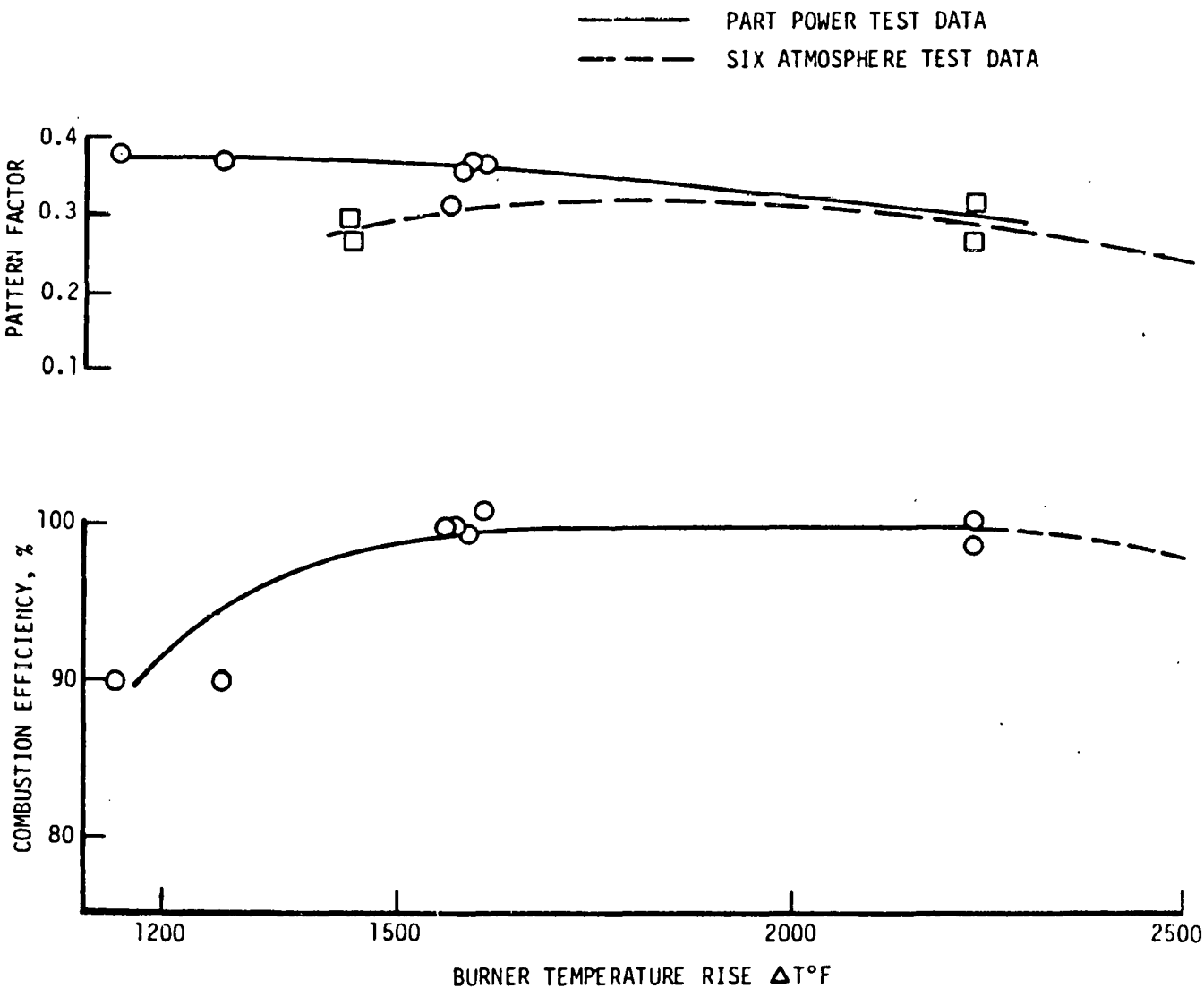

HTT-II-641A

Figure 6.51

TSTR 60° SECTOR COMBUSTION PERFORMANCE WITH OVERBOARD AIR BLEED (CONFIGURATION IIa)

CONDITIONS: 6 ATMOSPHERES COMBUSTOR PRESSURE
520°F COMBUSTOR INLET TEMPERATURE
JET A FUEL

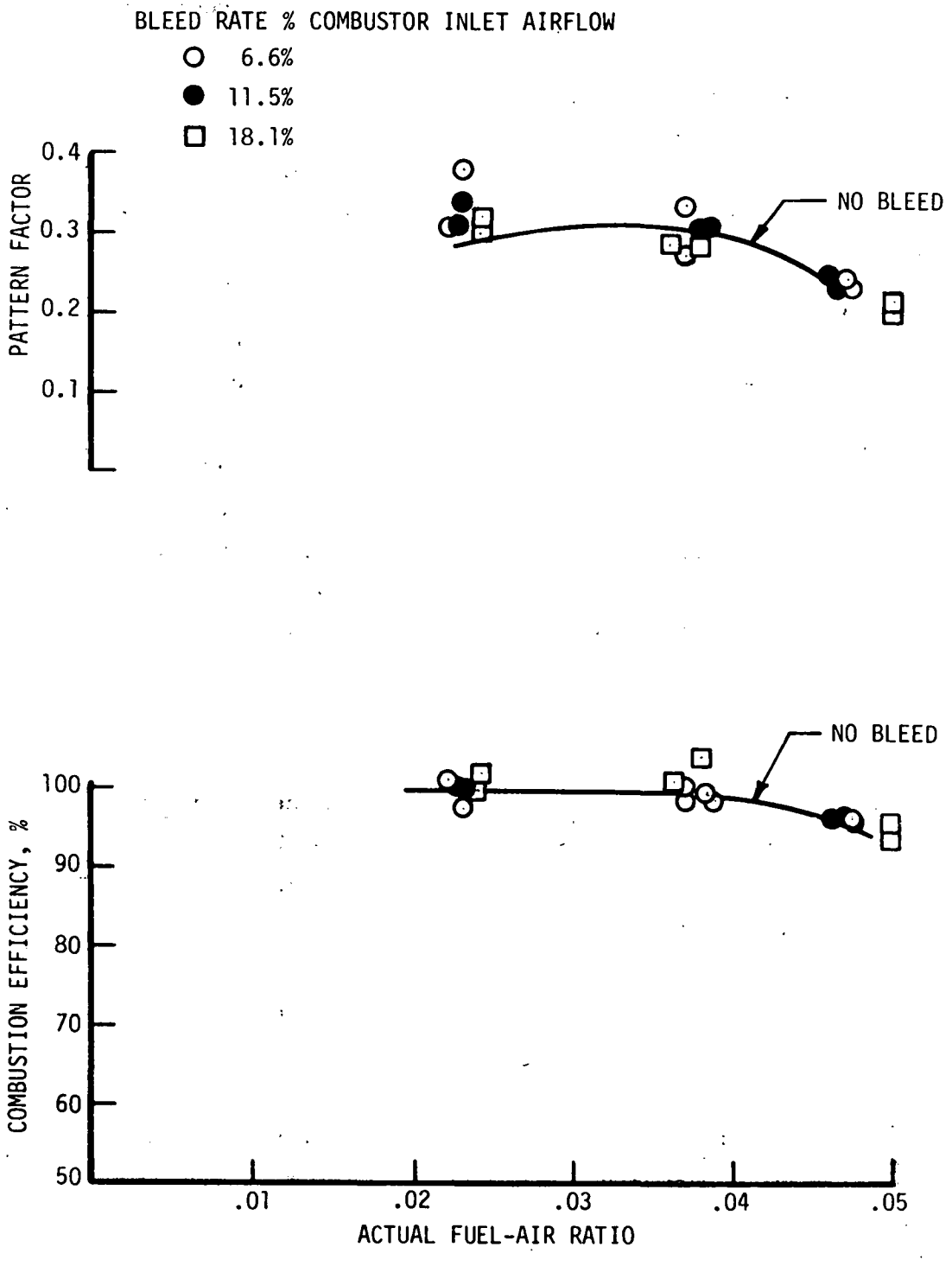

HTT-II-640

Figure 6.52

Configuration IIIa

Combustion performance/durability tests were conducted at six atmospheres to evaluate three cooling schemes for metal temperature reduction at the rear section of the inner combustor liner. The first of these, designated Configuration IIIa, consisted of three rows of sweat cooling holes immediately forward of the hot area. With this arrangement, a cooling film is produced when the high velocity main combustor hot gas stream deflects the cool air jets emerging from the sweat cooling holes normal to the liner surface. The holes in each row are staggered to establish uniform film coverage over the affected surface area.

The three rows of 0.125 inch diameter sweat cooling holes provided 4.1% of the combustor airflow immediately upstream of the area to be cooled. An additional 1% airflow was added to the splashplate cooling knuckle of the fifth inner wall panel upstream. The complete cooling scheme is shown in Figure 6.53. Some additional local cooling (approximately 0.58%) was also incorporated downstream of the primer/igniter location. The resultant overall combustor airflow distribution of Configuration IIIa is shown in Figure 6.54; this represents a cooling airflow increase of approximately 5.4% over Configuration IIa.

Metal temperature levels at the rear of the inner liner were measured by fifteen thermocouples embedded at three circumferential locations in each of five axial planes. The first plane, approximately 1.35 inches downstream of cooling panel edge #5, planes #2, #3 and #4 coincide with the three rows of sweat cooling holes while plane #5 is at the critical last cooling panel nugget. Test results as shown in Figures 6.55 and 6.56 indicate that this arrangement satisfactorily lowered metal temperatures to below 1500°F in the critical areas. A comparison of predicted metal temperatures is included with the measured results in these figures.

The sweat cooling modification adversely affected combustor performance to the extent that both temperature pattern factor and apparent combustion efficiency were unacceptably low, as shown in Table 6-4.

TSTR DISTILLATE FUEL COMBUSTOR CONFIGURATION IIIa
INNER LINER REAR WALL COOLING MODIFICATIONS

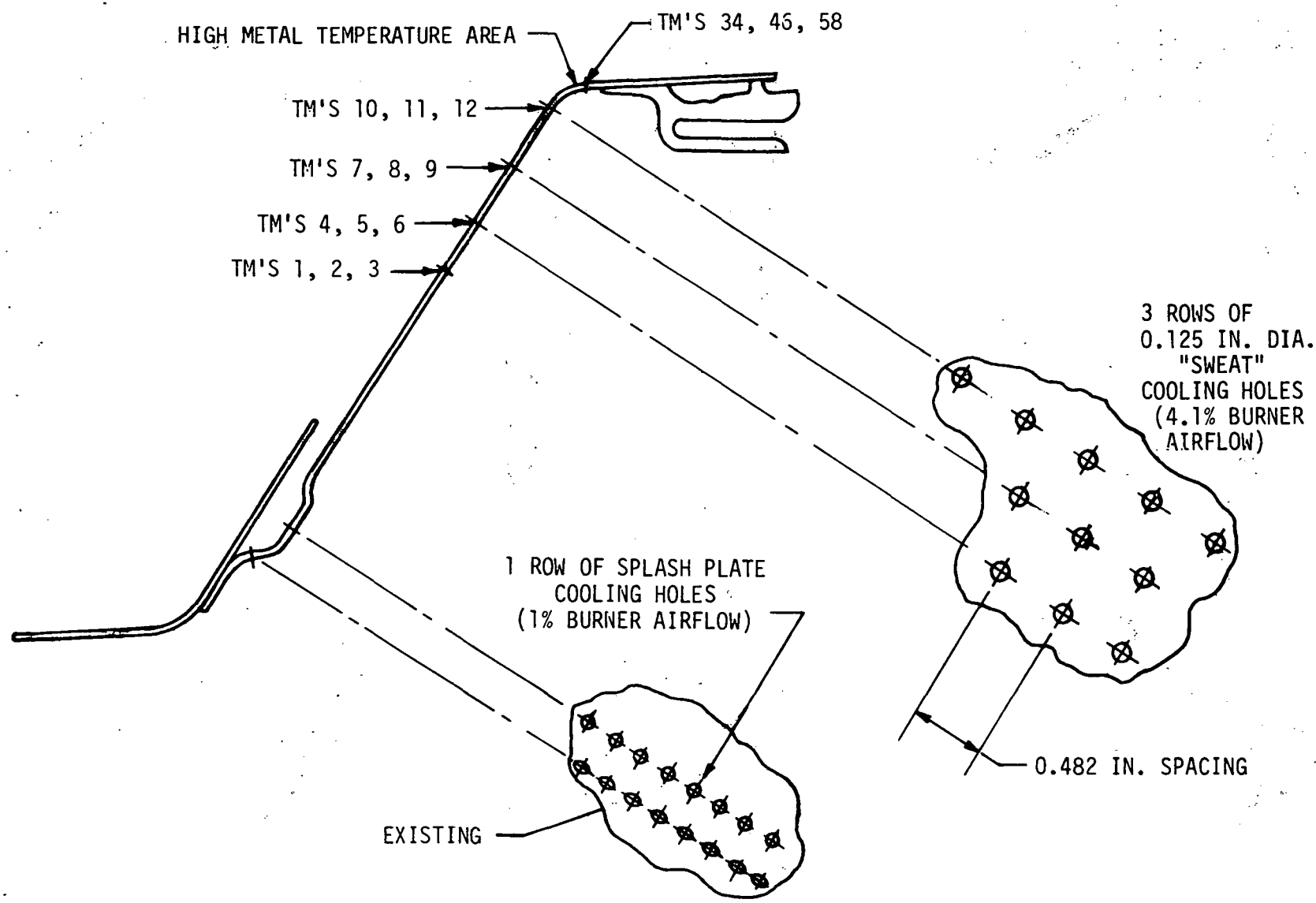

Figure 6.53

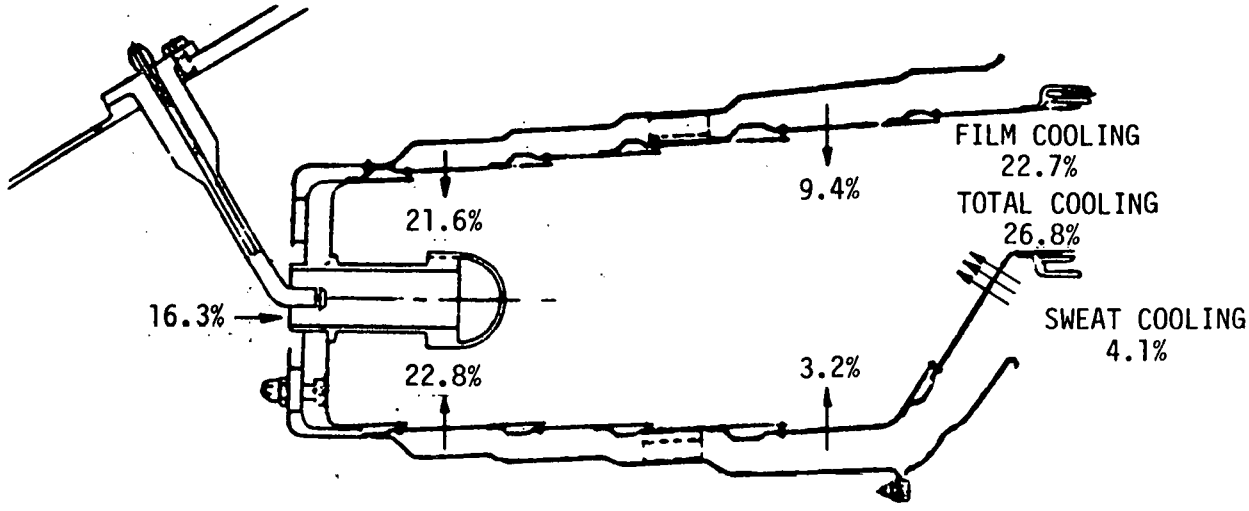

CONFIGURATION IIIa

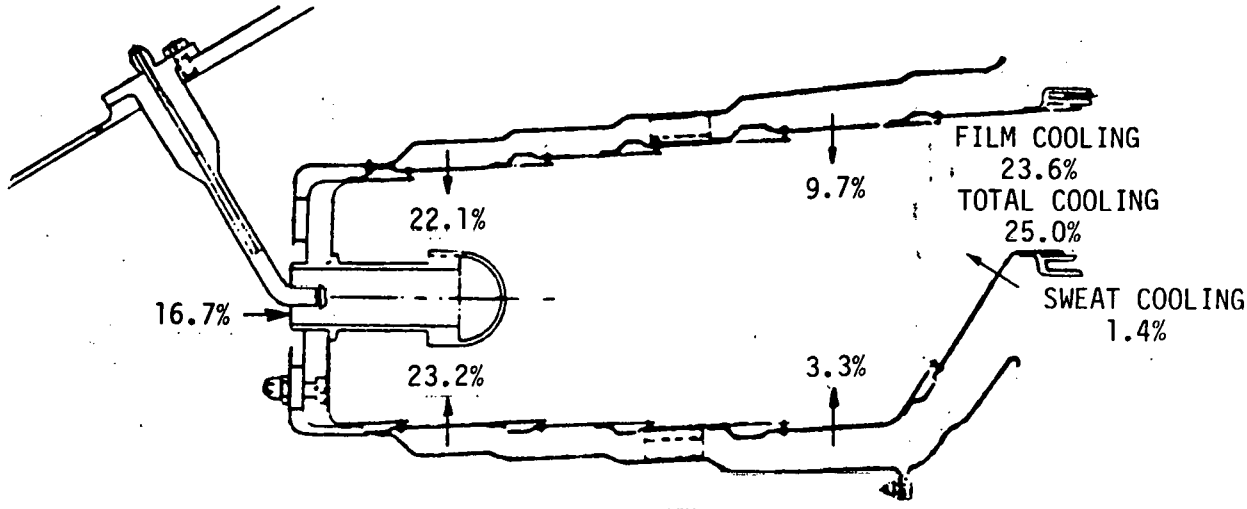

CONFIGURATION IVa

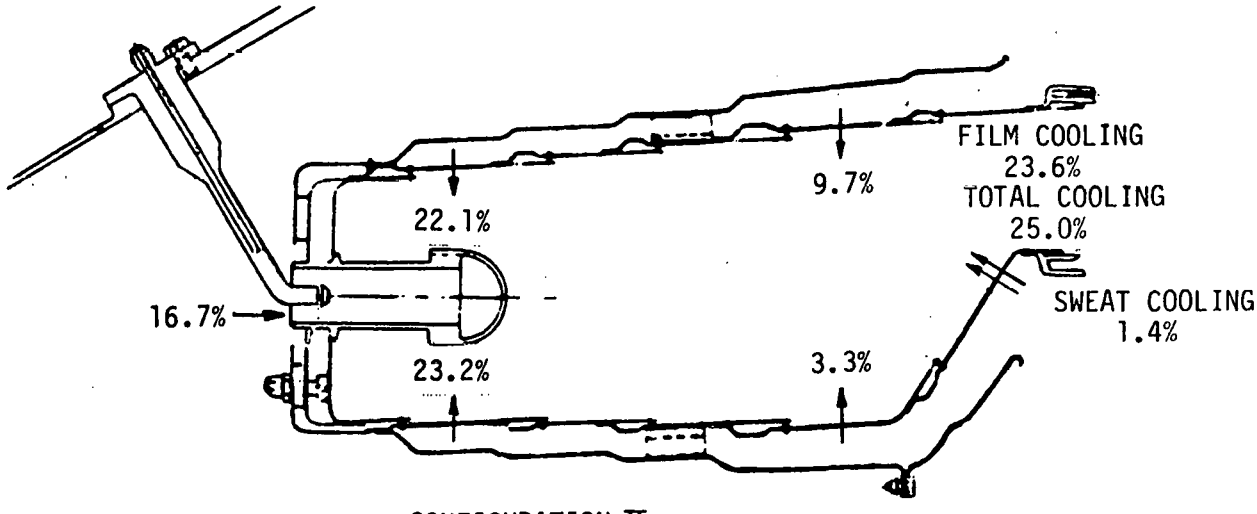

CONFIGURATION Va

TSTR DISTILLATE FUEL COMBUSTOR CONFIGURATIONS

Figure 6.54

TSTR DISTILLATE FUEL 60° SECTOR COMBUSTOR RIG
INNER LINER METAL TEMPERATURE
COMBUSTOR CONFIGURATION IIIa
INLET TEMPERATURE 525°F
(See Figure 6.53)

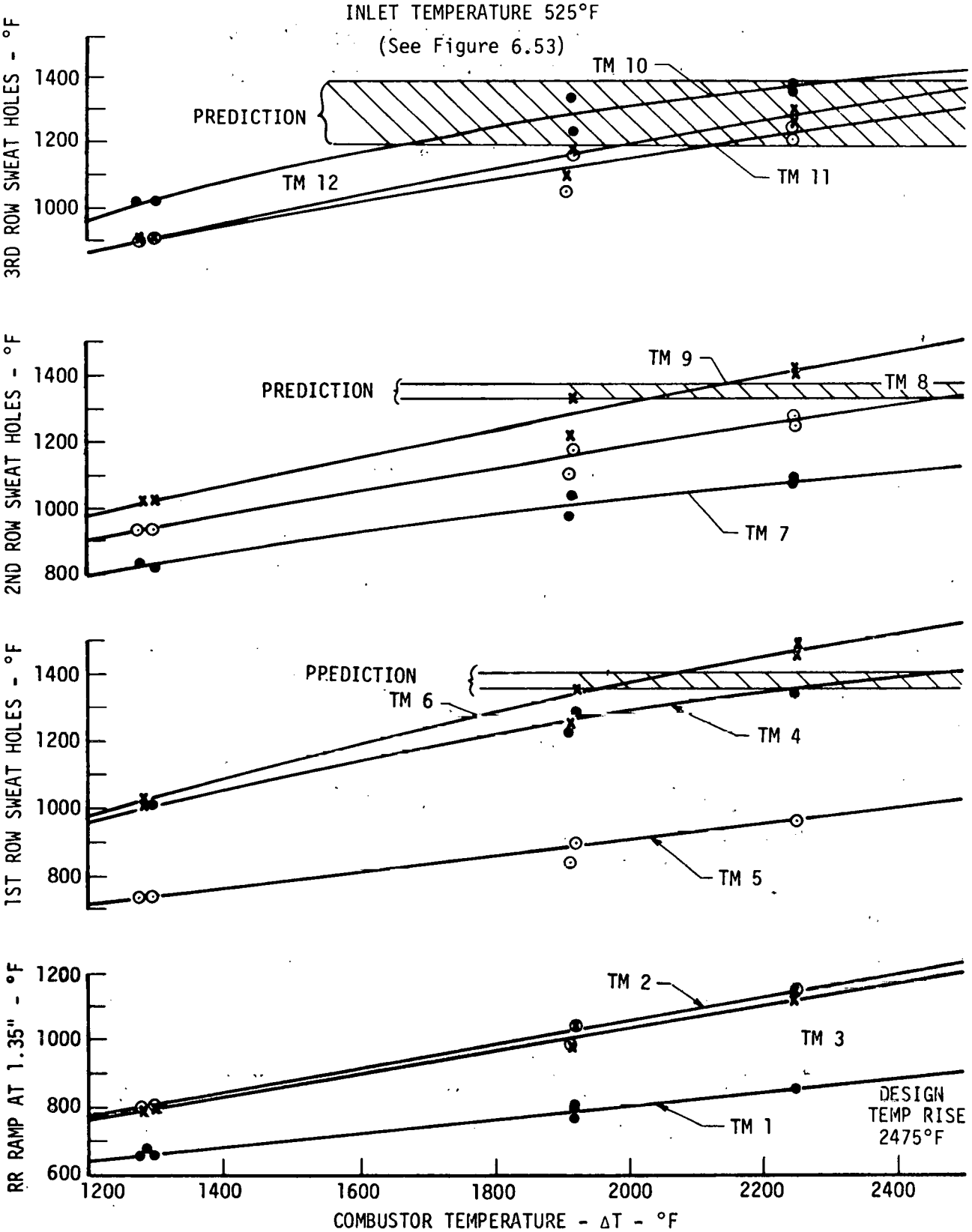

Figure 6.55

TSTR DISTILLATE FUEL 60° SECTOR COMBUSTOR RIG
INNER LINER METAL TEMPERATURE AT #6 NUGGET
COMBUSTOR CONFIGURATION IIIa
INLET TEMPERATURE 525°F
(See Figure 6.53)

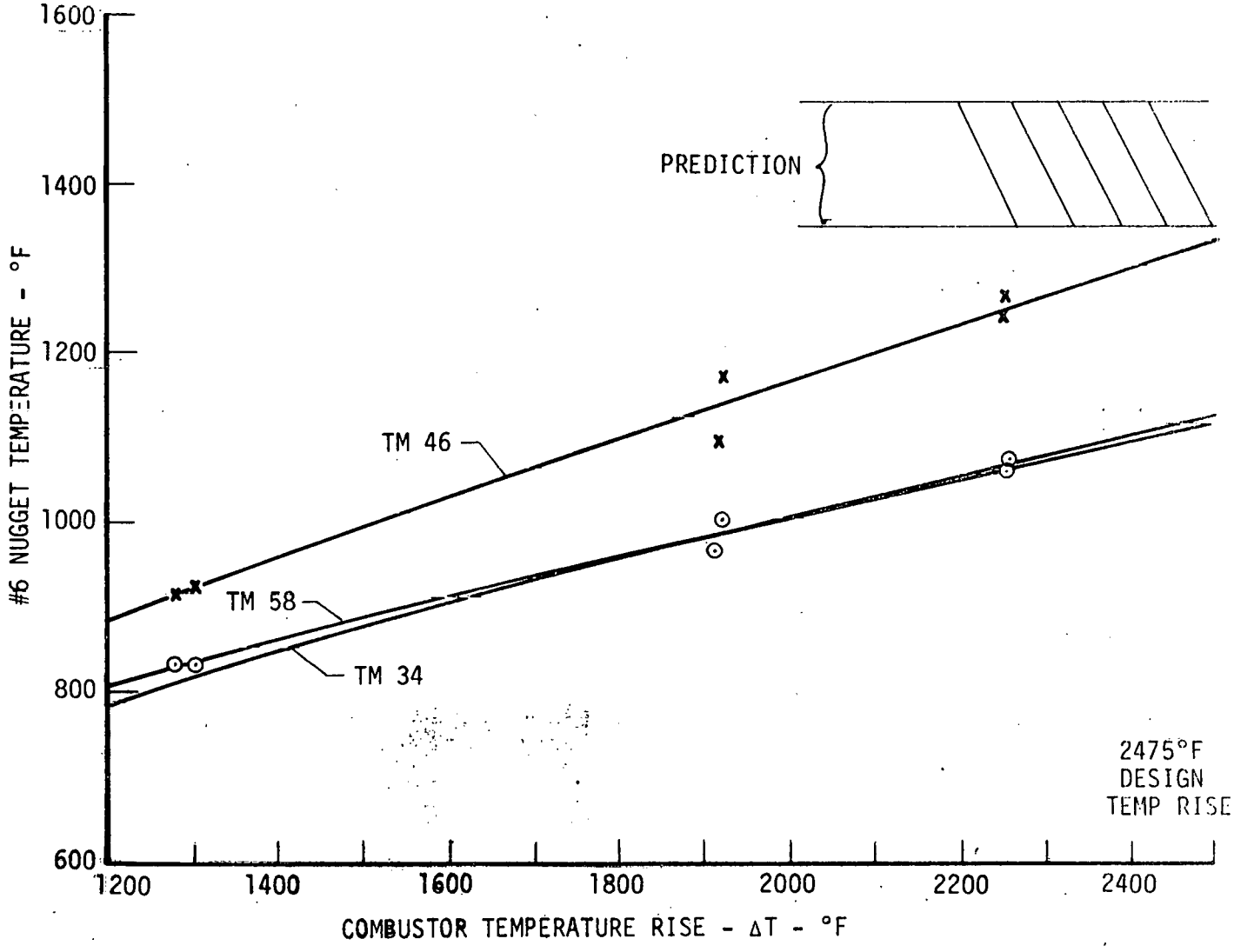

Figure 6.56

Table 6-4

TSTR 60° SECTOR COMBUSTOR PERFORMANCE SUMMARY

Configuration	Combustion Efficiency % At F/A .043	Radial Profile Factor $\frac{T_{max\ avg}}{T_{avg}}$/Span %	Temperature Pattern Factor At F/A .043	Maximum Temperatures Rear-Inner Wall, °F At F/A .043
IIa	97.5	1.12/40%	.245	Over 1600
IIIa	90.5	1.13/65%	.280	1350
IVa	95.5	1.08/40%	.250	1600
Va	97.5	1.09/40%	.230	1520

Configuration IVa

In an effort to minimize performance effects, the sweat cooling hole scheme of combustor Configuration IIIa was modified by closing the front two rows of .125 holes, thereby significantly reducing the quantity of cooling air. This modification (Figure 6.54) was identified as Configuration IVa, was tested at six atmospheres to evaluate the effect on performance and cooling effectiveness. As shown by the performance summary Table 6-4, some performance improvement was accomplished, but at the expense of inner liner cooling effectiveness. Analysis of the sweep probe temperature data from the tests of both Configurations IIIa and IVa resulted in the conclusion that the changes in performance were caused by excessive penetration of the cooling air jets into the hot gas stream.

Configuration Va

In order to reduce cooling air penetration into the hot gas stream, and thereby improve deflection of the cooling air to produce a more effective cooling film, the sweat cooling arrangement of Configuration IIIa was modified to utilize two rows of smaller holes as shown in Figure 6.57, and identified as Configuration Va. As shown in Figure 6.54 combustor overall airflow distribution for Configurations IVa and Va were the same.

Performance tests of Configuration Va at six atmospheres indicated satisfactory combustor performance and adequate cooling of the rear inner liner as shown in Table 6-4 and Figure 6.58. Although, the combustor exit radial, average temperature profile was slightly warmer than the target profile at 88% span as shown in Figure 6.59, the Configuration Va performance was judged to be adequate for the follow-on turbine vane cascade test program. Subsequent analysis of the cascade test results indicated that the TSTR combustor exit gas stream maximum temperature should be reduced at the outermost radius of the annulus for optimum vane cooling. As shown in Figure 6.59, the originally targeted maximum temperature goal at the 88% span thermocouple location was achieved by Configuration Va in the combustor development program.

TSTR DISTILLATE FUEL COMBUSTOR CONFIGURATION Va
INNER LINER REVISED
REAR WALL SWEAT COOLING

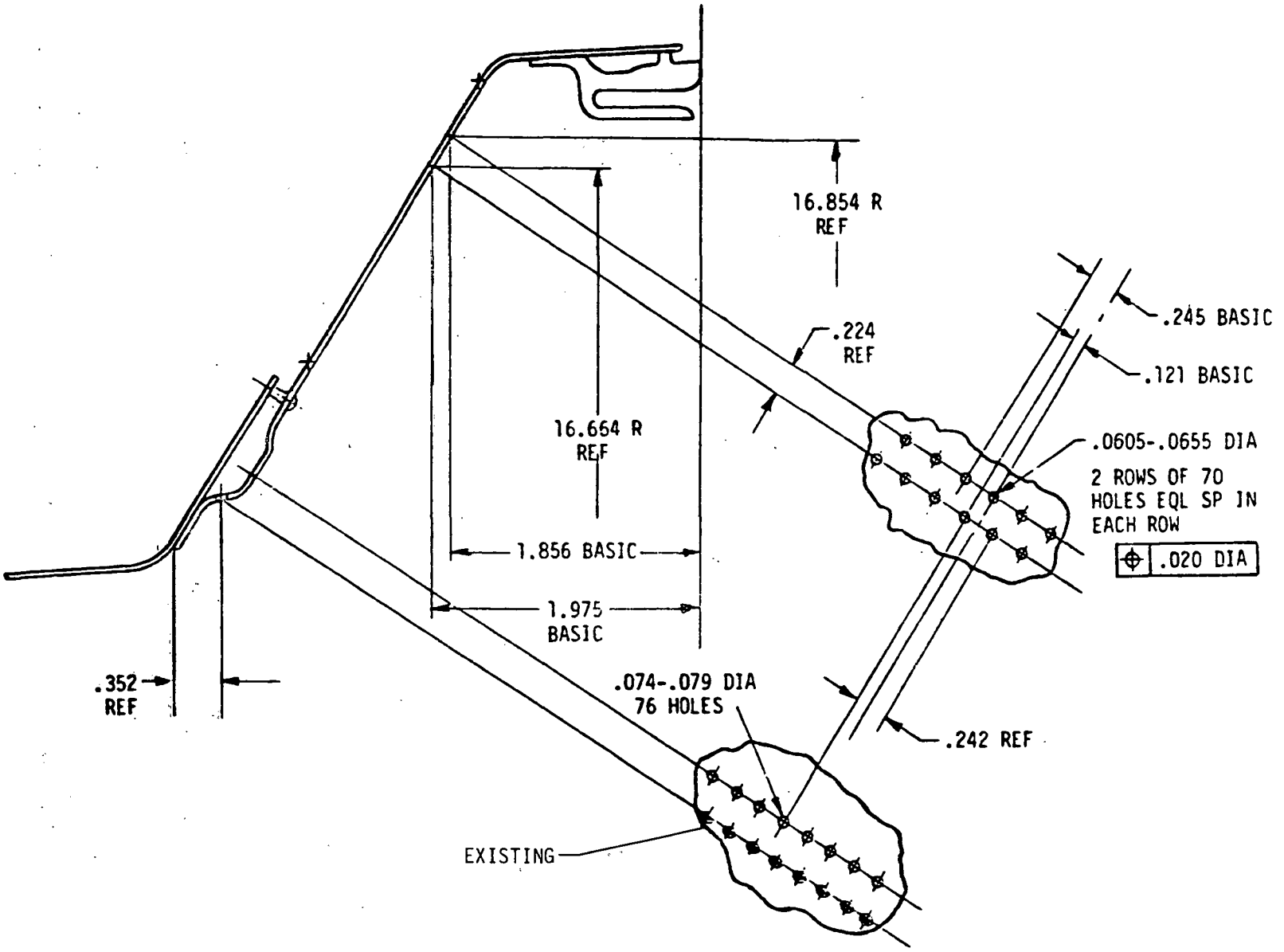

Figure 6.57

TSTR 60° SECTOR COMBUSTOR RIG
6 ATM TM = 525°F
CONFIGURATION Va
INNER LINER METAL TEMP. @ #6 NUGGET
(See Figure 6.53)

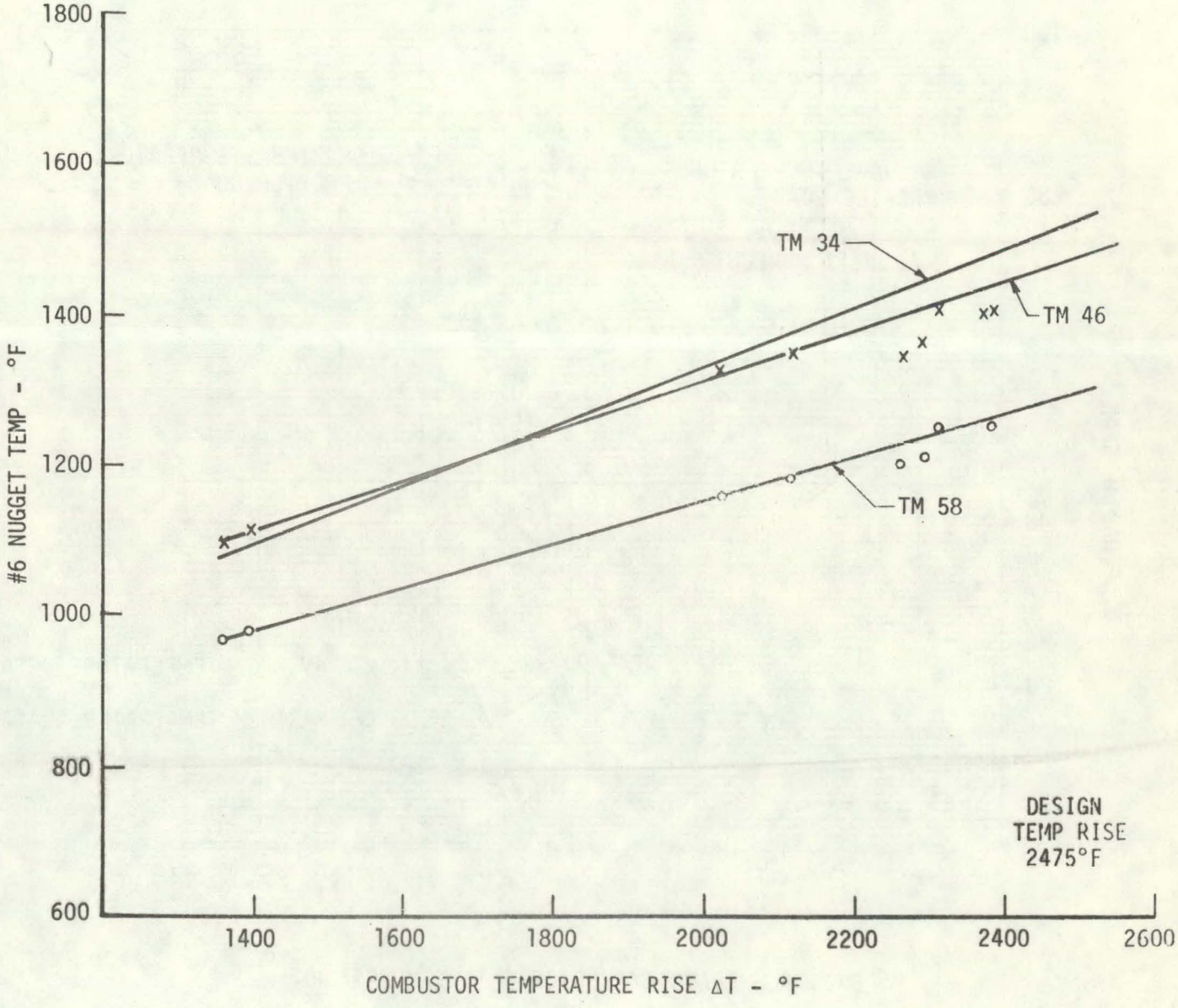

Figure 6.58

JET A FUEL

60° COMBUSTOR SECTOR EXIT

AVERAGE AND MAXIMUM TEMPERATURE SURVEYS

CONFIGURATION Va

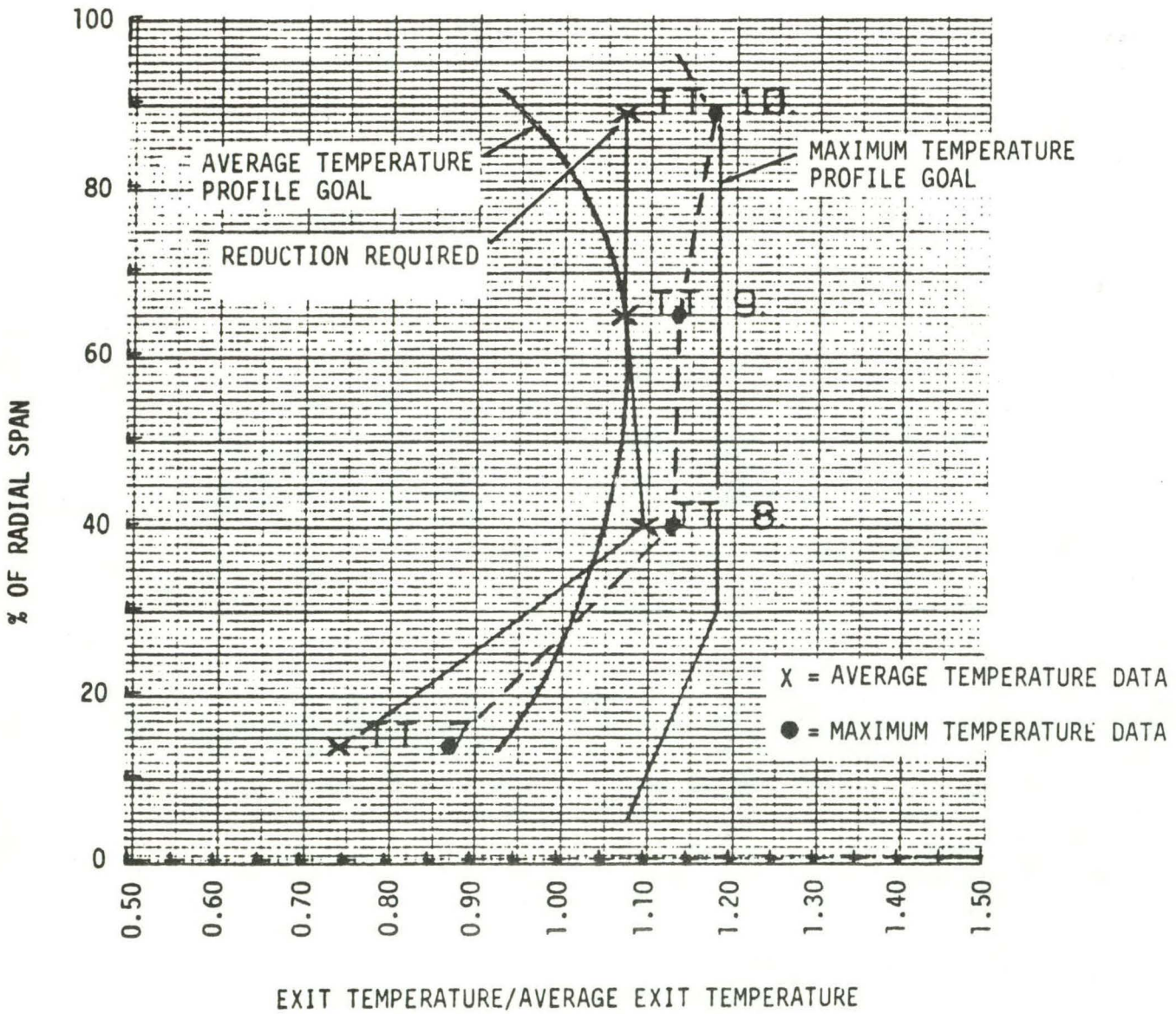

Figure 6.59

HTT-II-733A

The combustor exit temperature pattern of Configuration Va as shown by Figures 6.60 and 6.61 indicates the area in which a need for reduction of temperature was indicated by the cascade test.

Configuration Va Through Xa

Following the turbine vane cascade test, the 60° combustor sector rig was prepared for further development testing to lower the maximum exit temperature level at the outermost radius of the annulus. The original and revised goals are compared in Figure 6.62. The combustor modifications to achieve the revised goals included redistribution of both the primary combustion air and dilution zone airflows between the combustor inner and outer liners. As shown in Figures 6.63 and 6.64, combustor primary and dilution zone changes were incorporated in the following sequence:

Configuration VIa incorporated a reduction in primary zone airflow with a higher percentage through the outer liner (55% outer, 45% inner liner) and redirecting all of the inner liner dilution flow to the outer liner. Overall combustor liner pressure drop was increased approximately 1.5 percentage points to 5.25% by this modification.

Configuration VIIa revised the primary zone outer/inner liners air flow split to make them equal and incorporated a secondary zone immediately downstream of the primary zone by shifting some airflow from primary and outer liner dilution zones.

Configuration VIIIa modified Configuration VIIa by adding low penetration holes in the outer liner dilution zone. The effect of the increased dilution zone area was to reduce liner pressure loss from 5.25% to 5.0%.

Configuration IXa modified Configuration VIIIa by further addition of low penetration holes in the outer liner dilution zone by modification of the dilution slots.

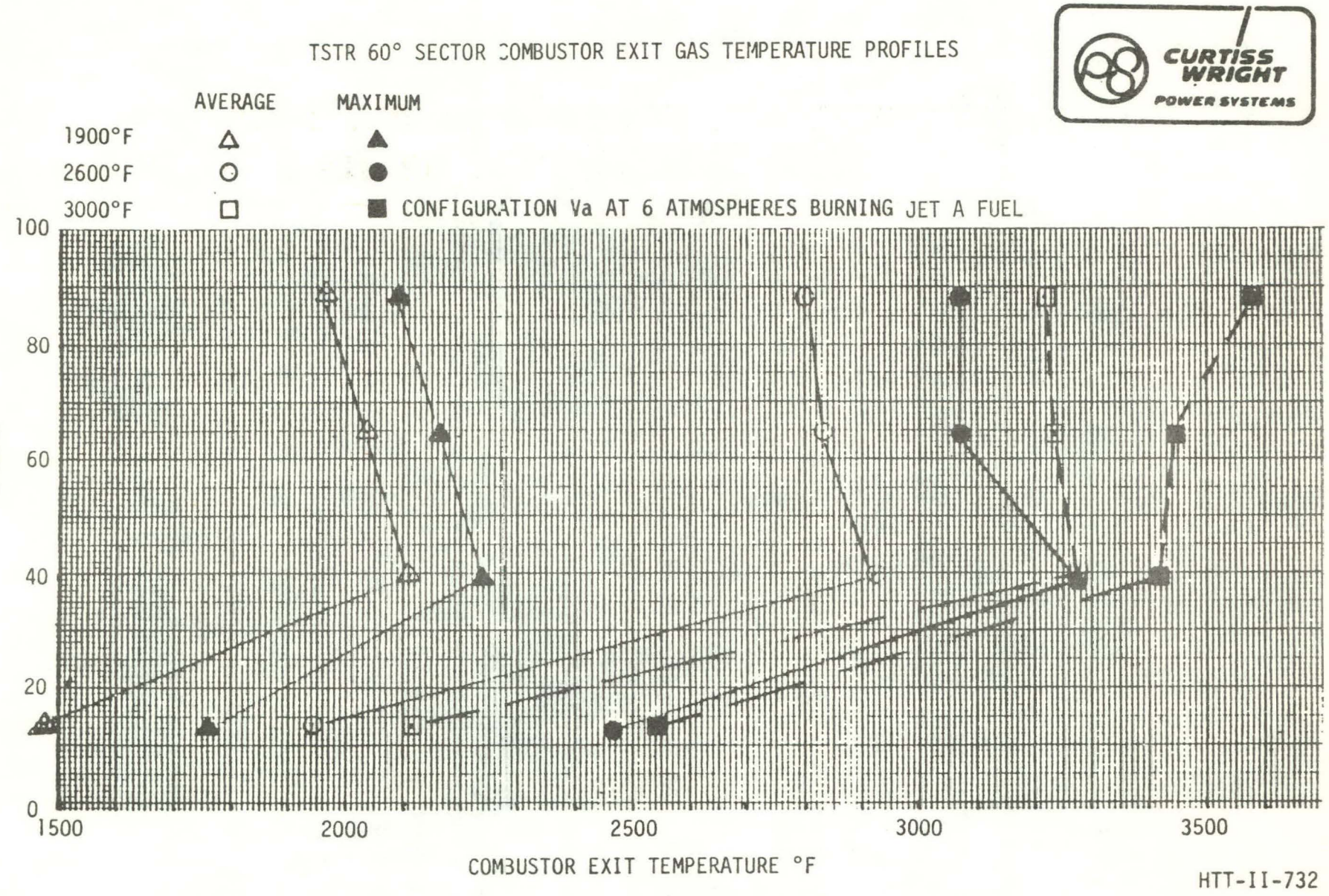
TSTR 60° SECTOR COMBUSTOR EXIT GAS TEMPERATURE PROFILES
AVERAGE
MAXIMUM
1900°F
2600°F
3000°F
CONFIGURATION Va AT 6 ATMOSPHERES BURNING JET A FUEL
% SPAN
100
80
60
40
20
0
1500
2000
2500
3000
3500
COMBUSTOR EXIT TEMPERATURE °F
HTT-II-732

Figure 6.60

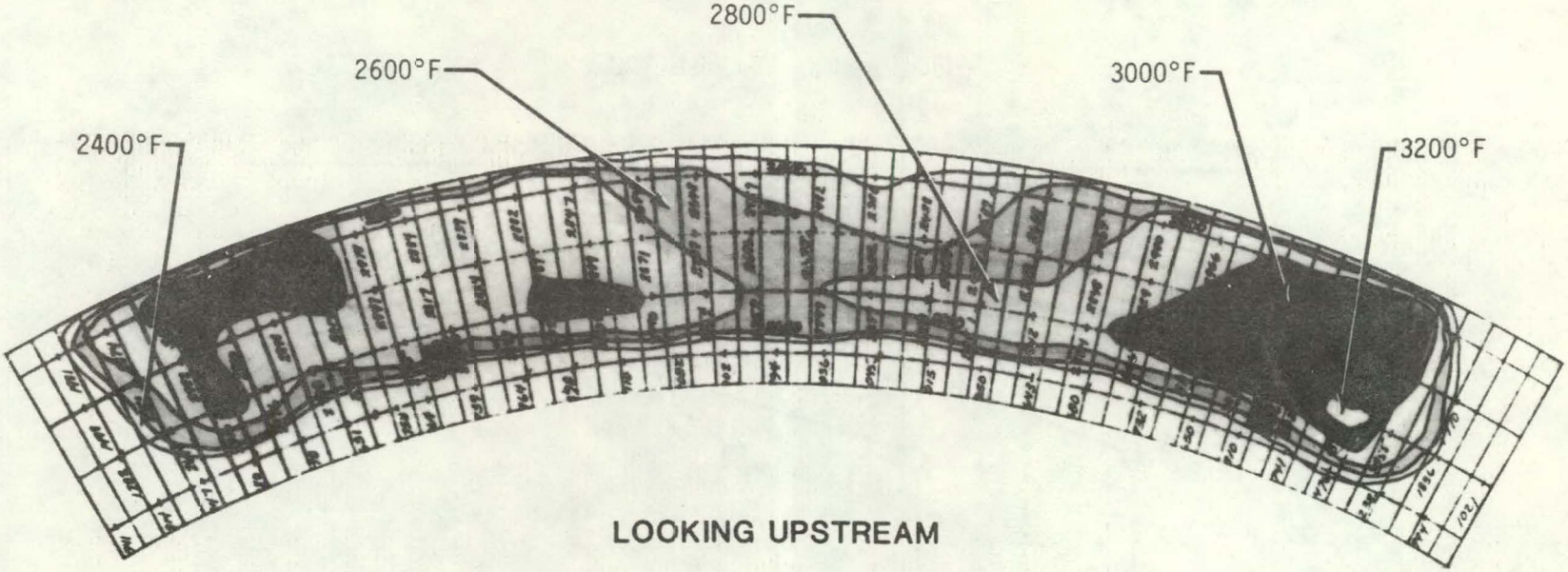

COMBUSTOR CONFIGURATION Va

TIME: 5/29/80 11:22:23

TEMP. MAX. 3275°F TEMP. AVG. 2600°F

COMBUSTOR INLET TEMP. 525°F

COMBUSTOR INLET PRESS. 6 ATM

FUEL JET A

TSTR 60° SECTOR COMBUSTOR RIG
EXIT TEMPERATURE PATTERN VARIATION

HTT-II-791

Figure 6.61

60° TSTR COMBUSTOR RADIAL AVG/MAX TEMPERATURE PROFILE TARGETS

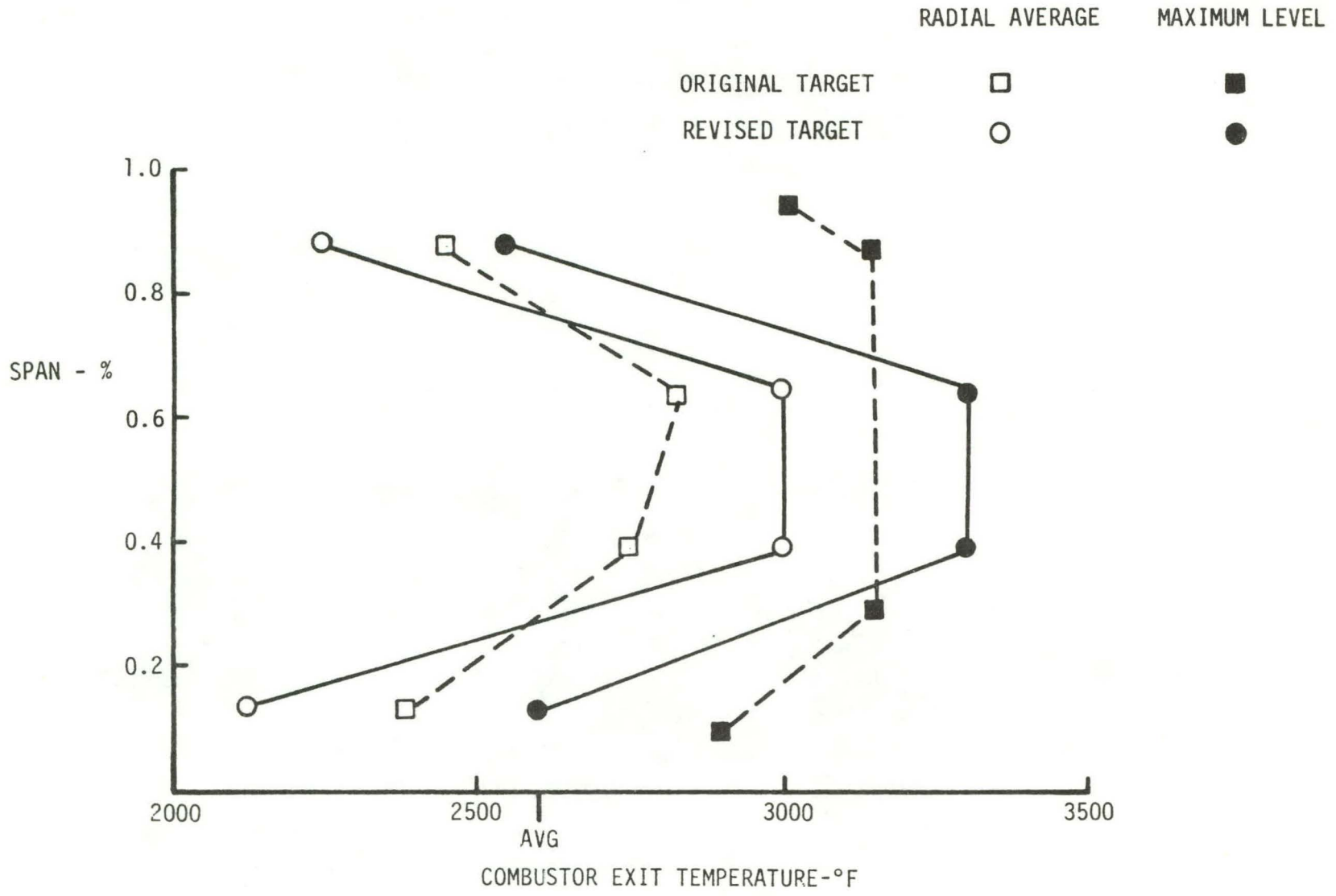

HTT-II-792

Figure 6.62

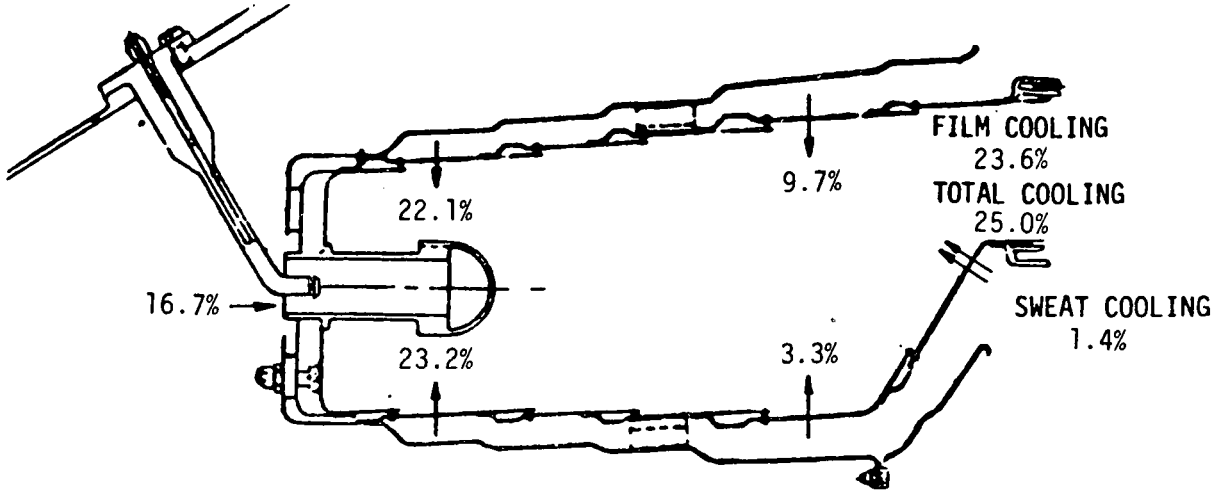

CONFIGURATION Va

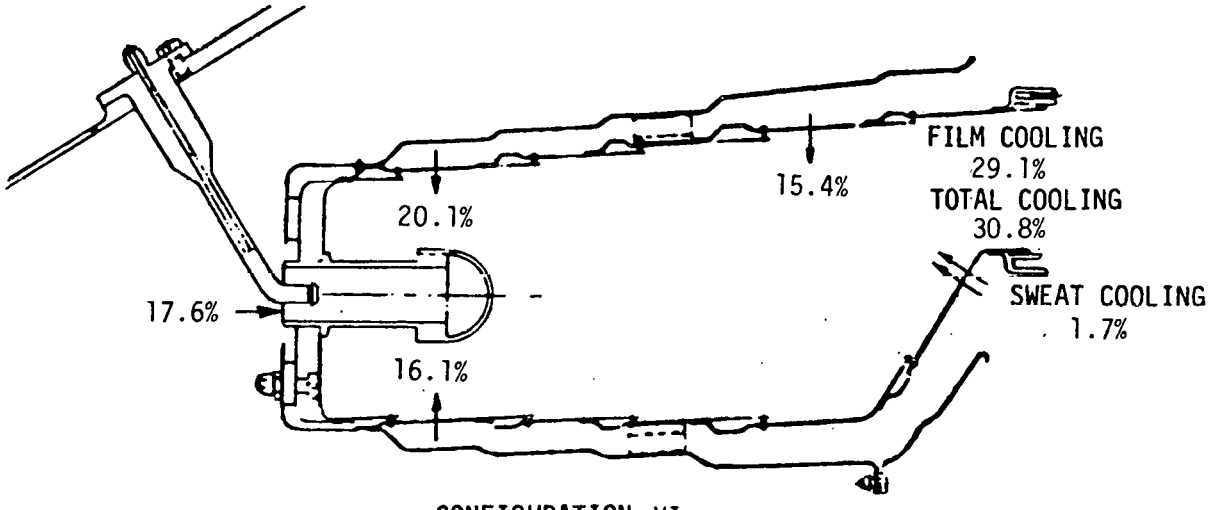

CONFIGURATION VIa

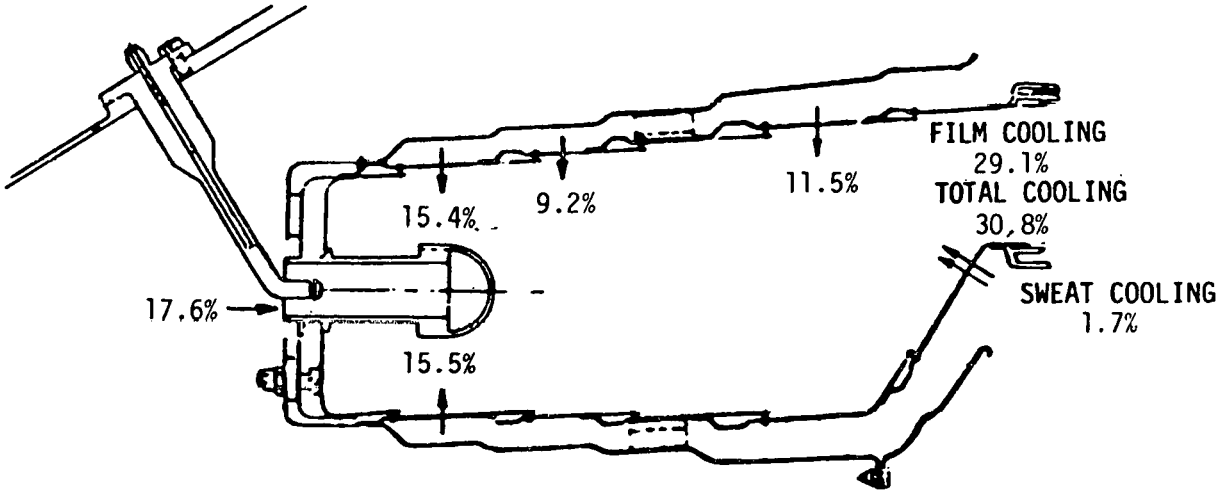

CONFIGURATION VIIa

TSTR LIQUID-FUELED COMBUSTOR CONFIGURATIONS

Figure 6.63

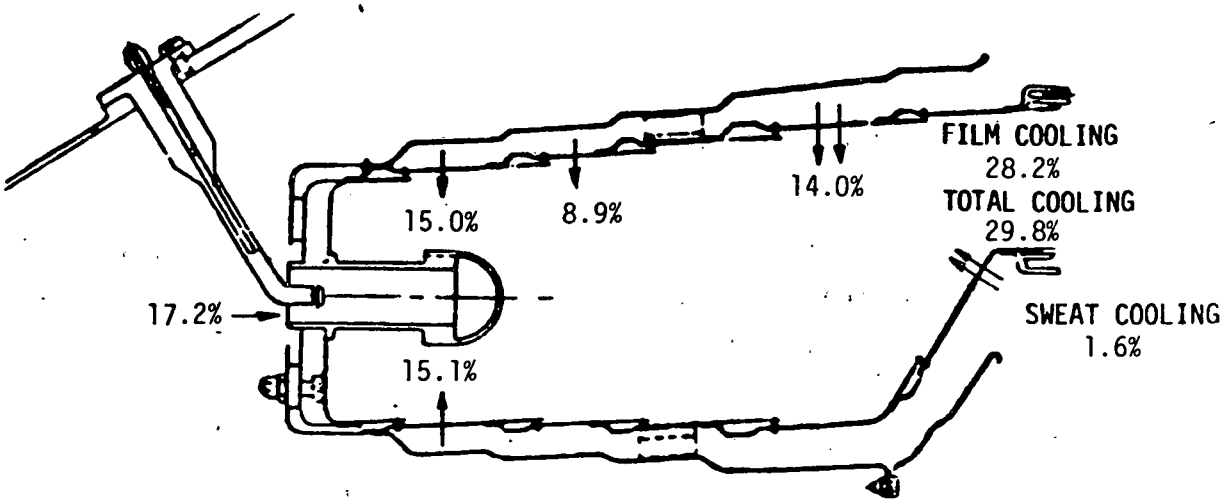

CONFIGURATION VIIIa

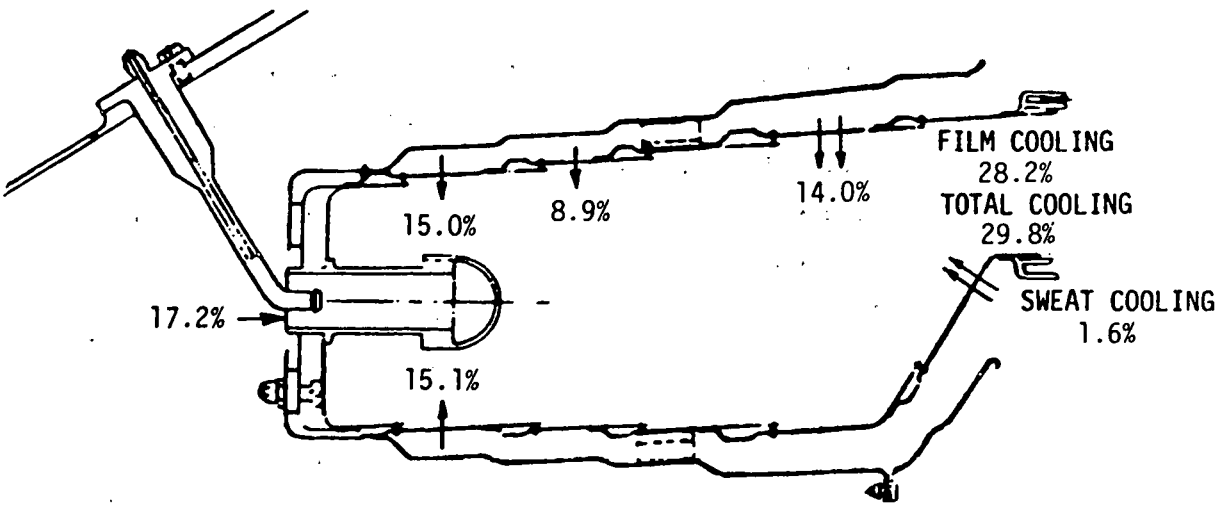

CONFIGURATION IXa

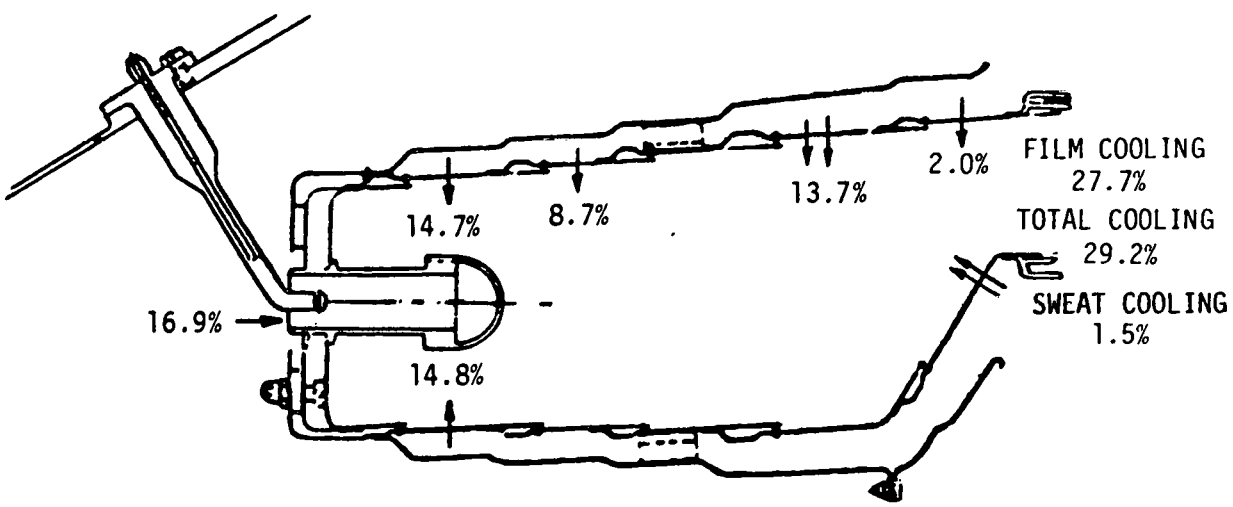

CONFIGURATION Xa

TSTR LIQUID-FUELED COMBUSTOR CONFIGURATIONS

Figure 6.64

Configuration Xa modified Configuration IXa by restoration of the dilution slots configurations of Configuration VIIIa and further addition of low penetration dilution holes in the outer liner panel (#15) downstream of the dilution zone. This increase of dilution hole area further reduced the liner cold pressure drop to approximately 4.8% (total hot loss = 6.5%).

The results of the test program conducted with the above modifications to the TSTR 60° sector burner rig are given by Tables 6-5 and 6-6. Although combustor exit temperature profile goals were not exactly achieved by the final Configuration Xa, it was judged that the demonstrated performance and durability of this configuration was satisfactory for incorporation into the TSTR cascade rig and full-round burner. As shown in Figures 6.65 and 6.66 the outermost portion of the combustor exit annulus temperature achieved the average radial target of 2250°F, while the maximum temperature was reduced approximately 350°F from the baseline Configuration Va. Visual inspection of the 60° combustor sector after approximately 15 hours test at 6.0 ATM indicated excellent durability as shown by Figure 6.67. Based on these results, Configuration Xa was released to the TSTR.

Table 6-5

TSTR 60° SECTOR COMBUSTOR PERFORMANCE SUMMARY

Configuration	Combustion Efficiency % At F/A .043	Radial Profile Factor $\frac{T_{max\ avg}}{T_{avg}}$/Span %	Temperature Pattern Factor At F/A .043	Maximum Temperatures Rear-Inner Wall, °F At F/A .043
VIa *				
VIIa	97.0	1.12/40%	.255	1520
VIIIa	97.5	1.13/40%	.220	1500
IXa	97.0	1.15/40%	.230	1600
Xa	97.0	1.18/40%	.230	1600

* Tests Terminated Prior to Full Evaluation

Table 6-6

COMPARISON OF EXIT TEMPERATURE PROFILES WITH TSTR 60° COMBUSTOR SECTOR RIG

CONFIGURATIONS 2600°F AVERAGE EXIT TEMPERATURE - JP-5 FUEL

	88% Span		64% Span		40% Span		13% Span	
Combustor Configuration	Max. °F	Avg. °F	Max. °F	Avg. °F	Max. °F	Avg. °F	Max. °F	Avg. °F
Previous (Baseline) Configuration Va	3070	2800	3070	2830	3280	2920	2460	1940
	Δ°F	Δ°F	Δ°F	Δ°F	Δ°F	Δ°F	Δ°F	Δ°F
Goal	-520	-550	+230	+170	+ 20	+ 80	+140	+180
			CHANGE FROM BASELINE					
Secondary Zone Configuration VIIa	- 60	-210	+ 10	+ 30	- 90	+110	-200	- 20
First Dilution Change Configuration VIIIa	-270	-330	+ 40	+ 60	- 40	+130	- 90	+ 50
Second Dilution Change Configuration IXa	-250	-415	+110	+ 45	- 35	+180	- 20	+ 95
Third Dilution Change (Final) Configuration Xa	-340	-550	+130	+ 10	+ 70	+320	-130	+200

60° COMBUSTOR SECTOR
COMBUSTOR EXIT AVG/MAX TEMPERATURE PROFILES

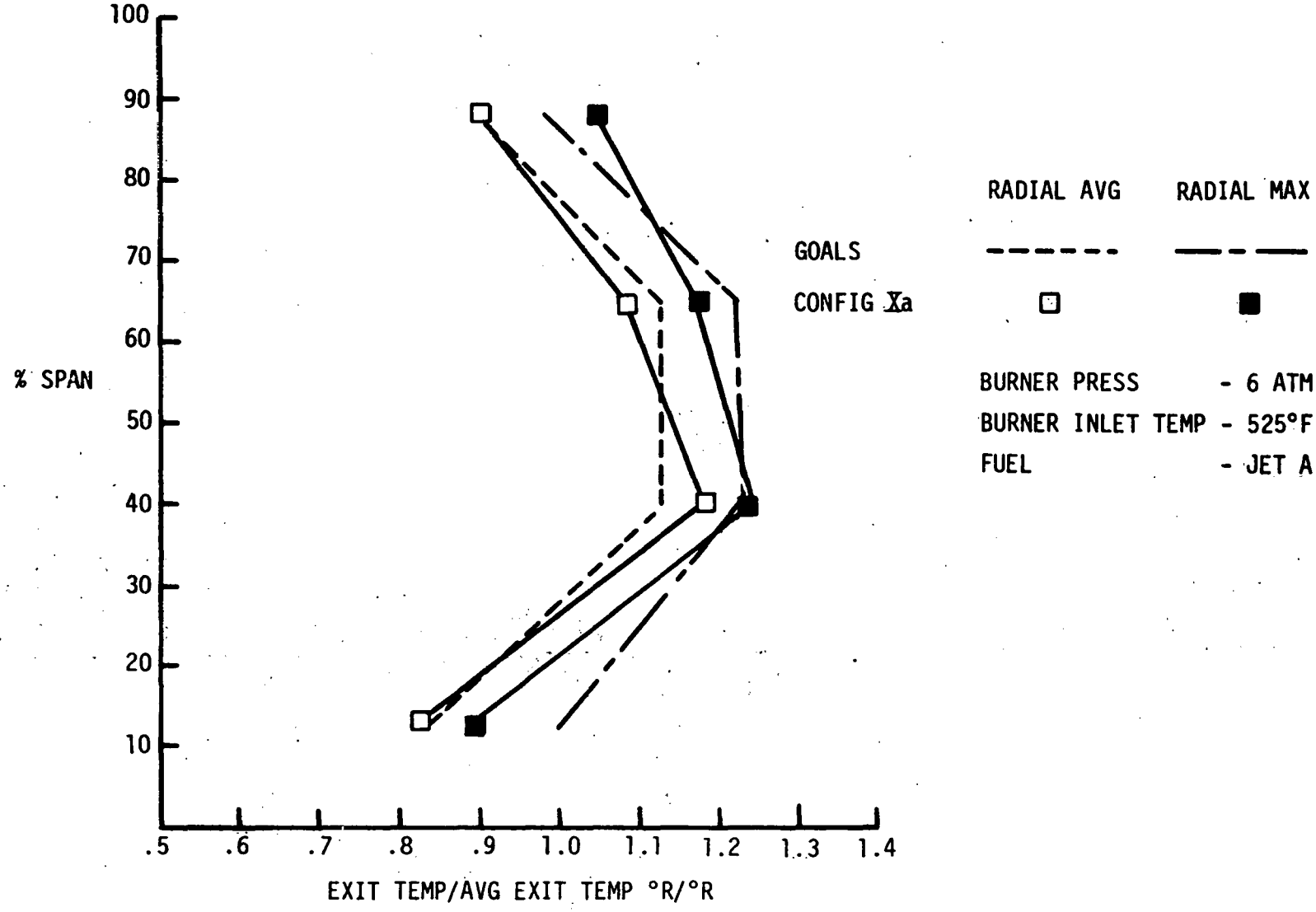

HTT-II-795A

Figure 6.65

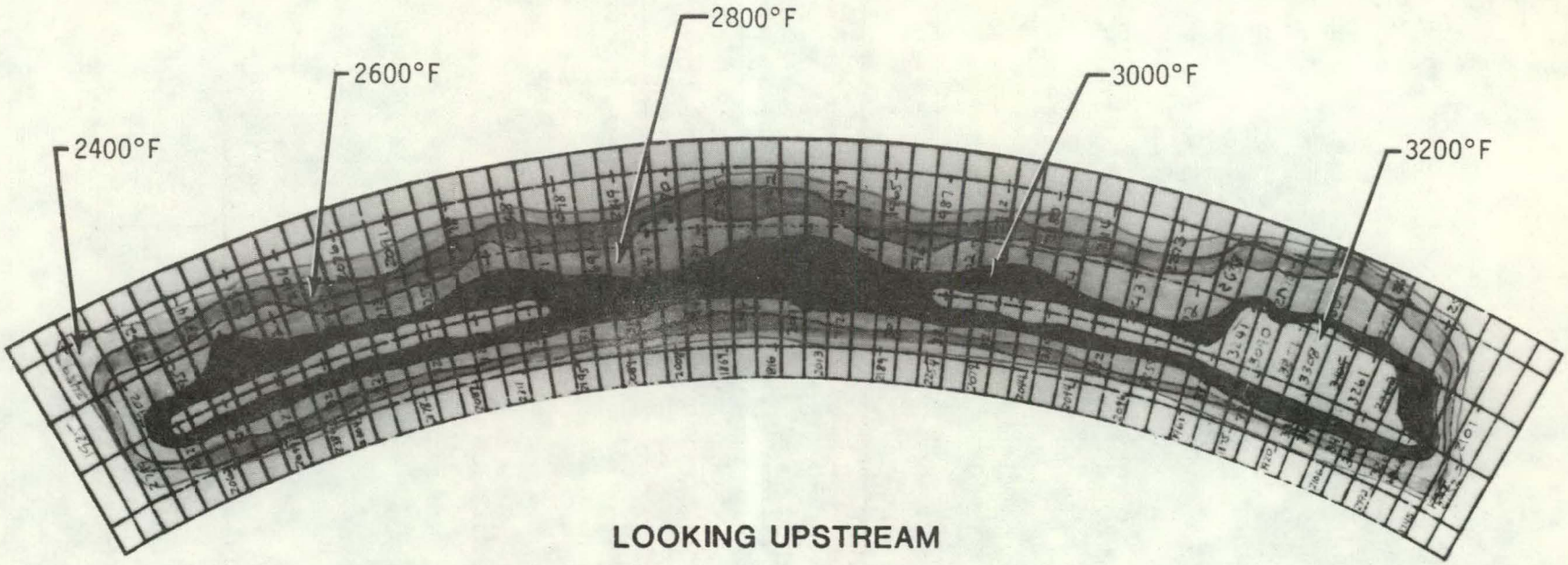

COMBUSTOR CONFIGURATION Xa

TIME: 9/24/80 09:31:31

TEMP. MAX. 3428°F TEMP. AVG. 2600°F

COMBUSTOR INLET TEMP. 525°F

COMBUSTOR INLET PRESS. 6 ATM

FUEL JET A

TSTR 60° SECTOR COMBUSTOR RIG
EXIT TEMPERATURE PATTERN VARIATION

HTT-II-794

Figure 6.66

TSTR COMBUSTOR 60° SECTOR DURABILITY CONDITION (20 TEST HOURS)

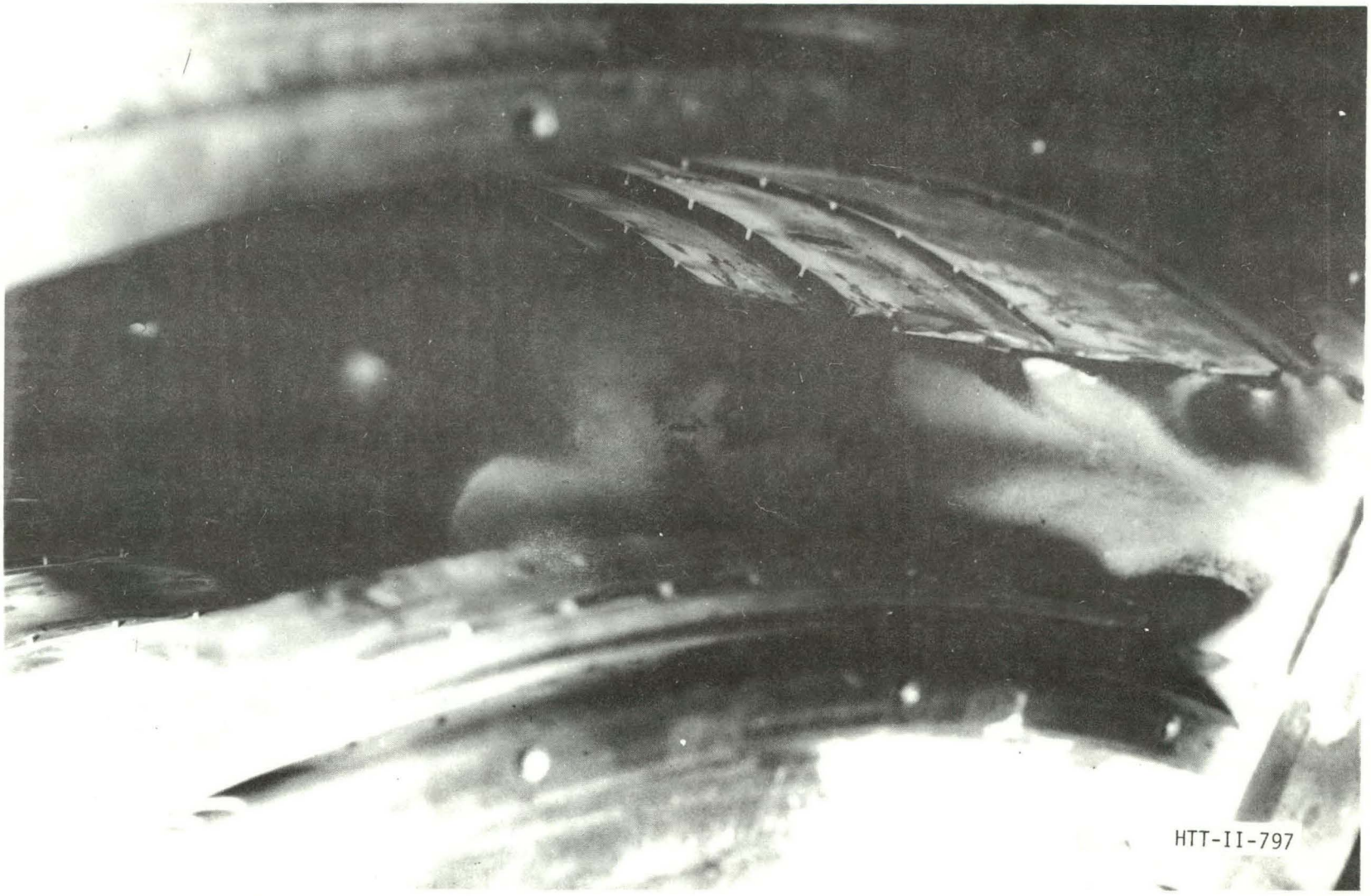

Figure 6.67

Section 7.0
CONCLUSION

The TSTR combustor development program to demonstrate durability and performance up to 3000°F was conducted in a 60° sector (cut from a full-round combustor) test rig at pressure levels up to 6 atmospheres. Following the development program of 130 test hours, the 60° sector combustor rig was installed ahead of a turbine cascade sector for evaluation of the cooling effectiveness of the TSTR turbine vanes. Upon successful demonstration up to 2800°F combustor exit temperature with the cascade, combustor Configuration Xa was considered acceptable for, and was released for TSTR installation.

☆U.S. GOVERNMENT PRINTING OFFICE: 1982-546-085/3225